Enhancing Groundwater Recharge in Malta:

Proposing a Ground Permeability Model for Infiltration Boreholes in Maltese Limestone

By

Ryan Worley

Dissertation submitted to the Faculty for the Built Environment, University of Malta in part fulfilment of the requirements for the attainment of the degree of Master of Engineering (Civil Engineering)

July 2024

L-Università ta' Malta

University of Malta Library – Electronic Thesis & Dissertations (ETD) Repository

The copyright of this thesis/dissertation belongs to the author. The author's rights in respect of this work are as defined by the Copyright Act (Chapter 415) of the Laws of Malta or as modified by any successive legislation.

Users may access this full-text thesis/dissertation and can make use of the information contained in accordance with the Copyright Act provided that the author must be properly acknowledged. Further distribution or reproduction in any format is prohibited without the prior permission of the copyright holder.

L-Università ta' Malta

FACULTY/~~INSTITUTE/CENTRE/SCHOOL~~ for the Built Environment

DECLARATIONS BY POSTGRADUATE STUDENTS

(a) Authenticity of Dissertation

I hereby declare that I am the legitimate author of this Dissertation and that it is my original work.

No portion of this work has been submitted in support of an application for another degree or qualification of this or any other university or institution of higher education.

I hold the University of Malta harmless against any third party claims with regard to copyright violation, breach of confidentiality, defamation and any other third party right infringement.

(b) Research Code of Practice and Ethics Review Procedures

I declare that I have abided by the University's Research Ethics Review Procedures. Research Ethics & Data Protection form code BEN-2024-00012.

As a Master's student, as per Regulation 77 of the General Regulations for University Postgraduate Awards 2021, I accept that should my dissertation be awarded a Grade A, it will be made publicly available on the University of Malta Institutional Repository.

ACKNOWLEDGEMENTS

I would like to express my deepest gratitude to the following individuals, whose support, guidance, and encouragement have been invaluable throughout the course of my dissertation.

I am profoundly grateful to my dissertation supervisor Dr. Adrian Mifsud *B.E&A.(Hons.), M.Sc.(Lond.), Ph.D.(Melit.), DIC, Eur. Ing. Perit* for his immense patience and for always finding the time to assist and guide me. His great enthusiasm for my research and his unwavering support whenever I encountered roadblocks have been invaluable. Dr. Mifsud made me believe in my potential to succeed and helped me develop a deep appreciation and understanding of the complexities of geotechnical engineering.

I would like to express my sincere gratitude to Mr. Emmanuel Magro and the rest of the team at *Solidbase Laboratory* for allowing me to accompany them during borehole coring operations in order to conduct the necessary permeability testing. Their support in providing me any essential data was crucial for the completion of my research.

I wish to extend my thanks to Dr. Kevin Gatt *B.E.&A.(Hons.), M.Sc.(Lond.), MBA, Ph.D, MCIWEM, CEng* for guiding me towards this research topic and for his patience during my moments of indecisiveness. His energy and motivation inspired me to pursue my path in civil engineering and his passion for water and environmental engineering instilled in me a desire to improve our environment and prioritize a more sustainable future.

Lastly, I extend my heartfelt thanks to those closest to me who have consistently supported me throughout my journey: my family, my friends, and my significant other.

To all of you, I extend my deepest gratitude. Your contributions and assistance have been crucial to the completion of this dissertation, and I am forever grateful for your support.

I take full responsibility for any shortcomings in this dissertation.

ABSTRACT

Malta faces ongoing challenges in securing potable water due to its geographical and climatic limitations. Historically, the Maltese relied on groundwater and rainwater storage, but modern reliance on aquifer pumping has led to over-extraction, particularly from the mean sea level aquifer.

Despite the high risks observed on water resources in Malta, the rate of urban development has contributed to soil-sealing effects without the implementation of any mitigation measures, resulting in an increase in flash flooding and a decline in permeable areas for groundwater recharge.

This dissertation examines past and present water conservation practices and proposes infiltration boreholes for managed aquifer recharge (MAR) in Malta's limestone strata. By analysing local ground conditions, the study aims to estimate recharge rates through a simplified dry well model and evaluate the feasibility of MAR as part of a broader and more streamlined aquifer recharge strategy.

A parametric model was developed to predict recharge rates, demonstrating that water head loss, flow velocity, and volumetric flowrate in emptying infiltration boreholes decrease over time. The model also highlights the significant impact of fissure concentration and infill material on flowrate estimations, as well as the differences between primary and secondary permeability. The model was created to map directly onto existing local drilling record data, in order to facilitate direct input of rock quality designation (RQD) values and borehole dimensions and to hasten the estimation and design process of local MAR projects.

Further testing is required to refine the model and increase confidence in site-specific predictions, especially regarding flow resistance factors within fissures.

Keywords

Limestone, Hydrogeology, Groundwater recharge, Boreholes, Water conservation

TABLE OF CONTENTS

LIST OF FIGURES

LIST OF TABLES

ABBREVIATIONS

a	Fissure aperture
A_{BH}	Cross-sectional area of borehole
A_f	Fissure flow area
AM	Ambjent Malta
ASR	Aquifer-Storage-Recovery
ASTR	Aquifer-Storage-Transfer-Recovery
BC	Blue Clay
CL	Coralline Limestone
cm	Centimetre
cm^3/s	Cubic centimetre per second
D	Diameter
dh	Change in height
Dl	Depth Index
dt	Change in time
e	Void ratio
ERA	Environment and Resources Authority
EU	European Union
EWA	Energy and Water Agency
F	Hvorslev Intake Shape Factor
F_F	Flow Factor due to Fissure Resistance
g	Acceleration due to gravity
GCD	Gouge Content Designation
GEO-INF	Rainwater Recovery Project in Malta
GIS	Geographic Information System
GL	Globigerina Limestone
h	Height
i	Hydraulic gradient
Ing.	Engineer title
k	Hydraulic conductivity
L	Length
LCL	Lower coralline limestone
LGL	Lower globigerina limestone
LIFE-IP	Life Integrated Project
LPI	Lithology Permeability Index
m/s	Metre per second
m^2	Square metre
m^3	Cubic metre

m^3/s	Cubic metre per second
MAR	Managed Aquifer Recharge
mm	Millimetre
mm^2	Millimetre squared
MSL	Mean Sea Level
MSLA	Mean Sea Level Aquifer
NFRP	National Flood Relief Project
NSO	National Statistic Office
P	Pressure
Q	Volume flowrate
Q_T	Total volume flowrate
r	Radius
RBMP	River Basin Management Plan
RMR	Rock Mass Rating
RQD	Rock Quality Designation
RVA	Range of Variability Approach
t	Unit for time
U.S.	United States
v	Velocity
WFD	Water Framework Directive
WSC	Water Services Corporation
°C	Degree Celsius
ρ	Density

1 INTRODUCTION

1.1 ENVIRONMENTAL CONTEXT

1.1.1 The Maltese Climate

With its Mediterranean climate characterized by little rainfall throughout the year and soaring temperatures, Malta faces a constant battle of freshwater availability. Between 1952 and 2020, the annual rainfall was observed to range from 274mm to 900mm, showing a high variability and unpredictability with very dry years and moderately wet years, averaging at around 545mm of total rainfall per year (NSO Malta, 2022).

The unpredictability of rainfall is compounded by high evaporation and evapotranspiration losses which exceed both annual rainfall and recharge volumes, as well as the observed negative trend of around 10mm of reduced rainfall per decade. This is an ever-increasing problem stemming from the climate change induced upward trend of mean air temperature, with a recorded increase of 0.2°C per decade since 1952 (NSO Malta, 2022). Figure 1.1 below shows the gradual reduction of total rainfall over the period 1952 to 2020.

Figure 1.1: Time Series of the Annual Total Rainfall for the Period 1952-2020 (NSO Malta, 2022)

Furthermore, the densely populated nature of the country, accommodating approximately 1,400 individuals per square kilometre, magnifies the strain on water resources, resulting in a severe water scarcity situation in the densely inhabited islands of Malta and Gozo (Sapiano, 2018).

For centuries, reservoirs had once served as important lifelines for the Maltese residents during long periods of drought, ensuring survival and wellbeing (alteraqua, 2022). However,

such structures are nowadays seen to be more of an inconvenience or an expense; where it is considered cheaper and easier to rely on the national grid or to extract groundwater free of charge than it is to retain and renovate these historical water conservation structures.

1.1.2 The Groundwater Aquifers

Malta's geology is made up of a series of sedimentary layers, predominantly of porous limestone, with a single middle layer of blue clay. The hydrogeology gives rise to two main fresh-water aquifers across the Maltese islands; the perched aquifers located above the clay layer, and the mean sea-level (MSL) aquifer, found deep in the lower globigerina and lower coralline layers (Bakalowicz & Mangion, 2003).

As in Figure 1.2, the perched aquifer may only be found within the rural-dominated north-western end of Malta. The MSL aquifers, however, can be found throughout Malta and Gozo and are the largest and most important aquifers for public water supply. It is these MSL freshwater lenses which are currently classified as "poor" due to over-abstraction and salinification (Sant, 2019).

The infiltration zone depth of the perched and sea level aquifers varies by 20-50m and 50-100m respectively from the surface (Bakalowicz & Mangion, 2003).

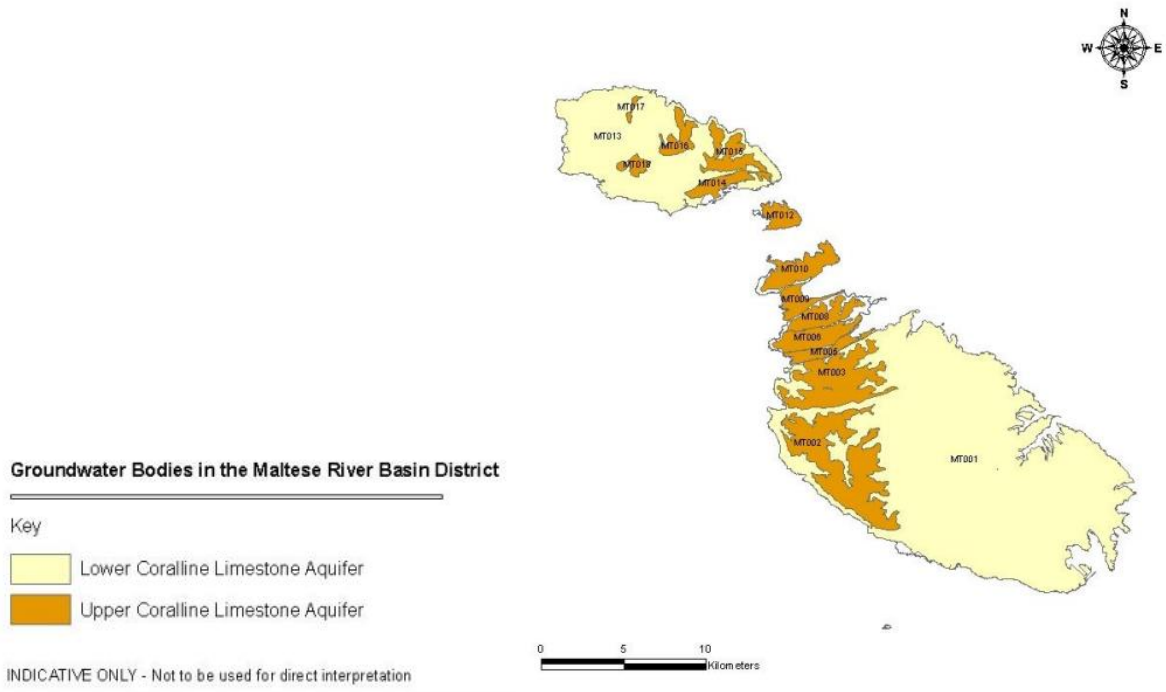

Figure 1.2: Groundwater Bodies as Designated under the Water Framework Directive (ERA, 2018)

1.2 History of Water Resource Management

Malta, positioned in a geographical location prone to water scarcity, has earned its reputation as one of the driest countries on Earth. The challenge of limited water resources has not only influenced the course of its history but has also left some form of an impact on its built and natural landscapes. Despite the many problems the country faces, once common sustainable practices of rainwater management have now long been brushed aside for more unsustainable sources of water (Ministry for Public Works and Planning, 2022), leaving historical stormwater infrastructure to be paved over by main roads and forgotten, or left to deteriorate and act simply as a monument of a distant ”archaic” past.

Within the last few centuries, a high number of dams and groundwater galleries were constructed throughout Maltese valleys. In the 1890s, a British engineer, Mr Osbert Chadwick, designed a series of dams in Wied il-Qlejgħa, now known as *Chadwick Lakes* (Borg, 2018). The purpose of these structures was to provide fresh water to farmers to irrigate their fields with. One of these structures can be seen in Figure 1.3. The surrounding area would also provide a secure habitat for flora and fauna.

In the 20th century, the construction of many more dams across Malta were ordered, which provided water for not only agricultural purposes, but also aided in groundwater recharge. In addition to this, dams were also constructed with the aim of reducing flooding in urbanized downstream areas. This especially became a widespread problem in the latter half of the century, which saw major soil-sealing practices and rapid urban development spilling into once-permeable valley watercourses (EWA & ERA, 2020).

Figure 1.3: Chadwick Lakes - Dam (RBMPLife, 2018)

In the 1970s, several soakaways were implemented, located next to arterial roads and the national airport, with the aim of reducing runoff and flooding along these routes (Ministry for Public Works and Planning, 2022). Such locations include Ħaż-Żebbuġ, Msida, Gudja, and Birżebbuġa's Ħas-Saptan region.

The effectiveness of a soakaway would depend largely on the type of ground material present, whereas a fractured and porous limestone would allow for quicker infiltration, without leaving stagnant semi-permanent water bodies. Some of the previously listed soakaways, however, fail to drain quickly and have resulted in the creation of new habitats around the semi-permanent pools (see Figure 1.4).

Figure 1.4: Ħaż-Żebbuġ Soakaway (2023)

For decades, the Maltese have been relying on groundwater pumping to source their potable and non-potable uses. However, with a growing population, it was recognised that groundwater quality was and still is deteriorating due to over abstraction and its consequence of an increased level of salinity due to sea-water intrusion (Abela, 2019). Thus, the 1980s saw the advent of desalination as an alternative source of water. As of 2023, Malta has four desalination plants producing up to two-thirds of potable water, with the remaining third being from the groundwater aquifers (Water Services Corporation, 2023).

However, the over-reliance of desalination has arguably given the population a false sense of security. The rapid urban sprawl coupled by a lack of proper enforcement led to building development either not having a well or else having a well which is not used. This has resulted in increased flooding in downstream urban areas, and high runoff velocities.

In 2015, the *National Flood Relief Project* (NFRP) was completed, which involved the digging of tunnels and the construction of new stormwater culverts to curb the growing problem of flooding in certain localities. As seen in Figure 1.5 and Figure 1.6, tunnels were dug with the intention of draining the localities of Attard, Birkirkara, and Msida amongst others (European

Commission, 2019). One of the main foci of the project was to alleviate the flash flooding which occurred in urbanized valleys such as in Qormi, Birkirkara, and Msida.

It is ironic that in a water-scarce country, Malta has sought to invest considerably in the project with the sole aim in collecting stormwater and discharging it to the sea as quickly as possible rather than investing in green infrastructure which manages and harvests rainwater at source. Instead, the soil-sealing practices and the reliance of grey infrastructure in urban developments have resulted in extreme volumes of runoff which end up flowing out to sea. In turn, groundwater recharge is significantly reduced, and the re-harvesting of potable water back from the sea is required through energy-intensive desalination.

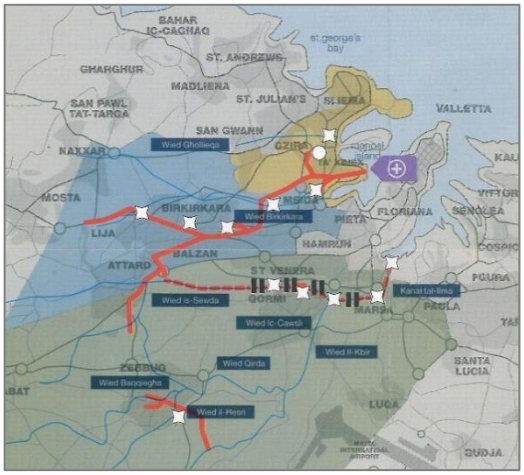

Figure 1.5: NFRP Leaflet Map of Project (The Ministry for Resources and Rural Affairs, n.d.)

Figure 1.6: NFRP Tunnel (Floodlist, 2014)

Despite the project's heavy focus on hastening the transportation of runoff to the sea, the NFRP also included a soakaway reservoir in Gżira which allows for the storing of valley runoff and groundwater aquifer recharge. This reservoir can hold up to 10,000 cubic metres of rainwater (Times of Malta, 2012). In this instance, the focus was not necessarily only to enhance groundwater infiltration, but to also prevent further flooding within Gżira.

This practice of the quick removal of water applies not only to public spaces and urbanized valleys but also within the individual buildings, where rainwater harvesting techniques are far from a usual sight. According to Malta's regulation office's *Technical Guidance Document F*, it is a requirement for every new building to have an underground rainwater cistern sized according to roof area and for this to be used for non-potable uses (Malta Ministry for Resources and Infrastructure Services Division Building, Regulations Office, 2006). Due to lack of enforcement, often enough, cisterns are either undersized, omitted or not connected to second class water supplies thus overflowing into the street and contributing to flooding of downstream locations.

There have been significant opposition to any proposals within natural valleys over the past few decades, and new dam proposals are no longer made because of claims of significant environmental damage caused by prior dam projects from the 20th century. The environmental authorities are currently concentrating on maintaining and renovating existing dam structures to ensure as little disruption as possible to the currently existing nature which has developed.

1.3 Water Resource Strategies

Currently, the water resources in Malta and Gozo are managed according to the EU Water Framework Directive, which has developed into requirements which every EU member state must develop and adapt towards to safeguard water quality and quantity, and natural ecosystems (Caruana, T. M., 2017). The directive has brought about the *LIFE Integrated Projects* and the *River Basin Management Plans* which ensure compliance by EU member states to the environmental and water management goals.

The LIFE Integrated Project (LIFE IP)

The LIFE Integrated Project is an EU-funded initiative which supports the execution of regional, multi-regional, or national environmental and climate plans, programs, and strategies. The project helps Malta in particular with the preparation and implementation of the *River Basin Management Plans* (RBMP), also known as the *Water Catchment Management Plans (WCMP)*.

The LIFE IP in Malta, spanning from 2018 to 2025, is led by the Energy & Water Agency (EWA). The project has engaged multiple stakeholders to collaborate and accomplish the environmental goals outlined by the EU Water Framework Directive.

INVESTMENT IN LIFE PROJECTS IN MALTA (€ million)

	TOTAL INVESTMENT	EU CONTRIBUTION
ALL LIFE projects	39	23.2
Nature & Biodiversity	13.3	17.2
Circular Economy & Quality of Life	21.4	13.4
Climate Change Mitigation & Adaptation	0	0
Others - NGOs, Preparatory, Technical Assistance	4	2.5
Clean Energy Transition	0.2	0.1

Figure 1.7: Life IP Investment in Malta (EU CINEA, 2022)

Malta's River Basin Management Plan (RBMP)

Keeping in line with the EU Water Framework Directive, it is required that Malta prepares and conforms to a water catchment management strategic plan focused on managing the water environment at a river basin or water catchment district level. This plan would address flooding, groundwater pollution, water conservation, and ecosystem preservation.

As of March 2024, ERA has finalized the *3rd Water Catchment Management Plan*, which covers the next five years and is specifically supported through the LIFE IP Project (ERA (Environment and Resources Authority), 2022).

The project is commonly referred to within the EU as the *River Basin Management Plan (RBMP)*, however due to the size of Malta and the lack of permanent rivers, it is locally known as the *Water Catchment Management Plan (WCMP)* and addresses the entire country's main catchment and sub-catchment areas as well as each groundwater aquifer's status.

Table 8: *Classification of Risk to Good Groundwater Status*

GWB-Code	GWB-Name	Risk due to Chemical Contamination	Risk due to Sea Water Intrusion	At Risk Objectives			
				Quantitative Status	Qualitative Status	Use (Drinking Water)	Associated SW Bodies
MT001	Malta Mean Sea Level	X	X	X	X	X	
MT002	Rabat-Dingli Perched	X			X		X
MT003	Mgarr-Wardija Perched	X			X	X	
MT005	Pwales Coastal	X	X		X		
MT006	Mizieb Mean Sea Level		X	X	X	X	
MT008	Mellieha Perched	X			X		
MT009	Mellieha Coastal	X	X		X		
MT010	Marfa Coastal	X	X		X		
MT012	Comino Mean Sea Level	X			X		
MT013	Gozo Mean Sea Level	X	X	X	X	X	
MT014	Ghajnsielem Perched	X			X	X	
MT015	Nadur Perched	X			X		
MT016	Xaghra Perched	X			X		
MT017	Zebbug Perched	X			X		
MT018	Victoria-Kercem Perched	X			X		X

Figure 1.8: Groundwater Classification Table according to 3rd RBMP (ERA, 2024)

1.4 Statement of Intent

The aim of this dissertation is to highlight the ability to maximise the groundwater recharge potential in Malta using Managed Aquifer Recharge (MAR) methods, giving due attention to general feasibility, effectiveness, and other practical considerations.

The mean sea level aquifer in Malta demonstrates high abstraction rates beyond estimated recharge volumes and above their sustainable yield, and hence, natural watercourses and other collection points situated above globigerina or coralline limestone may be used to enhance aquifer recharge and promote climate-resilience by slowing down, collecting and infiltrating rain runoff.

In summary, the objectives of this dissertation are the following:

- To analyse Malta's past and present water management practices, in terms of stormwater management, groundwater security and flood prevention.
- To present viable forms of MAR in catchment areas as a means of aquifer recharge of the mean sea-level aquifer.
- To derive a method of efficiently designing infiltration boreholes in Maltese limestone.
- To propose a model with which aquifer recharge projects can be analysed and prioritised on their potential recharge volume.

1.5 Research Questions

Can Maltese watercourses be used to effectively capture large volumes of stormwater runoff, and to accelerate safe and efficient groundwater aquifer recharge?

Are existing methods of Managed Aquifer Recharge applicable to the Maltese context?

Can water permeability rates in Maltese rock strata be reliably estimated through analysis and modelling of its pores and fractures?

Can complex ground conditions be modelled to derive the most effective method of enhancing groundwater recharge?

Can the obtained and analysed data be used to create and implement a national strategy for water conservation in Malta?

1.6 Dissertation Structure

Chapter 2 is divided into two sections: the first offers a general overview of MAR systems both locally and internationally, while the second introduces the theory related to rock permeability and rock quality.

Chapter 3 delves into the theoretical framework and equations used to develop a ground permeability model tailored for dry wells in MAR, and also details the required water permeability tests and their procedures.

Chapter 4 describes the step-by-step creation of the parametric model using *Microsoft Excel*.

Chapter 5 provides a final analysis and discussion, where a model sensitivity analysis is presented to illustrate the model's practical application and expected results. This chapter would also present the results from the conducted on-site water permeability tests.

Chapter 6 discusses the success or otherwise of the predictive model, highlighting key conclusions and limitations. This chapter also evaluates the parametric model's effectiveness and potential integration into a broader national water conservation strategy.

2 LITERATURE REVIEW

2.1 MANAGED AQUIFER RECHARGE (MAR)

Managed Aquifer Recharge is the purposeful engineered recharge of groundwater through surface infiltration or deep injection methods for water conservation and subsequent recovery or for environmental benefit (National Ground Water Association, 2022). MAR often provides one of the cheapest guarantees of water security and supply for towns and small communities (Dillon, 2005).

Due to the Maltese islands' population's reliance on groundwater and the current over-abstraction crisis seen in the MSL aquifer, MAR has significant potential for widespread adoption on a national scale.

2.1.1 MAR Systems

Recharge Dams

A 'recharge dam' is a structure built into a watercourse with the main goal of storing storm runoff for controlled groundwater surface recharge. They can either be designed as impermeable retaining dams, or permeable detention dams. Recharge dams can be especially effective in arid regions with no permanent rivers, where runoff can be held in one location long enough for ground infiltration to take place (Jaafar, 2014).

There are several factors which dictate the design and placement of a dam within a watercourse some of which are the physiography, geology, hydrology, sediment load, and infiltration capacity. The geology of the area must have sufficient permeability to allow for an acceptable recharge rate. The water storage volume, retention time, and the controlled downflow must all be matched to the catchment inflow to prevent flooding or unintended over-spilling (Standen, Kathleen et al., 2020).

When considering Maltese geology, the upper and lower coralline limestone is suitable for water infiltration due to the very porous and karstic nature of the rock. The globigerina limestone is less permeable, relying mainly on cracks and fractures for groundwater infiltration. This sub-layer is generally more suitable for temporary water storage and allows for semi-permanent ponding.

Types of Recharge Dams

Retaining Dams -- A retaining-type dam is designed to act as a reservoir along a watercourse. As seen in Figure 2.1, these dams serve to hold back water and raise the water level, generally acting as permanent pools of water with losses only occurring due to evaporation and infiltration. May be designed with a spillway or as a weir for overspilling.

Weirs -- A 'weir' or 'check dam' is a low dam often found in rivers and watercourses which are designed for overspilling and help raise water level, control flooding, and slow the rate of flow (Fowler, 2015). Such dams are usually designed specifically as a buffer for high rainfall periods, protecting any downstream settlements.

When considering the Maltese valley's wet and dry periods, the weir would initially retain all runoff, until the water level reaches the crest and overspills, with further runoff flowing downstream. When runoff ceases, the weir once again acts as a retaining-type dam.

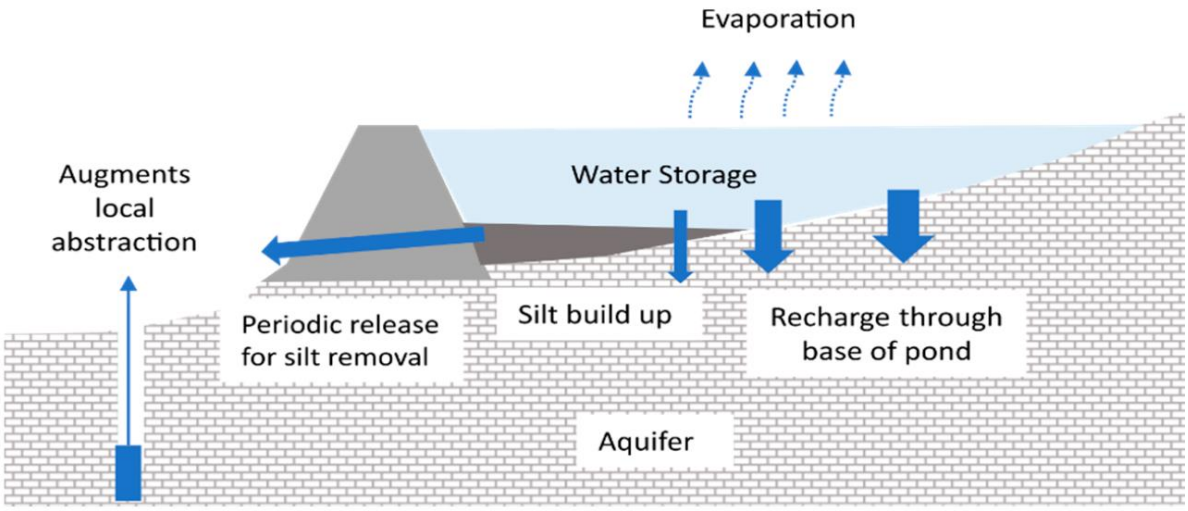

Figure 2.1: Retaining Recharge Dam (Standen et al., 2020)

Detention Dams -- A detention-type dam is designed for the temporary storage of stormwater along watercourses and for the controlled discharge of that floodwater downstream. A backwater effect would be created behind the dam, storing water for a period before it fully drains at a rate appropriate for the conditions. Permeable dams with continuous flow can avoid environmental risks to downstream habitats by ensuring a steady and slow stream of water, minimizing changes to the natural flow in the valley (Caruana, T. M., 2017).

Leaky Dams, a type of detention dam commonly seen in the UK, utilize natural materials to trap silt and debris in streams, reducing soil erosion and controlling water flow. Mimicking natural tree and branch obstructions, these dams serve as partial blockades with minimal ecological impact (Caruana, T. M., 2017).

Embankment Dams -- Recharge dams, made of engineered or natural materials, are constructed to retain water. Typically built with compacted soil and rock, the core of the dam is densely packed to prevent seepage that could erode it (ARGO-E GROUP, 2011). In Malta, earth-filled dams covered with limestone blocks are common, such as in Wied is-Sewda or the Santa Katarina watercourse. These dams prevent flooding, improve water retention, and provide vehicular access across the watercourses. Regular maintenance is required to prevent sediment and organic matter buildup. Such dams must be designed to resist the erosion effects of water seepage, thus causing rapid failure of the dam.

Environmental Impacts of Dams

Valleys in Malta support diverse ecosystems that can be significantly impacted by dam construction. Changing sedimentary and hydrological flows can harm existing habitats and species, necessitating environmental impact assessments. Each valley requires a tailored approach to balance benefits and impacts. (Mifsud & Bonello, 2010).

Dam construction can disrupt habitats by raising upstream water levels and stopping downstream flow. Permeable leaky dams with low water levels are recommended to mitigate these effects. Storm runoff, carrying soil and nutrients, naturally cleans valleys and supports vegetation. Impermeable barriers, however, block sediment transport, reducing reservoir storage and necessitating regular cleaning (Glen Canyon Institute, 2018).

Regular cleaning and renovation of valley structures are crucial to minimize ecological disturbance. While larger dams face sediment accumulation issues, smaller local dams typically avoid these risks. Sediment build-up can clog outlets, reducing discharge and risking overflow (Schellenberg et al., 2017), making regular maintenance essential.

Renovating and optimizing existing structures are considered the least risky and most beneficial interventions. Many old dams have altered valley hydrology and require adaptation. Due to neglect and siltation, many structures are now ineffective.

Case Studies of Recharge Dams

Recharge dams are not very common in mainland Europe. European countries normally have easily accessible fresh water in the forms of streams and lakes, and hence, it would be an unnecessary expense to construct dams specifically for the purpose of recharging the groundwater aquifers. Engineered recharge dams and artificial ponds are more likely to be found in hotter mediterranean countries where there is a serious risk of droughts.

A large number of embankment dams and weirs may already be found along most natural valleys within the Maltese islands. Wied is-Sewda features a series of embankment dams which assist with flood control, groundwater recharge, and private access to fields. A weir is also found nearing the end of the watercourse (See Figure 2.2) before transitioning into an urban canal which discharges in Marsa, forming part of the NFRP network.

Figure 2.2: Wied is-Sewda Weir Dam (DOI Malta, 2021)

Portugal is a southern European country which experiences water scarcity and an over-reliance on surface water bodies/streams. This has led to serious risks of major cities completely running out of water during long periods of drought (Standen, Kath et al., 2023). It is common for such countries, which normally have steady streams in the wetter months, to construct dams to block the watercourses and consume water from the surface-reservoir, without much thought on the extraction of groundwater. However, this subterranean source of water should not be ignored, as the volume of groundwater at aquifers normally far exceed any constructed dam or basin capacity.

One would find many recharge dams in India to sustain irrigation water availability from groundwater. In fact, more than 200,000 recharge dams have been constructed in India (Standen, Kathleen et al., 2020). Some of these dams would be constructed out of earthen fill, usually in more rural areas, and may have a capacity of almost one million gallons of water (Arora, 2016). An obvious positive for the chosen material would be how cost-effective it is and yet can help sustain water security for thousands of lives.

Lastly, one may look at Israel for a comparative study in preserving water resources in arid climates of little rainfall. The ‘Liman’ irrigation system is often used in the water-scarce regions

of Israel. This system makes use of earthen dam structures and basins to collect rainwater within desert wadi (valley) watercourses.

Small fruit tree groves and crops would receive freshwater from the resulting oasis, where surface runoff would soak into the ground and persist throughout the drier, hotter months (Keren Kayemeth LeIsrael-Jewish National Fund, 2022).

Infiltration Basins

An infiltration basin is a method of managed aquifer recharge which makes use of surface-spreading, to maximise the infiltration surface area. A water-collecting basin can be formed from the construction of dikes and dams, or from a natural or excavated depression which collects diverted runoff (INOWAS & TU Dresden, 2018). They are typically designed with permeable soil or engineered media that allow stormwater to easily infiltrate into the ground. Basins may also serve a secondary purpose of protecting against flooding, acting as an urban soakaway. As such, infiltration basins are often incorporated in urban areas as green infrastructure which helps mimic natural hydrological processes (Ministry for Public Works and Planning, 2022). However, such an implementation normally requires large flat areas, highly permeable ground materials or natural rivers to achieve efficient recharge rates.

Malta does not have the available space for wide surface-spreading infiltration, and hence, more concentrated watercourse infiltration may be required. Locally, deep quarries in fractured rock may act as an infiltration basin or soakaway.

Environmental Impacts of Basins

Infiltration basins will require a large area which will ultimately end up flooded, potentially damaging existing ecosystems. In addition to this, infiltration basins are normally not suitable for locations of industrial activity, where pollutants may collect and sit within the basin and end up infiltrating and contaminating groundwater aquifers (susDrain, 2023). Nonetheless, with sufficient depth between the surface and the aquifer, the ground material and the vegetation found within the basin can help further filter pollutants from already suitably clean rain runoff.

Case Studies of Basins

Groundwater recharge is important in California, U.S. This state is particularly susceptible to prolonged dry weather and sudden intense storms. In fact, it is well known that California has a Mediterranean climate, similar to what Malta experiences. Therefore, there have been projects which divert a percentage of river runoff from the primary stream and collect the separated runoff in above-ground infiltration basins. As seen in Figure 2.3, these basins would gradually replenish the groundwater aquifer, benefiting the residents and the agricultural sector (California Department of Water Resources, 2023). Even though the creation of wide recharging basins outside of quarry soakaways is not applicable to the Maltese context, water volume and infiltration calculations may still be investigated.

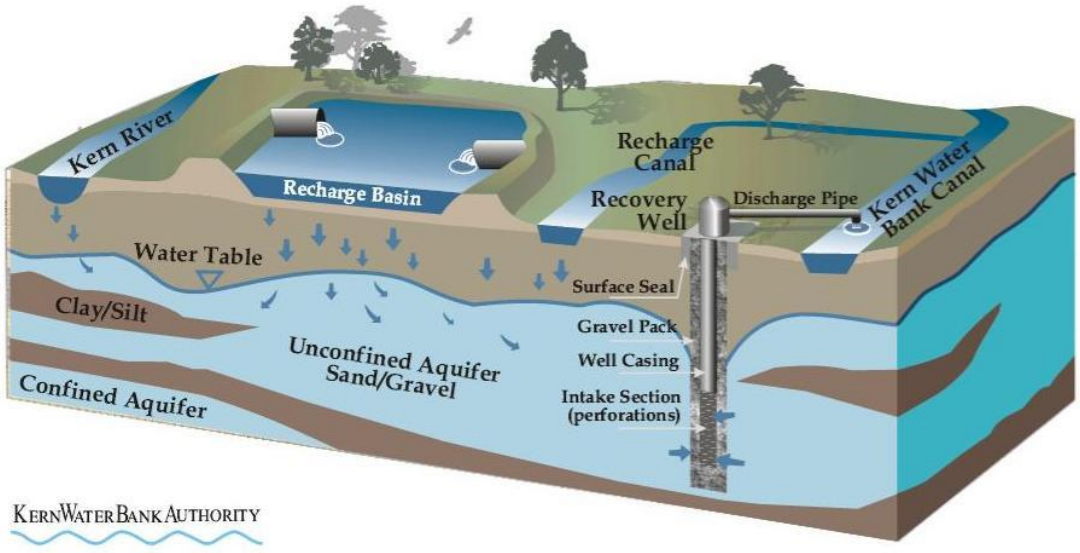

Figure 2.3: California's Groundwater Management System (Kern Water Bank Authority, 2021)

Infiltration Dry Wells

Infiltration wells, also known as dry wells, allow for deep injection of water back into the ground by means of a pit, shaft, or borehole. Injection can be done through gravity flow or by artificial pumping. Through this method of managed aquifer recharge, one would be able to dramatically improve the rate of recharge by bypassing large depths of rock strata, thus reducing the travel time for surface water to recharge the groundwater aquifers.

The pit or borehole would be filled with varying grades of packed gravel, sand, and sometimes geotextile mesh to effectively filter the collected water and enhance aquifer recharge.

Types of Dry Wells

Pit Dry Wells -- A pit dry well allows for recharge of shallow aquifers, where the rock strata itself may be too impermeable for regular surface-spreading MAR (Gale, 2005). This type of infiltration well is the simplest form and can function as a soakaway if it is sufficiently large. These wells are typically shallow, and if a structure is required, they are constructed using precast cylindrical walls or a plastic tank placed within a hand-dug hole in the soil.

A dry well can be open pit or covered. Open pit wells receive runoff water directly from above, whilst closed pit wells would be fed directly from a source pipe and often include a buffer chamber through which runoff is initially filtered or settled.

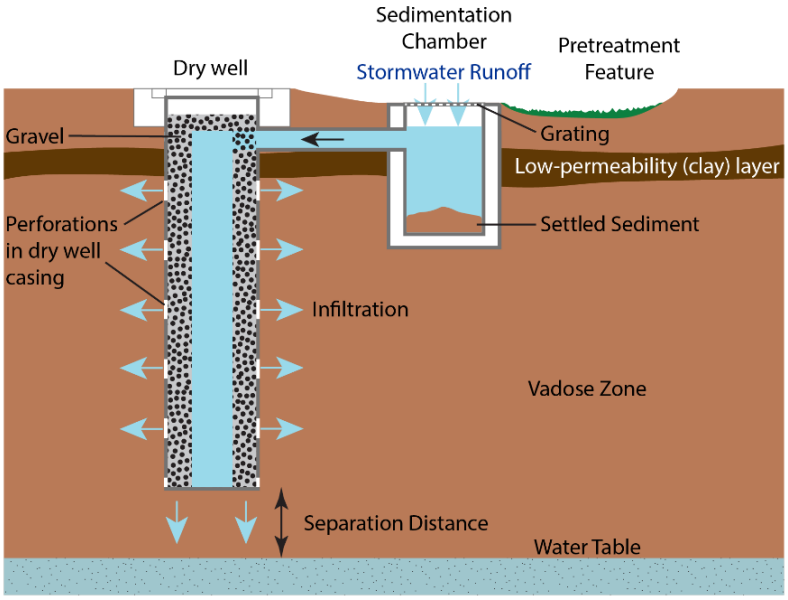

Figure 2.4: Typical USA dry well design with pretreatment features (Edwards & Mandler, 2017)

Borehole Dry Wells -- Drilled boreholes allow for the injection of water past semi-to-fully impermeable rock strata and into deep aquifers. The design of such a borehole requires careful engineering considerations, as well as the filter medium found within. This type of MAR is advantageous in land-scarce areas, where a collection of infiltration boreholes may be drilled at proximity to each other (Gale, 2005). Drilled boreholes also allow for Aquifer-Storage-Recovery (ASR), where water can be stored or pumped out according to demand from the same wells (Bouwer, H. et al., 1990). However, it is generally recommended to have Aquifer-Storage-Transfer-Recovery (ASTR), where recovery boreholes are at a distance from the injection boreholes, such as what is seen in Figure 2.5. This method would make use of the water-treatment capacity of the aquifer and the material it is found in (Gale, 2005).

Considering the space available within Malta and the potential requirement to be as unobtrusive as possible to the existing natural environment, the only available choice of well

to enhance recharge would be to opt for drilled boreholes, and not pits. In addition, the focus of the proposal is to enhance recharge rates and hence only boreholes for water injection are considered and not for recovery.

Infiltration boreholes can be dug in groups within dam reservoirs, with a designed depth for enhanced groundwater recharge. Sufficient depth between the freshwater lens and the infiltration boreholes may be required to ensure enough water-purification takes place as water seeps through the rock material before it reaches the aquifer. This consideration is especially important in areas within the groundwater protection zone, where abstraction sources and underground galleries are found. The filter medium within the borehole should also be engineered to sufficiently filter the storm runoff.

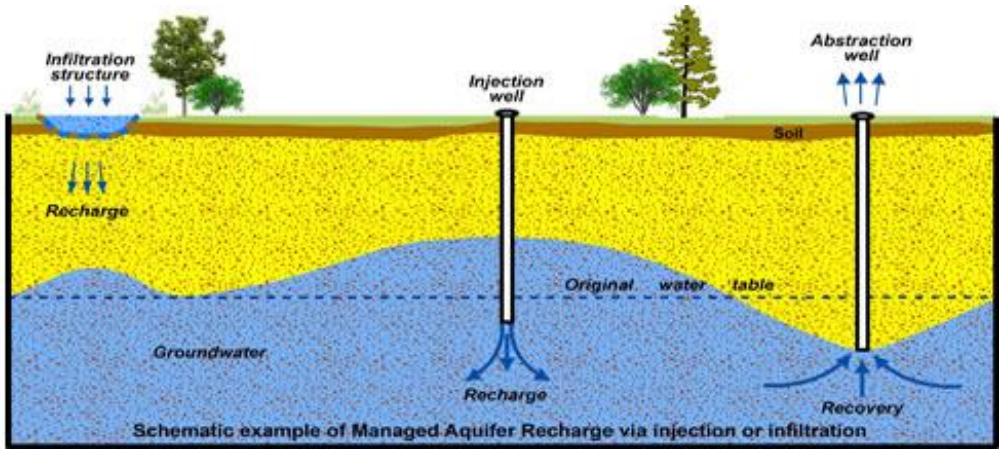

Figure 2.5: Managed Aquifer Recharge (Green Suffolk, 2021)

Environmental Impacts of Dry Wells

Infiltration boreholes are effective MAR methods and generally more environmentally friendly than basins or dams which would require the flooding of surfaces. In addition to this, evaporation losses are a minimum when there is no reliance of surface-spreading. Boreholes would generally require much less space, and groups can be confined to small, concentrated areas. Despite this, the effectiveness of infiltration boreholes is enhanced when they are paired with other forms of MAR, such as with soakaways and basins. After all, the boreholes require a pool of water at surface or a constant runoff stream from which transfer can occur.

When infiltration boreholes are paired with dammed basins, one can expect an increased water infiltration rate from the stormwater that gravitates to these areas. However, it is extremely important that the borehole and the material in it be carefully designed.

The natural ground material usually acts as an effective filter at great depths and ensures safe water quality standards. However, the artificial bypass may cause the aquifer to become more susceptible to contamination. Therefore, adequate protective measures and filter media

should be selected when implementing a recharge well. This would also be necessary to prevent sediment and soil from clogging the fill material, rendering the borehole ineffective.

Borehole clogging may be due to an accumulation of inorganic and organic solids, silt particles and microorganism cells (Bouwer, Herman, 2002). As with infiltration basins, recharge wells may not be suitable next to industrial areas of high contamination risk. This may also be of risk in agricultural areas where pesticides and fertilizers can pollute the water table (Bexfield et al., 2021). Nonetheless, this is mainly a regulatory issue which should be addressed by the relevant authorities.

Case Studies of Dry Wells

Spain has several managed aquifer recharge systems. Since the late 20th century, engineered recharging wells have been constructed across the country. In the 80s, infiltration wells in Daimiel National Park were constructed (Fernández-Escalante, 2018). These wells help mitigate the serious impact caused by drought on the wetlands and the over-exploitation of the groundwater aquifer in the area by irrigation, thus ensuring climate resiliency and futureproofing.

In India, extensive implementations of reverse boreholes are currently being done in areas where the deep groundwater has been overexploited. A series of injection boreholes wells can be found along the Narwana branch canal in India which directly recharge a confined aquifer (Kaledhonkar et al., 2003). It has been estimated that the water recharges at a rate of 7.2m^3 per day per borehole. Such an amount of water can accumulate and recharge the aquifers quite substantially when many of them are strategically placed.

Figure 2.6: Borehole wells at MDH soakaway under test (Ministry for Public Works and Planning, 2022)

Infiltration boreholes can also be paired with soakaways. Using Mater Dei Hospital's soakaway as a case study (Figure 2.6), this system is space and cost efficient and has been observed to drain completely from full within 24 hours, effectively managing the runoff generated from an area of 140,275m^2 (Ministry for Public Works and Planning, 2022). The borehole casings protrude 30cm from the pit floor level, preventing sediments from clogging the boreholes.

2.1.2 Managed Aquifer Recharge in Malta

The 2nd RBMP's development process has demonstrated the considerable obstacles Malta must overcome to meet the EU Water Framework Directive's good status objectives. These difficulties result from a variety of specific social, environmental, and economic problems unique to a Mediterranean small island state with a high population, such as: Water Scarcity and Drought Conditions, High Population Density, Saline Intrusion and Pollutant Contamination (EWA et al., 2020).

There are several LIFE IP Project measures which Malta is working to uptake to improve the status of our water resources. One of which would be the implementation of various MAR methods. The first step in widespread MAR adoption would be to trial the concept in a number of locations, ideally with vulnerable groundwater resources, and monitor the results.

The Pwales MAR Project

As of writing this dissertation, the Pwales coastal aquifer, which is situated in the north of Malta, is aimed to be purposefully recharged as a pilot project of an ongoing MAR scheme co-funded by the EU under the RBMP project '*LIFE 16 IPE MT 008*' (RBMP LIFE, 2023). Due to its high salinity and nitrate concentration, the Pwales aquifer has a low-quality rating and cannot be used for most irrigation needs (WSC & EWA, 2020).

The investigation of the region's hydro-geological features was the first phase in the MAR programme. The design and implementation of the MAR system come next. Monitoring the water quality and level both before and after the MAR plan is implemented is a crucial part of the project. A nearby water-reclaiming plant normally supplies irrigation water to the nearby fields. However, when there is little demand for this water, recharge will be carried out as the ultra-filtrated reclaimed water will be injected into the ground, driving the salinity of the coastal aquifer down.

The GEO-INF Project

GEO-INF, a rainwater recovery project that was carried out in 2012-13 by *Ing*. Marco Cremona of *Sustech Consulting*, focused on the installation of rainwater injection boreholes in various schools around Malta. The purpose of this project was to monitor the performance and feasibility of reverse boreholes in the adoption of compact infiltration systems as a means of rooftop water conservation and runoff reduction (Ministry for Public Works and Planning, 2022).

The impact of GEO-INF was recorded as substantial, with each installation contributing to the recovery of approximately 100,000 litres of water annually and ensures that more rainwater is conserved and reaches the groundwater aquifers (Atlas Insurance, 2023).

Figure 2.7: GEO-INF Installation (N. Borg, 2012)

2.1.3 Environmental Considerations

Runoff Pollutants

Managed aquifer recharge raises important environmental considerations, particularly concerning the potential impact of runoff pollutants on the underlying aquifer. As stormwater lands and travels on impervious urban surfaces, it carries with it a variety of pollutants such as heavy metals, hydrocarbons, pathogens, and suspended solids (Pitt et al., 1999). These contaminants can pose a threat to the quality of the receiving aquifer, potentially leading to serious groundwater contamination. This risk is elevated especially after long dry periods,

where the 'first flush phenomenon' may deposit a rapid increased level of contaminants to the valleys, and hence, higher levels of treatment would be required (Caruana, M., 2009).

Careful assessment and management of infiltration well systems are therefore essential to mitigate the risk of introducing harmful substances into the aquifer. Environmental authorities consider this factor to be one of the most important considerations which often prevents artificial recharge projects from taking place. However, intense vegetation in natural valleys may mitigate this issue as the flora filters the runoff pollutants.

Water Abstraction Galleries

Malta's abstraction galleries were dug in areas of high groundwater recharge and abstraction potential, and thus, can be commonly found be beneath some of Malta's largest natural valley systems. These sea-level subterranean structures form integral components of groundwater management in regions like Malta, but also present unique environmental considerations in relation to pollutant transport and extraction.

As mentioned previously, runoff pollutants pose a significant threat to the quality of groundwater in an area. Abstraction tunnels, whilst initially meant to spread the abstraction and prevent saline up-coning, may inadvertently become conduits for the migration of pollutants, potentially compromising the quality of the water. Managed aquifer recharge locations and depths must be considered carefully to minimize the risk of permanently contaminating groundwater which is extracted for the national water network.

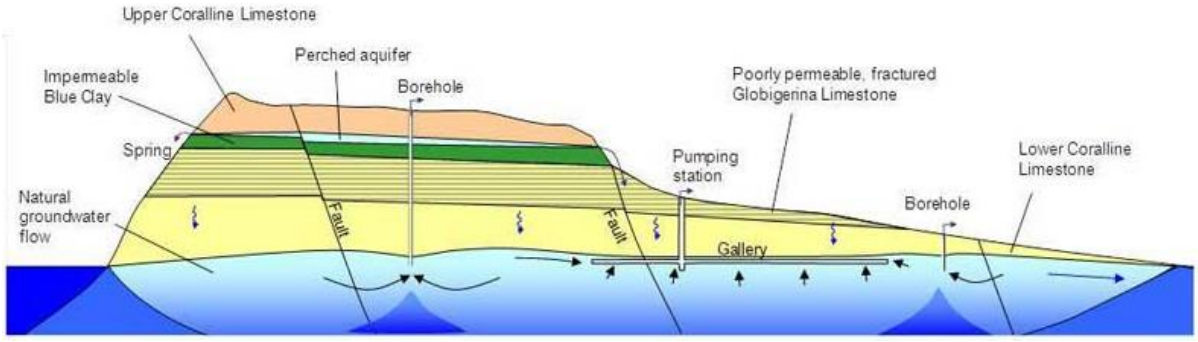

Figure 2.8: Schematic cross section of Malta with aquifers (British Geological Survey, 2024)

Groundwater Safeguard Zones

The Groundwater Safeguard Zones comprise of a network of protection buffer zones designed to protect and conserve the groundwater bodies across the Maltese islands for purposes of abstraction and consumption (EWA & ERA, 2024). These zones implement additional land use, development, and discharge control measures to prevent pollutants from entering the water bodies.

Safeguard zones are specifically positioned around underground abstraction galleries and abstraction pumps and the water quality is actively monitored. These zones are defined and highlighted in the 2nd and 3rd *River Basin Management Plans* for Malta among other defined environmental protective areas.

Nonetheless, the entire country's water resources remain susceptible to widespread pollution. Malta's accession to the EU in 2004 introduced stringent regulations, particularly targeting the agricultural sector due to the risk of nitrate pollution in groundwater bodies, leading to a nation-wide EU classification of being a "Nitrate Vulnerable Zone" (ERA (Environment and Resources Authority), 2020).

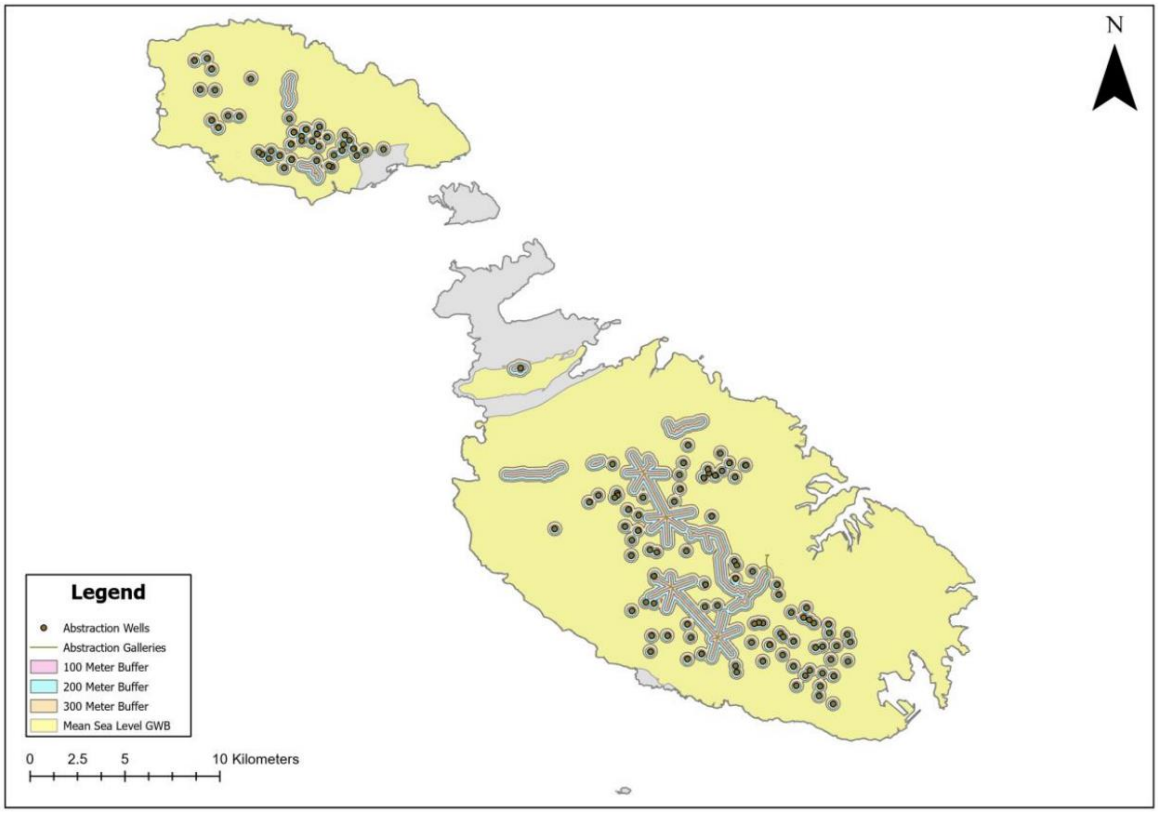

Figure 2.9: Groundwater Safeguard Zones (EWA & ERA, 2024)

Environmental Flow

The environmental flows (e-flows) in relation to river or valley systems are described as the minimum or recommended flow necessary to support the ecological health of the environment.

In the past, early methods like the Montana method focused on maintaining minimum flow levels to protect aquatic life. This method, which would rely on the average daily discharge or the mean annual flow, would provide minimum percentages of total water flow which should be retained after any interventions which may otherwise impede the flow of the river

(Tennant, 1976). However, these methods can be considered as low-confidence and may not consider flow fluctuations or any other effects. To overcome these shortcomings, more holistic approaches such as the Range of Variability Approach (RVA) have been developed.

The RVA (Richter et al., 1996) characterizes hydrological indicators, including flow variability and non-flow events, to better mimic natural flow regimes and preserve river ecosystems. This method is particularly suitable for temporary waterways, where flow intermittency plays a crucial role (D'Ambrosio et al., 2017).

Similar approaches offer a deeper comprehension of the variability of water flow, allowing for the creation of flow patterns that are environmentally friendly. Factors to consider include anticipating low-water periods, preserving the shape of rivers, and supporting the life cycles of indigenous species, all of which improve the accuracy of evaluations of environmental flows in rivers that sometimes run dry.

One of the best methods in finding balance in the environmental flow would be to conduct an extensive habitat and flow simulation, however this is out of scope for this dissertation and would require extensive research to simulate the many variables within the many local valley systems.

2.2 HYDROGEOLOGICAL CONSIDERATIONS

2.2.1 Water Loss Classification

When rainfall reaches the ground, it undergoes various forms of loss, which flood hydrologists categorize into four types:

1. Interception by vegetation; Occurs where plants absorb or slow down runoff.
2. Evaporation from the ground surface; Occurs naturally during rainfall into the atmosphere.
3. Depression storage along the ground surface; Depressions and holes which act like small reservoirs and only release water when their capacity is exceeded.
4. Infiltration into the soil, rock, or a combination of both; Depends on porosity and fracture-level of the ground.

(U.S. Dept. of the Interior, Bureau of Reclamation, 1987)

Normally, under high rain runoff conditions, the first three losses may be quite minimal. Nonetheless, all these factors must be considered when deciding on the type of storage and recharge interventions. Rain runoff will generally have many losses in catchments of a high prevalence of permeable agricultural land and little urbanized area. This information is important for modelling a catchment and deriving the volume of water entering a valley which is able to be captured by dams and infiltration boreholes.

Everything said, it is very difficult to accurately measure specific values of volume loss, or what percentage of the catchment area is contributing to rain runoff. Due to the many variables of the ground and the catchment area, one can only estimate a percentage, ideally by considering the worst-case scenario. In addition, losses do not occur linearly. Initial rainfall is seen to be absorbed much quicker in dry conditions than in already-saturated conditions due to a higher matric potential gradient (Lili et al., 2008).

However, yet another hidden factor would be how long the ground has been dried for. Drought conditions may in fact make flooding much worse, due to the shrinking of the soil structure and the development hydrophobicity, and hence, a reduction in infiltration (Katwala, 2022).

2.2.2 Local Rock Strata

In the local context, the three primary rock types which affect water infiltration are the following: Coralline Limestone (CL), Globigerina Limestone (GL), and Blue Clay (BC). Of course, the clay layer acts as an impermeable layer upon which the perched aquifers can be found. The limestone layers, however, each have varying degrees of permeability. The upper and lower coralline limestone in of itself has a fairly permeable rock mass, with many voids present throughout. The globigerina limestone, in particular the lower globigerina sub-layer, is considered as an aquitard and is significantly less permeable (Bakalowicz & Mangion, 2003). This strata mainly transmits water through rock discontinuities (See Figure 2.10).

The ideal site for groundwater recharge would be one with very fractured and porous rock strata. In addition to this, if one were fortunate enough to locate a phreatic tube or cave under the surface, this would bring about such high permeability rates only limited by the size and transmissivity of the borehole itself.

Another note of importance for groundwater recharge is the available rock depth within which water can seep through. Sites already found close to sea-level, and hence, close to the MSL aquifer, may already be too saturated and too low of a potential gradient to enhance recharge. One also must not forget the water quality risks associated with injecting directly into the aquifer.

It is a given that a site within the blue clay layer will do little to enhance groundwater recharge and will only serve to retain water. In such a case, the only solutions would be to dig infiltration wells which serve to recharge the perched aquifer, or to bore through the deep clay layer entirely.

Figure 2.10: Fissures as seen in locally excavated sites (Newspoint UM, 2023)

2.2.3 Ground Permeability Variations

Permeability rates for managed aquifer recharge systems can vary depending on the following:

1. The primary permeability of the rock layers (lithological variations).
2. The degree of fissuring and voids (fault-line cracking and karst dissolution).
3. The depth of a dry well (an increased wetted area and water pressure).
4. The diameter of a dry well (an increased wetted area).

(Ministry for Public Works and Planning, 2022)

One critical aspect in the selection and justification of a recharge proposal lies in the comparison of water volume that permeates the ground before and after the intervention. However, our present methodologies exhibit significant limitations in accurately obtaining the infiltration rates within our geological formations. At best, we have resorted to approximations derived from extensive testing to estimate permeability values. However, the inherent variability of on-site conditions renders the development of an accurate model for ground seepage and drainage behaviour almost unfeasible without conducting an on-site test of the rock. (Cedergren Harry, 1997)

The concept of on-site real-time experimentation in relation to the unpredictability of hydrogeology was presented by O. Chadwick in a statement he once made on the design of dams in Wied il-Qlejgħa:

> "The ultimate height of each dam was to be determined experimentally, commencing with a low dam, and increasing its height according to the actual results observed from year to year" (Chadwick, n.d., as stated in, Morris, 1952)

Hydrogeological concepts are based on certainties (or lack thereof), since weather patterns and the ground condition itself varies too much to derive neat conclusions. Presently, the most effective method of deriving ground permeability would be to conduct in-depth tests at each specific location to prevent varying unrealistic results.

The GEO-INF project in Malta, as described in subsection 2.1.2, involved extensive permeability testing conducted at numerous sites in Malta. These tests revealed a notable absence of consistent correlation among transmissivity values, even when the underlying geological material was identical. Evidently, the permeability of a given material is predominantly dependent upon local characteristics such as voids, fractures, and other site-specific attributes. Consequently, to establish a precise estimate for groundwater recharge in specific catchment areas, it becomes apparent that the excavation of boreholes and controlled testing remains a necessary step.

2.3 THEORETICAL FRAMEWORK

In this section, we shift focus to the theoretical framework that underpins water infiltration and permeability. Understanding the various equations and principles that govern these processes is crucial for developing an accurate ground permeability model through porous and fractured rock.

This knowledge is essential for the practical application of designing and optimizing managed aquifer recharge projects in Malta.

2.3.1 Rock Mass Classification Systems

On-site rock can be analysed through boreholes and be given rating classifications depending on various characteristics. These labels would help predict the behaviour and properties of the rock such as the expected compressive strength, shear strength, and rock mass permeability.

The Rock Quality Designation (RQD) – Depends on the fracture concentration.

The Gouge Content Designation (GCD) – Depends on the fracture infill material.

The Depth Index (DI) – Depends on the fracture depth within the rock mass.

The Lithology Permeability Index (LPI) – The permeability/porosity of the intact rock.

The Rock Mass Rating (RMR) – An overall assessment of the rock quality and stability.

2.3.2 Borehole Drilling Records

When a borehole is drilled and the core is recovered, the information is compiled in a document.

Typical borehole logs record the material and fissure variation throughout the length. The entire borehole would be divided into many ‘runs’, each with its own rock mass classification and detailed information on the discontinuities.

Each run is defined as the length drilled between successive manoeuvres of the drilling rig and rigger, where each manoeuvre entails assembly and disassembly of the drill string (drill pipe) to enable core retrieval or drilling/sampling tool replacement. For example, a run would consist of the following steps: assembling the drill string with a double core sample tool at the lower end with a specific available drilling depth, advancing the drill string until the sampler is full, and then dismantling the drill string to retrieve the core sample at the surface.

This document is important to accurately represent ground conditions in any digitized model, due to the consideration of how discontinuities may be concentrated in some locations and not others and would record larger voids found within a specific run.

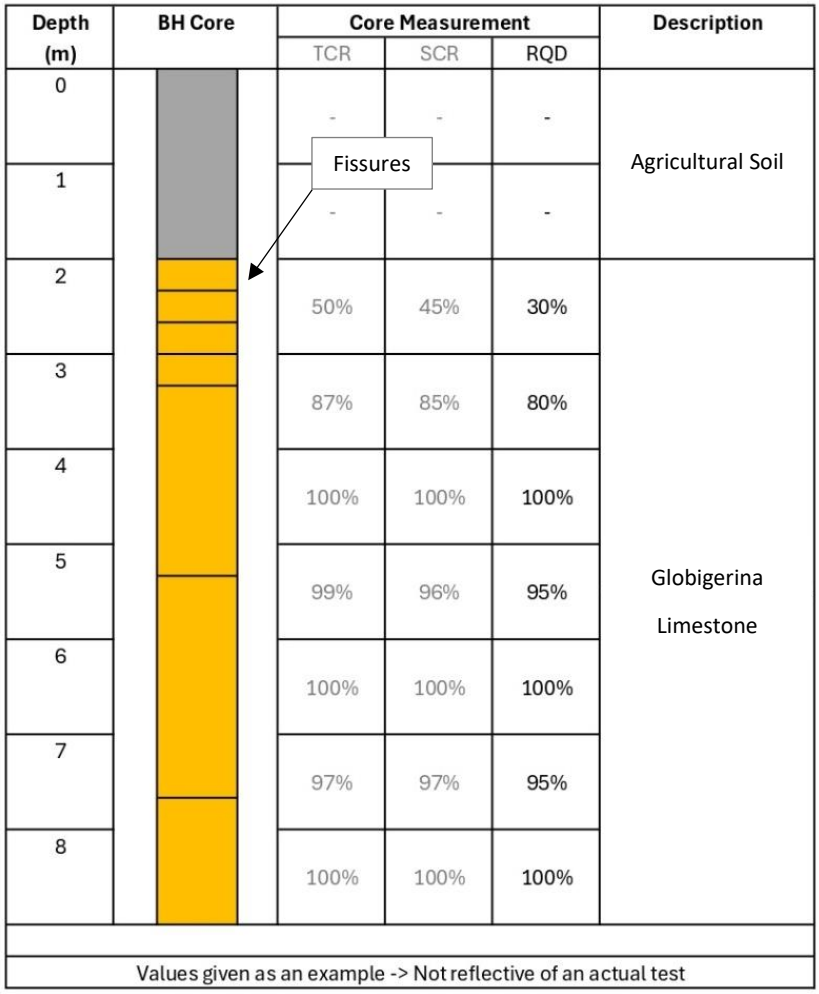

Figure 2.11: Simplified Representation of a BH Drilling Record (2024)

2.3.3 Geological Permeability Theory

Most widespread literature only consider permeability rates of wells for the purposes of groundwater abstraction, with not as much research done for the opposite. Initial assumptions may be that the existing abstraction permeability equations may be reversible to represent infiltration, however this is an inaccurate assumption.

The variables in common by both types of well would include the wetted area, rock mass permeability and the discontinuity concentration. However, it is important to note that infiltration rates within a dry well borehole also rely on the hydraulic pressure generated by the captured water height (water head), and its distance from the water table.

The two main contributors to water flow in the ground are the primary and secondary permeabilities, the first which depends on the materials inherent pore permeability, and the second which depends on the water flow which may occur through cracks, fissures, and other such discontinuities.

Primary Permeability

Darcy's law is an important equation which describes laminar water flow through a regular porous medium. This equation lays out the "basis for many experimental determinations of permeability that measure seepage quantity" (Cedergren, 1997):

$$Q = kiAt$$

Equation 1

Where *Q* is the water volume discharge seeping through the ground, *k* is the coefficient of hydraulic conductivity, *i* is the hydraulic gradient, *A* is the area which is normal to the direction of flow, and *t* is the time taken for a water particle to go from one position to another.

When certain seepage properties are known in laboratory testing, such as hydraulic conductivity, one can determine the infiltration rate. However, Darcy's Law only applies to the permeability of the intact rock itself, the ground's porosity, as opposed to a fissured rock mass.

M. J. Hvorslev, in his book "Time Lag and Soil Permeability in Ground-water Observations" (1951), expanded on the concept of Darcy's Law and derived a number of permeability formulas with varying infiltration conditions (See Appendix A). These formulas were originally used to find the hydraulic conductivity '*k*' of a soil through on-site or laboratory testing. However, if a rough value for k is known, then the volume flowrate '*Q*' may be estimated. These formulas were fundamental in establishing the theory for primary permeability within the parametric model, albeit being mainly applicable to homogenous porous media, such as uniform layers of soil.

An estimate of steady-state infiltration through a dry well in porous coralline limestone can be calculated by using Case F to represent coralline underlying globigerina, and Case G for representing a dry well found entirely in coralline limestone or any other highly porous medium (See Figure 2.12; Full Chart on Appendix A).

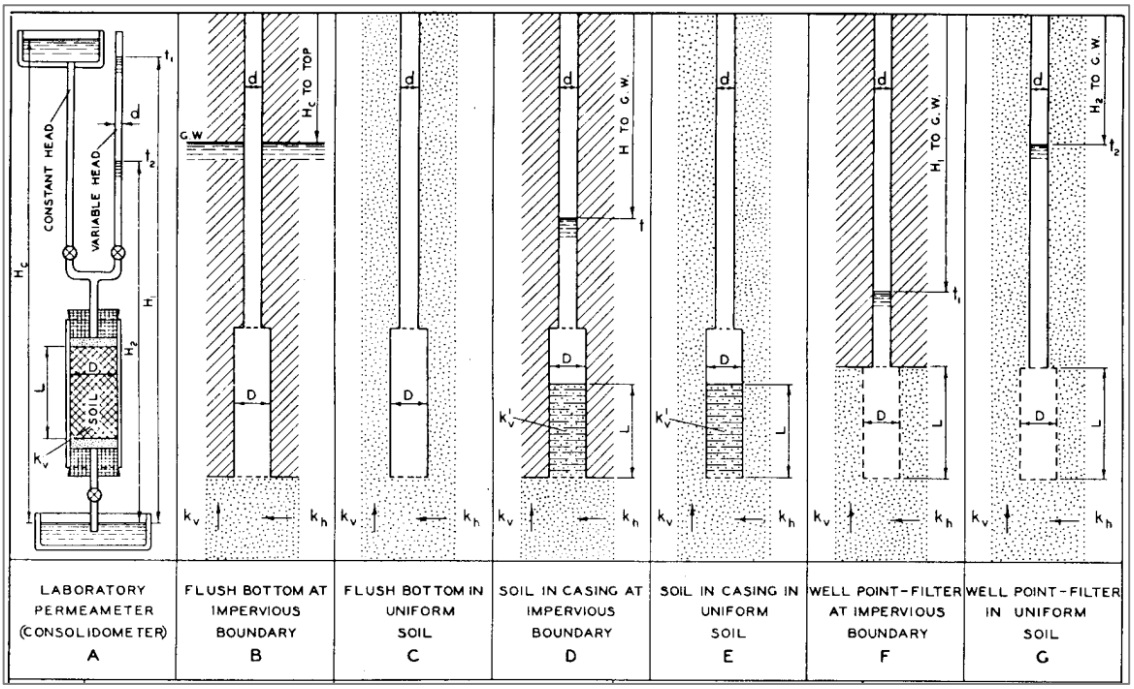

Figure 2.12: Chart of Permeability Cases for the Determination of Permeability (Hvorslev, 1951)

The Hvorslev solutions as well as many other methods aim to derive an estimate of ground permeability by also considering the nature of a vertical well, and how water pressure affects the permeability along the well's depth. However, the vast majority of these equations would have been derived through empirical means, whereas extensive on-site testing would occur within the researchers own geological regions and they would attempt to fit an equation which closely relates to the real-world observations.

Secondary Permeability

When analysing fractured rock masses, the permeability of the ground depends on factors such as the concentration, size, and orientation of the fractures. For permeability estimation of fractured rock it is normally best assumed that the intact rock porosity is almost impermeable, with most of the water infiltration occurring within the discontinuities in a given time period. To determine accurate site-specific permeability values, a comprehensive 3D fluid flow model of the on-site ground characteristics may be necessary. However, this is not very feasible, especially for the proposal of Managed Aquifer Recharge (MAR) projects, considering the numerous variables that are not easily quantifiable and measurable on-site.

For a more efficient assessment of the hydraulic conductivity of a rock mass, it's essential to consider both 1] theoretical approaches, which establish relationships based on fundamental laws, and 2] empirical methods, which rely on ground testing and comparative analysis of results. Several equations have been formulated to estimate the hydraulic conductivity of rock masses based on a rock's visual characteristics, typically derived from previous borehole

testing. These equations are contingent upon various on-site rock classifications, including Rock Quality Designation (RQD), Gouge Content Designation (GCD), Depth Index (DI), Lithology Permeability Index (LPI), and Rock Mass Rating (RMR).

However, Z. Şen (1996) concluded that rock quality designations alone may not be sufficient enough to estimate the hydraulic conductivity of a fractured rock. Fracture aperture, despite the minor effects to the final RQD value, is not fully represented in its effects to the ground permeability. This is especially the case when considering how recovered cores may lose the fracture width information since on-site suspended support is removed. In fact, an RQD of 100% may still exhibit sparse wide apertures which would provide sufficiently high permeability, since some RQD equations only consider the minimum length of core pieces.

Şen derived the following equation which relates RQD to hydraulic conductivity, by using the fracture width as a variable:

$$RQD = 100\left(1 + 600\frac{k}{a^3}\right)\exp\left(-600\frac{k}{a^3}\right)$$

Equation 2

Where RQD is the rock quality designation as a percentage, k is the hydraulic conductivity, and a is the aperture width.

When displaying this equation as a chart, one can more clearly visualise the large permeability variation dependent on aperture width (Figure 2.13).

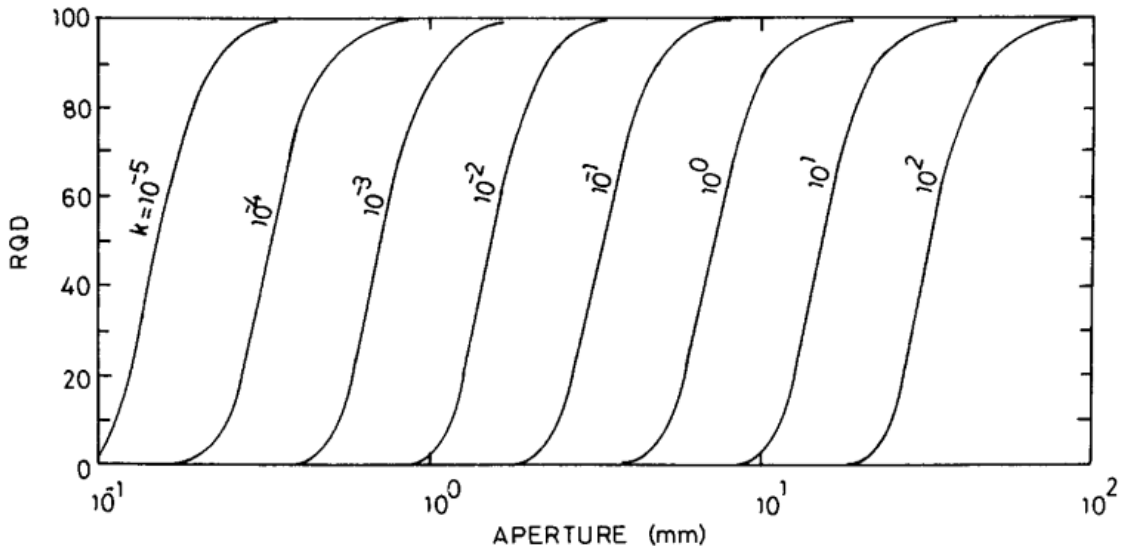

Figure 2.13: Permeability-RQD-Fracture Aperture Chart (Şen, 1996)

Once the hydraulic conductivity value is determined, the borehole can be sized accordingly to meet the desired water outflow rate, which relies on the exposed surface area within the borehole, commonly referred to as the wetted area. Moreover, the volume of water flowing through the rock is contingent upon the water pressure within the system. Consequently, the maximum water volume flows when the water head reaches the surface.

An important factor to remember is that each researcher's equation derivation would ultimately depend on their own specific on-site rock characteristics, and hence, it is difficult to make an instant assumption that these equations would be valid for the Maltese context.

2.4 Concluding Remarks

The literature review aimed to familiarise the reader with key elements related to groundwater and the deployment of managed aquifer recharge systems, drawing upon previous research and well-established knowledge.

The first part introduced the reader to the concept of managed aquifer recharge, and the various methods one may employ to achieve enhanced groundwater infiltration rates.

The second part introduced the reader to the fundamental theoretical concepts of ground permeability and rock designation. These concepts would be analysed and developed upon by others researching in this field of study and would provide me the necessary basics to begin developing the methodology for a ground permeability model.

If all aspects are considered, and the proposal is designed in a holistic and intelligent manner, Malta may benefit greatly from MAR interventions. By implementing such interventions in the sub-catchments of high rainfall and runoff, ecological and economical values can be derived from securing the groundwater resource as a sustainable storage of freshwater. If deemed successful, such MAR interventions may be applied to many other sub-catchment areas across Malta and Gozo.

From all the research gathered in the literature review, it was deemed that Infiltration Boreholes may be the MAR solution of highest potential in Malta.

There are several reasons as to why infiltration boreholes are considered as an excellent option for MAR in Malta:

1. *Limited Surface Space for localized and compact solutions*

   There isn't much room for extensive water management infrastructure in Malta because of its dense population. Compact and well-suited to the island's spatial limitations, infiltration boreholes provide an effective solution.

2. *Geological Conditions and the prevalence of highly fissured limestone*

   Malta's local geological strata are made up of heavily fissured limestone, some of which are prone to the formation of cavities and caves; All of which are favourable to the efficient operation of infiltration boreholes.

3. *Efficiency in infiltration by bypassing more impermeable layers*

   Particularly in urban settings, infiltration boreholes are an effective way to get around less permeable surface layers. Natural watercourses can also hold more water and slow down runoff.

4. *Mitigation of surface runoff and flooding*

   Infiltration boreholes aid in preventing downstream flooding by limiting excess runoff. This is especially crucial in rural and urban areas where excessive rainfall can cause serious flooding problems.

5. *Protection against seawater intrusion*

   Malta's coastal aquifers are vulnerable to seawater intrusion, which lowers the quality of the water. These aquifers can be replenished with freshwater by strategically positioned infiltration boreholes, raising the quality of the water that is available for local use.

The next chapter will outline the methodology employed to gather and analyse data for constructing a ground permeability model for assessing potential local solutions.

3 METHODOLOGY

3.1 INTRODUCTION

The methodology of this dissertation centres on building an informative predictive model of water runoff which is collected and infiltrated into the ground, where many variables are present, in order to guide the proposal of MAR projects around Malta. This dissertation specifically focuses on the recharge of the mean sea level aquifer, and hence, the main sedimentary rock layers considered are lower globigerina limestone and lower coralline limestone. However, the thought process may also be applied to perched aquifers.

Through the methodology, the relevant authorities would have the ability to assess multiple locations and sub-catchment areas around Malta for managed aquifer recharge and create a priority list before intense invasive interventions are actually implemented.

For the purposes of this dissertation, the predictive model focuses on designing infiltration boreholes to maximize ground infiltration with minimal spatial requirements. Given Malta's limited surface space and the predominance of fissured rock in the local strata, infiltration boreholes are deemed an effective MAR solution. This model was built to consider the many parameters involved in the design of site-specific infiltration boreholes, with the result of predicting the infiltration flowrate and efficiency of the system (Figure 3.1).

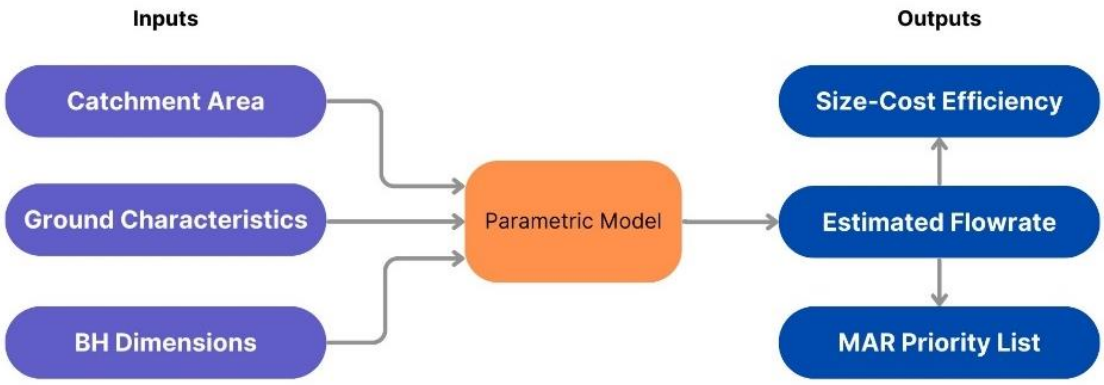

Figure 3.1: Informative Diagram of Parametric Model Inputs & Outputs (2024)

This dissertation's derived guidelines for 'Managed Aquifer Recharge' seek to answer the following quantitative questions:

1. Is the chosen location's geology suitable for enhanced water recharge?
2. Is there sufficient water inflow to justify the construction of further MAR systems? What is the volume of water entering the collection point?
3. What is the volume of water infiltrating in the ground? Can the infiltration rate be estimated reliably from core recovery information?
4. What is the permissible volume of water flowing downstream?

3.2 DATA COLLECTION

Existing research papers and articles were assessed which covered the following topics:

1. Maltese flood management and risk zones
2. Maltese rock permeability
3. Existing groundwater recharge proposals
4. The design of dams and water boreholes
5. Ground Permeability and Seepage Literature
6. The ecology and protected habitats of valleys
7. The overall geological characteristics of catchment areas

Local architects, engineers knowledgeable in this field, and environmental authorities were consulted to gain insight on designing aquifer recharge structures, in terms of design requirements, construction methods, and safety precautions:

1. '*Ambjent Malta'* was consulted on the common concerns of MAR development in protected areas such as valleys, as well as which ground conditions around Malta may be ideal for groundwater recharge projects.
2. Hydrology and geotechnical engineers were consulted on the design of infiltration boreholes, as well as the estimation of permeability from ground characteristics.
3. Through '*Solidbase Laboratory*', tests were done on-site to boreholes to test the permeability rate of various rock types and ground conditions to calibrate my estimation model.

3.3 Selection of Catchment Area Case Studies

The selection of local valleys as case studies in the implementation of managed aquifer recharge was based on:

- Sites already noted by authorities as having high redevelopment and recharge potential.
- Sites with a sizable water catchment area.
- Sites overlying the mean sea level aquifer.
- Sites with enough available space for interventions.
- Sites which may already have existing MAR and flood-control structures.

An online WEBGIS map which highlights the main catchment areas and all the data collected through the LIFE-IP project (LIFE IP & Project Green, 2023) was studied to derive information on the existing structures and ecosystems along many watercourses, as well as the nation-wide potential for MAR projects.

The GIS Geological Map of the Maltese Islands was also be studied to identify the expected type of ground material present and the major faults at permeability test sites and potential catchment areas for managed aquifer recharge.

These two sources proved useful to locate two examples of catchment areas upon which the parametric model was applied. The analysis and results are explained in Section 5.2.

3.4 MAR Intervention Design Parameters

3.4.1 Rainfall Catchment Area

In each catchment area, the amount of rainfall collected depends on both the rate of rainfall and the surface area of the catchment. To gauge the volume of water reaching the collection point of the Managed Aquifer Recharge (MAR) Project, we consider the average annual rainfall rate.

We calculate the volume flowrate (Q) using the equation:

$$Annual\,Q = Catchment\,Area \times \%\,Runoff \times Average\,Annual\,Rainfall$$

Equation 3

As previously mentioned in subsection 2.2.1, the runoff volume is influenced by various factors like permeable soil and water-collecting depressions within the catchment area. Urban areas with impermeable surfaces tend to accumulate rain runoff.

In addition to estimating the inflow of runoff through a watercourse, it's crucial to determine the required outflow for environmental purposes, ensuring downstream sections of the valley receive adequate water and nutrients. However, quantifying this outflow may prove to be challenging and may be more qualitative in nature as predicting downstream water requirements is complex. This step may also involve the design of retaining dams, whether permeable or not, to ensure that the required water for infiltration is captured within the collection point.

Once the inflow-outflow dynamics are understood, the amount of water to be captured and infiltrated is derived. Varying the number and dimensions of boreholes allows us to identify the most cost-effective and efficient solution for the MAR Project.

3.4.2 Borehole Infiltration Parameters

Integrating the Infiltration Borehole Model into the Managed Aquifer Recharge (MAR) Project necessitates meticulous consideration of design parameters, processes, and geological characteristics to ensure optimal infiltration of water into the aquifer. Pre-establishing a set of design parameters for a set of infiltration boreholes led to the design of a parametric model, allowing for the identification of the most efficient dry wells based on dimensional variables and the discontinuity concentration. Here's an overview of the design parameters and considerations involved:

Design Parameters:

1. Dimension Variables: Borehole diameter, depth, and spacing are optimized to maximize water infiltration while ensuring structural integrity and operational efficiency.
2. Rock Type: Globigerina and Coralline limestone exhibit different water transmission properties. Globigerina tends to be more impermeable with extremely small pores, where transmission of groundwater primarily occurs through fissures. Coralline is significantly more porous, where the karstic dissolution of limestone provides a high void content in the intact rock.
3. Discontinuity Concentration: RQD values are assessed to determine the rock mass quality and guide the design of borehole parameters for optimal performance.
4. Fissure Properties: The fissure width and its infill material will affect the allowable water flowrate moving through the system.
5. Location & Catchment Area: The available impermeable catchment area as well as whether existing flood control and recharge structures are already found within the catchment area. Integration of dry wells within dam basins can aid in enhancing groundwater recharge.

Ground Permeability and Seepage Analysis:

1. Theoretical and Empirical Equations: Ground permeability and seepage literature were consulted to develop theoretical and empirical equations, accounting for both porous rock and fractured rock conditions. These equations estimate the hydraulic conductivity of the ground and subsequent flow permeability rate.
2. Variability in Permeability: Permeability values vary across sites and down the length of the borehole itself, with particular focus on globigerina and coralline limestone which are the predominant strata through which water infiltrates in the region. Site-specific permeability assessments guide the selection of infiltration locations and borehole design.

Equations and Models:

1. Flow Equations: Mathematical models such as hydrology flow equations are employed to calculate the volume of water infiltrating into the aquifer through the boreholes.
2. Pipe Equations: Hydraulic equations governing flow through pipes are utilized to design boreholes through fractured rock as a simplification of the system to optimize water flow rates.
3. Pressure Equations: Pressure equations are employed to evaluate the hydraulic head and pressure distribution within the borehole system, ensuring efficient water infiltration.
4. Hydraulic Conductivity Equations: Equations assessing hydraulic conductivity in a porous medium aid in estimating groundwater flow rates and optimizing borehole placement and design for coralline limestone.

3.5 Ground Permeability Model for Dry Wells

This dissertation introduces a theoretical approach to estimating potential water infiltration within managed aquifer recharge (MAR) projects, surpassing the traditional method of repeatedly pumping water into a borehole, and conducting a falling-head test at each location to determine ground permeability.

The model aims to simplify complexities inherent in ground conditions, offering a conservative estimation of water flow to assess the viability of a site for MAR projects. Developed on Microsoft Excel, the model employs conventional equations for water flow to establish an in-out model of the proposed location.

The parametric model requires input data derived from an initial recovered core; by obtaining the Rock Quality Designation (RQD), average fracture width, and infill material. This streamlined approach enhances efficiency in project evaluation and should help with surface-level analysis of MAR locations around Malta.

Part of the model considers the volume flowrate of water as the borehole empties. The drop in flowrate over time may not be an important factor when deciding on the number of boreholes required to capture the catchment area's water input. However, in order to calibrate and prove the model to be realistic, the head loss over time is required. From the results in the model, and the results from on-site tests, the model itself can be calibrated and proved to depict the ground permeability more accurately.

3.5.1 Primary Permeability Flow

The primary permeability would depend on the rock type and the input borehole dimensions. In this instance, the model would assume primary permeability only for coralline limestone.

First and foremost, the hydraulic conductivity for coralline limestone is derived through on-site testing, and many such values have already been found. However, these values would likely vary due to ground uncertainties and natural variations.

Once a conservative value of the material's hydraulic conductivity *K* is empirically derived separately through various testing, Hvorslev's formulae for infiltration through a porous medium can be applied, as highlighted in Section 2.3.3.

For a constant head situation, Hvorslev provides equations for both deep and shallow flow cases, which were further simplified and detailed by J. Massmann (2004) in his report on estimating infiltration rates for stormwater dry wells.

The simplified Hvorslev deep and shallow flow field solution is as follows (Massmann, 2004):

[Deep Flow – Case F]

$$Q = \frac{2\pi KLH}{\ln\left[\frac{2L}{r} + \sqrt{1+\left(\frac{2L}{r}\right)^2}\right]}$$

Equation 4

[Shallow Flow – Case G]

$$Q = \frac{2\pi KLH}{\ln\left[\frac{4L}{r} + \sqrt{1+\left(\frac{4L}{r}\right)^2}\right]}$$

Equation 5

Where Q is the water volume discharge rate, K is the saturated hydraulic conductivity (permeability), H is the height of water in the well, L is the wetted length of the dry well exposed to the porous medium, and r is the radius of the well.

Deep and shallow fields specifically refer to flow in confined and unconfined aquifers respectively, and these equations consider ellipsoid-shaped infiltration bulbs as the water permeates along the depth of the borehole.

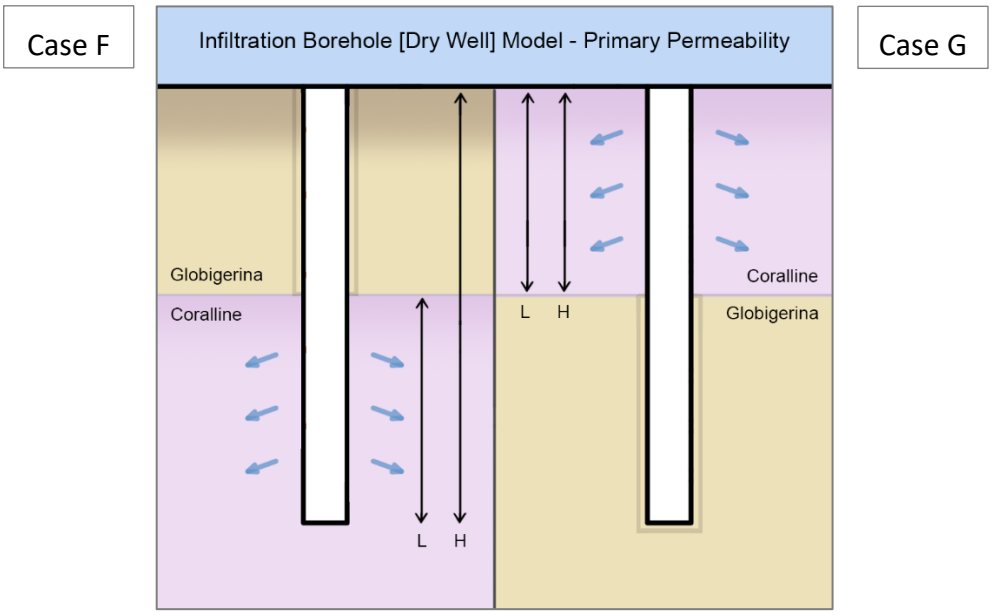

Figure 3.2: Dry Well Primary Permeability in Varying Strata Diagram (2024)

If an infiltration borehole is located purely within coralline limestone, Equation 5 can be directly applied to the dimensions of the borehole (Case G). However, when considering a variation in rock strata, the values would need to be adjusted to consider the lack of pore permeability through globigerina limestone, and whether a large water head is being applied.

Depending on the level of impermeability exhibited by the globigerina limestone, Equation 4 may be required (Case F).

Both globigerina and coralline limestone can contain fissures, which contribute to secondary permeability through rock discontinuities. The total flow rate from primary permeability, such as in coralline limestone, must be combined with the secondary permeability.

Generally, pore permeability in rock is very low compared to the secondary permeability through fissures. Calculating the secondary permeability is more complex but essential for determining the total flow rate out of the borehole.

3.5.2 Secondary Permeability Flow

By leveraging data gathered on the fissures and their distribution throughout the borehole depth, we derive the hypothetical cross-sectional area for water flow along this depth. The model estimates secondary permeability by converting complex fissure data into a simplified pipe model, with water flowing out of the BH cavity wall through these pipes (Figure 3.3).

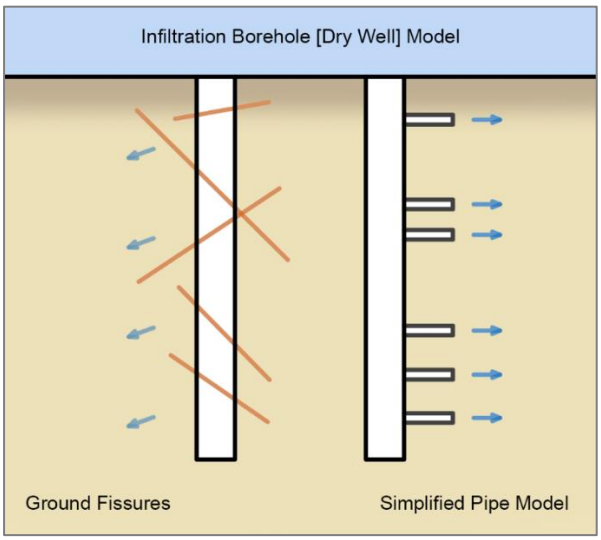

Figure 3.3: Dry Well Secondary Permeability Simplified Model Diagram (2024)

Flow Area of Fissures

To streamline calculations for determining outflow, the borehole depth is subdivided into numerous small slices or segments. This segmentation aids in simplifying the process of computing outflow for each segment.

Assuming horizontal plane cuts as the fissures, the total area of flow out of the system is calculated by multiplying the aperture width by the circumference of the borehole:

$$Af = a \times (2\pi r)$$

Equation 6

Where A_f is the available fissure area for flow, a is the aperture width, and 2r is the radius of the borehole.

Flow Velocity of Fissures

The maximum flowrate, that being the initial flowrate, occurs when the head is at its peak height, and each fissure is experiencing its highest possible water pressure, thus inducing a water velocity at each fissure due to each respective hydraulic head.

To estimate the velocity at each fissure in a dry well, Bernoulli's equation can be employed under the initial assumption of energy conversion at dry well entry and exit without losses, as expressed by the equation:

$$P_1+\left(\frac{1}{2}\ \rho\ \left(v_1\right)^2\right)+\left(\rho\, gh_1\right)=P_2+\left(\frac{1}{2}\ \rho\ \left(v_2\right)^2\right)+\left(\rho\, gh_2\right)$$

Equation 7

Where *P* is the existing applied pressure, *ρ* is the density of the fluid, *v* is the velocity of the fluid, *g* is the acceleration due to gravity, and *h* is the height of the fluid from a specific datum point.

The equation can be further simplified to better represent the problem in question, since virtually no kinetic energy would be present at the surface of the dry well, and no potential energy to be considered at the bottom of the dry well:

$$\rho\, gh_1=\frac{1}{2}\rho\ \left(v_2\right)^2$$

Equation 8

Here, the potential energy at the dry well's surface convert into kinetic energy at its openings. Additionally, it can be assumed that the air pressure at the surface is around the same as the air pressure at the other end of the fractures in the ground. This however is a broad assumption since air being trapped within fractures may still occur and slow down water flow.

Modifying Bernoulli's equation further yields the equation for velocity at each opening:

$$v=\sqrt{(2\, gh\ )}$$

Equation 9

This value for velocity represents the hypothetical velocity when no energy losses occur. To be realistic, a resistance factor would be multiplied by every subsequent velocity at each timestep and at each fracture, to cater for friction and flow resistances.

Volume Flowrate through the Borehole

Under constant head, the calculation may only require the addition of each volume flowrate equation at each fissure, where the fundamental hydrological volume flowrate equation is used:

$$Q = Av$$

Equation 10

Total volume flowrate through the BH requires the addition of each individual fissure's flowrate, each with differing velocities and flow areas at each segment:

$$Q_T = A_1 v_1 + A_2 v_2 + A_3 v_3 + \ldots$$

Equation 11

However, one must consider that the velocities in reality would be dramatically lower than the values derived purely through this method. In reality, velocity would be significantly lower due to potential resistances and energy losses in the system.

In order to accurately calibrate the borehole permeability model to consider resistances to flow, the second part of the model needed to be designed, which catered to the analysis of falling-head infiltration, in order to facilitate a direct comparison to real-world permeability tests.

Sections 3.5.3 and 4.3 go into more detail on these permeability tests and how they are utilized for model calibration.

Volume Flowrate through an Emptying Borehole

Calculating the flowrate within an emptying water tank with a single opening is simple to understand, utilizing the hydrological volume flowrate equation with no additional variables. However, introducing multiple openings at different heights complicates the scenario significantly.

When the dry well has fractures along its entirety, the head drop occurs rapidly initially. However, as the water level declines, fewer openings are available to carry the flowrate, resulting in a gradual lessened output. Therefore, it's crucial to consider the effects of each individual opening within the dry well over specific timesteps. The analysis of these openings would occur at a chosen spacing depending on the borehole's segment height division as well as how conservative of a value I wished to derive.

Despite the curved reduction in flowrate, Bernoulli's equation for velocity demonstrates Torricelli's Law, where velocity increases linearly with depth, regardless of the number of openings, as velocity depends on the head height (Figure 3.4).

The calculations of flowrate variation with time are typically conducted iteratively, which is where the software *Microsoft Excel* comes into play. As seen up until now, determining the initial flowrate at t=0 is straightforward, involving the calculation of velocity at each height, thereby deriving the summed volume flowrate. However, the rate of change of head loss at each timestep must be determined to find subsequent changes in velocity.

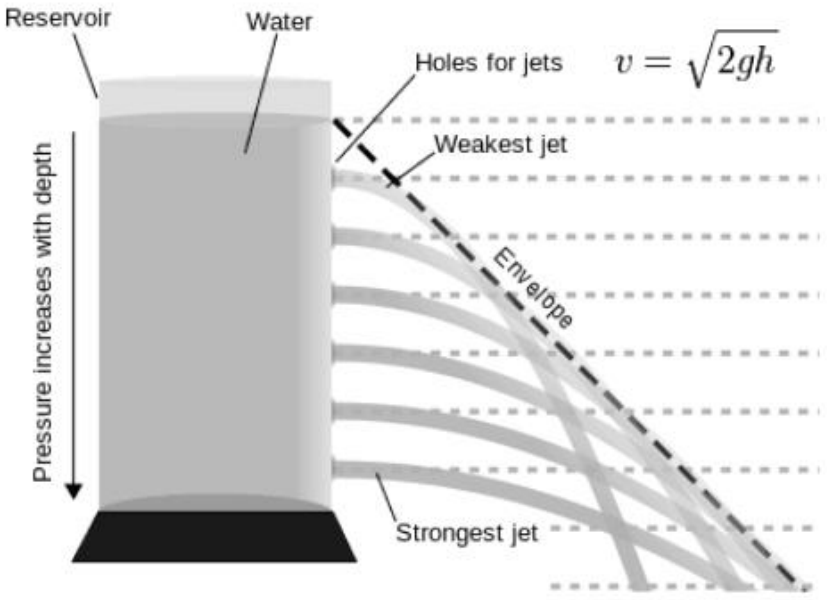

Figure 3.4: Torricelli's Law Diagram (Cook, 2015)

A derived equation describes the rate of head decrease in the dry well relative to the outflow and the cross-sectional area (CSA) of the well:

$$\frac{Q_T}{A_{BH}} = \frac{dh}{dt}$$

Equation 12

Where Q_T is the total volumetric flowrate, A_{BH} is the cross-sectional area of the borehole, dh is the incremental height, and dt is the incremental time. The resulting units on either side of the formula are in m/s.

Increasing borehole diameter decreases the rate of change of head loss due to the larger volume of water within the borehole. Conversely, a greater number of openings or fissures

throughout the borehole increases the outflow rate, thus enhancing the rate of change of head loss.

This equation is iteratively applied at each timestep to determine subsequent head losses which are re-introduced as the new head value until the tank is empty (Figure 3.5):

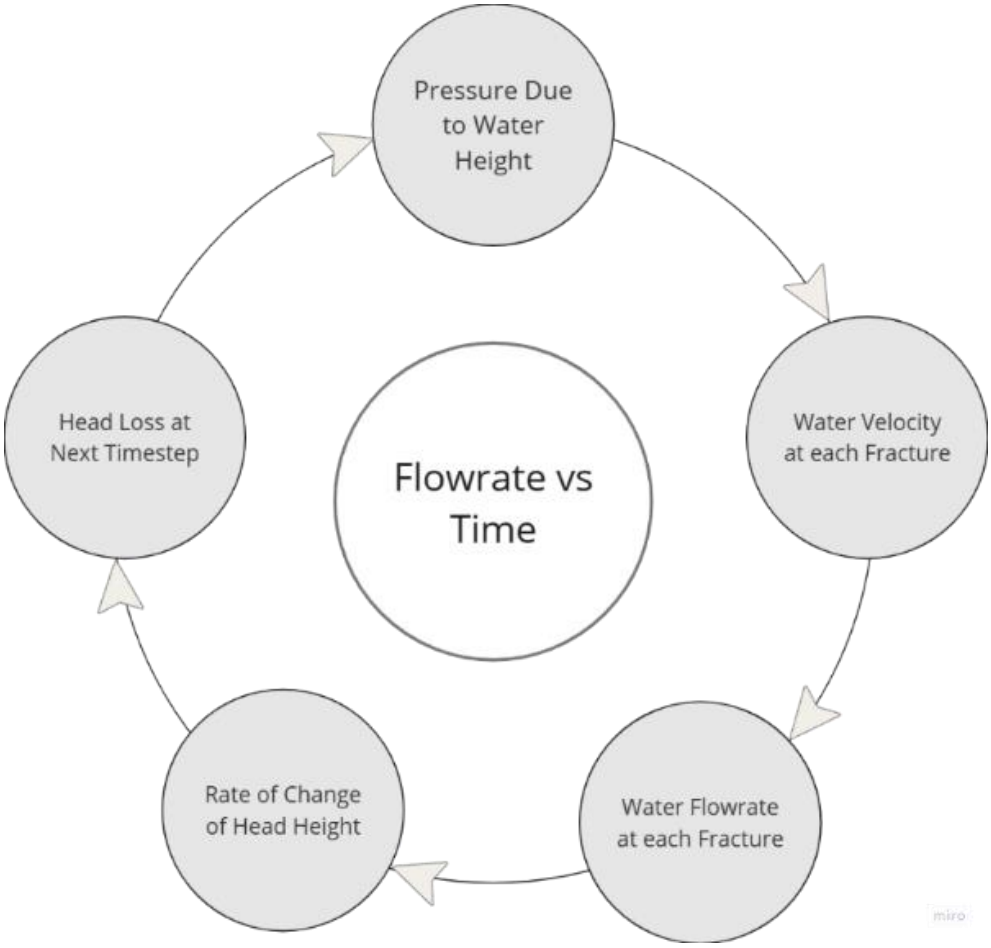

Figure 3.5: Looped Flow Calculation due to Head Loss (2024)

3.5.3 Flow Resistance Considerations

The previous section outlined the necessary equations for the model's theoretical foundation. In practice, water infiltration encounters resistances from various factors, which must be considered to accurately estimate ground conditions.

The simplified model uses the pipe flow equation $Q = Av$, but Darcy's law $Q = kiAt$ emphasizes the importance of the hydraulic gradient. Variations like the pressure gradient depend on the 'effective length' and 'pressure difference' between the start and end of water flow. A long effective length or a small pressure difference results in a shallow pressure gradient. These variables are complex and not directly applicable to ground fissures and pores, making the

problem intricate. The effective length concept may apply to an underground fissure but cannot be directly measured or identified.

To address this, an alternative method was developed to account for flow resistance, moving away from the initial parametric model's smooth, lossless pipe assumption. A flow factor concept was established to consider unknown resistances, such as effective length, fissure roughness, and hydraulic gradient, along with identifiable resistances like fissure infill material type.

An empirical approach was adopted to derive a table of flow factors, though this remains a crude estimation. This approach, covered in sub-section 4.3, relies on falling-head permeability tests which need to be conducted in various ground conditions in order to derive these resistance factors. Of course, the higher the number of tests done, the larger the confidence in these factors and the many difference factors which can actually be recorded depending on various identifiable ground conditions. These factors, derived from many on-site ground permeability testing, would be able to estimate water permeability for future site analyses.

In order to apply the flow factor to the model, it would be multiplied by each fissure's velocity to find the subsequent reduction in velocity after the flow resistances are considered:

$$v_{final} = v_{initial} \times F_F$$

Equation 13

Where $v_{initial}$ is the lossless initial velocity, F_F is the Flow Factor due to flow resistances, and v_{final} is the resulting final velocity.

The decision to simplify energy-loss variables into single factors was driven by the complexity and unpredictable variability of real-world ground conditions. While pressure or hydraulic gradients typically affect the volume flow rate, determining the effective length of a ground fissure or the roughness throughout the fissure is impossible.

The adoption of a simplified factor not only further refined the estimation but also aligned with the original objective of providing a rapid preliminary solution to support managed aquifer recharge projects in Malta.

3.6 On-Site Testing

Falling-head permeability tests were conducted on a number of boreholes of known rock and fissure characteristics to derive a rough estimate on the resistance to flow. A table of these factors would be recorded, each tied to a specific fissure infill characteristic, since any variations in this infill material will widely affect the final permeability rate.

Falling-Head Percolation Test:

To conduct a falling head test, the appropriate equipment and sufficient preparation is required to accurately record the rate of head loss per unit time.

Equipment:

- Water Level Meter Sensor – An instrument of specific length with an electric buzzer and light to indicate when the probe contacts water.
- Stop watch – To check the rate of head loss after a decided specific interval.
- Water Supply – To entirely fill the borehole.

Test Process:

1. A borehole is dug, and the core is recovered to record the RQD and fissure characteristics.
2. The borehole is flushed to ensure no obstructions in the cavity.
3. The borehole is filled to the top with pumped water.
4. Using a water level sensor and a stopwatch, the head loss is recorded at regular and frequent time intervals (Figure 3.6).
5. The reading process can stop when steady state conditions are met or close to being met, such as with very slow dissipation.
6. The percolation / permeability rate can be derived from the resulting curved graph.

Test Data

Elapsed Time (mins)	Water Level (mbgl)	Water Level (mOD)
0	0.00	163.52
1	0.81	163.21
2	1.51	163.13
3	2.12	163.09
4	2.64	163.06
5	3.08	163.04
6	3.46	163.01
7	3.70	163.00
8	3.88	162.99
9	4.03	162.97
10	4.15	162.96
11	4.24	162.95
12	4.32	162.93
13	4.38	162.94
14	4.41	162.91
15	4.43	162.91
16	4.45	162.91
17	4.47	162.90
18	4.48	162.89
19	4.49	162.89
20	4.49	162.88
21	4.50	162.88
22	4.50	162.88
23	4.50	162.88
24	4.51	162.88
25	4.51	162.88
26	4.51	162.88
27	4.51	162.88
28	4.51	162.88
29	4.51	162.88
30	4.51	162.88
31	4.51	162.88
32	4.51	162.88
33	4.51	162.88
34	4.52	162.88
35	4.52	162.88

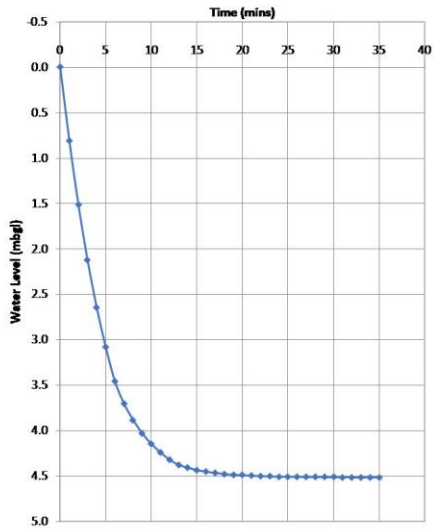

Calculated Permeability (k)

k =	5.42E-05 m/s

Figure 3.6: Example of Falling Head Test (Stuart Wells Ltd., 2022)

Figure 3.7: Equipment for Falling Head Test (2024)

3.7 INTERPRETED HYDRAULIC CONDUCTIVITY

Through knowing the borehole dimensions and the recorded head loss, a value for conductivity *K* can be found for each borehole.

Hvorslev (1951) had derived a method which first requires the derivation of the *Intake Shape Factor*, a factor which depends on the dimensions of the borehole:

$$F = \frac{2\pi L}{\left(\ln\left[\frac{L}{D} + \sqrt{1 + \left(\frac{L}{D} \right)^2} \right] \right)}$$

Equation 14

Where *L* is the length of the borehole, *D* is the diameter of the borehole, and *F* is the *Intake Factor* for a cylindrically shaped intake.

Thus, the Hvorslev Slug Test Method can then be used:

$$K = A \times \frac{\ln\left(\frac{h_1}{h_2} \right)}{F\left(t_2 - t_1 \right)}$$

Equation 15

Where *A* is the cross-sectional area of the borehole, h_1 is the initial water height, h_2 is the secondary water height due to head loss, t_1 is the starting time, t_2 is the time taken for the head loss to reach h_2, and *F* is the intake factor as found previously.

3.8 Assumptions and Limitations

Ground Permeability

This dissertation aims to offer a guideline for selecting suitable locations for managed aquifer recharge projects in Maltese valleys. To develop a practical model for estimating ground permeability, several assumptions were necessary.

The design methodology for infiltration boreholes assumed that knowledge of the Rock Quality Designation (RQD) and average fracture widths would suffice to estimate permeability. However, on-site variations may still occur.

The design method may overestimate or underestimate the on-site permeability:

- Ground conditions can differ between boreholes, influenced by borehole diameter and whether fissures are penetrated or missed entirely.
- Rock fissures may be filled with impermeable materials like clay deeper within the fissures which may not be initially visible from borehole coring.
- Some fissures may be short and inadequately extend for sufficient water infiltration.
- Fissures which extend into larger karstic voids and phreatic tubes may significantly increase permeability rates, flow being limited only by the borehole diameter.

Model Creation and Calibration

To establish the theoretical framework, it was assumed that all fissures are horizontal and planar. Consequently, at any given segmented height, water would permeate through the entire circumference of the borehole at an equal flow rate. In reality, fissures are rarely horizontal and often occur at steep vertical angles. However, it is possible that the heightened flow rate on the downward side of a fissure plane and the reduced flow rate on the opposite upward side could average out, justifying the overall horizontal plane assumption.

Calibrating the parametric model necessitates a comprehensive series of on-site tests to establish an accurate table of ‘resistance’ flow factors, which vary depending on simplified ground characteristics. Conducting falling-head tests on both empty and infilled fissures is crucial, as it leads to significantly different final permeability values.

An encompassing resistance factor is necessary because it is impractical to accurately derive pressure gradients or hydraulic gradients through ground fissures. These gradients may depend entirely on the effective length of the fissure, its orientation, and any variations in the fissure aperture along the faulted plane. Deriving these fissure properties would require an extensive ground analysis method that penetrates the subsurface to create a 3D map, which

is beyond conventional means. Therefore, to streamline the MAR design process, these uncertainties must be simplified to a certain extent, while still providing a conservatively reliable form of guidance.

All things considered, achieving a high level of confidence in these resistance factors is important to ensure that the parametric model is reliable in dictating managed aquifer recharge locations. However, a high confidence level may be challenging due to time and access constraints during the writing of this dissertation.

Hydraulic Conductivity

As with previously mentioned limitations, one cannot assign a single value of conductivity to the rock strata, or to boreholes within the same site. What may result is a range of conductivity values, especially when one considers the fact that head loss in fractured globigerina limestone occurs entirely due to the number of fissures, which is an unpredictable variable.

Assumptions for conductivity are also reflected by the Hvorslev Intake Shape Factor. This factor's equation was derived for isotropic homogeneous soil, and it would be inaccurate to say that fractured rock follows these properties.

4 MODEL CREATION

4.1 INTRODUCTION

This chapter explores the function of the parametric model in more detail, and how it has been set up to cater for varying ground characteristics with the aim of deriving meaningful insights and conclusions. This phase is crucial for understanding the effectiveness of estimating the ground permeability through simplification methods of Maltese rock strata in order to encourage and streamline the development of managed aquifer recharge projects across the Maltese islands.

Figure 4.1: Flowchart of Parametric Model Design Process (2024)

4.2 PARAMETRIC INFILTRATION MODEL

4.2.1 Starting Parameters

A list of starting values would be used to gradually build up the model. These values would come to be the initial values that would need to be derived from any on-site testing in order to assess a managed aquifer recharge project:

- Borehole Diameter – 0.11m
- Borehole Depth – 10m
- RQD Percentages – 0-100% with core runs of 1m
- Fissure Aperture Average Width – 1mm

To create the model, the BH depth was divided into 100 segments. Such a segment number was chosen to ensure the accuracy of the model with a smooth-curve solution whilst also being practical with the number of rows to calculate and visualise. The input borehole depth would therefore be split along the 100 segments and the volume flowrate would be found at each of these segments. For the purposes of this example, water head within the BH is also taken as the full BH depth. However, this can be adjusted as required.

4.2.2 Flowrate through Pores

Using a programmable drop-down list, the user would either select either Globigerina Limestone or Coralline Limestone and provide the depth of the first layer of rock (inputs in red). Choosing globigerina would automatically disable the primary permeability calculations only for that section of the borehole.

Rock Type:			**Rock Length:**	
Upper Rock:	Globigerina Limestone	->	8	m
Lower Rock:	Coralline Limestone	->	2	m

Table 1: Establishing the Ground Materials & Depths

This table (Table 1) would allow for a fully customizable ground model, whether the ground in question is fully globigerina, fully coralline, or features both.

Depending on the selected input rock type for the top or bottom strata, the model chooses between the calculation of Hvorslev's shallow flow, or deep flow (as highlighted in Section 3.5.1). In this instance of GL above CL, the deep flow equation is applied, considering 2 metres of pore permeability within CL. Hvorslev's equations consider the borehole dimensions and the hydraulic conductivity *K* of CL, all separate input values for the model.

It is important to note that existing values for hydraulic conductivity vary greatly since they are based on many on-site tests and rock characteristics. According to De Biase et al., (2021), the porosity of LCL varies greatly from 7 to 20%, and the average hydraulic conductivity of LCL of the MSLA was measured to be $1x10^{-4}$ m/s. However, this value for *K* was measured from on-site pumping tests which likely also factored in secondary permeability through fissures, so this value is unusable for this section.

Many sources, such as that of Notario & Diaz (1998), list the hydraulic conductivity of various unfractured sedimentary rock types to be in a range of $x10^{-5}$ and $x10^{-10}$. Therefore, the value of $5x10^{-7}$ was adopted for the purposes of this dissertation. It is important to note, however, that this value is not factual.

Primary Permeability Calculations Table		
Hydraulic Conductivity K of CL (Input) :	5x10^-7	$m^3/s/m^2$
Hvorslev Flow Calculation: Lower Rock (DEEP FLOW):	0.00126	m^3/s
Coralline Limestone (CL) BH Length : Lower Rock:	2	m
Final Pore Permeability Q Flow : Lower Rock:	0.00126	m^3/s

Table 2: Primary Permeability Calculations

Thus, the primary permeability flowrate is found at the maximum initial flowrate, occurring when the borehole is full and in steady-state conditions. As the reader may recognise later on, this calculation can be linked with the head-loss section of the model (Table 5) by adding a separate column for Q_{pore}, since the pore permeability would also lessen over time.

4.2.3 Flowrate through Fissures

The hydrology flowrate equation normally applied to pipes may be applied to each fissure/segment, where the 'area of pipe' in this instance can be substituted by the available aperture area (Equation 10):

$$Q = Av$$

This equation, along with the Darcy's Law variation, forms to basis of the digital model.

Fissure Number from Rock Quality Designation

In order to simplify the analysis process for MAR locations, the RQD values per run as stated in the recovered borehole report should be directly transferable to the model. Table 3 had been created to directly emulate the core run lengths and their assigned RQD values.

Fissure Distribution Table [Borehole Log Runs]

Core Run: (#)	Core Length Input Values: (m)	RQD Input Values: (%)	Core Run Max Depth: (m)	Fissured Lengths: (m)	Fissure Number per Run: (#)	Fissure Number per Segment: (#)
-	-	-	-	-	-	-
1	1	50	1	0.5	5	0.5
2	1	80	2	0.2	2	0.2
3	1	50	3	0.5	5	0.5
4	1	95	4	0.05	0.5	0.05
5	1	100	5	0	0	0
6	1	100	6	0	0	0
7	1	90	7	0.1	1	0.1
8	1	100	8	0	0	0
9	1	100	9	0	0	0
10	1	100	10	0	0	0

Table 3: RQD Inputs for Fissure Distribution

From an RQD Value, a conservative estimate on the number of fissures present in the core run can be calculated. It is important to note that the following method is a way of conservatively interpreting the number of fissures. In reality, more fissures may be present which may not be considered if the core pieces in between them exceed 10cm in length.

E.g. With RQD = 80%

~0.8m of the 1m run is made of intact rock, whilst ~0.2m of the run is fissured, chosen with a distance of 10cm between fissures.

Since the typical RQD Equation considers fractured cores as pieces smaller or equal to 10cm, a conservative estimate would be to assume all pieces are bordering on 10cm, for 'minimal' permeability.

10cm pieces of core within a 0.2 metre length of fissures would result in around 2 fissures, each with an initial aperture width of 1mm (Figure 4.2).

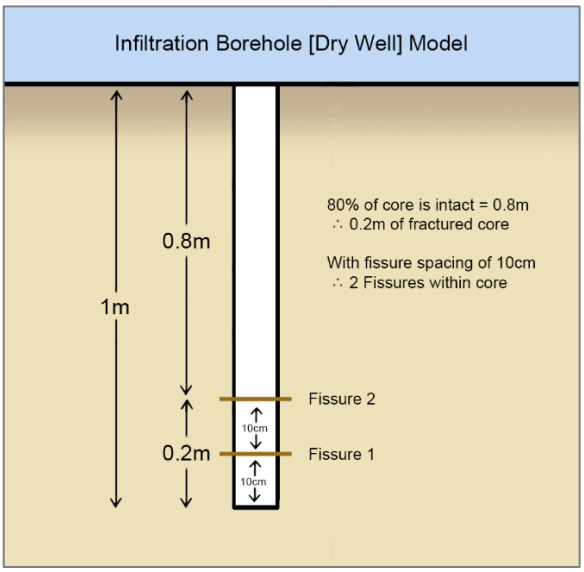

Figure 4.2: Diagram of Fissure Number Assessment (2024)

The number of fissures per metre run would then be adjusted to reflect the number of fissures per segment of the borehole model. The model was designed to consider 100 segments along the borehole height.

Assuming plane horizontal fissures passing through the borehole, using Equation 6, fissure area at Segment:

$= (\text{Aperture Width}) * (2 \pi r)$

$= (1\text{mm}) * (2 * \pi * (110/2))$

= 345.58 mm^2 of available flow area per fissure

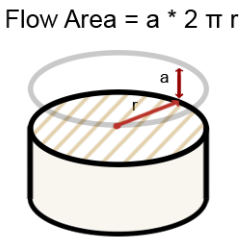

Figure 4.3: 3D Diagram of Fissure Plane & Flow Area (2024)

Establishing the Initial Velocity

The velocity equation derived from Bernoulli's Equation, see Equation 9, is applied to each fissure/segment to find the initial velocity within the first timestep:

$v = \text{sqrt}(2*g*h)$

A table is drawn (Table 4), and a condition is set so if the height of the fissure is greater than the height of the water head in the borehole, the resulting velocity will equal zero. This would apply for future timesteps when the head height falls below a number of fissures.

Segment/Slice Number (#):			0	1	2	3	4	...	100
Height of Slice Openings from Bottom (m):			10	9.9	9.8	9.7	9.6	...	0
Timesteps	**BH Head**	**Velocity**	v0	v1	v2	v3	v4	...	v100
(s)	(m)	(m/s)							
0	10		0	1.4007	1.9809	2.4261	2.8014	...	14.0071

Table 4: Velocity at Timestep 0

Calculating Initial Flowrate and Head Loss

After determining both variables in the flow rate equation - the fissure area and the fissure velocity - the volume flow rate passing through each fissure, and consequently through the infiltration borehole as a whole, can be calculated.

A second table is drawn (Table 5) to tabulate the found flowrates at each fissure, where the total flowrate can then be summed up. Stopping here would be sufficient for steady-state conditions. However, further calculations are required for head-loss conditions.

The rate of change of water head equation can then be applied (Equation 12):

$$Q_T/A_{BH} = dh/dt$$

Where Q_T is the total summed flowrate, A_{BH} is the cross-sectional area of the borehole, *dh* is the change in water height, and *dt* is the timestep.

Fracture Area Per Segment (m2):				0.0001728	0.0001728	0.00017279	0.00017	0.000173	...	0.00000
Volume Flowrate Table:										
Time steps	**Head**	**Qtotal**	**dh/dt**	q0	q1	q2	q3	q4	...	q100
(s)	(m)	(m3/s)	(m/s)							
0	10	0.02564	2.69762	0.00000	0.00024	0.00034	0.00040	0.00048	⋯	0.00000

Table 5: Flowrate at Timestep 0

When taking the time step between each head loss iteration '*dt*' as 1s, the final change in water height '*dh*' after 1s can be found through Equation 12:

$$dt * Q_T / A_{BH} = dh$$

Therefore, the value for '*dh*' is reduced from the initial water head to find the next water height in the next timestep. This process (finding the velocity, flowrate, and head loss) is repeated for t=1, t=2, t=∞ …

Summarized Results from Starting Parameters:

Timesteps	**Head**	**Qtotal**	**dh/dt**	**dh**
(s)	(m)	(m3/s)	(m/s)	(m)
0	10.00	0.0256	2.6976	2.6976
1	7.30	0.0043	0.4503	0.4503
2	6.85	0.0032	0.3355	0.3355
3	6.52	0.0028	0.2990	0.2990
4	6.22	0.0026	0.2714	0.2714
5	5.95	0.0024	0.2541	0.2541
6	5.69	0.0023	0.2407	0.2407
7	5.45	0.0022	0.2273	0.2273
8	5.22	0.0020	0.2138	0.2138
9	5.01	0.0019	0.2003	0.2003
10	4.81	0.0018	0.1868	0.1868
11	4.62	0.0016	0.1731	0.1731

Table 6: Results of Change in Flow with Timesteps

Flow Factors due to Fissure Resistance

Adding the flow factor to the parametric model was a simple addition, where each velocity at each fissure is multiplied by the factor. This factor would vary from 0 to 1, with 1 being unimpeded flow with no losses or resistances.

The resulting head loss graph from on-site borehole testing is compared to the model's head loss graph, and the curves are matched by adjusting the resistance factor until they are sufficiently overlapping each other.

Due to the wide variabilities of fissures at different locations, it was ideal to obtain multiple average factors depending on the defining characteristics. A fissure infilled with clayey soil would be largely impermeable, whilst an empty fissure would have a factor depending on the average roughness. These factors were added within a drop-down list which are easily selectable in the parametric model.

Borehole Filter Material

The borehole cross-sectional area is used in calculating the rate of head loss with time, since a large diameter borehole would experience a slower head loss than if the borehole was much narrower. This cross-sectional area would be further reduced when the water filtering medium is added into the borehole.

The minimum percentage area which can be taken by loose gravel may be estimated to fill around 50% of the available area. Of course, with finer materials, less voids may be present, greatly limiting the volume of water available within the borehole at any given time.

The filter material may be defined in the model with a drop-down list menu presenting the most common gravel types and the area reduction percentage. The void ratio may then be multiplied by the empty cross-sectional area of the borehole to find the new available area, as seen below (Equation 16):

$$A_{BH} = \pi r^2 \times e$$

Equation 16

Where A_{BH} is the final cross-sectional area used in Equation 13, r is the radius of the borehole cavity, and e is the void ratio of the fill material.

List for BH filter material:
Gravel [0.50 void ratio]
Coarse Sand [0.45 void ratio]
Fine/Silty Sand [0.40 void ratio]
No Filter Material

Figure 4.4: BH Filter Materials

Another important consideration is the hydraulic permeability of the filler material itself. While the model assumes no impedance to head loss, filling the borehole cavity with material can slow water flow, potentially reducing the flow rate over time.

This effect must be accounted for to ensure accurate predictions and effective borehole design for managed aquifer recharge projects. However, this effect is normally only detrimental when the filter medium's permeability is less than the borehole walls' permeability.

Borehole Casing

A number of sites require the usage of permanent borehole casing within looser material, such as soil at surface level, in order to prevent internal collapse and subsequent blocking of the cored hole. This casing can be considered within the model with an input depth value. This value is tied into the resulting flowrates at each segment by halting flow entirely.

Taking an example, a 0.5m depth of soil and sediment may require a casing, resulting in an impermeable layer which blocks any flow within that initial depth (See Table 7).

Table of Resulting Values at t=0 with BH Casing of 0.5m					
Segment	Depth	Discharge Velocity	Fissure Num.	Fissure Area	Flowrate
(#)	(m)	(m/s)	(#)	(m2)	(m3/s)
	h	v		A	Q=Av
0	0	0	0.5	0.00017	0
1	0.1	0.0700	0.5	0.00017	0
2	0.2	0.0991	0.5	0.00017	0
3	0.3	0.1213	0.5	0.00017	0
4	0.4	0.1401	0.5	0.00017	0
5	0.5	0.1566	0.5	0.00017	0
6	0.6	0.1716	0.5	0.00017	2.964E-05
7	0.7	0.1853	0.5	0.00017	3.202E-05

Table 7: Blocking of Flowrate from 0m to 0.6m Depth due to Casing

Visualising the Borehole Model

Managing a large number of input parameters can be challenging, making visualization essential. Visualizing the borehole as inputs are varied allows for a clearer understanding of the model. The key aspects to display include overall dimensions, average fissure placement, and borehole casing.

While setting up depth, diameter, and casing variables is straightforward, configuring fissure data is more complex (Table 8). This involved presenting the average fissure number per segment along the entire length of the borehole. These fissure numbers were then added together one segment at a time. Each whole number reached would place a fissure at that specific segment.

This would end up aiding the user in understanding the ground characteristics which have been input, and the resulting designed borehole. The result is shown in Figure 4.5.

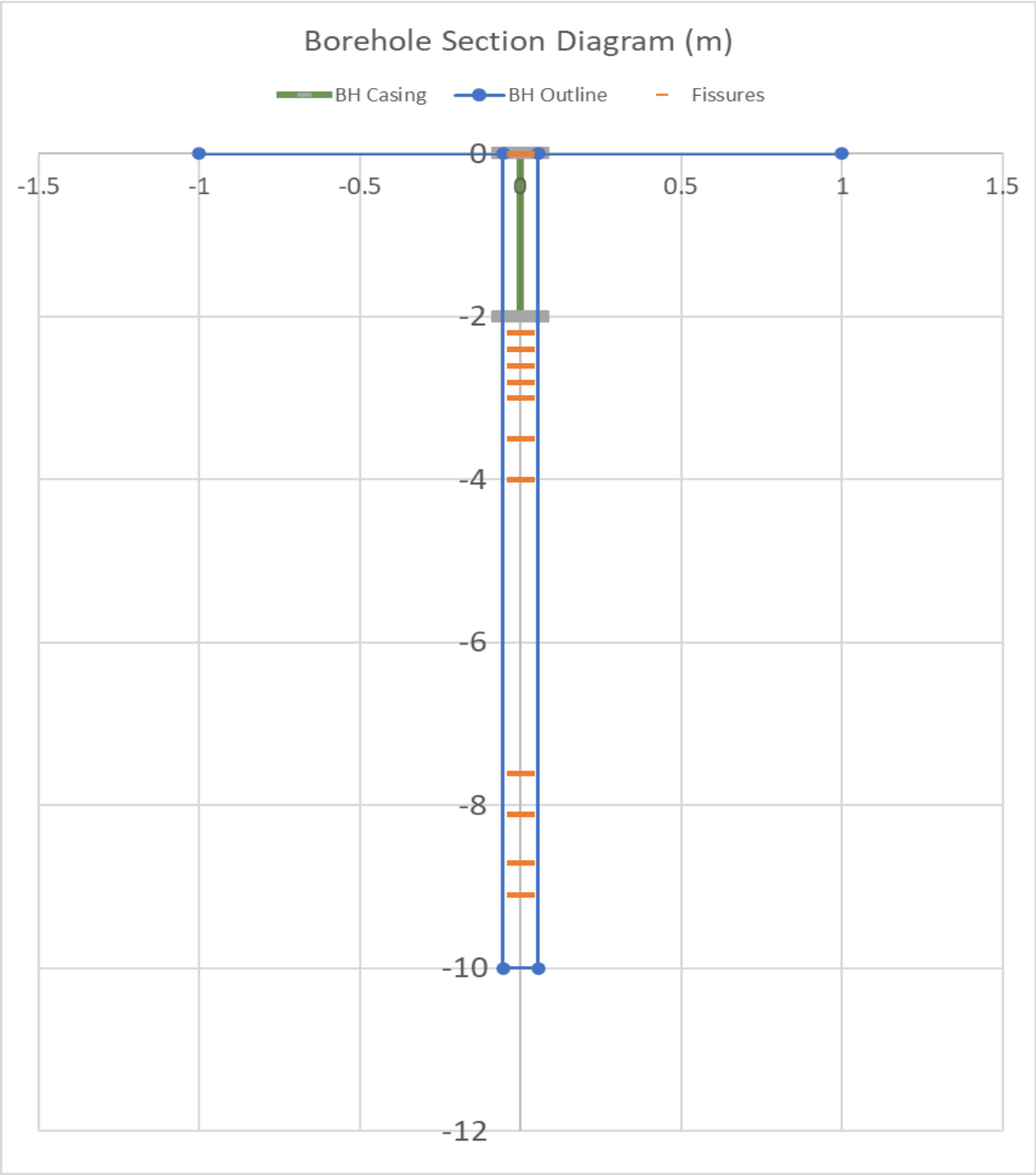

Figure 4.5: BH Section Chart

Segment Num (#)	1	2	3	4	5	6	7
Segment Depth (m)	0.094	0.188	0.282	0.376	0.47	0.564	0.658
Fissure Area (m_2)	0.00041	0.00041	0.00041	0.00041	0.00041	0.00041	0.00041
Fissure Amount (#)	0.94	0.94	0.94	0.94	0.94	0.94	0.94
Fissure Addition	0.94	1.88	2.82	3.76	4.7	5.64	6.58
Draw Fissure? (Y/N)	N	Y	Y	Y	Y	Y	Y

Table 8: Converting Fissure Data into Visual Graph Data

4.3 Model Calibration

The fissure flow factor 'F_F' considers the unknown variable resistances to flow, depending on the fissure characteristics. The flow factor is multiplied by all values in the water velocity table for fissure flow.

Below is an example of how adjusting the flow factor changes the parametric model's head loss curve:

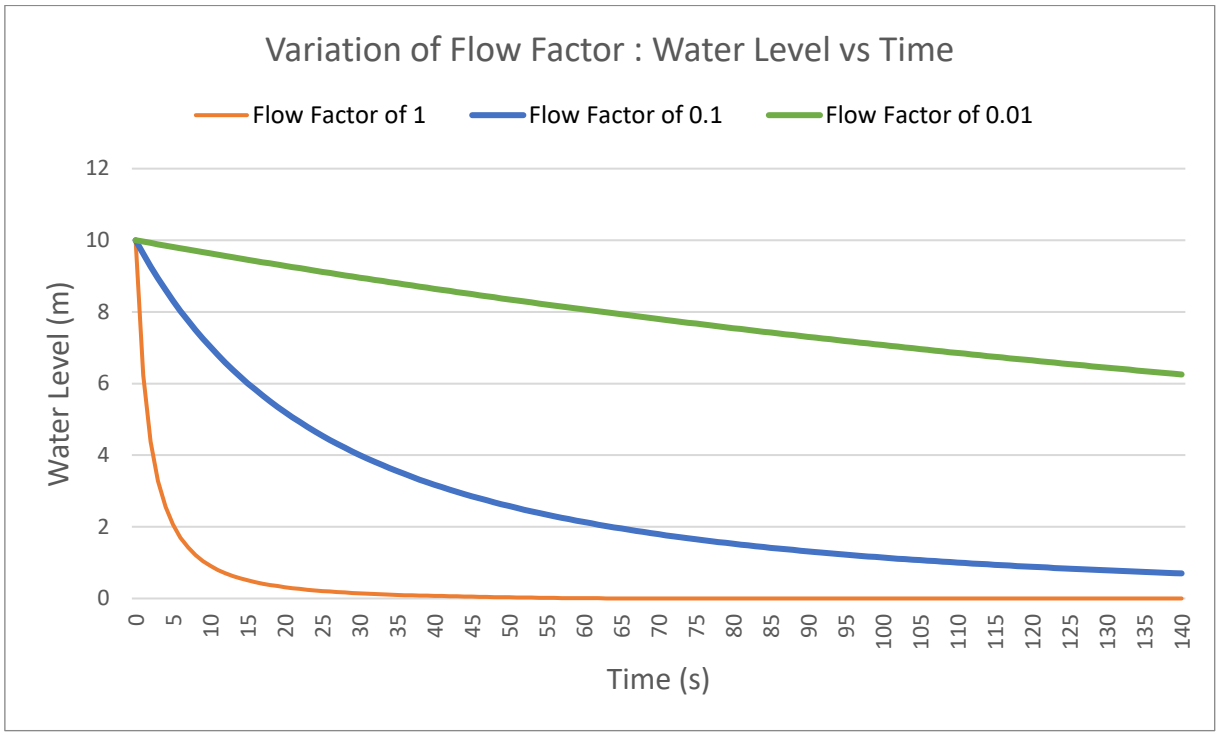

Figure 4.6: Variation of Flow Factor on Head Loss

After tabulating the rate of head loss of various on-site falling head permeability tests from sites of differing ground characteristics, the results were depicted in a series of graphs. A trendline can be drawn between all the individual time recordings, and a gradually decreasing curve should be visible, as the rate of head loss decreases over time. This can be seen in the permeability test sheets in Appendix C.

Once the core drilling records are received and the preliminary BH and fissure data is input into the parametric model, the permeability test's head loss curve is then superimposed onto the parametric model's curve, so as to facilitate the trial-and-error approach of inputting and adjusting the flow factors until a curve which best fits the test's trend line is found.

On the next page is a number of examples of how adjusting the flow factor changes the parametric model's head loss curve, making use of an on-site test trend line that would need to be compared to.

Comparison of Flow Factor Adjustment in Relation to On-Site Test Results (Test ID: Att.T1):

Flow Factor of 0.5 (Low Resistance):

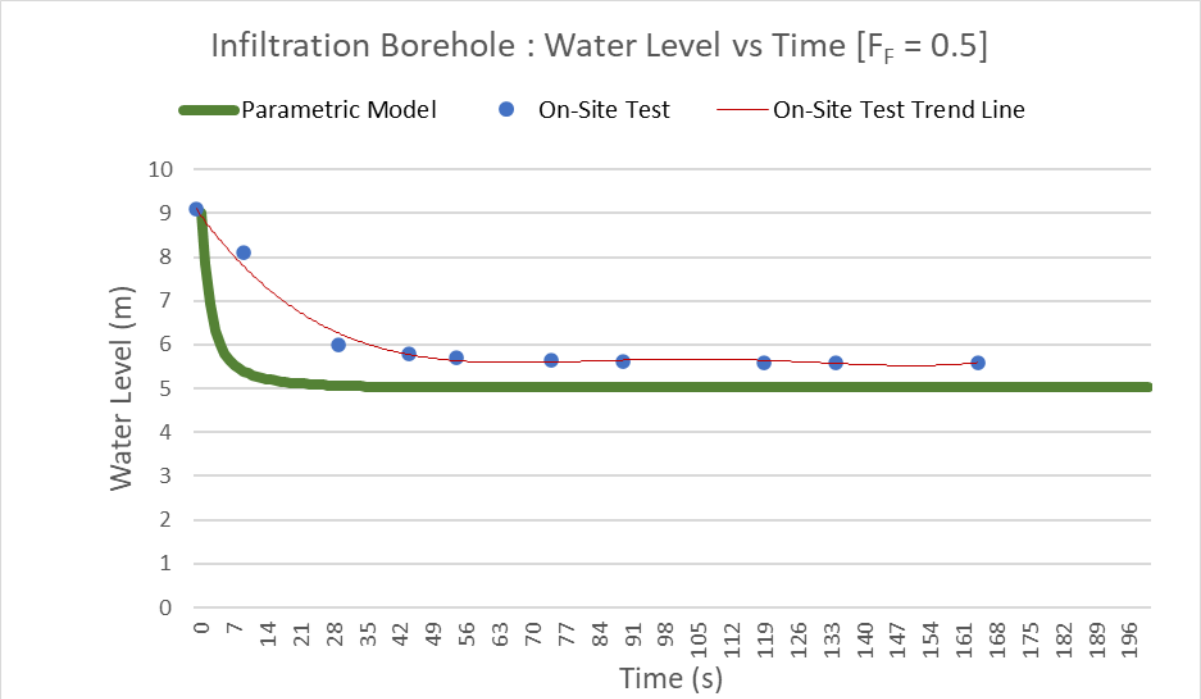

Figure 4.7: Att.T1 Test Values overlayed with Flow Factor = 0.5

Flow Factor of 0.005 (High Resistance):

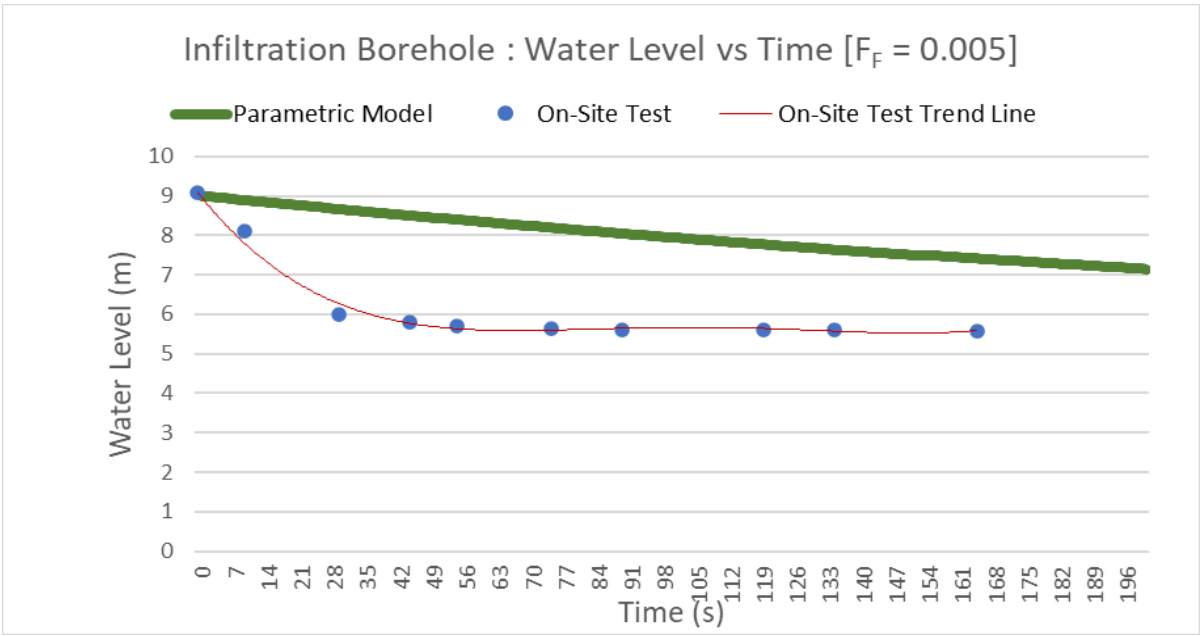

Figure 4.8: Att.T1 Test Values overlayed with Flow Factor = 0.005

5 DATA ANALYSIS & DISCUSSION

5.1 MODEL SENSITIVITY ANALYSIS

This section provides a detailed sensitivity analysis of the ground permeability predictive model. The analysis examines the impact of various input parameters on the resulting flow rates and aims to draw meaningful conclusions from these observations.

5.1.1 Pores vs Fissures

The parametric model was tested through the comparison between primary and secondary permeability. Through this model, one can deduce the effectiveness fissures may have on ground permeability more than pure reliance on the pores of intact rock.

Two versions of the same model were set with the following initial base parameters:

V1: Coralline Limestone; *V2*: Globigerina Limestone

Borehole Depth = 10m

Borehole Diameter = 0.1m

V1: Coralline Limestone hydraulic conductivity of 5×10^{-7} m/s

V2: Fissure Aperture Width of 1mm

RQD Input = 90% spread throughout the entire depth; 1m core runs

Initial outputs revealed that fissures through globigerina limestone produce a significantly greater flowrate, than the reliance of coralline limestone pore permeability.

Q_{Pore} results in a flowrate of 42.5819cm^3/s

Alternatively, $Q_{fissure}$ only came close in value to Q_{Pore} when only a single fissure was introduced at the base of the borehole (Final 1m Run: RQD=90%). In addition, a Flow Factor of 0.001 was required, representing a degree of infill within the fissure (See Figure 5.1).

From these findings, one can conclude that MAR Projects should always be located in highly fissured areas, to maximize on the recharge potential, and one should not rely on the porous nature of CL to accomplish enhanced aquifer recharge.

Nonetheless, it may be advantageous to locate fissured areas within CL, to make use of both permeabilities within infiltration boreholes.

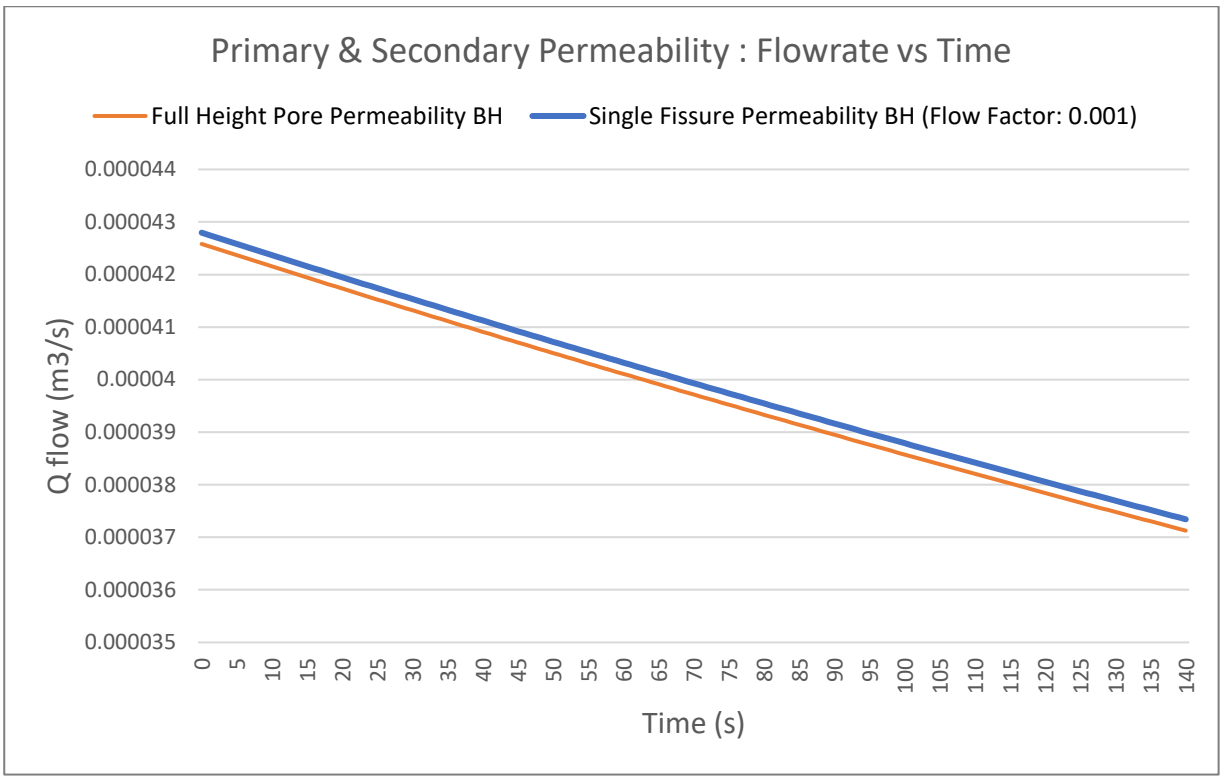

Figure 5.1: Primary vs Secondary Permeability in BHs

5.1.2 Depth vs Diameter

In this sub-section, the parametric model is tested through the variation of depth and diameter and its effects on secondary permeability. Through this model, one is able to find more efficient borehole dimensions to maximise ground permeability or cost efficiency.

The model was set with the following initial base parameters:

Globigerina Limestone

Borehole Depth = 10m

Borehole Diameter = 0.1m

RQD Input = 90% spread throughout the entire depth; 1m core runs

Aperture Width of 1mm

Flow Factor of 0.05

The resulting output Q flowrate due to the aforementioned parameters = 1477cm^3/s

In a hypothetical scenario where the flowrate was required to be doubled, one may ask the question:

"*Is it more cost effective to increase the diameter or the depth of the borehole?*"

The answer is not straightforward, since it would depend entirely on if drilling a deeper borehole will expose more underground fissures through which water can flow.

Assuming that the 90% RQD continues throughout the rock depth, the values in Table 9 represent an increase in either the borehole diameter or the borehole depth respectively. Both parameter sets were adjusted until they result in an equal maximum volume flowrate of water of ~2950m^3/s, that being a 100% increase in the initial Q flowrate.

Version 1: Increased Diameter		Version 2: Increased Depth	
100	% increased Flowrate	100	% increased Flowrate
0	% increased Depth	60	% increased Depth
100	% increased Diameter	0	% increased Diameter
0.1	**m extra diameter**	**6**	**m extra depth**

Table 9: Diameter Increase vs Depth Increase Parameters

Additionally, a second question can be asked:

"Which measurement affects BH head loss the most? Diameter or depth?"

Assuming that the 90% RQD continues throughout the rock depth, the variance of the volume flowrate over time due to head loss was plotted and compared between the two alternate sets of parameters (Figure 5.2; See Appendix A for the full model data sheets):

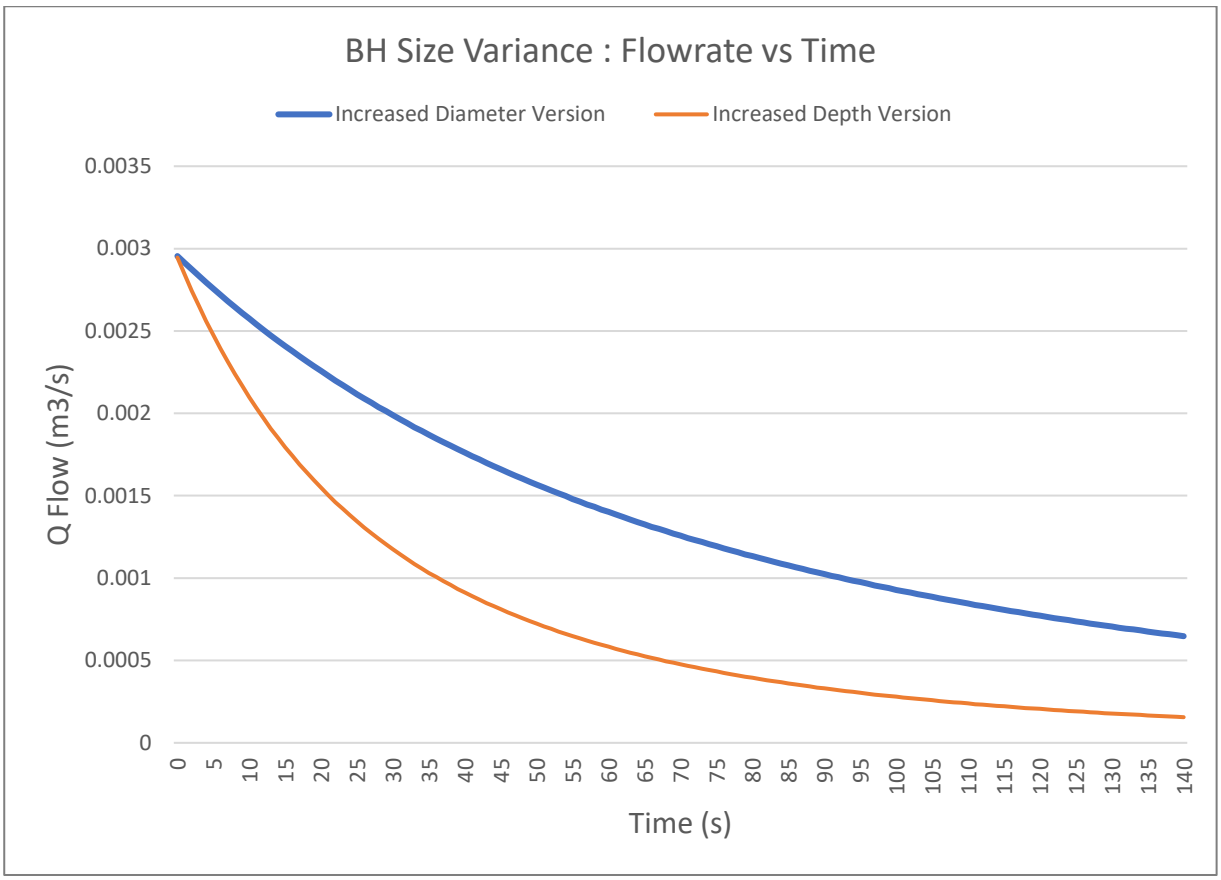

Figure 5.2: Flow Reduction Curves with BH Dimension Variance

The following table compares the volume capacity of each version of borehole of equal flowrate but different dimensions (Table 10):

Version 1: Increased Diameter		Version 2: Increased Depth	
Q	0.00295m^3/s	Q	0.00295m^3/s
0.2	m Diameter	0.1	m Diameter
10	m Depth	16	m Depth
0.3142	**m3 Total Water Volume**	**0.1257**	**m3 Total Water Volume**

Table 10: Diameter Increase vs Depth Increase - Volume Capacity 1

A method of analysing the change in volume capacity for each version is through a step-by-step percentage increase of both diameter and depth (Table 11):

Increased	Diameter	Depth
(%)	Volume (m3)	
0	0.0785	0.0785
10	0.0950	0.0864
20	0.1131	0.0942
30	0.1327	0.1021
40	0.1539	0.1100
50	0.1767	0.1178
60	0.2011	0.1257
70	0.2270	0.1335
80	0.2545	0.1414
90	0.2835	0.1492
100	0.3142	0.1571
Default of 0.1m ⌀ and 10m Depth		

Table 11: Diameter Increase vs Depth Increase - Volume Capacity 2

'Depth vs Diameter' Observations:

1. In order to increase initial flowrate by 100%, the diameter had to also be doubled with an increase of 100%, albeit at a small change of 10cm. On the other hand, depth needed to be increased by 6 metres, at a 60% increase in total depth.
2. The resulting curves showed that an increased diameter retains an elevated flowrate far exceeding the increase in depth during a falling-head flow event.

'Depth vs Diameter' Conclusions:

1. If the required boring machinery is available, it may be more efficient and practical to increase flowrate by increasing the borehole diameter, than it is to core deeper boreholes. This conclusion is valid only when assuming relatively constant ground and fissure characteristics. A change in rock type or fissure amount at much deeper depths may thereby change this assumption entirely.
2. An increased borehole diameter leads to larger volume capacity at any given segment of the borehole which would take longer to deplete. Therefore, water pressure is retained for a longer period of time.
3. Further to the previous point, an increased borehole diameter leads to an overall larger volume of water within the borehole, despite the fact that the depth increase required an extensive additional 6 metres. These conclusions however do not consider other aspects which are involved in the design of MAR projects, one being any space constraints which would limit the borehole diameter.

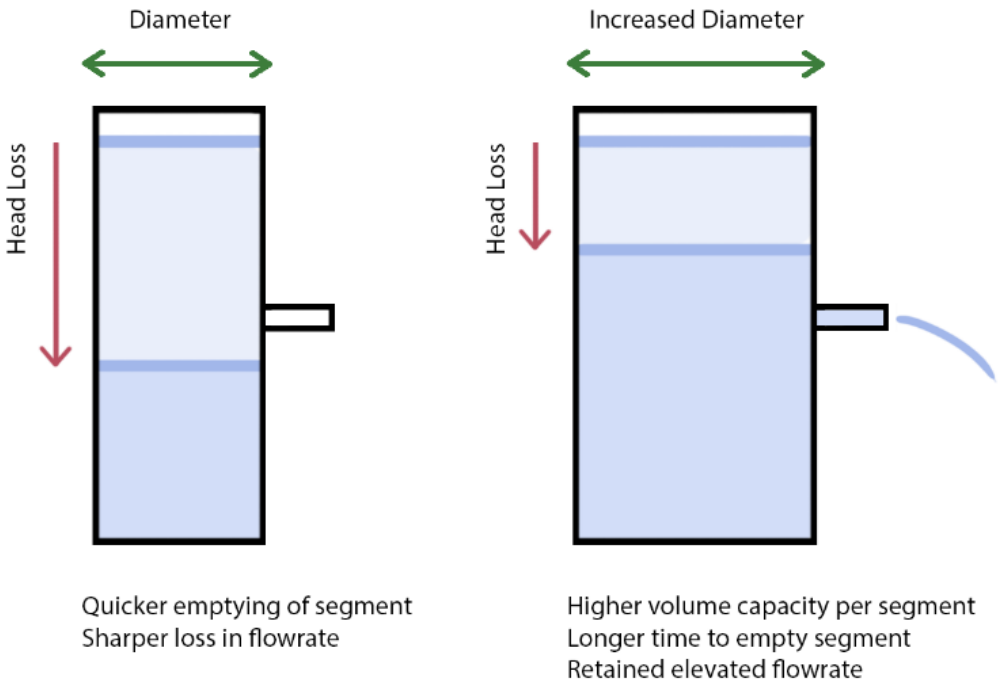

Figure 5.3: Increased Diameter of BH Diagram

5.1.3 Flowrate vs Diameter

Instead of considering the change over time during falling-head conditions, the change of initial steady-state flowrate depending on the borehole dimension variables can also be visualised and plotted to identify any correlation:

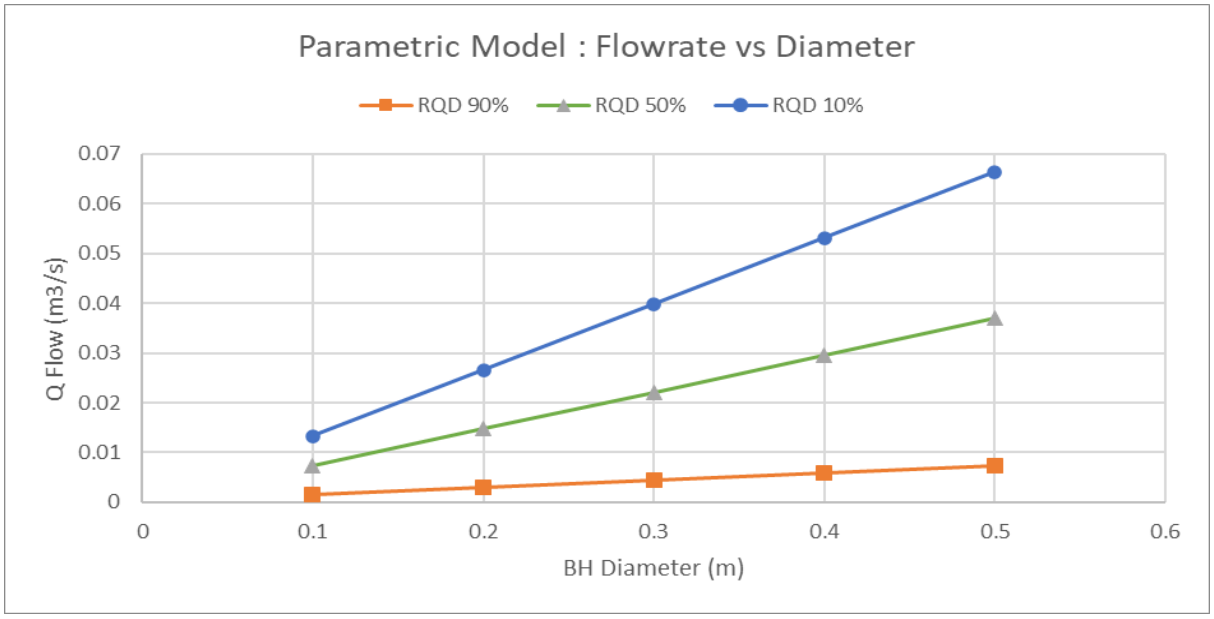

Figure 5.4: Chart of Flowrate Increase with Diameter Increase with Varying RQD Spread

'Flowrate vs Diameter' Observations:

1. It was found through the model that flowrate increased linearly with diameter. This result is to be expected, since the equation Q=Av would consider velocity as the 'constant' at any given fissure depth. The only variable is the increase in exposed fissure area for flow.
2. It was also noted that more fissured rock will result in a larger increase in flowrate with a diameter increase than less fissured rock.

'Flowrate vs Diameter' Conclusions:

1. If the site conditions are unsuitable for efficient aquifer recharge due to largely intact rock, then it will likely still not be suitable even if the borehole diameter were to be increased.
2. Highly fractured rock will result in large increases in flowrate when diameter is increased when compared to mainly intact rock.

5.1.4 Fissure Concentration Variance

Using the same initial parameters from 5.1.2 but varying the RQD spread to reflect varying ground conditions, where the first figure represents fissures on the lower-half of the borehole, and the second figure represents the fissures on the upper-half:

Fissure Distribution Table [Borehole Log Runs]

Core Run: (#)	Core Length Input Values: (m)	RQD Input Values: (%)	Core Run Max Depth: (m)	Fissured Lengths: (m)	Fissure Number per Run: (#)	Fissure Number per Segment: (#)
1	1	100	1	0	0	0
2	1	100	2	0	0	0
3	1	100	3	0	0	0
4	1	100	4	0	0	0
5	1	100	5	0	0	0
6	1	90	6	0.1	1	0.1
7	1	90	7	0.1	1	0.1
8	1	90	8	0.1	1	0.1
9	1	90	9	0.1	1	0.1
10	1	90	10	0.1	1	0.1

Table 12: RQD Variation 1

Fissure Distribution Table [Borehole Log Runs]

Core Run: (#)	Core Length Input Values: (m)	RQD Input Values: (%)	Core Run Max Depth: (m)	Fissured Lengths: (m)	Fissure Number per Run: (#)	Fissure Number per Segment: (#)
1	1	90	1	0.1	1	0.1
2	1	90	2	0.1	1	0.1
3	1	90	3	0.1	1	0.1
4	1	90	4	0.1	1	0.1
5	1	90	5	0.1	1	0.1
6	1	100	6	0	0	0
7	1	100	7	0	0	0
8	1	100	8	0	0	0
9	1	100	9	0	0	0
10	1	100	10	0	0	0

Table 13: RQD Variation 2

The following head-loss graph is plotted, showing the reduction in volume flowrate between each fissure spread type (Figure 5.5; See Appendix A for the full model data sheets):

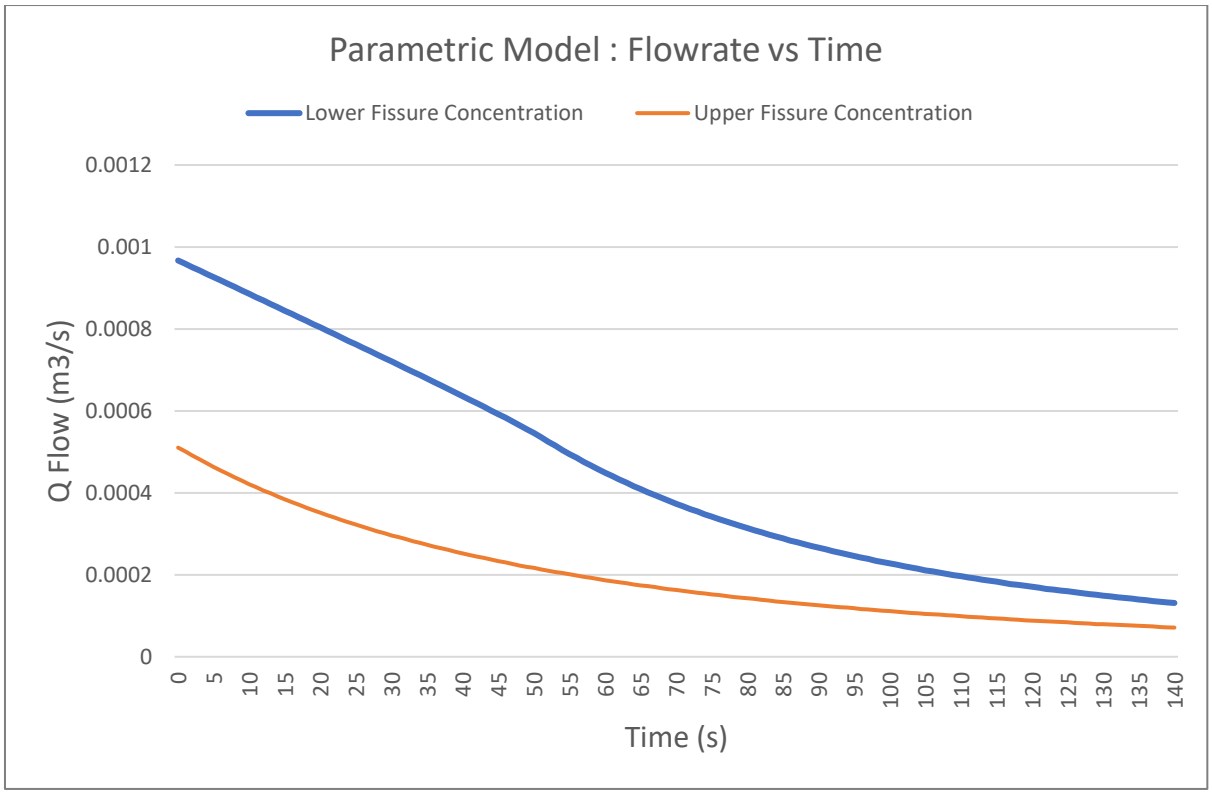

Figure 5.5: Flow Reduction Curves with Fissure Concentration Variance

'Fissure Concentration Variance' Observations:

1. A larger flowrate is recorded when fissures are located at larger depths.
2. Flowrate stagnates when fissures are located close to the surface.
3. Lower fissure concentration leads to a more drastic loss in flowrate.

These three points are relevant when it comes to designing infiltration boreholes in globigerina limestone. Real-world observations indicate that the rock surface tends to be the most fissured section due to being within the weathered zone.

'Fissure Concentration Variance' Conclusions:

1. Due to Torricelli's law applied to the parametric model's theoretical framework, fissures experiencing larger water pressures will experience an increased outflow velocity.
2. Fissures close to the surface do not experience large water pressures, and hence, the flowrate is slow. Additionally, as the head loss approaches the 'last fissure' within the upper concentration, flow will halt, and semi-permanent water stagnation will result.

5.2 Application to Rainfall Catchment Areas

A number of potential sites were inspected through various maps and imagery, and two were selected based on the requirements as outlined in Section 3.3.

The following sites were selected based on Section 3.3, and their results were analysed:

- Wied is-Sewda (Wied il-Kbir Catchment Area, Ħal-Qormi)
- Wied Katarina (Wied il-Għasel Catchment Area, Burmarrad)

The in-depth analysis of each of these sub-catchments can be found in Appendix B.

5.2.1 Observations & Conclusions

The ground infiltration model could serve as a foundation for designing an extensive MAR network along Maltese watercourses. Enhancing groundwater recharge throughout the watercourse length is one of the most efficient and space-saving methods for conserving rain runoff. Concentrating water capture methods in a single location is often unfeasible for certain catchment areas. However, pairing infiltration boreholes with existing embankment dams could still be advantageous. By doing so, the volume of water held within the basin can be effectively infiltrated at one spot, preventing the borehole from being overwhelmed and reducing the risk of water discharging out to sea.

This method of designing the most efficient and effective infiltration borehole may be applicable to smaller, localized catchment areas, such as rainwater collected from rooftops. However, its necessity might be questionable for such applications. Since the model requires investigating ground fissure conditions through a single borehole, and rooftop catchment areas would likely only need one infiltration borehole, the minimal intervention approach becomes less relevant. This negates the need for extensive time, effort, and financial resources dedicated to a full MAR project, as the project would essentially be complete after digging a single borehole.

5.3 Falling Head Permeability Tests

This sub-section deals with the on-site water permeability tests which took place at various locations around Malta, and the analysis process of the recorded results.

The result sheets for the falling head permeability tests are presented in Appendix C, with their subsequent parametric model comparison sheets. The borehole drilling records are also found in Appendix C for each tested borehole, which include the core runs and their assigned RQD percentages.

To facilitate the comparison and analysis between the two permeability curves, several assumptions were made:

- RQD percentage values between 98% and 99% were treated as 100% to account for human-caused breakages to facilitate storage and transportation of core pieces.
- Average fissure widths were assumed for certain drilled boreholes because such data cannot be reliably retained from a recovered core unless a camera is lowered into the borehole cavity.
- A “best fit” trendline curve was used for curve comparison and model calibration due to the risk of human errors in timing affecting individual readings.

The following process took place to obtain and analyse the data from the falling head permeability tests:

1. Water depth vs time interval readings, with more concentrated timings at the start of the test and further apart timings once the flowrate slows significantly.
2. Recorded values are compiled digitally and plotted in a graph. A trend-line is drawn.
3. Upon receiving the borehole drilling records, the RQD data is input into the parametric model, along with the borehole dimensions and ground characteristics.
4. The parametric model’s head loss curve and the on-site test’s head loss curve is compared, and a flow factor is obtained.
5. Observations and conclusions are derived.

The following sites were tested, and their results were analysed:

- Attard [Tested by the author, 2024]
- Kalkara [Tested by the author, 2024]
- Birkirkara [GEO-INF, Tested by N. Borg, 2012]
- Fgura [GEO-INF, Tested by N. Borg, 2012]

Each site was also labelled with a short code in order to simplify the referencing process between each document and result sheet:

Test Reference Code = (Locality) . (Test Number of BH)

Ex: Attard site, 1st test which occurred on the specified borehole = "Att.T1"

Attard	Kalkara	Birkirkara	Fgura
Att.T1	Kal.T1	Bir.T2	Fgu.T2

Table 14: List of Test Sites & Their Created Reference Codes

Detailed analyses of each borehole's results are available in Appendix B, which includes the input and output processes and the derivation of each flow factor. These results are summarized in Table 15.

5.3.1 Observations

Att.T1 in particular showed that the parametric model's theoretical framework may in fact accurately describe ground permeability through fractures.

The on-site head loss curve of Att.T1 occurs at a varying slope very similar to the parametric model's head loss curve. This may signify that fractures throughout an infiltration borehole may conservatively yet accurately emulate flow similar to the simplified theory of pipe flow and emptying tanks with multiple openings (See Figure 5.6; Full results & analysis in Appendix B). This point is confirmed due to the low percentage difference of head loss at specific timesteps.

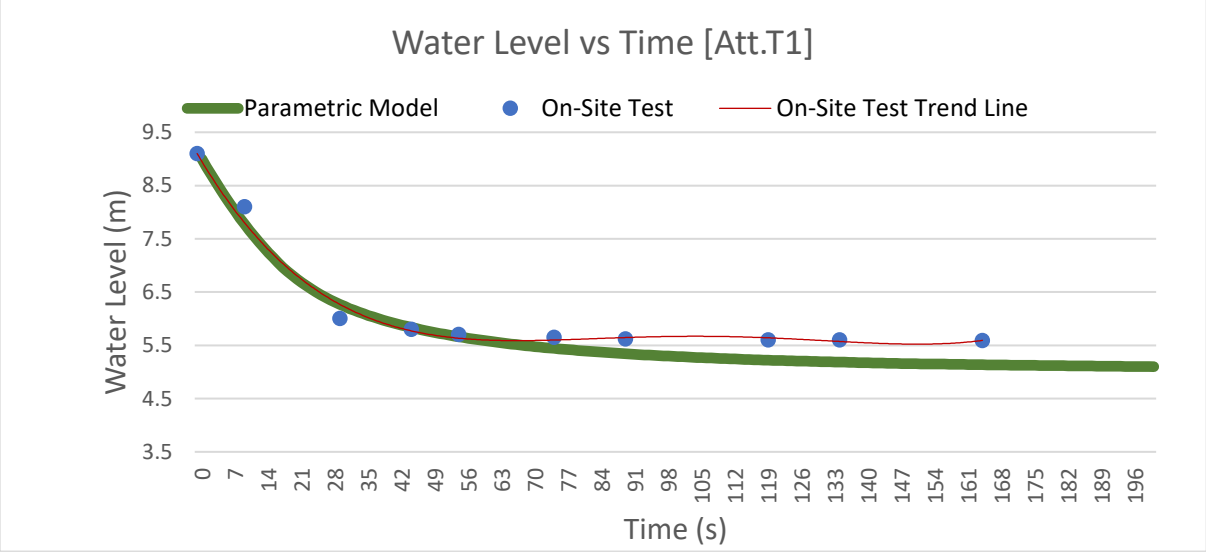

Figure 5.6: Att.T1 Test Values overlayed with Flow Factor = 0.065

A number of boreholes had their RQD variations concentrated at the surface, in what is known as the weathered zone. However, borehole casings installed through this layer prevents the ability to make use of the fractures for enhanced secondary permeability. Nonetheless, casings are usually required to prevent the core wall from crumbling and collapsing into the space.

A number of reasons may explain an unexpected halt in head loss or extremely low flowrates within some of the infiltration boreholes:

1. A significant number of fissures are infilled with an impermeable material.
2. The fissures may not be deep in length and quickly fill with water throughout the initial filling process.
3. The fissures may have been sufficiently deep in length but were subsequently filled with water during the coring, cleaning, and filling process, or due to rainy weather conditions.
4. The fissures may have been initially not infilled, but the coring, cleaning and filling process may have introduced core debris and saturated mud into the fissures and subsequent smearing of the mud on the borehole walls. (As may have been the case for Kal.T1).

5.3.2 Summarized Results

Location	Attard [Att.T1]	Kalkara [Kal.T1]	Birkirkara [Bir.T2]	Fgura [Fgu.T2]
Max Q (cm^3/s)	1220	9.55	31.8	6.67
F_F ($x10^{-3}$)	65	0.21	0.5	0.065
Infill	No Infill	Clayey Soil	Red Clayey Soil	Red Clayey Soil
RQDs	Moderate	Low	High	Low
BH Depth (m)	9	8	21	22
BH Diameter (m)	0.10	0.10	0.14	0.10
Height MSL (m)	+68	+37	+39	+43

Table 15: Summarized Table of Results for Permeability Tests & Model Calibration Flow Factors

Analysis of Results:

1. A correlation between the initial flowrate and the Flow Factor, since the largest flow factor is linked to highest initial flowrate, and the lowest flow factor is linked to the lowest initial flowrate. This makes sense since the flow factor calculation directly adjusts the resulting flowrate.
2. Tests in highly fractured rock (low RQD) still showed the lowest Flow Factors, indicating high resistance to flow. This finding was contrary to initial expectations.
3. Boreholes with fissures infilled with clayey soil had the three lowest Flow Factors.

4. The borehole without recorded infill material had the highest Flow Factor, indicating low resistance to flow.
5. No correlation was observed between borehole depth and Flow Factor.
6. No correlation was observed between MSL height and Flow Factor.
7. Not enough data on the effect of borehole diameter on Flow Factor.

Conclusions:

1. The RQD values and its spread may not immediately dictate the flowrate through the borehole. The more prominent factor would be the infill material characteristics.
2. Borehole depth would also not necessarily dictate flowrate. Depth would only have a prominent effect if the drilled core reached porous coralline limestone or caves and phreatic tubes.
3. Fissures infilled with clayey soil exhibit extreme resistance to flow when compared to empty fissures. Bir.T2 and Fgu.T2 boreholes were both recorded to have a number of fissures infilled with “Terra Rossa”.
4. Significantly more testing needs to be done to consider having a reliable flowrate estimate due to the potential variability of Flow Factors. In particular, more tests should be done to determine if fissures without any infill material accurately emulate the flow through a simplified pipe model, similar to the results in Att.T1.

6 CONCLUSIONS & FINAL REMARKS

6.1 RESEARCH INTENTION

The main aim of this dissertation was to assess whether the complexity of ground conditions in the Maltese islands can be estimated and simplified to derive a conservative yet useful conclusion to the guidance of potential managed aquifer recharge sites. While the strategic placement of managed aquifer recharge facilities within high-flow catchment areas, particularly valleys, is logical, the diverse and site-specific nature of ground conditions necessitated a nuanced approach to site assessment and prioritization.

Conventional ground-testing techniques often involve invasive methods, which may be impractical or challenging to implement in certain catchment areas. In such cases, the ability to estimate potential infiltration rates at specific collection points becomes invaluable, allowing for informed decision-making without the need for extensive on-site intervention.

While an array of wide-diameter dry wells would be advantageous for maximizing infiltration, it is impractical to implement such a project without prior knowledge of what permeability rates one would expect. The use of single small-diameter cores can suffice to determine rock quality designation and rock porosity, thus minimizing the risk of investing resources in unsuitable sites.

By deriving the material depths and RQD percentages throughout the rock strata, the prepared computer model (Figure 6.1) may be used to optimize site-specific infiltration borehole diameter and depth, maximizing water infiltration while minimizing time and costs. The sensitivity analysis conducted in Chapter 5 exhibited the influence of parametric variations on infiltration rates.

The development of the ground model involved extensive research and iterative refinement. Starting from a rudimentary impermeable pipe concept with one opening, the model evolved into an advanced borehole model incorporating varying fissure depths and resistance characteristics.

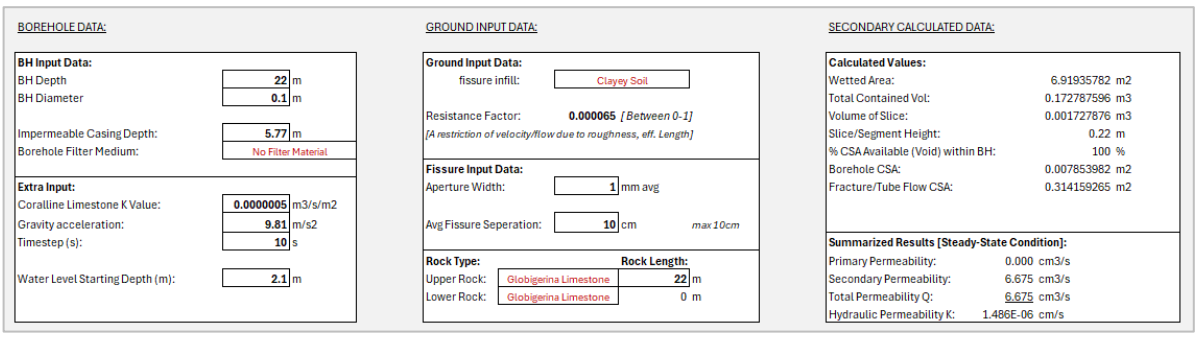

Figure 6.1: Input & Output Data of Parametric Model

6.2 Permeability Tests & The Flow Factor

The second phase of the dissertation, which involved locating suitable sites for the falling head permeability tests, proved to be labour-intensive and challenging. Some initially promising sites were hindered by issues such as borehole collapse, particularly in areas with agricultural soil and loose surface rock.

Overcoming these challenges required effective communication, strategic planning, and perseverance. Upon completion of the permeability tests, additional waiting time was necessary for the documentation and logging of recovered cores to obtain the RQD values.

Certain assumptions also had to be made during the analysis stage of the permeability tests in order to derive the flow factor for those specific site conditions. As it stands, these factors are of low confidence. However, providing that the established theoretical model within this dissertation is applied to more locations, further tests can be conducted to refine these factors for many different site characteristics.

An issue that remains unaddressed is the potential variability in the hydraulic conductivity of Coralline Limestone. As observed in one of the permeability tests (Kal.T1), the cored surface was likely coated with saturated clayey mud, which significantly reduced secondary permeability. This coating could also impact primary permeability. This issue may be solved by washing the borehole with a high-pressure jet.

One proposed solution is to apply the Flow Factor to the pore flowrate. However, this solution's efficacy remains uncertain, as almost no coralline limestone sites were encountered during the research for this dissertation. Consequently, it is unclear whether the Flow Factor, used to represent fissure resistances, can also be applied to the blocking of pores. Further research involving sites with coralline limestone is necessary to validate this approach.

6.3 Parametric Model Review

The parametric model was built from a theoretical framework which resulted in a number of predictions on the behaviour of infiltration boreholes in local fractured rock strata:

1. The water head loss in an emptying BH decreases with time.
2. The flow velocity through fissures in an emptying BH decreases with time.
3. The volumetric flowrate in an emptying BH decreases with time.
4. Fissure concentration may provide a rough estimate of ground infiltration in local rock strata through the use of RQD percentages along a borehole’s depth.

The first three points were proved to be correct through the variable head permeability tests conducted on on-site boreholes.

Regarding to the fourth point, fissure amount and location may have a correlation to ground permeability, but the main deciding factor on the flowrate volume appears to be the infill material and its resistance to flow.

An important observation to note is that the flow rate from secondary permeability is significantly higher than that from primary permeability. This indicates that infiltration boreholes are predominantly effective in fractured rock, rather than relying solely on pore permeability.

One of the research questions listed at the start of the dissertation was the following:

> "Can water permeability rates in Maltese rock strata be reliably estimated through analysis and modelling of its pores and fractures?"

After reviewing the results from the parametric model, one can assume that the theory behind the model may be accurate enough to guide future managed aquifer recharge projects. However, the only way to properly test the model would be to conduct significantly more permeability tests on recovered core boreholes, in order to continuously recalibrate and increase the confidence in the results. Due to time and access constraints, the model may presently be of low confidence and final permeability results may still unpredictably vary from site to site (See Table 15 for the obtained F_F values as of writing this paper).

The primary limitation of the ground permeability model is to obtain flow factors which consider the many unknown flow resistances within fissures: infill material, roughness, effective infiltration depth, and hydraulic gradient.

Obtaining a wider table of flow factors depending on a wider range of fissure and rock characteristics will further increase the confidence and accuracy of the model (Table 16). As such, through many more tests, the parametric model may become a very powerful tool in the estimation of groundwater recharge.

Proposed Table of Flow Factors F_F for MAR Ground Model ($x10^{-3}$)					
Fissure Infill Type:	No Infill	Coarse Sands	Fine Sands	Clayey Silt	Clay
Globigerina Limestone:					
Coralline Limestone:					

Table 16: Proposed Table of Flow Factors to be Derived

6.4 Streamlining Managed Aquifer Recharge Projects

Malta urgently needs to address local water scarcity and the deteriorating status of its groundwater bodies. Simplifying the processes for determining ground permeability and designing Managed Aquifer Recharge (MAR) projects can expedite the implementation of effective water management solutions. To this end, a flow-chart has been drafted to facilitate the preliminary analysis of valleys in Malta, aimed at optimizing the initiation and execution of MAR projects.

The established parametric model covers a portion of the chart; however, further research and development may be done on the environmental feasibility, the proposal or otherwise of a dam for a more holistic MAR project, and a more extensive cost-benefit analysis of such proposals.

To address the first two research questions posed at the beginning of this dissertation, it is evident that Maltese catchment areas and water courses can effectively capture and infiltrate stormwater runoff, and existing MAR methods are applicable in the Maltese context. Historically, structures such as recharge dams have been employed for this purpose. It has also been observed through excavation work that a large number of Maltese valleys have developed along fault lines, where the rock is inherently more fractured than other areas.

Infiltration boreholes, a form of MAR used in other countries and contexts, also hold potential. However, further local research is necessary to predict water permeability accurately and to determine whether permeability decreases over time due to sedimentation buildup.

The process of analysing a site and determining ground fissure characteristics plays a crucial role in guiding the optimal depth and design of a borehole array. By accurately identifying fissure locations, time and cost efficiency can be significantly improved. If the final stretch of rock within a borehole is found to lack fissures entirely, extending the borehole further or shortening it can prevent unnecessary drilling through impermeable layers.

On-site variable head permeability tests often reveal that fissures which are concentrated in the upper portion of the borehole lead to a complete halt in water flow at a certain depth. This insight allows for more targeted drilling and optimized borehole design, ensuring that resources are utilized effectively to enhance groundwater recharge.

6.5 Potential for National Water Strategy

Given the difficulties associated with water scarcity, which are made worse by the effects of climate change and groundwater pollution, the possibility of a national water strategy in Malta is critical.

Innovative approaches that improve groundwater recharge while reducing the consequences of runoff and flooding downstream are needed to address these problems. Infiltration borehole design is a crucial part of this strategy, and it is explored in depth in this dissertation. These boreholes can be extremely helpful in capturing and storing significant amounts of water from rain runoff, and they provide a way to force contaminants from groundwater outwards and serve as a buffer between the groundwater table and seawater intrusion.

The proposal of a parametric model simplifies the procedure for choosing, designing, and ranking managed aquifer recharge projects. Any insights derived from inputting the ground conditions and catchment details may prove a vital step in a wider national water strategy.

By taking these steps, this strategy can support Malta's water management practices' long-term sustainability and resilience in addition to addressing the country's current problems with water scarcity.

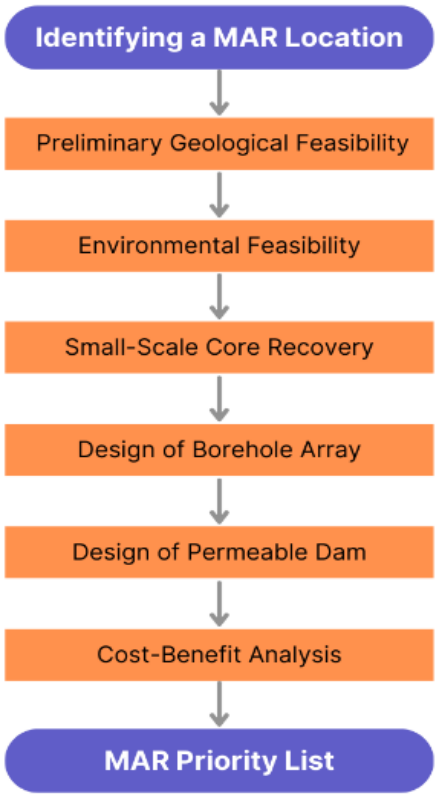

Figure 6.2: MAR Proposal Flow-Chart (2024)

6.6 Recommendations for Future Research

Identification and Derivation of Flow Resistance Factors in Fissured Rock

This research has employed simplified hydraulic equations to estimate ground permeability, incorporating flow factors to account for various ground conditions and fissure characteristics. Future research could focus on identifying a broader range of resistance factors or developing new methods to replace the current approach for more accurate estimations.

Long-Term Reduction of Infiltration Borehole Permeability

Investigating the impact of sedimentation on the permeability of infiltration boreholes is crucial. Sediment accumulation can reduce hydraulic conductivity, affecting the long-term effectiveness of managed aquifer recharge (MAR). Future studies could explore methods such as incorporating catch pits, geotextiles, and filter materials to prevent sediment buildup. Additionally, the issue of long-term borehole wall collapse, as observed in the GEO-INF Project, suggests the need for research into stabilization techniques.

Design of Permeable Dams in Valleys

Optimizing the design of permeable dams in valleys could enhance MAR projects by improving environmental flow and reducing upstream flooding risks. Future research should aim to balance water retention for recharge with the preservation of natural flow regimes, which are vital for ecosystem health and biodiversity. This involves refining design parameters to achieve the best outcomes for both water management and ecological sustainability.

REFERENCES

Abela, K. (2019, Aug 12,). Groundwater crisis remains 'unchanged' . *Times of Malta* https://timesofmalta.com/articles/view/groundwater-crisis-remains-unchanged.728363

Adi Associates. (2020a). *Catchment Summary Report 1 - Għasel.* (). RMBP Life project Geoportal: Valley Management Unit - Project Green. https://lifeip-rbmp-geoportal-valleymanagement.hub.arcgis.com/pages/masterplans

Adi Associates. (2020b). *Catchment Summary Report 2 – Kbir.* (). RMBP Life project Geoportal: Valley Management Unit - Project Green. https://lifeip-rbmp-geoportal-valleymanagement.hub.arcgis.com/pages/masterplans

alteraqua. (2022, April 11,). Malta's water saving heritage: Relic of the past or guide to the future? *Times of Malta* https://timesofmalta.com/articles/view/maltas-water-saving-heritage-relic-of-the-past-or-guide-to-the-future.947494

ARGO-E GROUP. (2011, May,). *Earth / Rockfill Dams* . www.geoengineer.org. Retrieved September 5, 2023, from https://www.geoengineer.org/education/dam-engineering/earth-rockfill-dams

Arora, S. (2016, Jan 16,). 4 recharge dams for groundwater. *The Times of India* https://timesofindia.indiatimes.com/city/gurgaon/4-recharge-dams-for-groundwater/articleshow/50599532.cms

Atlas Insurance. (2023, Aug 30,). *GEO-INF: Innovating Water Sustainability.* www.atlas.com.mt. Retrieved May 28, 2024, from https://www.atlas.com.mt/geo-inf/

Bakalowicz, M., & Mangion, J. (2003). *The limestone aquifers of Malta: their recharge conditions from isotope and chemical surveys*

Bexfield, L. M., Belitz, K., Lindsey, B. D., Toccalino, P. L., & Nowell, L. H. (2021). Pesticides and Pesticide Degradates in Groundwater Used for Public Supply across the United States: Occurrence and Human-Health Context. *Environmental Science & Technology; Environ Sci Technol, 55*(1), 362-372. 10.1021/acs.est.0c05793

Borg, J. (2018). *L-inginier Chadwick u H'Attard*. Attard : Soċjetà Mużikali 'La Stella Levantina'.

Borg, N. (2012). *Research on the use of infiltration boreholes for flood mitigation and to enhance groundwater recharge : geo-inf*. University of Malta; Faculty for Built Environment. Department of Architecture and Urban Design.

Bouwer, H., Pyne, R. D. G., & Goodrich, J. A. (1990). Recharging ground water. *Civil Engineering (New York, N.Y.1983), 60*(6), 63-66.

Bouwer, H. (2002). Artificial recharge of groundwater: hydrogeology and engineering. *Hydrogeology Journal, 10*(1), 121-142. 10.1007/s10040-001-0182-4

California Department of Water Resources. (2023, Mar 31,). *Groundwater Recharge in California.* water.ca.gov. Retrieved June 26, 2023, from https://water.ca.gov/Programs/Groundwater-Management/Groundwater-Recharge

Caruana, M. (2009). *Assessing the effectiveness of soakaways as a means for groundwater recharge*. University of Malta; Faculty for the Built Environment. Department of Civil and Structural Engineering.

Caruana, T. M. (2017). *Environmental criteria for valley management to support water conservation*. University of Malta; Institute of Earth Systems.

Cedergren Harry. (1997). Permeability; Summary Comments. *Seepage, Drainage, and Flow Nets* (pp. 69). Wiley-Interscience; 3rd edition.

Cedergren, H. R. (1997). *Seepage, Drainage, and Flow Nets* (3rd ed.). John Wiley & Sons.

D'Ambrosio, E., De Girolamo, A., Barca, E., Ielpo, P., & Rulli, M. C. (2017). Characterising the hydrological regime of an ungauged temporary river system: a case study. *Environmental Science and Pollution Research, 24*10.1007/s11356-016-7169-0

Dillon, P. (2005). Future management of aquifer recharge. *Hydrogeology Journal, 13*(1), 313-316. 10.1007/s10040-004-0413-6

ERA (Environment and Resources Authority). (2020, July,). *Nitrates Directive .* era.org.mt. Retrieved May 27, 2024, from https://era.org.mt/topic/nitrates-directive/#:~:text=All%20of%20Malta%20was%20designated,and%20Rural%20Affairs%20in%202011.

ERA (Environment and Resources Authority). (2022a, May 12,). *ERA | About Us.* era.org.mt. Retrieved July 17, 2023, from https://era.org.mt/about-era/

ERA (Environment and Resources Authority). (2022b, July 6,). *Water Catchment Management Plan .* era.org.mt. Retrieved July 20, 2023, from https://era.org.mt/topic/water-catchment-management-plan-2/

European Commission. (2019, Feb 11,). *New flood-prevention infrastructure helps keep Malta safe and dry
.* floodlist.com. Retrieved June 24, 2023, from https://ec.europa.eu/regional_policy/en/projects/malta/new-flood-prevention-infrastructure-helps-keep-malta-safe-and-dry

EWA (Energy and Water Agency). (2022, Sep 3,). *EWA | About Us.* energywateragency.gov.mt. Retrieved July 17, 2023, from https://energywateragency.gov.mt/about-us/

EWA, & ERA. (2020). *Significant Water Management Issues in the Malta River Basin District.* ().Energy & Water Agency. https://energywateragency.gov.mt/wp-content/uploads/2022/04/Significant-Water-Management-Issues-Document_final-1.pdf

EWA, & ERA. (2024). *The 3rd River Basin Management Plan for the Malta Water Catchment District*. Environment and Resources Authority (ERA).

EWA, ERA, & WSC. (2020). *LIFE 16 IPE MT 008 | Optimising the implementation of the 2nd RBMP in the Malta River Basin District .* ().Energy & Water Agency. https://www.rbmplife.org.mt/content/life-integrated-project-booklet

Fernández-Escalante, E. (2018). *Managed Aquifer Recharge in Spain .* ().International Association of Hydrogeologists. https://recharge.iah.org/files/2018/06/Spain-MAR-Fernandez-jun18.pdf

Fowler, W. (2015, *What is A Weir | Weir Structure | Weir Design | SANI-TRED.* Sanitred.com. Retrieved September 10, 2023, from https://sanitred.com/waterproofing-weir-dam/

Gale, I. (2005). *Strategies for Managed Aquifer Recharge (MAR) in semi-arid areas.* (). 7 Place de Fontenoy, 75352 Paris 07 SP, France: United Nations Educational, Scientifi c and Cultural Organization (UNESCO). https://recharge.iah.org/files/2017/01/Gale-Strategies-for-MAR-in-semiarid-areas.pdf

Glen Canyon Institute. (2018), *All Dams are Temporary – Sedimentation .* www.glencanyon.org. Retrieved August 2, 2023, from https://www.glencanyon.org/all-dams-are-temporary-sedimentation/#:~:text=Because%20dams%20are%20built%20to,are%20destroyed%20by%20natural%20floods.

Government of Malta. (2021), *Ambjent Malta Background.* environmentcms.gov.mt. Retrieved July 17, 2023, from https://environmentcms.gov.mt/en/ambjentmalta/Pages/home.aspx

Government of Malta. (2023, May 15,). *Project Green | About Us.* project.green. Retrieved July 19, 2023, from https://project.green/about/

Hvorslev, M. J. (1951). *Time Lag and Soil Permeability in Ground-Water Observations.* (). Mississippi, U.S.A: Waterways Experiment Station, Corps of Engineers, U.S. Army. https://luk.staff.ugm.ac.id/jurnal/freepdf/Hvorslev1951-USACEBulletin36.pdf

INOWAS, & TU Dresden. (2018, May 20,). *Infiltration ponds and basins .* inowas.com. Retrieved August 8, 2023, from https://inowas.com/infiltration-ponds-and-basins/

Jaafar, H. H. (2014). Feasibility of groundwater recharge dam projects in arid environments. *Journal of Hydrology (Amsterdam), 512*, 16-26. 10.1016/j.jhydrol.2014.02.054

Kaledhonkar, M. J., Singh, O. P., Ambast, S. K., Tyagi, N. K., & Tyagi, K. C. (2003). Artificial Groundwater Recharge through Recharge Tube Wells: A Case Study. *Journal of the Institution of Engineers (India): Agricultural Engineering Division,* (84), 28-32. https://www.researchgate.net/publication/250915289_Artificial_groundwater_recharge_through_recharge_tubewells_A_case_study

Katwala, A. (2022, Aug 19,). *How Long Droughts Make Flooding Worse* . Wired. Retrieved Nov 20, 2023, from https://www.wired.co.uk/article/drought-causing-floods

Keren Kayemeth LeIsrael-Jewish National Fund. (2022, Aug 8,). *What is a Liman?* . www.kkl-jnf.org. Retrieved September 14, 2023, from https://www.kkl-jnf.org/organization-chief-scientist/water-for-israel/water-in-the-desert/limans/what-is-a-liman/

Lili, M., Bralts, V. F., Ying-hua, P., Han, L., & Ting-wu, L. (2008). Methods for measuring soil infiltration: State of the art. *International Journal of Agricultural and Biological Engineering, 1*, 22-30. https://api.semanticscholar.org/CorpusID:55932015

Malta Ministry for Resources and Infrastructure Services Division Building, Regulations Office. (2006). *[Document] F, technical guidance : minimum requirements on the energy performance of buildings regulations*. Malta : Building Regulations Office, Services Division.

MaltaToday. (2011, June 2,). Wied il-Ghasel rehabilitation works given go-ahead . https://www.maltatoday.com.mt/news/national/10495/wied-il-ghasel-rehabilitation-works-given-go-ahead

Massmann, J. (2004). *An Approach For Estimating Infiltration Rates for Stormwater Infiltration Dry Wells*. Washington State Department of Transportation Research Office.

Mifsud, B., & Bonello. (2010, Aug 11,). Keeping The watercourse clean . *Malta Independent* https://www.independent.com.mt/articles/2010-08-11/news/keeping-the-watercourse-clean-278634/

Ministry for Public Works and Planning. (2022). *Green Stormwater Infrastructure Guidance Manual [Malta].* (). https://meae.gov.mt/en/Public_Consultations/MTI/Documents/Green%20Stormwater%20Infrastructure%20Guidance%20Manual.pdf

Morris, T. O. (1952). *The water supply resources of Malta*. Malta : Government Printing Office.

National Ground Water Association, U. (2022), *Managed Aquifer Recharge* . www.ngwa.org. Retrieved August 7, 2023, from https://www.ngwa.org/what-is-groundwater/groundwater-issues/managed-aquifer-recharge

NSO Malta. (2022). *The State of the Climate 2022.* (). Valletta: National Statistics Office Malta. https://nso.gov.mt/wp-content/uploads/Climate-publication-2022.pdf

Parks Malta Head Office. (2022), *PARKS Malta - About Us.* parksmalta.com. Retrieved September 4, 2023, from https://parksmalta.com/about/

Pitt, R., Clark, S., & Field, R. (1999). Groundwater contamination potential from stormwater infiltration practices. *Urban Water, 1*(3), 217-236. 10.1016/S1462-0758(99)00014-X

Richter, B. D., Baumgartner, J. V., Powell, J., & Braun, D. P. (1996). A Method for Assessing Hydrologic Alteration within Ecosystems. *Conservation Biology, 10*(4), 1163-1174. 10.1046/j.1523-1739.1996.10041163.x

Sant, G. (2019, April 7,). Malta's groundwater drought . *Times of Malta* https://timesofmalta.com/articles/view/maltas-groundwater-drought.706673

Sapiano, M. (2018, August 30,). *Interview — Malta: water scarcity is a fact of life.* www.eea.europa.eu. Retrieved June 23, 2023, from https://www.eea.europa.eu/signals/signals-2018-content-list/articles/interview-2014-malta-water-scarcity

Schellenberg, G., Donnelly, R., Holder, C. & Ahsan, R. (2017, Feb 22,). *Dealing with Sediment: Effects on Dams and Hydropower Generation .* www.hydroreview.com. Retrieved August 2, 2023, from https://www.hydroreview.com/world-regions/north-america/dealing-with-sediment-effects-on-dams-and-hydropower-generation/#gref

Şen, Z. (1996). Theoretical RQD-porosity-conductivity-aperture charts. *International Journal of Rock Mechanics and Mining Sciences & Geomechanics Abstracts, 33*(2), 173-177. 10.1016/0148-9062(95)00059-3

Seychell, J. (2000). *Valleys : taking Wied is-Sewda as a case study*

Standen, K., Costa, L., Hugman, R., & Monteiro, J. P. (2023). Integration of Managed Aquifer Recharge into the Water Supply System in the Algarve Region, Portugal. *Water, 15*(12)10.3390/w15122286

Standen, K., Costa, L. R. D., & Monteiro, J. (2020). In-Channel Managed Aquifer Recharge: A Review of Current Development Worldwide and Future Potential in Europe. *Water (Basel), 12*(11), 3099. 10.3390/w12113099

susDrain. (2023, *Infiltration basins.* www.susdrain.org. Retrieved September 4, 2023, from https://www.susdrain.org/delivering-suds/using-suds/suds-components/infiltration/infiltration-basin.html

Tennant, D. L. (1976). Instream Flow Regimens for Fish, Wildlife, Recreation and Related Environmental Resources. *Fisheries, 1*(4), 6-10. 10.1577/1548-8446(1976)001

U.S. Dept. of the Interior, Bureau of Reclamation. (1987). *Design of Small Dams*. U.S. Government Printing Office.

Water Services Corporation (WSC). (2023). *WSC Annual Report 2022 .* (). https://www.wsc.com.mt/wsc-annual-report-2022/

WSC, & EWA. (2020), *Development of a Managed Aquifer Recharge Scheme in the Pwales Groundwater Body.* www.rbmplife.org.mt. Retrieved September 6, 2023, from https://www.rbmplife.org.mt/content/development-managed-aquifer-recharge-scheme-pwales-groundwater-body

APPENDIX A

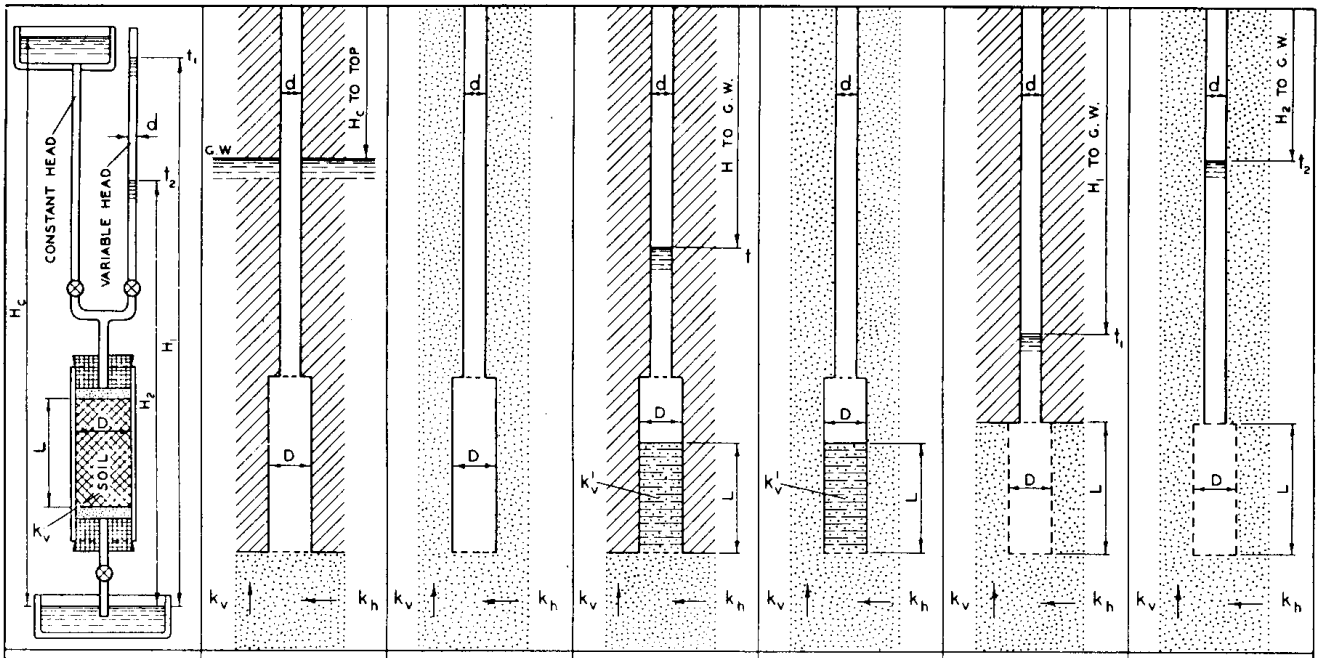

A	B	C	D	E	F	G
LABORATORY PERMEAMETER (CONSOLIDOMETER)	FLUSH BOTTOM AT IMPERVIOUS BOUNDARY	FLUSH BOTTOM IN UNIFORM SOIL	SOIL IN CASING AT IMPERVIOUS BOUNDARY	SOIL IN CASING IN UNIFORM SOIL	WELL POINT-FILTER AT IMPERVIOUS BOUNDARY	WELL POINT-FILTER IN UNIFORM SOIL

CASE	CONSTANT HEAD	VARIABLE HEAD	BASIC TIME LAG
A	$k_v = \frac{4 \cdot q \cdot L}{\pi \cdot D^2 \cdot H_c}$	$k_v = \frac{d^2 \cdot L}{D^2 \cdot (t_2 - t_1)} \ln \frac{H_1}{H_2}$ $k_v = \frac{L}{t_2 - t_1} \ln \frac{H_1}{H_2}$ FOR $d = D$	$k_v = \frac{d^2 \cdot L}{D^2 \cdot T}$ $k_v = \frac{L}{T}$ FOR $d = D$
B	$k_m = \frac{q}{2 \cdot D \cdot H_c}$	$k_m = \frac{\pi \cdot d^2}{8 \cdot D \cdot (t_2 - t_1)} \ln \frac{H_1}{H_2}$ $k_m = \frac{\pi \cdot D}{8 \cdot (t_2 - t_1)} \ln \frac{H_1}{H_2}$ FOR $d = D$	$k_m = \frac{\pi d^2}{8 \cdot D \cdot T}$ $k_m = \frac{\pi \cdot D}{8 \cdot T}$ FOR $d = D$
C	$k_m = \frac{q}{2.75 \cdot D \cdot H_c}$	$k_m = \frac{\pi \cdot d^2}{11 \cdot D \cdot (t_2 - t_1)} \ln \frac{H_1}{H_2}$ $k_m = \frac{\pi \cdot D}{11 \cdot (t_2 - t_1)} \ln \frac{H_1}{H_2}$ FOR $d = D$	$k_m = \frac{\pi \cdot d^2}{11 \cdot D \cdot T}$ $k_m = \frac{\pi \cdot D}{11 \cdot T}$ FOR $d = D$
D	$k_v' = \frac{4 \cdot q \cdot \left[\frac{\pi}{8} \cdot \frac{k_v'}{k_v} \cdot \frac{D}{m} + L\right]}{\pi \cdot D^2 \cdot H_c}$	$k_v' = \frac{d^2 \cdot \left[\frac{\pi}{8} \cdot \frac{k_v'}{k_v} \cdot \frac{D}{m} + L\right]}{D^2 \cdot (t_2 - t_1)} \ln \frac{H_1}{H_2}$ $k_v = \frac{\frac{\pi}{8} \cdot \frac{D}{m} + L}{t_2 - t_1} \ln \frac{H_1}{H_2}$ FOR $k_v' = k_v$, $d = D$	$k_v' = \frac{d^2 \cdot \left[\frac{\pi}{8} \cdot \frac{k_v'}{k_v} \cdot \frac{D}{m}\right] + L}{D^2 \cdot T}$ $k_v = \frac{\frac{\pi}{8} \cdot \frac{D}{m} + L}{T}$ FOR $k_v' = k_v$, $d = D$
E	$k_v' = \frac{4 \cdot q \cdot \left[\frac{\pi}{11} \cdot \frac{k_v'}{k_v} \cdot \frac{D}{m} + L\right]}{\pi \cdot D^2 \cdot H_c}$	$k_v' = \frac{d^2 \cdot \left[\frac{\pi}{11} \cdot \frac{k_v'}{k_v} \cdot \frac{D}{m} + L\right]}{D^2 \cdot (t_2 - t_1)} \ln \frac{H_1}{H_2}$ $k_v = \frac{\frac{\pi}{11} \cdot \frac{D}{m} + L}{t_2 - t_1} \ln \frac{H_1}{H_2}$ FOR $k_v' = k_v$, $d = D$	$k_v' = \frac{d^2 \cdot \left[\frac{\pi}{11} \cdot \frac{k_v'}{k_v} \cdot \frac{D}{m} + L\right]}{D^2 \cdot T}$ $k_v' = \frac{\frac{\pi}{11} \cdot \frac{D}{m} + L}{T}$ FOR $k_v' = k_v$, $d = D$
F	$k_h = \frac{q \cdot \ln \left[\frac{2mL}{D} + \sqrt{1 + \left(\frac{2mL}{D}\right)^2}\right]}{2 \cdot \pi \cdot L \cdot H_c}$	$k_h = \frac{d^2 \cdot \ln \left[\frac{2mL}{D} + \sqrt{1 + \left(\frac{2mL}{D}\right)^2}\right]}{8 \cdot L \cdot (t_2 - t_1)} \ln \frac{H_1}{H_2}$ $k_h = \frac{d^2 \cdot \ln \left(\frac{4mL}{D}\right)}{8 \cdot L \cdot (t_2 - t_1)} \ln \frac{H_1}{H_2}$ FOR $\frac{2mL}{D} > 4$	$k_h = \frac{d^2 \cdot \ln \left[\frac{2mL}{D} + \sqrt{1 + \left(\frac{2mL}{D}\right)^2}\right]}{8 \cdot L \cdot T}$ $k_h = \frac{d^2 \cdot \ln \left(\frac{4mL}{D}\right)}{8 \cdot L \cdot T}$ FOR $\frac{2mL}{D} > 4$
G	$k_h = \frac{q \cdot \ln \left[\frac{mL}{D} + \sqrt{1 + \left(\frac{mL}{D}\right)^2}\right]}{2 \cdot \pi \cdot L \cdot H_c}$	$k_h = \frac{d^2 \cdot \ln \left[\frac{mL}{D} + \sqrt{1 + \left(\frac{mL}{D}\right)^2}\right]}{8 \cdot L \cdot (t_2 - t_1)} \ln \frac{H_1}{H_2}$ $k_h = \frac{d^2 \cdot \ln \left(\frac{2mL}{D}\right)}{8 \cdot L \cdot (t_2 - t_1)} \ln \frac{H_1}{H_2}$ FOR $\frac{mL}{D} > 4$	$k_h = \frac{d^2 \cdot \ln \left[\frac{mL}{D} + \sqrt{1 + \left(\frac{mL}{D}\right)^2}\right]}{8 \cdot L \cdot T}$ $k_h = \frac{d^2 \cdot \ln \left(\frac{2mL}{D}\right)}{8 \cdot L \cdot T}$ FOR $\frac{mL}{D} > 4$

NOTATION

D = DIAM., INTAKE, SAMPLE, CM
d = DIAMETER, STANDPIPE, CM
L = LENGTH, INTAKE, SAMPLE, CM
H_c = CONSTANT PIEZ. HEAD, CM
H_1 = PIEZ. HEAD FOR $t = t_1$, CM
H_2 = PIEZ. HEAD FOR $t = t_2$, CM
q = FLOW OF WATER, $CM^3/SEC.$
t = TIME, SEC.
T = BASIC TIME LAG, SEC.
k_v' = VERT. PERM. CASING, CM/SEC.
k_v = VERT. PERM. GROUND, CM/SEC.
k_h = HORZ. PERM. GROUND, CM/SEC.
k_m = MEAN COEFF. PERM., CM/SEC.
m = TRANSFORMATION RATIO
$k_m = \sqrt{k_h \cdot k_v}$ $m = \sqrt{k_h / k_v}$
$\ln = \log_e = 2.3 \log_{10}$

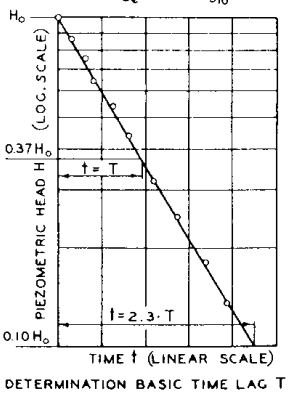

DETERMINATION BASIC TIME LAG T

ASSUMPTIONS

SOIL AT INTAKE, INFINITE DEPTH AND DIRECTIONAL ISOTROPY (k_v AND k_h CONSTANT) - NO DISTURBANCE, SEGREGATION, SWELLING OR CONSOLIDATION OF SOIL - NO SEDIMENTATION OR LEAKAGE - NO AIR OR GAS IN SOIL, WELL POINT, OR PIPE - HYDRAULIC LOSSES IN PIPES, WELL POINT OR FILTER NEGLIGIBLE

Fig. 18. Formulas for determination of permeability

STEADY STATE CONDITION (t=0) - SECONDARY PERMEABILITY

100 segments: (#)	Depth from Surface: (m)	Depth from Water Surface: (m)	Velocity Discharge t=0: (m/s) v	Fissure Num per Segment: (#)	Fissure Area per Segment: (m2) A	Q flow through fissures (m3/s) Q=Av
0	0	0	0	0.16	5.0265E-05	0
1	0.16	0.16	0.08858894	0.16	5.0265E-05	4.45297E-06
2	0.32	0.32	0.12528368	0.16	5.0265E-05	6.29744E-06
3	0.48	0.48	0.15344054	0.16	5.0265E-05	7.71276E-06
4	0.64	0.64	0.17717788	0.16	5.0265E-05	8.90593E-06
5	0.8	0.8	0.19809089	0.16	5.0265E-05	9.95713E-06
6	0.96	0.96	0.2169977	0.16	5.0265E-05	1.09075E-05
7	1.12	1.12	0.2343843	0.16	5.0265E-05	1.17814E-05
8	1.28	1.28	0.25056736	0.16	5.0265E-05	1.25949E-05
9	1.44	1.44	0.26576682	0.16	5.0265E-05	1.33589E-05
10	1.6	1.6	0.28014282	0.16	5.0265E-05	1.40815E-05
11	1.76	1.76	0.29381627	0.16	5.0265E-05	1.47688E-05
12	1.92	1.92	0.30688108	0.16	5.0265E-05	1.54255E-05
13	2.08	2.08	0.31941196	0.16	5.0265E-05	1.60554E-05
14	2.24	2.24	0.33146946	0.16	5.0265E-05	1.66615E-05
15	2.4	2.4	0.34310348	0.16	5.0265E-05	1.72463E-05
16	2.56	2.56	0.35435575	0.16	5.0265E-05	1.78119E-05
17	2.72	2.72	0.36526155	0.16	5.0265E-05	1.836E-05
18	2.88	2.88	0.37585103	0.16	5.0265E-05	1.88923E-05
19	3.04	3.04	0.38615023	0.16	5.0265E-05	1.941E-05
20	3.2	3.2	0.39618178	0.16	5.0265E-05	1.99143E-05
21	3.36	3.36	0.40596552	0.16	5.0265E-05	2.04061E-05
22	3.52	3.52	0.41551895	0.16	5.0265E-05	2.08863E-05
23	3.68	3.68	0.42485762	0.16	5.0265E-05	2.13557E-05
24	3.84	3.84	0.43399539	0.16	5.0265E-05	2.1815E-05
25	4	4	0.44294469	0.16	5.0265E-05	2.22648E-05
26	4.16	4.16	0.45171673	0.16	5.0265E-05	2.27058E-05
27	4.32	4.32	0.46032163	0.16	5.0265E-05	2.31383E-05
28	4.48	4.48	0.4687686	0.16	5.0265E-05	2.35629E-05
29	4.64	4.64	0.47706603	0.16	5.0265E-05	2.398E-05
30	4.8	4.8	0.4852216	0.16	5.0265E-05	2.43899E-05
31	4.96	4.96	0.49324233	0.16	5.0265E-05	2.47931E-05
32	5.12	5.12	0.50113471	0.16	5.0265E-05	2.51898E-05
33	5.28	5.28	0.50890471	0.16	5.0265E-05	2.55803E-05
34	5.44	5.44	0.51655784	0.16	5.0265E-05	2.5965E-05
35	5.6	5.6	0.52409923	0.16	5.0265E-05	2.63441E-05
36	5.76	5.76	0.53153363	0.16	5.0265E-05	2.67178E-05
37	5.92	5.92	0.53886547	0.16	5.0265E-05	2.70863E-05
38	6.08	6.08	0.54609889	0.16	5.0265E-05	2.74499E-05
39	6.24	6.24	0.55323774	0.16	5.0265E-05	2.78088E-05
40	6.4	6.4	0.56028564	0.16	5.0265E-05	2.8163E-05
41	6.56	6.56	0.56724598	0.16	5.0265E-05	2.85129E-05
42	6.72	6.72	0.57412194	0.16	5.0265E-05	2.88585E-05
43	6.88	6.88	0.58091652	0.16	5.0265E-05	2.92E-05
44	7.04	7.04	0.58763254	0.16	5.0265E-05	2.95376E-05
45	7.2	7.2	0.59427266	0.16	5.0265E-05	2.98714E-05
46	7.36	7.36	0.60083941	0.16	5.0265E-05	3.02015E-05
47	7.52	7.52	0.60733516	0.16	5.0265E-05	3.0528E-05
48	7.68	7.68	0.61376217	0.16	5.0265E-05	3.08511E-05
49	7.84	7.84	0.62012257	0.16	5.0265E-05	3.11708E-05
50	8	8	0.62641839	0.16	5.0265E-05	3.14872E-05
51	8.16	8.16	0.63265156	0.16	5.0265E-05	3.18005E-05
52	8.32	8.32	0.63882392	0.16	5.0265E-05	3.21108E-05
53	8.48	8.48	0.64493721	0.16	5.0265E-05	3.24181E-05
54	8.64	8.64	0.65099309	0.16	5.0265E-05	3.27225E-05
55	8.8	8.8	0.65699315	0.16	5.0265E-05	3.30241E-05
56	8.96	8.96	0.66293891	0.16	5.0265E-05	3.33229E-05
57	9.12	9.12	0.66883182	0.16	5.0265E-05	3.36192E-05
58	9.28	9.28	0.67467325	0.16	5.0265E-05	3.39128E-05
59	9.44	9.44	0.68046455	0.16	5.0265E-05	3.42039E-05
60	9.6	9.6	0.68620697	0.16	5.0265E-05	3.44925E-05
61	9.76	9.76	0.69190173	0.16	5.0265E-05	3.47788E-05
62	9.92	9.92	0.69755	0.16	5.0265E-05	3.50627E-05
63	10.08	10.08	0.7031529	0.16	5.0265E-05	3.53443E-05
64	10.24	10.24	0.70871151	0.16	5.0265E-05	3.56237E-05
65	10.4	10.4	0.71422685	0.16	5.0265E-05	3.5901E-05
66	10.56	10.56	0.71969994	0.16	5.0265E-05	3.61761E-05
67	10.72	10.72	0.72513171	0.16	5.0265E-05	3.64491E-05
68	10.88	10.88	0.7305231	0.16	5.0265E-05	3.67201E-05
69	11.04	11.04	0.73587499	0.16	5.0265E-05	3.69891E-05
70	11.2	11.2	0.74118824	0.16	5.0265E-05	3.72562E-05
71	11.36	11.36	0.74646366	0.16	5.0265E-05	3.75214E-05
72	11.52	11.52	0.75170207	0.16	5.0265E-05	3.77847E-05
73	11.68	11.68	0.75690422	0.16	5.0265E-05	3.80462E-05
74	11.84	11.84	0.76207086	0.16	5.0265E-05	3.83059E-05
75	12	12	0.76720271	0.16	5.0265E-05	3.85638E-05
76	12.16	12.16	0.77230046	0.16	5.0265E-05	3.88201E-05
77	12.32	12.32	0.77736478	0.16	5.0265E-05	3.90746E-05
78	12.48	12.48	0.78239632	0.16	5.0265E-05	3.93275E-05
79	12.64	12.64	0.78739571	0.16	5.0265E-05	3.95788E-05
80	12.8	12.8	0.79236355	0.16	5.0265E-05	3.98285E-05
81	12.96	12.96	0.79730045	0.16	5.0265E-05	4.00767E-05
82	13.12	13.12	0.80220696	0.16	5.0265E-05	4.03233E-05
83	13.28	13.28	0.80708364	0.16	5.0265E-05	4.05684E-05
84	13.44	13.44	0.81193103	0.16	5.0265E-05	4.08121E-05
85	13.6	13.6	0.81674966	0.16	5.0265E-05	4.10543E-05
86	13.76	13.76	0.82154002	0.16	5.0265E-05	4.12951E-05
87	13.92	13.92	0.82630261	0.16	5.0265E-05	4.15345E-05
88	14.08	14.08	0.83103791	0.16	5.0265E-05	4.17725E-05
89	14.24	14.24	0.83574637	0.16	5.0265E-05	4.20092E-05
90	14.4	14.4	0.84042846	0.16	5.0265E-05	4.22445E-05
91	14.56	14.56	0.84508461	0.16	5.0265E-05	4.24786E-05
92	14.72	14.72	0.84971525	0.16	5.0265E-05	4.27113E-05
93	14.88	14.88	0.85432078	0.16	5.0265E-05	4.29428E-05
94	15.04	15.04	0.85890162	0.16	5.0265E-05	4.31731E-05
95	15.2	15.2	0.86345816	0.16	5.0265E-05	4.34021E-05
96	15.36	15.36	0.86799078	0.16	5.0265E-05	4.363E-05
97	15.52	15.52	0.87249986	0.16	5.0265E-05	4.38566E-05
98	15.68	15.68	0.87698575	0.16	5.0265E-05	4.40821E-05
99	15.84	15.84	0.88144881	0.16	5.0265E-05	4.43064E-05
100	16	16	0.88588938		0	0

		Fissure Q
Total BH Depth :	16 m	0.002945472
BH Diameter:	0.1 m	m3/s
Water Start Depth :	0 m	*[Summed]*
Total Casing Depth :	0 m	**Pore Q**
Flow Factor :	0.05	0
		m3/s

FISSURE DISTRIBUTION TABLE [Borehole Log Runs]

Depth Increase

Core Run: (#)	Core Length Input Values: (m)	RQD Input Values: (%)	Core Run Max Depth: (m)	Fissured Lengths: (m)	Fissure Number per Run: (#)	Fissure Number per Segment: (#)
-	-	-	-	-	-	-
1	2	90	2	0.2	2	0.16
2	2	90	4	0.2	2	0.16
3	2	90	6	0.2	2	0.16
4	2	90	8	0.2	2	0.16
5	2	90	10	0.2	2	0.16
6	2	90	12	0.2	2	0.16
7	2	90	14	0.2	2	0.16
8	2	90	16	0.2	2	0.16
9						
10						
11						
12						
13						
14						
15						

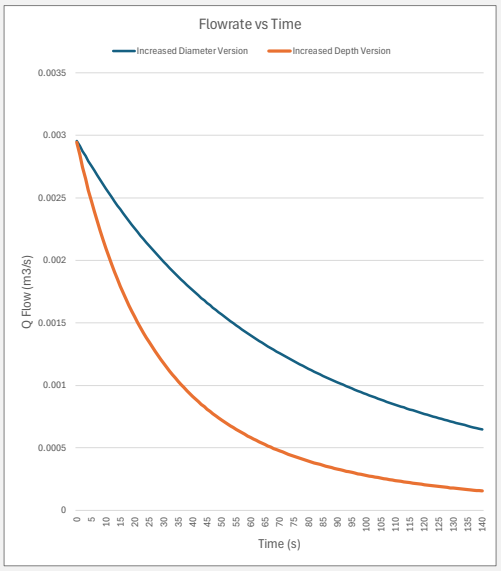

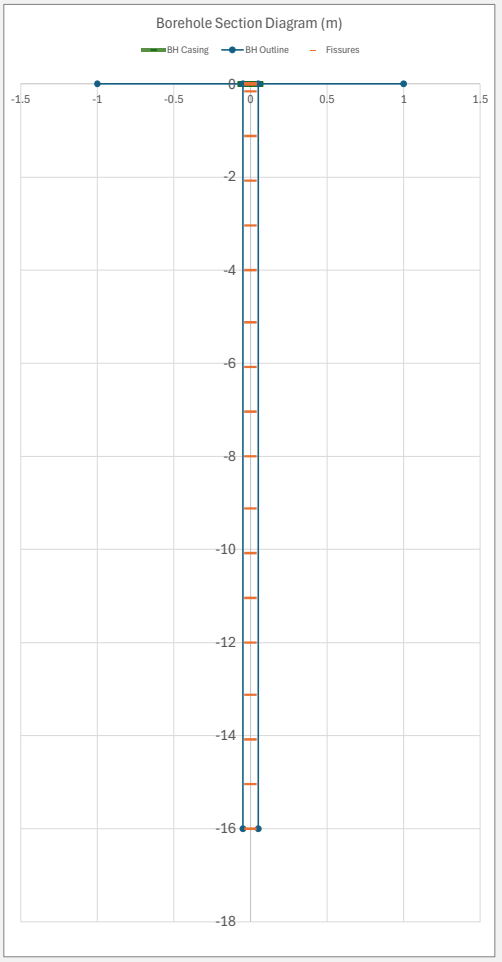

STEADY STATE CONDITION (t=0) - SECONDARY PERMEABILITY

100 segments: (#)	Depth from Surface: (m)	Depth from Water Surface: (m)	Velocity Discharge t=0: (m/s) v	Fissure Num per Segment: (#)	Fissure Area per Segment: (m2) A	Q flow through fissures (m3/s) Q=Av
0	0	0	0	0.1	6.2832E-05	0
1	0.1	0.1	0.07003571	0.1	6.2832E-05	4.40047E-06
2	0.2	0.2	0.09904544	0.1	6.2832E-05	6.22321E-06
3	0.3	0.3	0.1213054	0.1	6.2832E-05	7.62184E-06
4	0.4	0.4	0.14007141	0.1	6.2832E-05	8.80095E-06
5	0.5	0.5	0.1566046	0.1	6.2832E-05	9.83976E-06
6	0.6	0.6	0.17155174	0.1	6.2832E-05	1.07789E-05
7	0.7	0.7	0.18529706	0.1	6.2832E-05	1.16426E-05
8	0.8	0.8	0.19809089	0.1	6.2832E-05	1.24464E-05
9	0.9	0.9	0.21010712	0.1	6.2832E-05	1.32014E-05
10	1	1	0.22147235	0.1	6.2832E-05	1.39155E-05
11	1.1	1.1	0.23228216	0.1	6.2832E-05	1.45947E-05
12	1.2	1.2	0.2426108	0.1	6.2832E-05	1.52437E-05
13	1.3	1.3	0.25251733	0.1	6.2832E-05	1.58661E-05
14	1.4	1.4	0.26204961	0.1	6.2832E-05	1.64651E-05
15	1.5	1.5	0.27124712	0.1	6.2832E-05	1.7043E-05
16	1.6	1.6	0.28014282	0.1	6.2832E-05	1.76019E-05
17	1.7	1.7	0.28876461	0.1	6.2832E-05	1.81436E-05
18	1.8	1.8	0.29713633	0.1	6.2832E-05	1.86696E-05
19	1.9	1.9	0.30527856	0.1	6.2832E-05	1.91812E-05
20	2	2	0.3132092	0.1	6.2832E-05	1.96795E-05
21	2.1	2.1	0.32094392	0.1	6.2832E-05	2.01655E-05
22	2.2	2.2	0.32849658	0.1	6.2832E-05	2.064E-05
23	2.3	2.3	0.33587944	0.1	6.2832E-05	2.11039E-05
24	2.4	2.4	0.34310348	0.1	6.2832E-05	2.15578E-05
25	2.5	2.5	0.35017853	0.1	6.2832E-05	2.20024E-05
26	2.6	2.6	0.35711343	0.1	6.2832E-05	2.24381E-05
27	2.7	2.7	0.3639162	0.1	6.2832E-05	2.28655E-05
28	2.8	2.8	0.37059412	0.1	6.2832E-05	2.32851E-05
29	2.9	2.9	0.37715381	0.1	6.2832E-05	2.36973E-05
30	3	3	0.38360136	0.1	6.2832E-05	2.41024E-05
31	3.1	3.1	0.3899423	0.1	6.2832E-05	2.45008E-05
32	3.2	3.2	0.39618178	0.1	6.2832E-05	2.48928E-05
33	3.3	3.3	0.4023245	0.1	6.2832E-05	2.52788E-05
34	3.4	3.4	0.40837483	0.1	6.2832E-05	2.56589E-05
35	3.5	3.5	0.41433682	0.1	6.2832E-05	2.60336E-05
36	3.6	3.6	0.42021423	0.1	6.2832E-05	2.64028E-05
37	3.7	3.7	0.42601056	0.1	6.2832E-05	2.67667E-05
38	3.8	3.8	0.43172908	0.1	6.2832E-05	2.71263E-05
39	3.9	3.9	0.43737284	0.1	6.2832E-05	2.74809E-05
40	4	4	0.44294469	0.1	6.2832E-05	2.7831E-05
41	4.1	4.1	0.44844732	0.1	6.2832E-05	2.81768E-05
42	4.2	4.2	0.45388324	0.1	6.2832E-05	2.85183E-05
43	4.3	4.3	0.45925483	0.1	6.2832E-05	2.88558E-05
44	4.4	4.4	0.46456431	0.1	6.2832E-05	2.91894E-05
45	4.5	4.5	0.46981379	0.1	6.2832E-05	2.95193E-05
46	4.6	4.6	0.47500526	0.1	6.2832E-05	2.98455E-05
47	4.7	4.7	0.4801406	0.1	6.2832E-05	3.01681E-05
48	4.8	4.8	0.4852216	0.1	6.2832E-05	3.04874E-05
49	4.9	4.9	0.49024994	0.1	6.2832E-05	3.08033E-05
50	5	5	0.49522722	0.1	6.2832E-05	3.1116E-05
51	5.1	5.1	0.50015498	0.1	6.2832E-05	3.14257E-05
52	5.2	5.2	0.50503465	0.1	6.2832E-05	3.17323E-05
53	5.3	5.3	0.50986763	0.1	6.2832E-05	3.20359E-05
54	5.4	5.4	0.51465522	0.1	6.2832E-05	3.23367E-05
55	5.5	5.5	0.51939869	0.1	6.2832E-05	3.26348E-05
56	5.6	5.6	0.52409923	0.1	6.2832E-05	3.29301E-05
57	5.7	5.7	0.52875798	0.1	6.2832E-05	3.32228E-05
58	5.8	5.8	0.53337604	0.1	6.2832E-05	3.3513E-05
59	5.9	5.9	0.53795446	0.1	6.2832E-05	3.38007E-05
60	6	6	0.54249424	0.1	6.2832E-05	3.40859E-05
61	6.1	6.1	0.54699634	0.1	6.2832E-05	3.43688E-05
62	6.2	6.2	0.55146169	0.1	6.2832E-05	3.46494E-05
63	6.3	6.3	0.55589118	0.1	6.2832E-05	3.49277E-05
64	6.4	6.4	0.56028564	0.1	6.2832E-05	3.52038E-05
65	6.5	6.5	0.56464591	0.1	6.2832E-05	3.54777E-05
66	6.6	6.6	0.56897276	0.1	6.2832E-05	3.57496E-05
67	6.7	6.7	0.57326695	0.1	6.2832E-05	3.60194E-05
68	6.8	6.8	0.57752922	0.1	6.2832E-05	3.62872E-05
69	6.9	6.9	0.58176026	0.1	6.2832E-05	3.65531E-05
70	7	7	0.58596075	0.1	6.2832E-05	3.6817E-05
71	7.1	7.1	0.59013134	0.1	6.2832E-05	3.7079E-05
72	7.2	7.2	0.59427266	0.1	6.2832E-05	3.73393E-05
73	7.3	7.3	0.59838533	0.1	6.2832E-05	3.75977E-05
74	7.4	7.4	0.60246992	0.1	6.2832E-05	3.78543E-05
75	7.5	7.5	0.606527	0.1	6.2832E-05	3.81092E-05
76	7.6	7.6	0.61055712	0.1	6.2832E-05	3.83624E-05
77	7.7	7.7	0.61456082	0.1	6.2832E-05	3.8614E-05
78	7.8	7.8	0.6185386	0.1	6.2832E-05	3.88639E-05
79	7.9	7.9	0.62249096	0.1	6.2832E-05	3.91123E-05
80	8	8	0.62641839	0.1	6.2832E-05	3.9359E-05
81	8.1	8.1	0.63032135	0.1	6.2832E-05	3.96043E-05
82	8.2	8.2	0.63420028	0.1	6.2832E-05	3.9848E-05
83	8.3	8.3	0.63805564	0.1	6.2832E-05	4.00902E-05
84	8.4	8.4	0.64188784	0.1	6.2832E-05	4.0331E-05
85	8.5	8.5	0.6456973	0.1	6.2832E-05	4.05704E-05
86	8.6	8.6	0.64948441	0.1	6.2832E-05	4.08083E-05
87	8.7	8.7	0.65324957	0.1	6.2832E-05	4.10449E-05
88	8.8	8.8	0.65699315	0.1	6.2832E-05	4.12801E-05
89	8.9	8.9	0.66071552	0.1	6.2832E-05	4.1514E-05
90	9	9	0.66441704	0.1	6.2832E-05	4.17466E-05
91	9.1	9.1	0.66809805	0.1	6.2832E-05	4.19778E-05
92	9.2	9.2	0.67175889	0.1	6.2832E-05	4.22079E-05
93	9.3	9.3	0.67539988	0.1	6.2832E-05	4.24366E-05
94	9.4	9.4	0.67902135	0.1	6.2832E-05	4.26642E-05
95	9.5	9.5	0.68262362	0.1	6.2832E-05	4.28905E-05
96	9.6	9.6	0.68620697	0.1	6.2832E-05	4.31157E-05
97	9.7	9.7	0.6897717	0.1	6.2832E-05	4.33396E-05
98	9.8	9.8	0.69331811	0.1	6.2832E-05	4.35625E-05
99	9.9	9.9	0.69684647	0.1	6.2832E-05	4.37842E-05
100	10	10	0.70035705	0.1	6.2832E-05	4.40047E-05

			Fissure Q
Total BH Depth :	10	m	0.002954755
BH Diameter:	0.2	m	m3/s
Water Start Depth :	0	m	*[Summed]*
Total Casing Depth :	0	m	**Pore Q**
Flow Factor :	0.05		0
			m3/s

FISSURE DISTRIBUTION TABLE [Borehole Log Runs]

Diameter Increase

Core Run: (#)	Core Length Input Values: (m)	RQD Input Values: (%)	Core Run Max Depth: (m)	Fissured Lengths: (m)	Fissure Number per Run: (#)	Fissure Number per Segment: (#)
-	-	-	-	-	-	-
1	1	90	1	0.1	1	0.1
2	1	90	2	0.1	1	0.1
3	1	90	3	0.1	1	0.1
4	1	90	4	0.1	1	0.1
5	1	90	5	0.1	1	0.1
6	1	90	6	0.1	1	0.1
7	1	90	7	0.1	1	0.1
8	1	90	8	0.1	1	0.1
9	1	90	9	0.1	1	0.1
10	1	90	10	0.1	1	0.1
11						
12						
13						
14						
15						

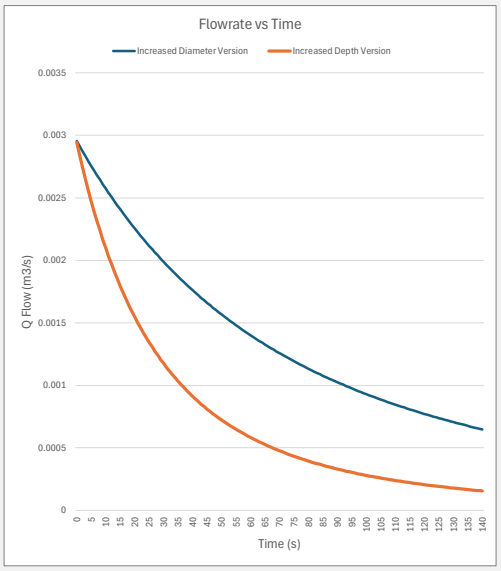

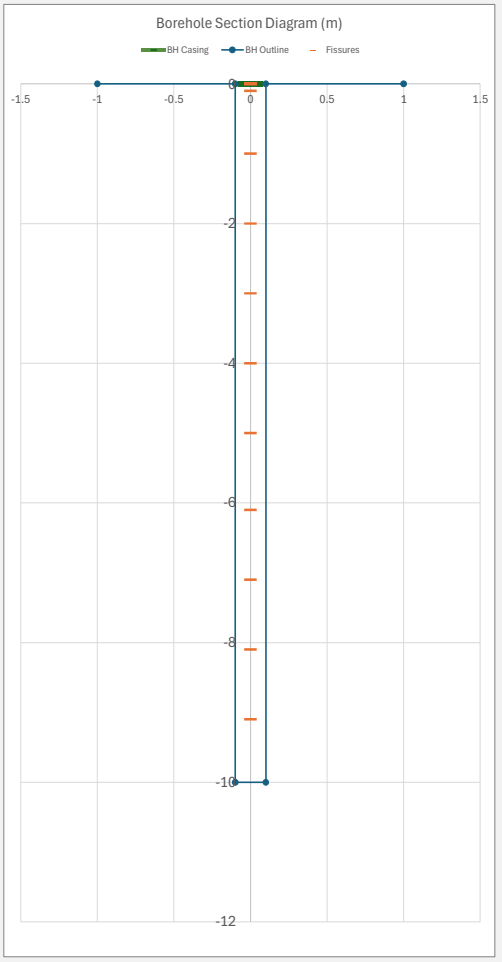

STEADY STATE CONDITION (t=0) - SECONDARY PERMEABILITY

100 segments: (#)	Depth from Surface: (m)	Depth from Water Surface: (m)	Velocity Discharge t=0: (m/s) v	Fissure Num per Segment: (#)	Fissure Area per Segment: (m2) A	Q flow through fissures (m3/s) Q=Av
0	0	0	0	0.1	3.1416E-05	0
1	0.1	0.1	0.07003571	0.1	3.1416E-05	2.20024E-06
2	0.2	0.2	0.09904544	0.1	3.1416E-05	3.1116E-06
3	0.3	0.3	0.1213054	0.1	3.1416E-05	3.81092E-06
4	0.4	0.4	0.14007141	0.1	3.1416E-05	4.40047E-06
5	0.5	0.5	0.1566046	0.1	3.1416E-05	4.91988E-06
6	0.6	0.6	0.17155174	0.1	3.1416E-05	5.38946E-06
7	0.7	0.7	0.18529706	0.1	3.1416E-05	5.82128E-06
8	0.8	0.8	0.19809089	0.1	3.1416E-05	6.22321E-06
9	0.9	0.9	0.21010712	0.1	3.1416E-05	6.60071E-06
10	1	1	0.22147235	0.1	3.1416E-05	6.95776E-06
11	1.1	1.1	0.23228216	0.1	3.1416E-05	7.29736E-06
12	1.2	1.2	0.2426108	0.1	3.1416E-05	7.62184E-06
13	1.3	1.3	0.25251733	0.1	3.1416E-05	7.93307E-06
14	1.4	1.4	0.26204961	0.1	3.1416E-05	8.23253E-06
15	1.5	1.5	0.27124712	0.1	3.1416E-05	8.52148E-06
16	1.6	1.6	0.28014282	0.1	3.1416E-05	8.80095E-06
17	1.7	1.7	0.28876461	0.1	3.1416E-05	9.07181E-06
18	1.8	1.8	0.29713633	0.1	3.1416E-05	9.33481E-06
19	1.9	1.9	0.30527856	0.1	3.1416E-05	9.59061E-06
20	2	2	0.3132092	0.1	3.1416E-05	9.83976E-06
21	2.1	2.1	0.32094392	0.1	3.1416E-05	1.00828E-05
22	2.2	2.2	0.32849658	0.1	3.1416E-05	1.032E-05
23	2.3	2.3	0.33587944	0.1	3.1416E-05	1.0552E-05
24	2.4	2.4	0.34310348	0.1	3.1416E-05	1.07789E-05
25	2.5	2.5	0.35017853	0.1	3.1416E-05	1.10012E-05
26	2.6	2.6	0.35711343	0.1	3.1416E-05	1.1219E-05
27	2.7	2.7	0.3639162	0.1	3.1416E-05	1.14328E-05
28	2.8	2.8	0.37059412	0.1	3.1416E-05	1.16426E-05
29	2.9	2.9	0.37715381	0.1	3.1416E-05	1.18486E-05
30	3	3	0.38360136	0.1	3.1416E-05	1.20512E-05
31	3.1	3.1	0.3899423	0.1	3.1416E-05	1.22504E-05
32	3.2	3.2	0.39618178	0.1	3.1416E-05	1.24464E-05
33	3.3	3.3	0.4023245	0.1	3.1416E-05	1.26394E-05
34	3.4	3.4	0.40837483	0.1	3.1416E-05	1.28295E-05
35	3.5	3.5	0.41433682	0.1	3.1416E-05	1.30168E-05
36	3.6	3.6	0.42021423	0.1	3.1416E-05	1.32014E-05
37	3.7	3.7	0.42601056	0.1	3.1416E-05	1.33835E-05
38	3.8	3.8	0.43172908	0.1	3.1416E-05	1.35632E-05
39	3.9	3.9	0.43737284	0.1	3.1416E-05	1.37405E-05
40	4	4	0.44294469	0.1	3.1416E-05	1.39155E-05
41	4.1	4.1	0.44844732	0.1	3.1416E-05	1.40884E-05
42	4.2	4.2	0.45388324	0.1	3.1416E-05	1.42592E-05
43	4.3	4.3	0.45925483	0.1	3.1416E-05	1.44279E-05
44	4.4	4.4	0.46456431	0.1	3.1416E-05	1.45947E-05
45	4.5	4.5	0.46981379	0.1	3.1416E-05	1.47596E-05
46	4.6	4.6	0.47500526	0.1	3.1416E-05	1.49227E-05
47	4.7	4.7	0.4801406	0.1	3.1416E-05	1.50841E-05
48	4.8	4.8	0.4852216	0.1	3.1416E-05	1.52437E-05
49	4.9	4.9	0.49024994	0.1	3.1416E-05	1.54017E-05
50	5	5	0.49522722	0	0	0
51	5.1	5.1	0.50015498	0	0	0
52	5.2	5.2	0.50503465	0	0	0
53	5.3	5.3	0.50986763	0	0	0
54	5.4	5.4	0.51465522	0	0	0
55	5.5	5.5	0.51939869	0	0	0
56	5.6	5.6	0.52409923	0	0	0
57	5.7	5.7	0.52875798	0	0	0
58	5.8	5.8	0.53337604	0	0	0
59	5.9	5.9	0.53795446	0	0	0
60	6	6	0.54249424	0	0	0
61	6.1	6.1	0.54699634	0	0	0
62	6.2	6.2	0.55146169	0	0	0
63	6.3	6.3	0.55589118	0	0	0
64	6.4	6.4	0.56028564	0	0	0
65	6.5	6.5	0.56464591	0	0	0
66	6.6	6.6	0.56897276	0	0	0
67	6.7	6.7	0.57326695	0	0	0
68	6.8	6.8	0.57752922	0	0	0
69	6.9	6.9	0.58176026	0	0	0
70	7	7	0.58596075	0	0	0
71	7.1	7.1	0.59013134	0	0	0
72	7.2	7.2	0.59427266	0	0	0
73	7.3	7.3	0.59838533	0	0	0
74	7.4	7.4	0.60246992	0	0	0
75	7.5	7.5	0.606527	0	0	0
76	7.6	7.6	0.61055712	0	0	0
77	7.7	7.7	0.61456082	0	0	0
78	7.8	7.8	0.6185386	0	0	0
79	7.9	7.9	0.62249096	0	0	0
80	8	8	0.62641839	0	0	0
81	8.1	8.1	0.63032135	0	0	0
82	8.2	8.2	0.63420028	0	0	0
83	8.3	8.3	0.63805564	0	0	0
84	8.4	8.4	0.64188784	0	0	0
85	8.5	8.5	0.6456973	0	0	0
86	8.6	8.6	0.64948441	0	0	0
87	8.7	8.7	0.65324957	0	0	0
88	8.8	8.8	0.65699315	0	0	0
89	8.9	8.9	0.66071552	0	0	0
90	9	9	0.66441704	0	0	0
91	9.1	9.1	0.66809805	0	0	0
92	9.2	9.2	0.67175889	0	0	0
93	9.3	9.3	0.67539988	0	0	0
94	9.4	9.4	0.67902135	0	0	0
95	9.5	9.5	0.68262362	0	0	0
96	9.6	9.6	0.68620697	0	0	0
97	9.7	9.7	0.6897717	0	0	0
98	9.8	9.8	0.69331811	0	0	0
99	9.9	9.9	0.69684647	0	0	0
100	10	10	0.70035705	0	0	0

		Fissure Q
Total BH Depth :	10 m	0.000510377
BH Diameter:	0.1 m	m3/s
Water Start Depth :	0 m	*[Summed]*
Total Casing Depth :	0 m	**Pore Q**
Flow Factor :	0.05	0
		m3/s

FISSURE DISTRIBUTION TABLE [Borehole Log Runs]

Upper Fissure Concentration

Core Run: (#)	Core Length Input Values: (m)	RQD Input Values: (%)	Core Run Max Depth: (m)	Fissured Lengths: (m)	Fissure Number per Run: (#)	Fissure Number per Segment: (#)
-	-	-	-	-	-	-
1	1	90	1	0.1	1	0.1
2	1	90	2	0.1	1	0.1
3	1	90	3	0.1	1	0.1
4	1	90	4	0.1	1	0.1
5	1	90	5	0.1	1	0.1
6	1	100	6	0	0	0
7	1	100	7	0	0	0
8	1	100	8	0	0	0
9	1	100	9	0	0	0
10	1	100	10	0	0	0
11						
12						
13						
14						
15						

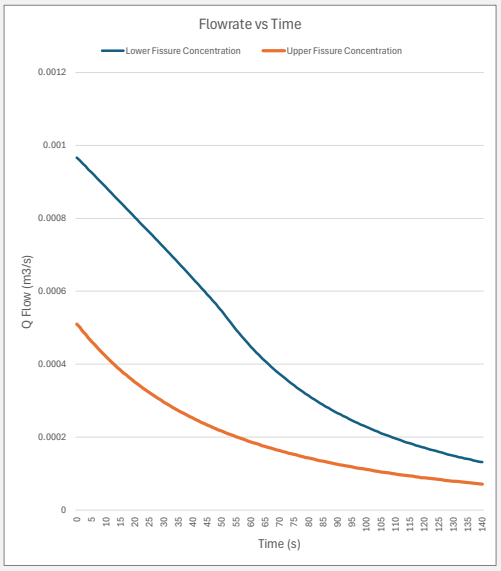

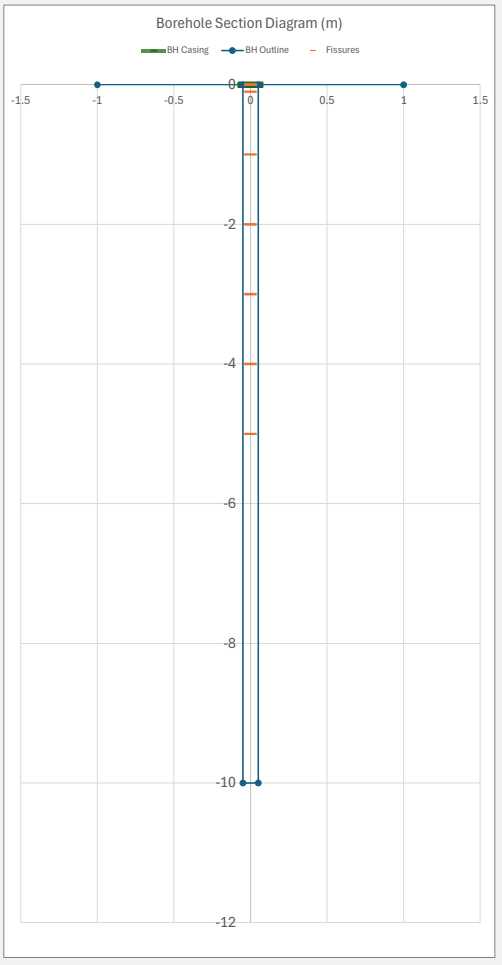

STEADY STATE CONDITION (t=0) - SECONDARY PERMEABILITY

100 segments: (#)	Depth from Surface: (m)	Depth from Water Surface: (m)	Velocity Discharge t=0: (m/s) v	Fissure Num per Segment: (#)	Fissure Area per Segment: (m2) A	Q flow through fissures (m3/s) Q=Av
0	0	0	0	0	0	0
1	0.1	0.1	0.07003571	0	0	0
2	0.2	0.2	0.09904544	0	0	0
3	0.3	0.3	0.1213054	0	0	0
4	0.4	0.4	0.14007141	0	0	0
5	0.5	0.5	0.1566046	0	0	0
6	0.6	0.6	0.17155174	0	0	0
7	0.7	0.7	0.18529706	0	0	0
8	0.8	0.8	0.19809089	0	0	0
9	0.9	0.9	0.21010712	0	0	0
10	1	1	0.22147235	0	0	0
11	1.1	1.1	0.23228216	0	0	0
12	1.2	1.2	0.2426108	0	0	0
13	1.3	1.3	0.25251733	0	0	0
14	1.4	1.4	0.26204961	0	0	0
15	1.5	1.5	0.27124712	0	0	0
16	1.6	1.6	0.28014282	0	0	0
17	1.7	1.7	0.28876461	0	0	0
18	1.8	1.8	0.29713633	0	0	0
19	1.9	1.9	0.30527856	0	0	0
20	2	2	0.3132092	0	0	0
21	2.1	2.1	0.32094392	0	0	0
22	2.2	2.2	0.32849658	0	0	0
23	2.3	2.3	0.33587944	0	0	0
24	2.4	2.4	0.34310348	0	0	0
25	2.5	2.5	0.35017853	0	0	0
26	2.6	2.6	0.35711343	0	0	0
27	2.7	2.7	0.3639162	0	0	0
28	2.8	2.8	0.37059412	0	0	0
29	2.9	2.9	0.37715381	0	0	0
30	3	3	0.38360136	0	0	0
31	3.1	3.1	0.3899423	0	0	0
32	3.2	3.2	0.39618178	0	0	0
33	3.3	3.3	0.4023245	0	0	0
34	3.4	3.4	0.40837483	0	0	0
35	3.5	3.5	0.41433682	0	0	0
36	3.6	3.6	0.42021423	0	0	0
37	3.7	3.7	0.42601056	0	0	0
38	3.8	3.8	0.43172908	0	0	0
39	3.9	3.9	0.43737284	0	0	0
40	4	4	0.44294469	0	0	0
41	4.1	4.1	0.44844732	0	0	0
42	4.2	4.2	0.45388324	0	0	0
43	4.3	4.3	0.45925483	0	0	0
44	4.4	4.4	0.46456431	0	0	0
45	4.5	4.5	0.46981379	0	0	0
46	4.6	4.6	0.47500526	0	0	0
47	4.7	4.7	0.4801406	0	0	0
48	4.8	4.8	0.4852216	0	0	0
49	4.9	4.9	0.49024994	0	0	0
50	5	5	0.49522722	0.1	3.1416E-05	1.5558E-05
51	5.1	5.1	0.50015498	0.1	3.1416E-05	1.57128E-05
52	5.2	5.2	0.50503465	0.1	3.1416E-05	1.58661E-05
53	5.3	5.3	0.50986763	0.1	3.1416E-05	1.6018E-05
54	5.4	5.4	0.51465522	0.1	3.1416E-05	1.61684E-05
55	5.5	5.5	0.51939869	0.1	3.1416E-05	1.63174E-05
56	5.6	5.6	0.52409923	0.1	3.1416E-05	1.64651E-05
57	5.7	5.7	0.52875798	0.1	3.1416E-05	1.66114E-05
58	5.8	5.8	0.53337604	0.1	3.1416E-05	1.67565E-05
59	5.9	5.9	0.53795446	0.1	3.1416E-05	1.69003E-05
60	6	6	0.54249424	0.1	3.1416E-05	1.7043E-05
61	6.1	6.1	0.54699634	0.1	3.1416E-05	1.71844E-05
62	6.2	6.2	0.55146169	0.1	3.1416E-05	1.73247E-05
63	6.3	6.3	0.55589118	0.1	3.1416E-05	1.74638E-05
64	6.4	6.4	0.56028564	0.1	3.1416E-05	1.76019E-05
65	6.5	6.5	0.56464591	0.1	3.1416E-05	1.77389E-05
66	6.6	6.6	0.56897276	0.1	3.1416E-05	1.78748E-05
67	6.7	6.7	0.57326695	0.1	3.1416E-05	1.80097E-05
68	6.8	6.8	0.57752922	0.1	3.1416E-05	1.81436E-05
69	6.9	6.9	0.58176026	0.1	3.1416E-05	1.82765E-05
70	7	7	0.58596075	0.1	3.1416E-05	1.84085E-05
71	7.1	7.1	0.59013134	0.1	3.1416E-05	1.85395E-05
72	7.2	7.2	0.59427266	0.1	3.1416E-05	1.86696E-05
73	7.3	7.3	0.59838533	0.1	3.1416E-05	1.87988E-05
74	7.4	7.4	0.60246992	0.1	3.1416E-05	1.89272E-05
75	7.5	7.5	0.606527	0.1	3.1416E-05	1.90546E-05
76	7.6	7.6	0.61055712	0.1	3.1416E-05	1.91812E-05
77	7.7	7.7	0.61456082	0.1	3.1416E-05	1.9307E-05
78	7.8	7.8	0.6185386	0.1	3.1416E-05	1.9432E-05
79	7.9	7.9	0.62249096	0.1	3.1416E-05	1.95561E-05
80	8	8	0.62641839	0.1	3.1416E-05	1.96795E-05
81	8.1	8.1	0.63032135	0.1	3.1416E-05	1.98021E-05
82	8.2	8.2	0.63420028	0.1	3.1416E-05	1.9924E-05
83	8.3	8.3	0.63805564	0.1	3.1416E-05	2.00451E-05
84	8.4	8.4	0.64188784	0.1	3.1416E-05	2.01655E-05
85	8.5	8.5	0.6456973	0.1	3.1416E-05	2.02852E-05
86	8.6	8.6	0.64948441	0.1	3.1416E-05	2.04042E-05
87	8.7	8.7	0.65324957	0.1	3.1416E-05	2.05224E-05
88	8.8	8.8	0.65699315	0.1	3.1416E-05	2.064E-05
89	8.9	8.9	0.66071552	0.1	3.1416E-05	2.07577E-05
90	9	9	0.66441704	0.1	3.1416E-05	2.08733E-05
91	9.1	9.1	0.66809805	0.1	3.1416E-05	2.09889E-05
92	9.2	9.2	0.67175889	0.1	3.1416E-05	2.11039E-05
93	9.3	9.3	0.67539988	0.1	3.1416E-05	2.12183E-05
94	9.4	9.4	0.67902135	0.1	3.1416E-05	2.13321E-05
95	9.5	9.5	0.68262362	0.1	3.1416E-05	2.14453E-05
96	9.6	9.6	0.68620697	0.1	3.1416E-05	2.15578E-05
97	9.7	9.7	0.6897717	0.1	3.1416E-05	2.16698E-05
98	9.8	9.8	0.69331811	0.1	3.1416E-05	2.17812E-05
99	9.9	9.9	0.69684647	0.1	3.1416E-05	2.18921E-05
100	10	10	0.70035705	0.1	3.1416E-05	2.20024E-05

			Fissure Q
Total BH Depth :	10	m	0.000967
BH Diameter:	0.1	m	m3/s
Water Start Depth :	0	m	*[Summed]*
Total Casing Depth :	0	m	**Pore Q**
Flow Factor :	0.05		0
			m3/s

FISSURE DISTRIBUTION TABLE [Borehole Log Runs]

Lower Fissure Concentration

Core Run: (#)	Core Length Input Values: (m)	RQD Input Values: (%)	Core Run Max Depth: (m)	Fissured Lengths: (m)	Fissure Number per Run: (#)	Fissure Number per Segment: (#)
-	-	-	-	-	-	-
1	1	100	1	0	0	0
2	1	100	2	0	0	0
3	1	100	3	0	0	0
4	1	100	4	0	0	0
5	1	100	5	0	0	0
6	1	90	6	0.1	1	0.1
7	1	90	7	0.1	1	0.1
8	1	90	8	0.1	1	0.1
9	1	90	9	0.1	1	0.1
10	1	90	10	0.1	1	0.1
11						
12						
13						
14						
15						

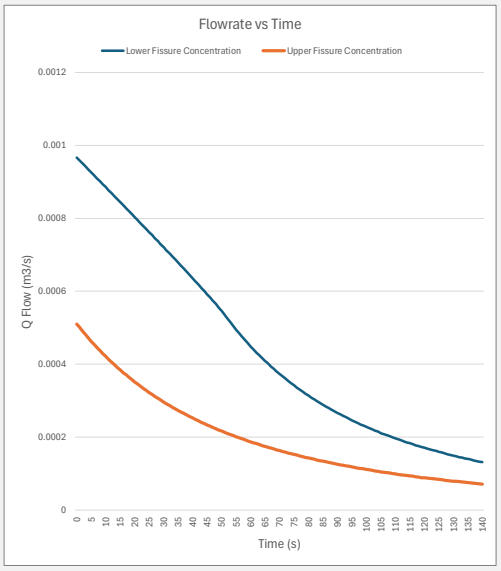

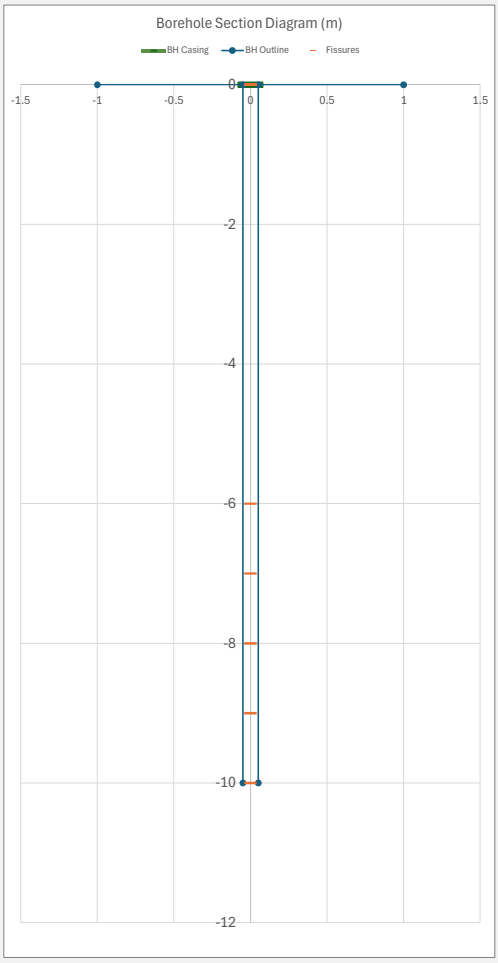

APPENDIX B

24/05/2024

BOREHOLE DATA ON PRIVATE LAND

Information & Permission Sheet

Information about the Study:

My name is Ryan Worley, and I am a Student at the University of Malta, reading for a *Masters in Civil Engineering*. My dissertation is about the infiltration of water through Maltese limestone, and how one can improve the groundwater recharge through the use of boreholes. This project is being conducted under the supervision of Dr Adrian Mifsud.

I am currently working with *Solidbase* and they are allowing me to perform water tests on a number of boreholes. However, since the boreholes and the information derived from recovered cores originate from your privately owned land, I require your written consent to use this data.

Please note that performing water permeability tests [*Falling Head Permeability Tests*] in boreholes have no negative consequences on the rock itself or any future development above.

Your Participation:

Any data collected from this research will be used solely for purposes of this study. Should you choose to participate, *Solidbase* may provide me with the relevant information on the ground underneath your site, and I would be able to conduct a water infiltration test on one or more boreholes found on-site.

Participation in this study is entirely voluntary; in other words, you are free to accept or refuse permission, without needing to give a reason. Should you choose to withdraw, any data collected from your site will be erased as long as this is technically possible.

Data Management:

The data collected will be anonymised in the dissertation. Your site's data may only be displayed on the research paper as being from a locality [For example - Location: Ħaż-Żebbuġ]. The data and any approved consent forms will only be kept in a private and secure location for up to three years after publication of the dissertation before being erased.

On the next sheet please find the '*Site Representative's Permission'* Section.

24/05/2024

Site Representative's Permission:

If you reply to this email with "I agree and consent to the study", it will signify that:

- You have read the information about the nature of the study, your involvement and data management.
- You have had the opportunity to ask questions about the study and your questions have been satisfactorily answered.
- You declare that you are 18 years or older.
- you understand that should you have any further queries, you can contact Ryan Worley through [redacted] or through the same email from which you received this consent form.
- You give permission to Ryan Worley to conduct permeability tests and to use borehole log data on the site in question.

Researcher

Ryan Worley

[redacted]

Supervisor

Dr Adrian Mifsud

[redacted]

Falling-Head Permeability Tests & The Application of their Results to the Ground Permeability Model for Infiltration Boreholes

The following sites were tested, and their results were analysed:

- Attard [Tested by R. Worley, 2024] Test #1
- Kalkara [Tested by R. Worley, 2024] Test #1
- Birkirkara [GEO-INF, Tested by N. Borg, 2012] Test #2
- Fgura [GEO-INF, Tested by N. Borg, 2012] Test #2

The following information for each test site is structured as the following:

1. Borehole Information
2. Fissure Distribution Table
3. Falling-Head Permeability Test Results
4. Parametric Model Overlay
5. Derivation of Flow Factor
6. Observations

See Appendix C for the full drilling records & model results.

Attard Site: Att.T1

The borehole was drilled within a private site by *Solidbase Laboratory Ltd* using a mobile drilling rig.

The borehole was drilled using a double core sampler, and the core was recovered.

The ground conditions were of fractured globigerina limestone, with no observed infill.

BH Dimensions:

9m	BH Depth
0.101m	BH Diameter
2m	Surface Casing Depth
0m	Initial Water Level Depth

Fissure Distribution Table (1) derived from Drilling Record:

Core Run (#)	Core Length Input Values (m)	RQD Input Values (%)	Core Run Max Depth (m)	Fissured Lengths (m)	Fissure Number per Run (#)	Fissure Number per Segment (#)
1	1	0	1	0	0	0
2	1	0	2	0	0	0
3	1	56	3	0.44	4.4	0.396
4	2	82.5	5	0.175	1.8	0.162
5	2	100	7	0	0	0
6	2	100	9	0	0	0

Note 1: Runs #1 and #2 were made up of agricultural soil, and hence, a casing was installed which spanned and covered the lengths.

Falling-Head Permeability Test Results:

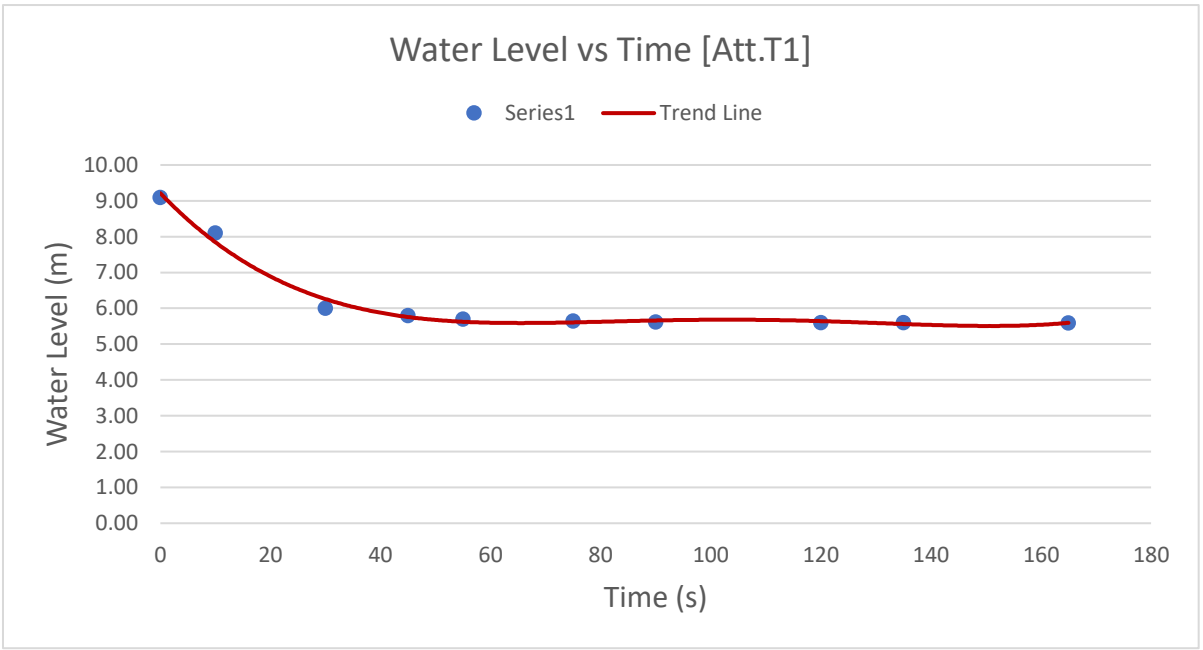

Model Overlay with Test Results (1):

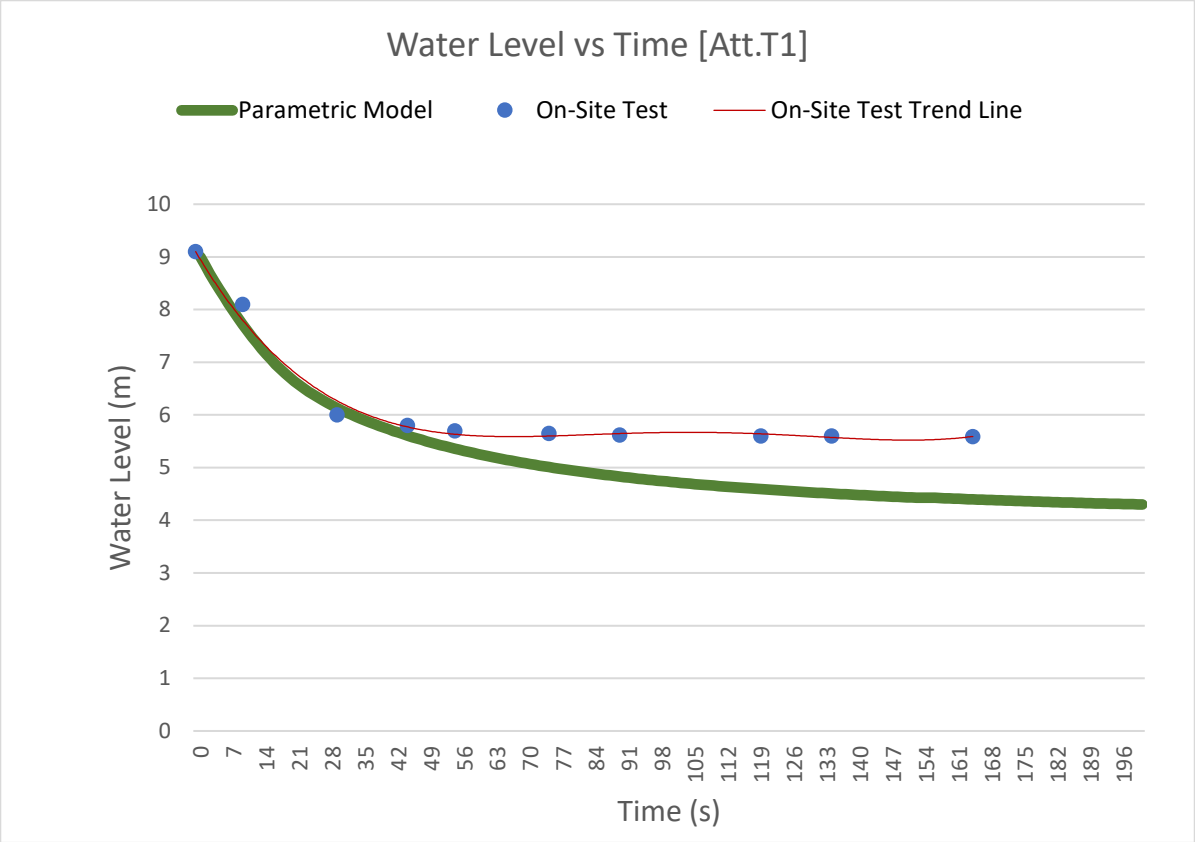

Observations (1):

The curves follow almost perfectly with each other, until 40 second mark, where the on-site test's head loss halted almost entirely at 3.5 metres from the surface (5.5 metres from the base of the borehole).

The halt in flowrate occurs within core run #4, through which the borehole drilling record listed an RQD of 82.5% over a depth of 2 metres.

However, by observing the images of the recovered core, it was noted that the core piece at a depth 4-5m exhibits little to no fractures along its length. Evidently, the majority of the fractures occur within the upper half of the 3-4m core piece

Therefore, it was seen as conclusive that the water level would drop only within 3m and 4m marks, at around the middle depth of around 3.5m.

If it were the case where the drilling record was set up to display 1m run cores along its entirety, then the following 'rough' estimations of RQD were derived:

Core Run #4 = 65% (1m)

Core Run #5 = 100% (1m)

Fissure Distribution Table (2) Adjusted for 1m Runs:

Core Run (#)	Core Length Input Values (m)	RQD Input Values (%)	Core Run Max Depth (m)	Fissured Lengths (m)	Fissure Number per Run (#)	Fissure Number per Segment (#)
1	1	0	1	0	0	0
2	1	0	2	0	0	0
3	1	56	3	0.44	4.4	0.396
4	1	65	4	0.35	3.5	0.315
5	1	100	5	0	0	0
6	1	100	6	0	0	0
7	1	100	7	0	0	0
8	1	100	8	0	0	0
9	1	100	9	0	0	0

Model Overlay with Test Results (2):

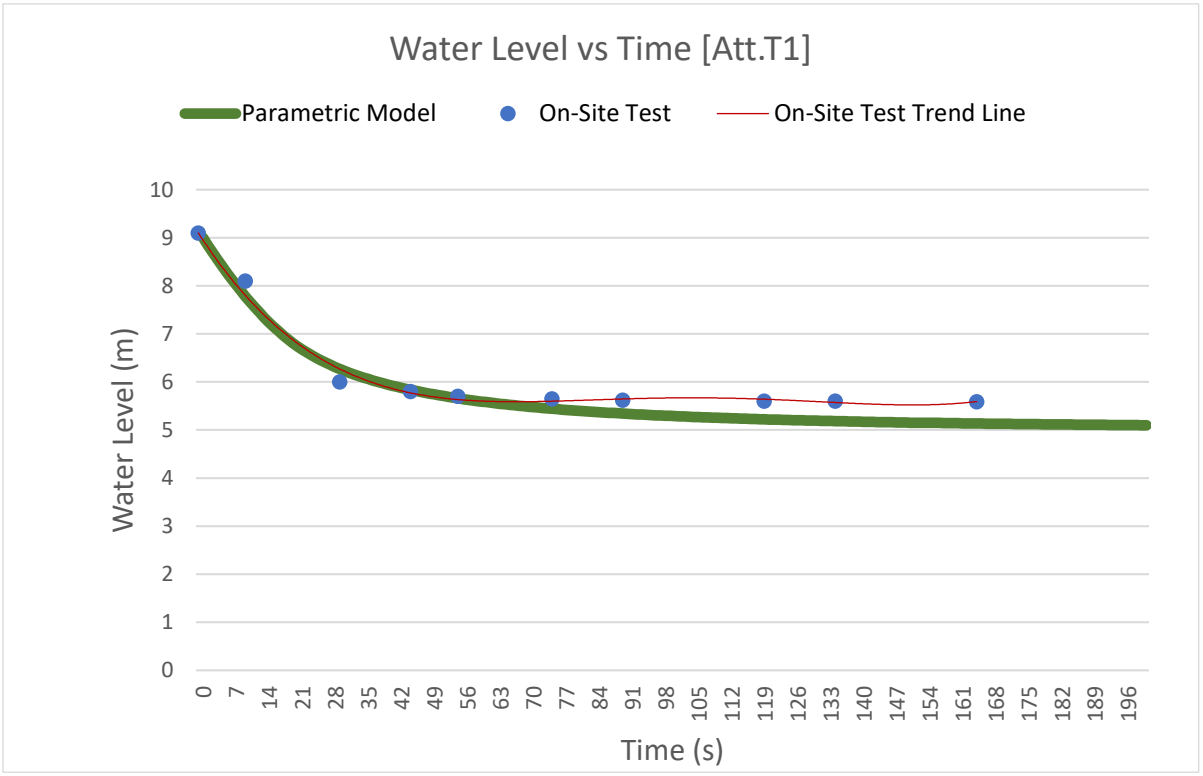

A flow factor of **0.065** was found to be the closest fit (for both RQD versions).

Observations (2):

The maximum velocity (steepest gradient) along the head loss curve was found to be 0.15722 m/s, and hence, the initial maximum flowrate was calculated as 1260 cm^3/s

The head loss curve created by the parametric model very accurately follows the curve created by the on-site permeability test, as seen below with the height difference percentages at specific timesteps:

Time Passed (s)	**P. Model Water Level** (m)	**On-Site Water Level** (m)	**Percentage Difference** (%)
0	9.000	9.10	1.11
10	7.753	8.10	4.47
30	6.332	6.00	5.24
45	5.900	5.80	1.62
55	5.716	5.70	0.28
75	5.487	5.65	2.97
90	5.381	5.62	4.45
120	5.250	5.60	6.67
135	5.209	5.60	7.51
165	5.155	5.59	8.43

Kalkara Site: Kal.T1

The borehole was drilled within a private site by *Solidbase Laboratory Ltd* using a mobile drilling rig.

The borehole was drilled using a single core sampler, and the core was recovered.

The ground conditions were of very weak fractured globigerina limestone, coralline limestone with fissure soil traces. Data unreliable since any fissures would have subsequently been filled during the drilling process.

BH Dimensions:

8m	BH Depth
0.101m	BH Diameter
0m	Surface Casing Depth
0m	Initial Water Level Depth

Fissure Distribution Table derived from Drilling Record and Assumptions:

Core Run (#)	Core Length Input Values (m)	RQD Input Values (%)	Core Run Max Depth (m)	Fissured Lengths (m)	Fissure Number per Run (#)	Fissure Number per Segment (#)
1.1	0.6	5	0.6	0..57	5.7	0.76
1.2	0.9	100	1.5	0	0	0
2	1.5	100	3	0	0	0
3	1.5	100	4.5	0	0	0
4	1.5	16	6	0.504	5	0.267
5	1	55	7	0.27	2.7	0.216
6	1	0	8	0.6	6	0.48

Falling-Head Permeability Test Results:

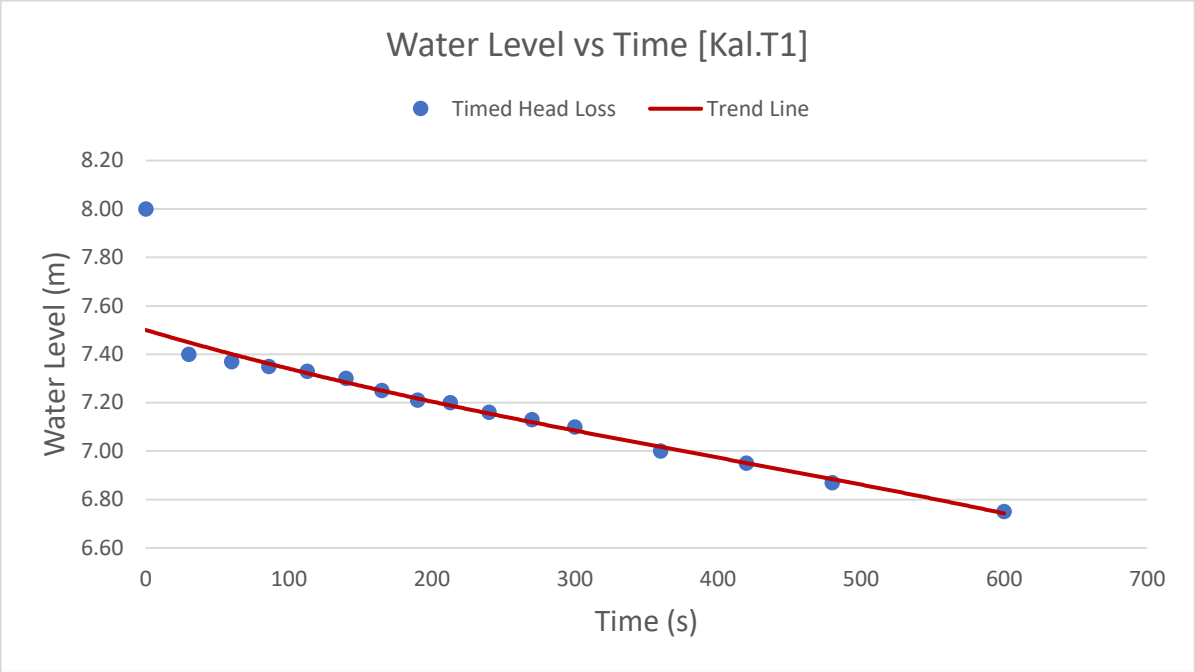

Note: Trend line is drawn with a y-intercept of 7.5m, since the rapid initial head loss occurs due to the surface fill material of ~0.5m.

Model Overlay with Test Results:

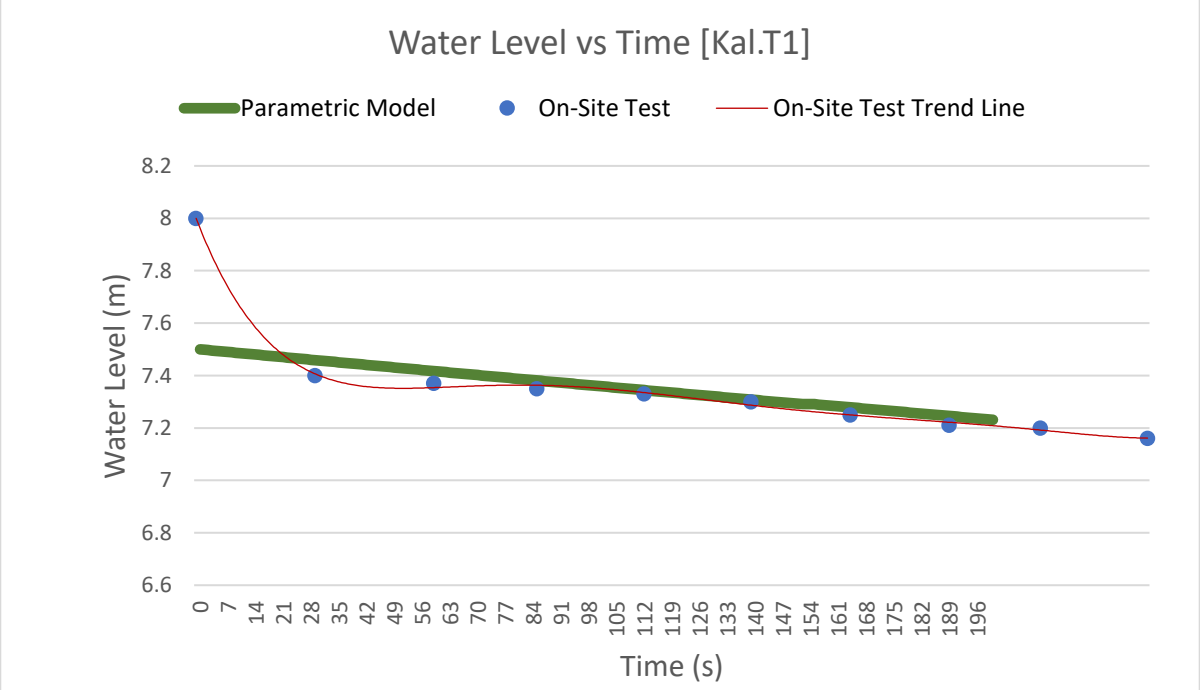

By lowering the starting water level's depth to 7.5m, the parametric model's head loss curve more accurately follows the trend line of the on-site test when a flow factor of **0.00021** is applied.

Observations:

When the recovered core was brought to the laboratory, concerns were raised about the viability of the test. The ground consisted of very weak rock, which may have been crushed by the simple sampler within the borehole cavity and mixed with the water. This could have resulted in any on-site fissures being forcefully infilled and blocked with the muddy mixture. This would also have an effect on Coralline Limestone porosity.

Drilling Record:

> 0.6m-4.5m: "Retrieved as soil due to use of simple sampler, (wackestone) limestone – GLOBIGERINA, Lower member"

From observing the recovered core, a large number of fractures are found throughout its length. The presence of a soft saturated clayey soil is evident, which likely infilled the fissures and slowed down permeability drastically.

In order to derive a conservative estimate of permeability, it was assumed that the lost fissure data is taken as fully intact rock (RQD = 100%) along this specific length of Globigerina.

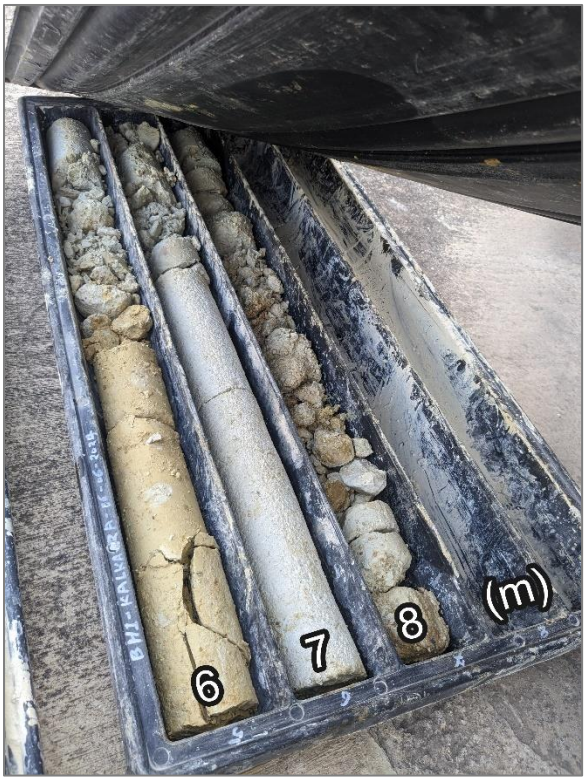

Birkirkara Site: Bir.T2

In order to obtain a wider range of test values, falling head permeability tests conducted by Nadine Borg (2012) relating to the GEO-INF Project were used to further refine the parametric model and attempt to find commonalities between flow factors.

The borehole was drilled within school boundaries by *Solidbase Laboratory* using a mobile drilling rig.

The borehole was drilled using a double core sampler, and the core was recovered.

The ground conditions were of weak fractured globigerina limestone, with 'terra rossa' infill.

BH Dimensions:

21m	Depth
0.14m	Diameter
5.4m	Surface Casing Depth
9m	Initial Water Level Depth

Fissure Distribution Table derived from Drilling Record:

Core Run (#)	Core Length Input Values (m)	RQD Input Values (%)	Core Run Max Depth (m)	Fissured Lengths (m)	Fissure Number per Run (#)	Fissure Number per Segment (#)
1	1	0	1	1	10	2.1
2	1	80	2	0.2	2	0.42
3	1	70	3	0.3	3	0.63
4	1	70	4	0.3	3	0.63
5	1	70	5	0.3	3	0.63
6	6	100	11	0	0	0
7	1	80	12	0.2	2	0.42
8	3	100	15	0	0	0
9	1	66	16	0.34	3.4	0.714
10	1	100	17	0	0	0
11	1	100	18	0	0	0
12	1	85	19	0.15	1.5	0.315
13	1	90	20	0.1	1	0.21
14	1	100	21	0	0	0

Falling-Head Permeability Test Results:

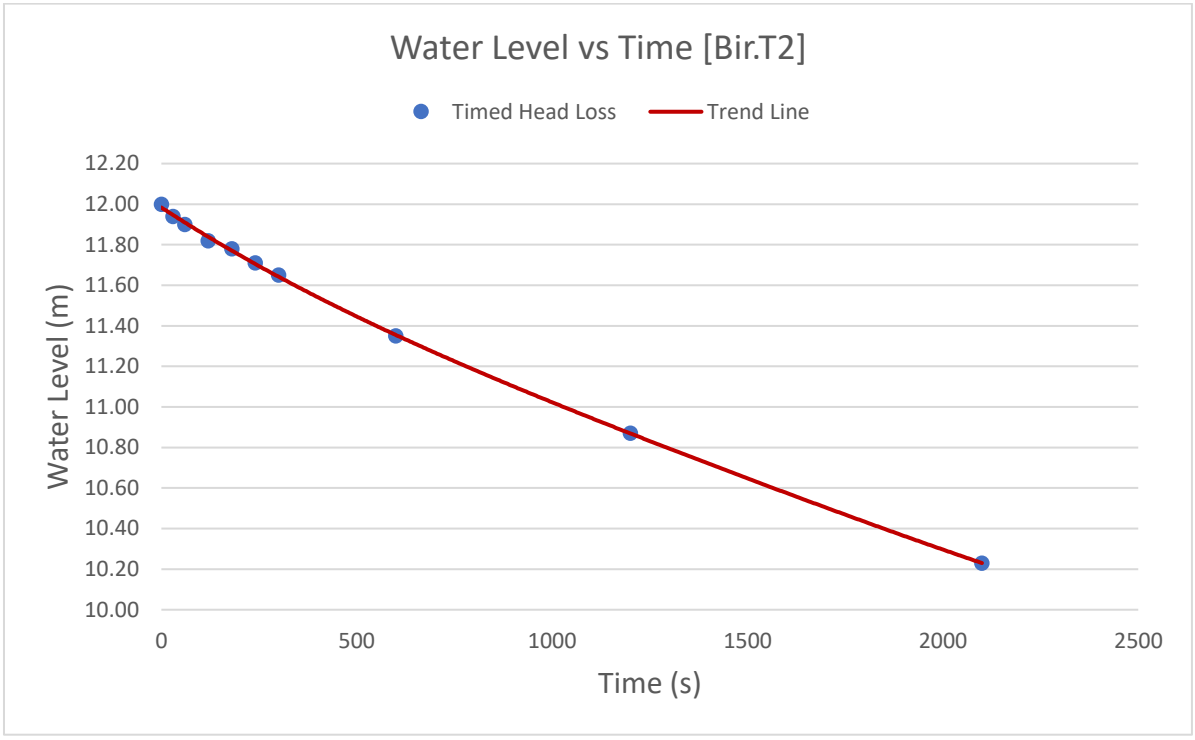

Model Overlay with Test Results:

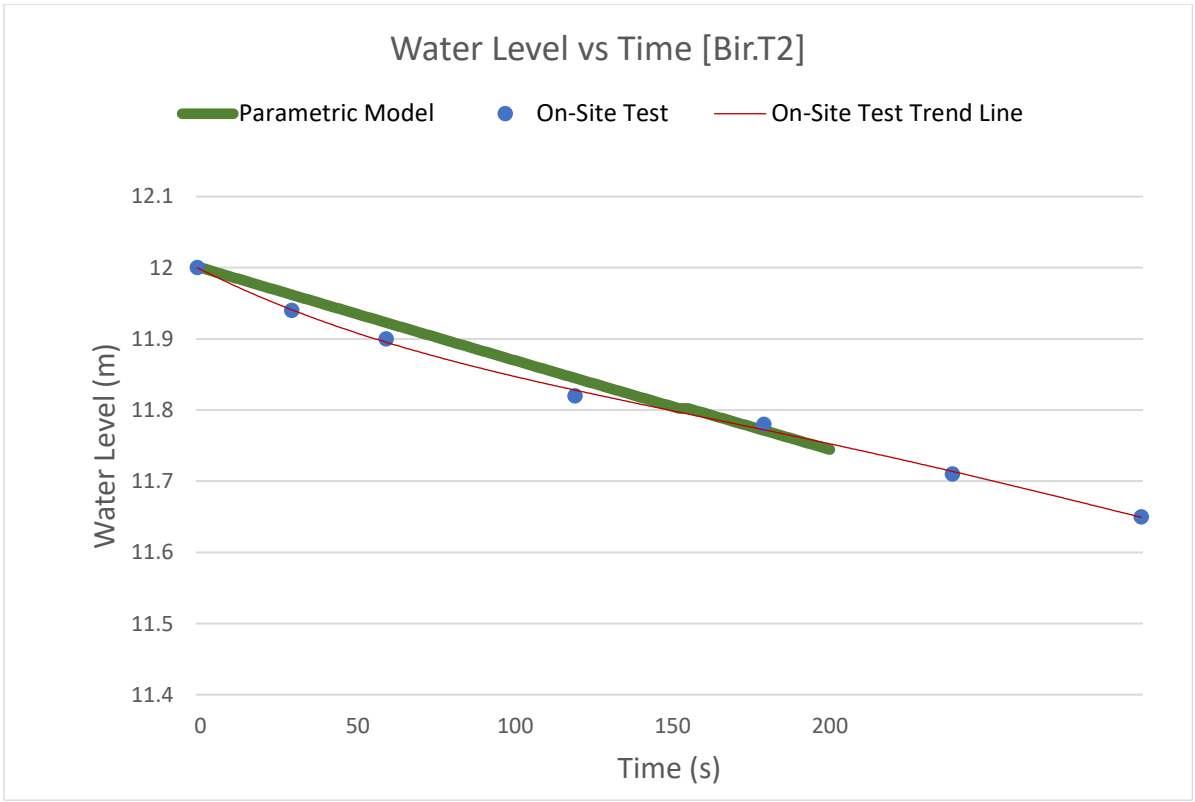

The parametric model's head loss curve more accurately follows the trend line of the on-site test when a flow factor of **0.0005** is applied.

Observations:

Bir.T2 exhibited a fairly low permeability, with a maximum initial flowrate of around 31cm^3/s. The test took more than an hour to conduct, and yet the head had only reduced by almost 2 metres.

The low permeability may be due to the lack of fissures at very far depths, whilst simultaneously, the fissures were observed to be infilled with a red soil (terra rossa infill).

Most of the fissures were found close to the surface, within the weathered zone. However, a borehole casing was installed throughout this layer, preventing the ability to make use of this layer for enhanced secondary permeability.

Fgura Site: Fgu.T2

The second site upon which a falling head permeability test was conducted by N. Borg (2012), relating to the GEO-INF Project.

The borehole was drilled within school boundaries by *Solidbase Laboratory* using a mobile drilling rig.

The borehole was drilled using a double core sampler, and the core was recovered.

The ground conditions were of fractured globigerina limestone of varying strength, with 'terra rossa' infill.

BH Dimensions:

22m	Depth
0.1m	Diameter
5.77m	Surface Casing Depth
2.1m	Initial Water Level Depth

Fissure Distribution Table derived from Drilling Record:

Core Run: (#)	Core Length Input Values: (m)	RQD Input Values: (%)	Core Run Max Depth: (m)	Fissured Lengths: (m)	Fissure Number per Run: (#)	Fissure Number per Segment: (#)
-	-	-	-	-	-	-
1	1.5	33.3	1.5	1	10	1.467
2	1.5	90	3	0.15	1.5	0.22
3	1.8	77.8	4.8	0.33	3.3	0.403
4	2	80	6.8	0.3	3	0.33
5	2.6	34.6	9.4	0.98	9.8	0.829
6	2.3	73.9	11.7	0.39	3.9	0.373
7	3	96.7	14.7	0.05	0.5	0.037
8	3	100	17.7	0	0	0
9	2	55	19.7	0.68	6.8	0.748
10	2	90	21.7	0.15	1.5	0.165
11	0.3	100	22	0	0	0

Falling-Head Permeability Test Results:

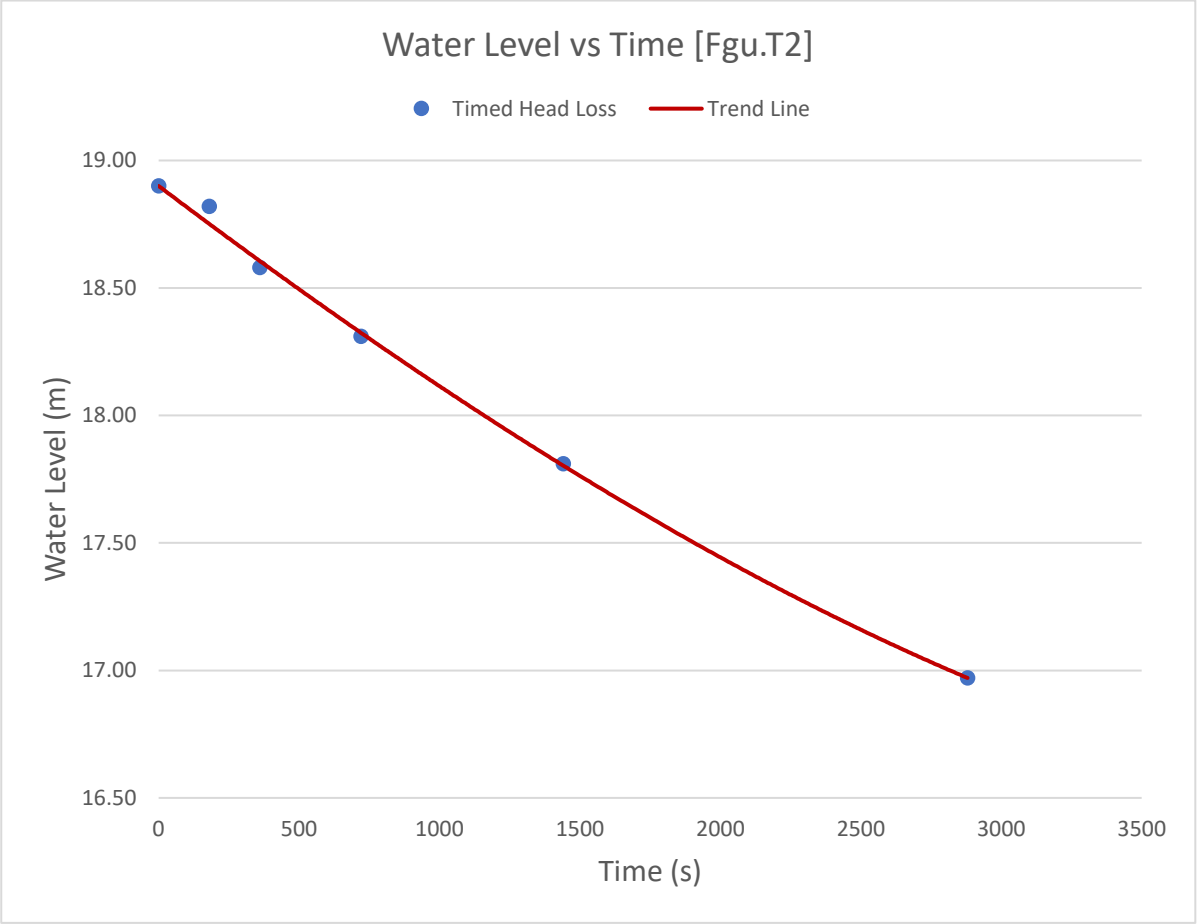

Model Overlay with Test Results:

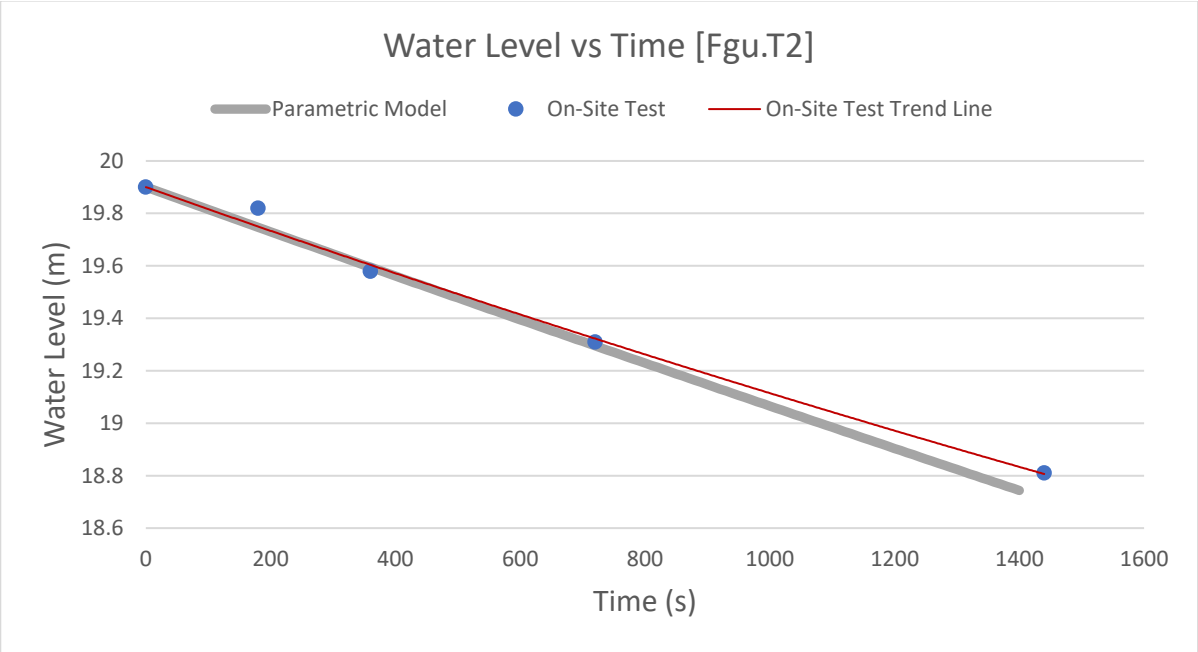

The parametric model's head loss curve more accurately follows the trend line of the on-site test when a flow factor of **0.000065** is applied.

A timestep of 10s was required for the model due to the low infiltration rate.

Observations:

RQD values vary greatly throughout the borehole's depth, however, due to the red clayey soil (terra rossa) infilling of the fissures, the flow factor come out to a very low value.

Most of the fissures were found close to the surface, within the weathered zone. However, a borehole casing was installed throughout this layer, preventing the ability to make use of a significant portion of this layer for secondary permeability.

Summarized Results of Tests:

Location	Attard [Att.T1]	Kalkara [Kal.T1]	Birkirkara [Bir.T2]	Fgura [Fgu.T2]
F_F ($x10^{-3}$)	65	0.21	0.5	0.065
Infill	No Infill	Clayey Soil	Clayey Soil	Clayey Soil
RQDs	Moderate	Low	High	Low
BH Depth (m)	9	8	21	22
BH Diameter (m)	0.10	0.10	0.14	0.10
Height MSL (m)	+68	+37	+39	+43

Application of Ground Permeability Model for Infiltration Boreholes to Rainfall Catchment Areas

The following sites were selected, and their results were analysed:

- Wied is-Sewda (Wied il-Kbir Catchment Area, Ħal-Qormi)
- Wied Katarina (Wied il-Għasel Catchment Area, Burmarrad)

The following information for each MAR site is structured as the following:

1. Sub-Catchment Information
2. Preliminary Borehole Dimensions
3. Ground Characteristics
4. Stormwater Flowrate
5. Infiltration Flowrate
6. Borehole Array

It is important to note that any RQD values are entirely fictitious and are only used to explain how the model can be used.

Wied is-Sewda

Wied is-Sewda is a sub-catchment of the Wied il-Kbir Catchment Area, spanning from Attard to Marsa. Wied is-Sewda is comprised of urban land concentrated within Ħal-Qormi, agricultural land, quarries for stone extraction, and a small percentage of natural garrigue and wooded areas (Adi Associates, 2020b).

As it stands, one can consider Wied is-Sewda to be an ecological desert with little to no value being derived apart from the retention of water to prevent downstream flooding (Caruana, T. M., 2017). The watercourse is neglected and often used as a dumping ground. The potential for a valley regeneration project is clear, with what one can consider as having close to no drawbacks or risks in implementing MAR projects.

Wied is-Sewda had already been recognised in the past as an important sub-catchment for groundwater pumping by O. Chadwick (Borg, J., 2018). The Tal-Ħlas Pumping Station is found in the heart of the valley and has been recorded to supply up to 10% of the daily extracted groundwater in Malta from its six underground galleries (Seychell, 2000).

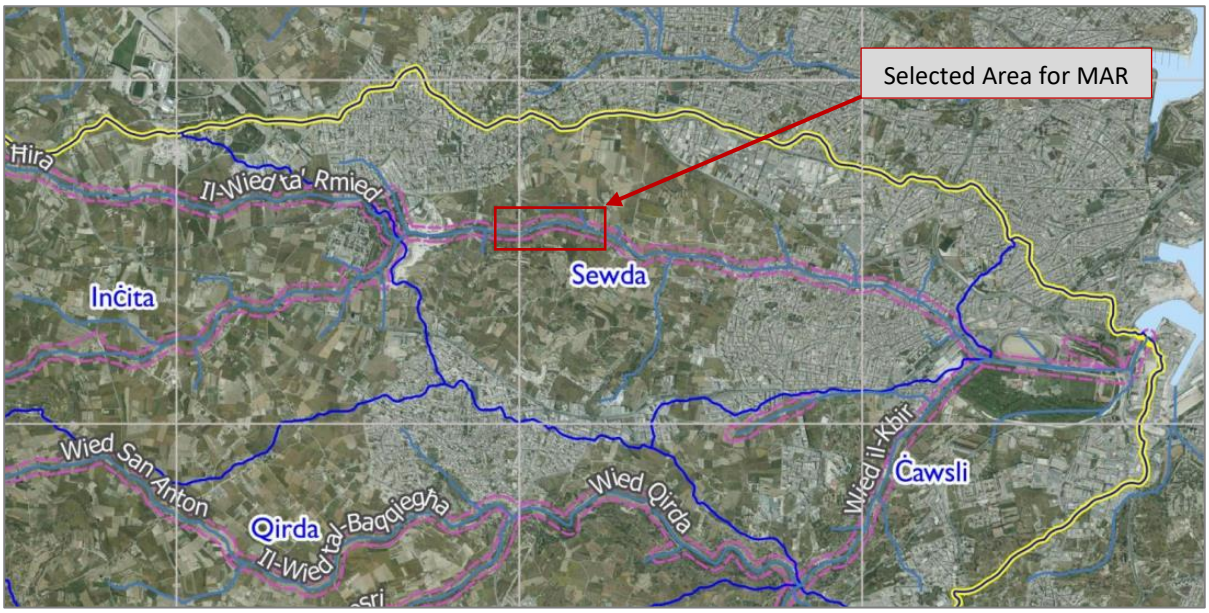

Wied is-Sewda, Water Sub-Catchments Map (Adi Associates Wied il-Kbir Summary Report, 2020)

Preliminary Borehole Dimensions:

- 15m BH depth [High distance from MSL aquifer]
- 0.1m diameter
- 5m of globigerina limestone overlying coralline limestone
- Fractures throughout the rock layers
- BH Casing of 2m depth
- Flow Factor of 0.02
- Coralline Limestone K = 5×10^{-7} m/s

Ground Characteristics:

The region is characterised by many major faults, with weathered globigerina limestone overlaying coralline limestone. Fissures may be found throughout.

For the purposes of this example, it is assumed that the ground layers consist of 5m of globigerina limestone overlying coralline limestone, therefore, 10m of primary permeability must be considered along with the secondary permeability from fissures.

Table 1: Fissure Distribution Table (With fictitious RQD values):

Core Run: (#)	Core Length Input Values: (m)	RQD Input Values: (%)	Core Run Max Depth: (m)	Fissured Lengths: (m)	Fissure Number per Run: (#)	Fissure Number per Segment: (#)
1	1	40	1	0.6	6	0.9
2	1	50	2	0.5	5	0.75
3	1	60	3	0.4	4	0.6
4	1	80	4	0.2	2	0.3
5	1	100	5	0	0	0
6	1	80	6	0.2	2	0.3
7	1	75	7	0.25	2.5	0.375
8	1	100	8	0	0	0
9	1	80	9	0.2	2	0.3
10	2	85	11	0.15	1.5	0.225
11	2	100	13	0	0	0
12	2	80	15	0.2	2	0.3

Stormwater Flowrate:

When considering Wied is-Sewda in Ħal-Qormi as a potential location for a managed aquifer recharge, the upstream catchment area would need to be considered.

The total upstream catchment area is equal to:

8.227km^2

When considering that the impermeable area represents 16% of the total catchment area:

131.627 Hectares of impermeable surface runoff.

With a mean annual rainfall of 543.4mm (NSO Malta, 2022), one can expect an average of 1.49mm of rainfall per day. Applying this to the entire catchment area would result in:

1959.6m^3 per day passing through the Wied is-Sewda Watercourse.

Infiltration Flowrate:

Using the catchment values obtained previously as well as the preliminary borehole dimension values:

Primary Permeability -> Using Hvorslev's Deep Flow Calculation = 70.496cm^3/s

Secondary Permeability -> Using the Fissure Distribution Table = 1055.398cm^3/s

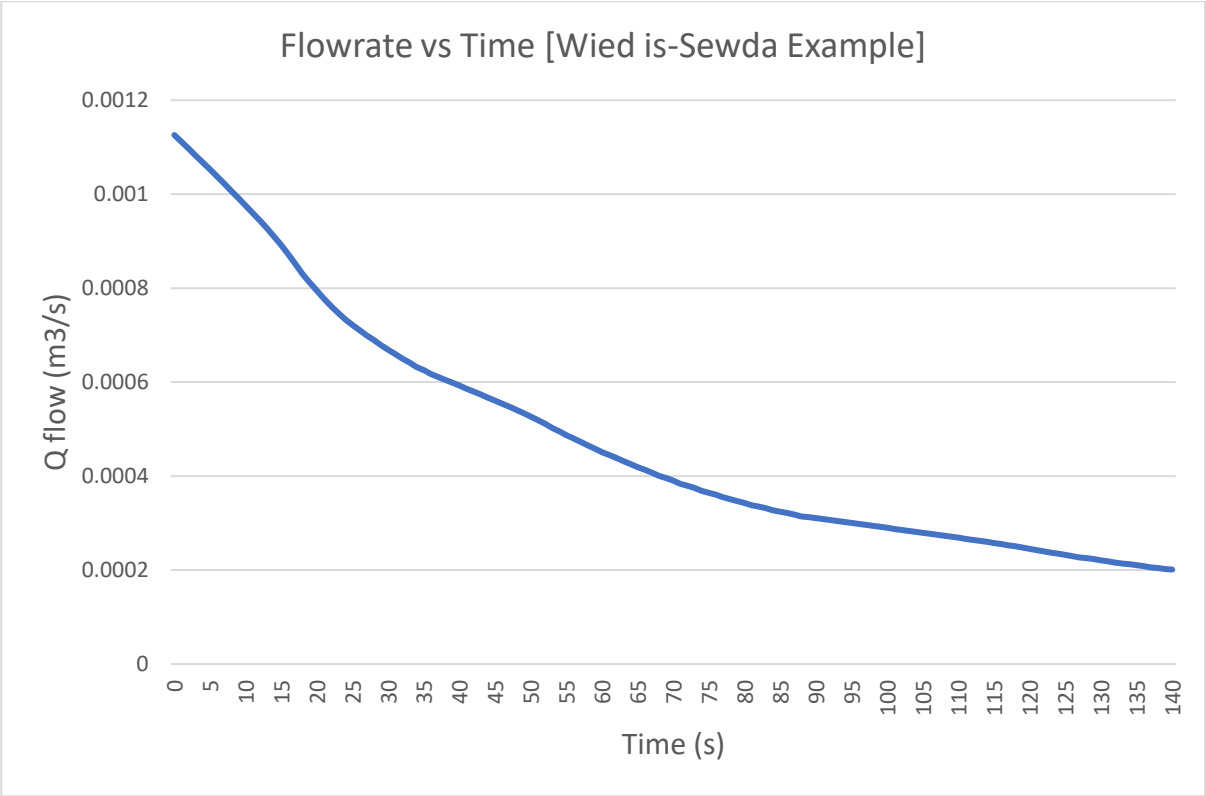

A total infiltration flowrate of 1125.894cm^3/s was calculated.

Thus, the number of boreholes required to capture the full entry flow was found to be:

~20 infiltration boreholes.

However, assuming a retained environmental flow of 60% for downstream areas,

~8 infiltration boreholes.

This value can be further reduced by adjusting the depth or the diameter.

In this case, doubling the borehole diameter to 0.2m would result in a halving of boreholes required; meaning, ~4 boreholes would be sufficient.

<u>Summary of Input & Output Data:</u>

BOREHOLE DATA:

BH Input Data:		
BH Depth	15	m
BH Diameter	0.1	m
Impermeable Casing Depth:	2	m
Borehole Filter Medium:	Gravel [0.50 void ratio]	
Extra Input:		
Coralline Limestone K Value:	0.0000005	m3/s/m2
Gravity acceleration:	9.81	m/s2
Timestep (s):	1	s
Water Level Starting Depth (m):	0	m

GROUND INPUT DATA:

Ground Input Data:		
fissure infill:	No Infill	
Flow Factor:	0.02 *[Between 0-1]*	
[A restriction of velocity/flow due to roughness, eff. Length]		
Fissure Input Data:		
Aperture Width:	1	mm avg
Avg Fissure Seperation:	10	cm *max 10cm*

Rock Type:		Rock Length:
Upper Rock:	Globigerina Limestone	5 m
Lower Rock:	Coralline Limestone	10 m

SECONDARY CALCULATED DATA:

Calculated Values:		
Wetted Area:	4.720242962	m2
Total Contained Vol:	0.117809725	m3
Volume of Slice:	0.001178097	m3
Slice/Segment Height:	0.15	m
% CSA Available (Void) within BH:	50	%
Borehole CSA:	0.003926991	m2
Fracture/Tube Flow CSA:	0.314159265	m2

Summarized Results [Steady-State Condition]:		
Primary Permeability:	70.496	cm3/s
Secondary Permeability:	1055.398	cm3/s
Total Permeability Q:	1125.894	cm3/s
Hydraulic Permeability K:	0.0003276	cm/s

Wied Katarina

The Katarina sub-catchment is situated within the broader Wied il-Għasel Catchment Area, stretching from Ta' Qali to Burmarrad. This research, however, focuses on the downstream segment of Wied il-Għasel, adjacent to the Industrial Estate and Santa Katerina chapel. This area is characterized by agricultural land, industrial activity, and mineral extraction quarries (Adi Associates, 2020a). Rainwater runoff from Dingli, Baħrija, and Wied il-Qlejgħa all converges in this area.

The Katarina watercourse has recently undergone redevelopment, incorporating stone embankment dams and raised pathways for the Wied il-Għasel nature trail (MaltaToday, 2011). These dams serve to mitigate downstream flooding in Burmarrad and St. Pauls Bay. Despite these improvements, the region contends with dust emissions from nearby quarries and industrial facilities, necessitating careful consideration of environmental pollutants. Nevertheless, implementation of a MAR project in this area could serve as a barrier against saline intrusion from the sea into the groundwater aquifer.

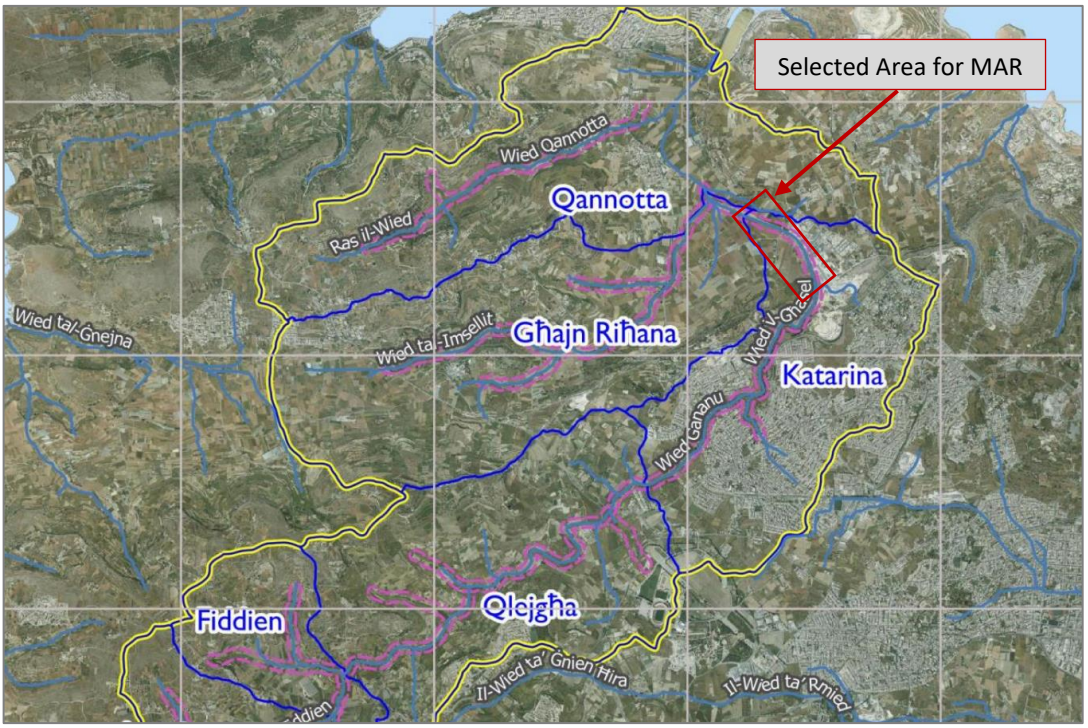

Wied Katarina, Water Sub-Catchments Map (Adi Associates Wied il-Għasel Summary Report, 2020)

Preliminary Borehole Dimensions:

- 10m BH depth [Small distance from MSL aquifer]
- 0.2m diameter
- 4m of globigerina limestone overlying coralline limestone
- Fractures throughout the rock layers
- BH Casing of 2m depth
- Flow Factor of 0.005
- Coralline Limestone K = 5×10^{-7} m/s

Ground Characteristics:

The region is characterised by many major faults, with weaky-consolidated to unconsolidated clayey sandy gravels, and globigerina limestone overlaying coralline limestone close to sea level. Due to region's surface soils, one may expect a very high resistance to flow within the fissures.

Fissure Distribution Table (With fictitious RQD values):

Core Run: (#)	Core Length Input Values: (m)	RQD Input Values: (%)	Core Run Max Depth: (m)	Fissured Lengths: (m)	Fissure Number per Run: (#)	Fissure Number per Segment: (#)
1	1	50	1	0.5	5	0.5
2	1	50	2	0.5	5	0.5
3	1	75	3	0.25	2.5	0.25
4	1	80	4	0.2	2	0.2
5	1	60	5	0.4	4	0.4
6	1	80	6	0.2	2	0.2
7	1	80	7	0.2	2	0.2
8	1	100	8	0	0	0
9	1	80	9	0.2	2	0.2
10	1	65	10	0.35	3.5	0.35

Stormwater Flowrate:

When considering Wied Katarina in Burmarrad as a potential location for a managed aquifer recharge, the upstream catchment area would need to be considered.

The total upstream catchment area is equal to:

21.667km^2

When considering the impermeable area to represent 18.36% of the total catchment area:

397.863 Hectares of impermeable surface runoff.

With a mean annual rainfall of 543.4mm (NSO Malta, 2022), one can expect an average of 1.48877mm of rainfall per day. Applying this to the entire catchment area would result in:

5923.265m^3 per day passing through the Wied Katarina Watercourse.

Infiltration Flowrate:

Using the catchment values obtained previously as well as the preliminary borehole dimension values:

Primary Permeability -> Using Hvorslev's Deep Flow Calculation = 34.393cm^3/s

Secondary Permeability -> Using the Fissure Distribution Table = 598.205cm^3/s

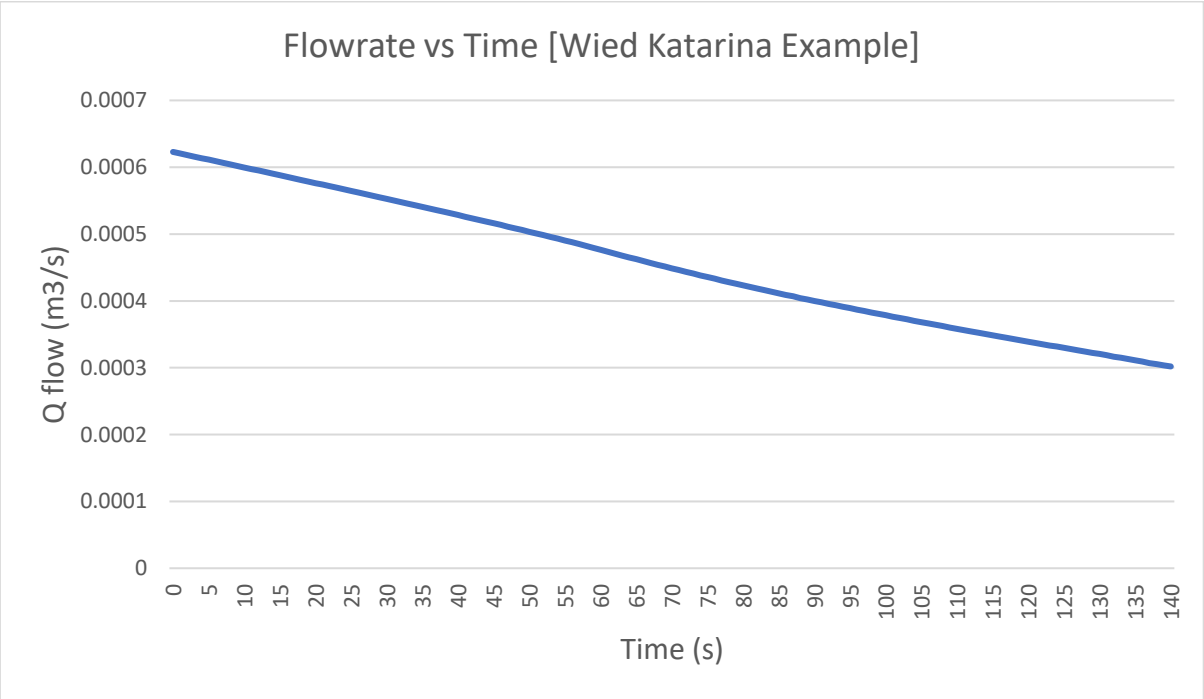

A total infiltration flowrate of 632.598cm^3/s was calculated.

Thus, the number of boreholes required to capture the full entry flow was found to be:

~115 infiltration boreholes.

However, assuming a retained environmental flow of 60% for downstream areas,

~45 infiltration boreholes.

It is clear that this many boreholes are an unpractical and unfeasible intervention to capture 40% of the entire flow of the Wied il-Għasel catchment.

A number of conclusions may be derived from these findings:

1. The infiltration boreholes for MAR for Wied Katarina can be spread out along the entirety of the catchment area.
2. The infiltration boreholes will have to have a larger diameter or will have to be deeper for a larger flowrate capacity.
3. It may be extremely beneficial to ensure that the infiltration boreholes are located within the embankment dam basins, so as to increase the pooling time for the water to infiltrate into the ground.
4. It is not required to capture that high volume of runoff, thus allowing for further downstream infiltration or discharge into the sea.

<u>Summary of Input & Output Data:</u>

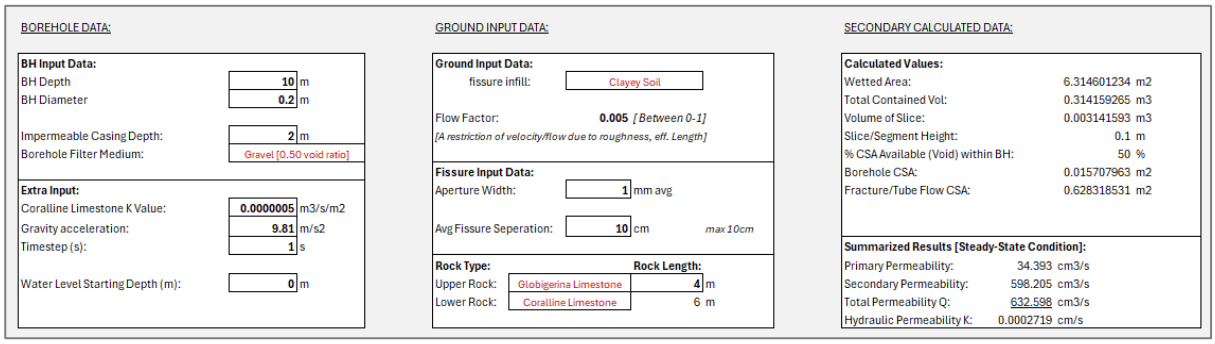

BOREHOLE DATA:

BH Input Data:		
BH Depth	10	m
BH Diameter	0.2	m
Impermeable Casing Depth:	2	m
Borehole Filter Medium:	Gravel [0.50 void ratio]	
Extra Input:		
Coralline Limestone K Value:	0.0000005	m3/s/m2
Gravity acceleration:	9.81	m/s2
Timestep (s):	1	s
Water Level Starting Depth (m):	0	m

GROUND INPUT DATA:

Ground Input Data:		
fissure infill:	Clayey Soil	
Flow Factor:	0.005 *[Between 0-1]*	
[A restriction of velocity/flow due to roughness, eff. Length]		
Fissure Input Data:		
Aperture Width:	1	mm avg
Avg Fissure Seperation:	10	cm *max 10cm*

Rock Type:		Rock Length:
Upper Rock:	Globigerina Limestone	4 m
Lower Rock:	Coralline Limestone	6 m

SECONDARY CALCULATED DATA:

Calculated Values:		
Wetted Area:	6.314601234	m2
Total Contained Vol:	0.314159265	m3
Volume of Slice:	0.003141593	m3
Slice/Segment Height:	0.1	m
% CSA Available (Void) within BH:	50	%
Borehole CSA:	0.015707963	m2
Fracture/Tube Flow CSA:	0.628318531	m2

Summarized Results [Steady-State Condition]:		
Primary Permeability:	34.393	cm3/s
Secondary Permeability:	598.205	cm3/s
Total Permeability Q:	632.598	cm3/s
Hydraulic Permeability K:	0.0002719	cm/s

APPENDIX C

Borehole Drilling Record

solidbase LABORATORY LTD.

page 1 of 2

BH1

Client:	Location:	Weather:	Date started:	Date completed:
	Attard	Fair	09/05/2024	09/05/2024
			Northings:	Eastings:

Job No:	Drill type:	Bit type/diameter:	Orientation:	Drilling fluid:	Ground level:	Water level:
J4237	CMV 600	Double Core	0	Water	69	0

Description	Depth (Actual depth)	Run (Drill time)	TCR %	SCR %	RQD %	f/m /m	Sampling/testing	Drilling progress	Returns
Light Yellowish Brown (2.5Y 6/3), loose, fine to coarse, silty gravel - MAN MADE, Limestone Fill	69.00	1 0.0	100.0					Advance Casing - Sampling	
Pale Brown (2.5Y 8/3), loose, coarse, cobbles - MAN MADE, Limestone Fill									
Brown (10YR 4/3), loose, fine to coarse, silty, with cobbles, sandy gravel - MAN MADE, Soil Fill	1.00 68.00	2 0.0	100.0					Advance Casing - Sampling	
Pale Brown (2.5Y 7/4), moderately weak, bioturbated, fine, rust stained, (wackestone) limestone - GLOBIGERINA, Lower member	2.00 67.00	3 0.1	100.0	68.0	56.0			Coring using double core sampler	
Discontinuity at 45°, rough sides, caliche traces, unclear									
	3.00 66.00	4 0.3	100.0	90.5	82.5		3.20 MC: 21.85% BD: 2057.01Kg/m³ UCS: 10.37N/mm²	Coring using double core sampler	
Discontinuity at 30°, rough sides, soil traces, unclear	4.00 65.00								

Legend:

GL: Ground level
AOD: Above Ordinance Datum
AMSL: Above mean sea level
RQD: Rock Quality Designation
TCR: Total core recovery
SCR: Solid core recovery
f: Fracture frequency
O/H: Open hole drilling

Clay, Silt, Sand, Gravel, Cobbles/ Boulders, Marl, Limestone, Recent

Topsoil (Recent deposits)
Man-made material (Recent deposits)
Quaternary Deposits (PLEISTOCENE, to HOLOCENE)
Upper Coralline Limst., Tal-Pitkal (MIOCENE, Tortonian to early Messinian)
Upper Coralline Limst., Mtarfa (MIOCENE, Tortonian to early Messinian)
Blue Clay - top weathered strata (MIOCENE, Langhian to Tortonian)
Blue Clay (MIOCENE, Langhian to Tortonian)
Upper Globigerina Limestone (MIOCENE, Burdigalian to early Langhian)
Middle Globigerina Limestone (MIOCENE, Aquitanian to Burdigalian)
Lower Globigerina Limestone (MIOCENE, Aquitanian)
Lower Coralline Limestone, Xlendi Member (OLIGOCENE, Chattian)
Lower Coralline Limestone, Attard Member (OLIGOCENE, Chattian)

UCS: Unconfined comp.strength
BD: Bulk density
MC: Moisture content
PP: Pocket penetrometer
PSV: Pocket shear vane
OED: Oedometer
SPT: Standard Penetration Test

Soil & rock colour references: Munsell notation (2009 charts)

Soil & rock strength descriptors: to BS 5930:1999

Borehole Drilling Record

BH1

Client:	Location:	Weather:	Date started:	Date completed:
	Attard	Fair	09/05/2024	09/05/2024
			Northings:	Eastings:

Job No:	Drill type:	Bit type/diameter:	Orientation:	Drilling fluid:	Ground level:	Water level:
J4237	CMV 600	Double Core	0	Water	69	0

Description	Depth (Actual depth)	Run (Drill time)	TCR %	SCR %	RQD %	f/m /m	Sampling/testing	Drilling progress	Returns
Pale Brown (2.5Y 7/4), moderately weak, bioturbated, fine, rust stained, (wackestone) limestone - GLOBIGERINA, Lower member	5.00 (64.00)	5 (0.3)	100.0	98.0	98.0			Coring using double core sampler	
	5.70						MC: 21.69% BD: 2045.91Kg/m³ UCS: 10.41N/mm²		
	6.00 (63.00)								
	7.00 (62.00)	6 (0.3)	100.0	99.0	98.0			Coring using double core sampler	
	7.85						MC: 20.48% BD: 2079.75Kg/m³ UCS: 10.23N/mm²		
Yellow (2.5Y 7/6), moderately weak, bioturbated, fine, rust stained, (wackestone) limestone - GLOBIGERINA, Lower member	8.00 (61.00)								
End of borehole	9.00 (60.00)								

Legend:

GL: Ground level
AOD: Above Ordinance Datum
AMSL: Above mean sea level
RQD: Rock Quality Designation
TCR: Total core recovery
SCR: Solid core recovery
f: Fracture frequency
O/H: Open hole drilling

Clay, Silt, Sand, Gravel, Cobbles/ Boulders, Marl, Limestone, Recent

Topsoil (Recent deposits)
Man-made material (Recent deposits)
Quaternary Deposits (PLEISTOCENE, to HOLOCENE)
Upper Coralline Limst., Tal-Pitkal (MIOCENE, Tortonian to early Messinian)
Upper Coralline Limst., Mtarfa (MIOCENE, Tortonian to early Messinian)
Blue Clay - top weathered strata (MIOCENE, Langhian to Tortonian)
Blue Clay (MIOCENE, Langhian to Tortonian)
Upper Globigerina Limestone (MIOCENE, Burdigalian to early Langhian)
Middle Globigerina Limestone (MIOCENE, Aquitanian to Burdigalian)
Lower Globigerina Limestone (MIOCENE, Aquitanian)
Lower Coralline Limestone, Xlendi Member (OLIGOCENE, Chattian)
Lower Coralline Limestone, Attard Member (OLIGOCENE, Chattian)

UCS: Unconfined comp.strength
BD: Bulk density
MC: Moisture content
PP: Pocket penetrometer
PSV: Pocket shear vane
OED: Oedometer
SPT: Standard Penetration Test

Soil & rock colour references: Munsell notation (2009 charts)

Soil & rock strength descriptors: to BS 5930:1999

Att.T1 BH1 (2024)

Falling Head Permeability Test (In-Situ)

Location: Attard
Company: Solidbase Laboratory

Test ID: Att.T1
Date: 09.05.2024

Borehole Data

BH Depth:	9	m
BH Diameter:	0.101	m
BH Casing Depth:	2	m
Site BH Number:	BH1	

Ground Data

Avg Fissure Width:	1	mm
Fissure Spread:	Surface Weathering	
Fissure Infill:	Unknown	
Ground Material:	Globigerina	

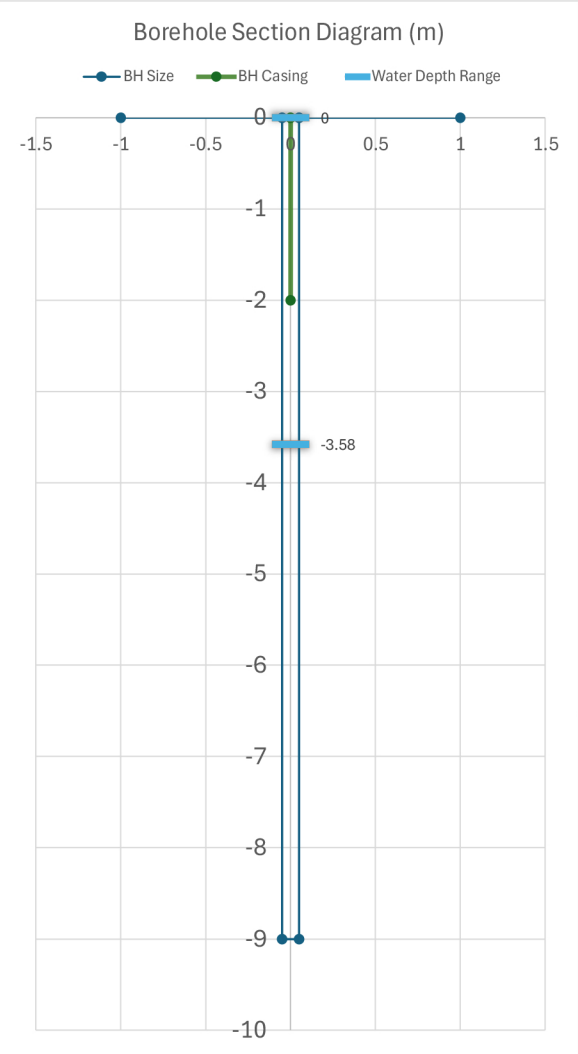

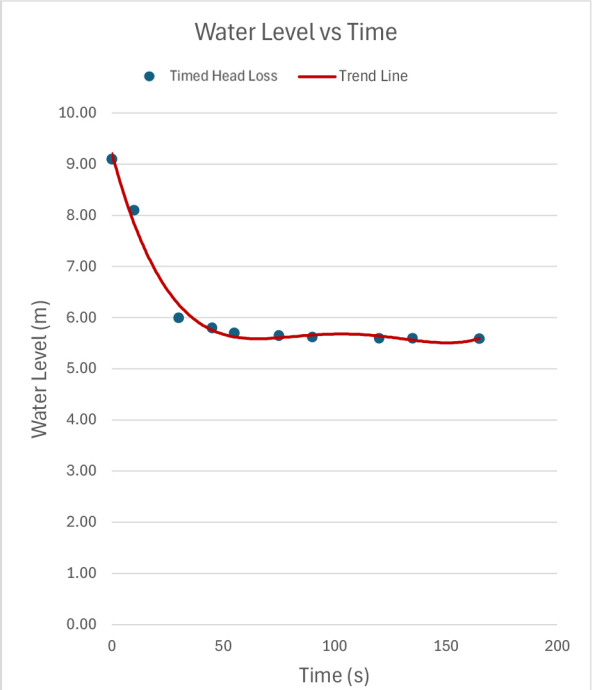

Notes:
Measurements taken from 9:30am to 10:00am after rainfall.
Requirement of Casing from 0-2m due to soil.
Large reduction in flow at 6m mark [Run #3].

Results:

Initial Water Level (Depth):	0	m
Final Water Level (Depth):	-3.58	m
Initial (Max) Flowrate Q:	0.00126	m3/s
Intake Factor Estimation F:	10.91033	
Initial (Max) Permeability K:	1.02E-05	m/s

Time	Time Passed (s)	Water Level Depth (m) Surface (-)	Base (+)
09:30	0	0	9.10
	10	1.00	8.10
	30	3.10	6.00
	45	3.30	5.80
	55	3.40	5.70
	75	3.45	5.65
	90	3.48	5.62
	120	3.50	5.60
	135	3.50	5.60
	165	3.51	5.59
	385	3.51	5.59
	625	3.53	5.57
	870	3.55	5.55
	1200	3.57	5.53
10:00	1800	3.58	5.52

Parametric Ground Model for Infiltration Dry Well (Original RQD)

Borehole Input Data

BH Depth:	9 m
BH Diameter:	0.101 m
BH Casing Depth:	2 m
BH Filter Medium:	No Filter Material

Ground Data

Ground Material:	Globigerina Limestone
Pore Hydraulic Conductivity:	0 m/s

Fissure Input Data

Avg Fissure Width:	1 mm
Fissure Spread:	Upper Concentration
Fissure Infill:	No Infill

Other Data

On-Site Test ID:	Att.T1
Starting Water Depth:	0 m
Timestep:	1 s

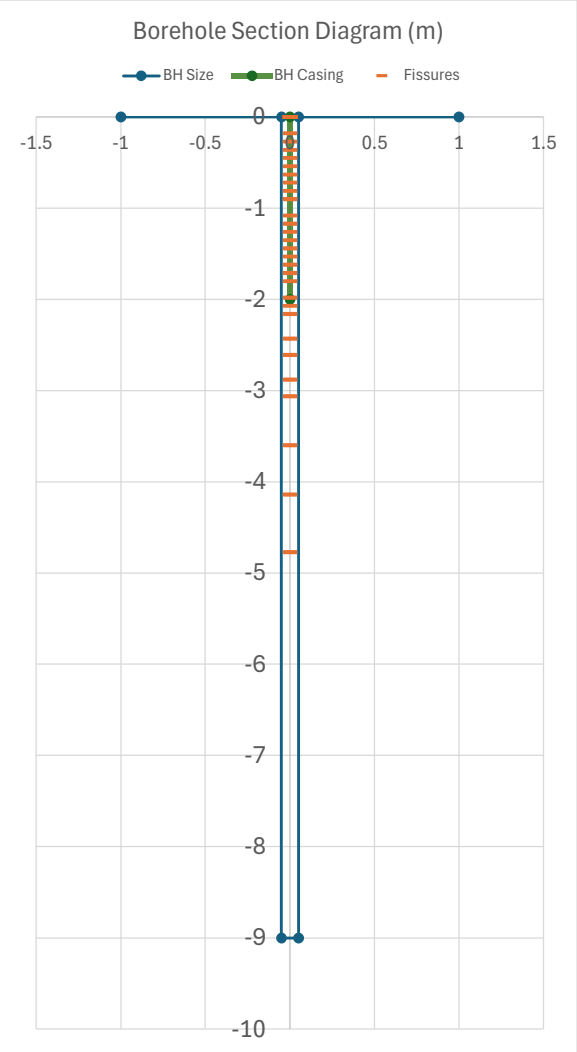

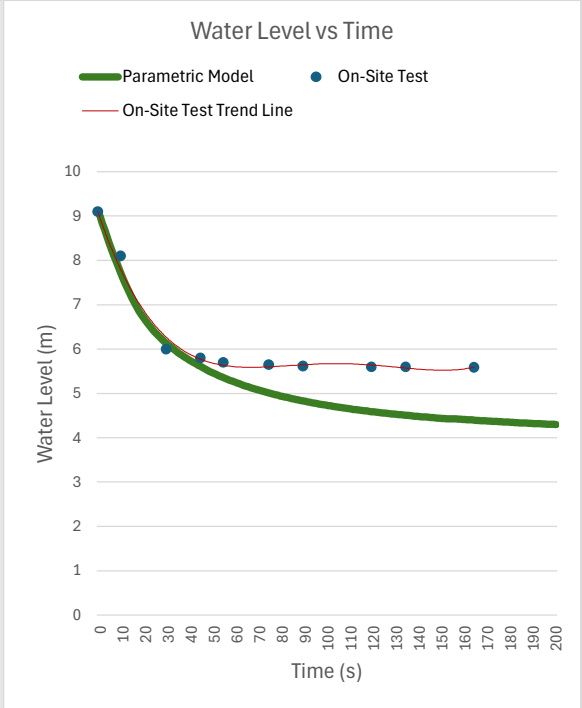

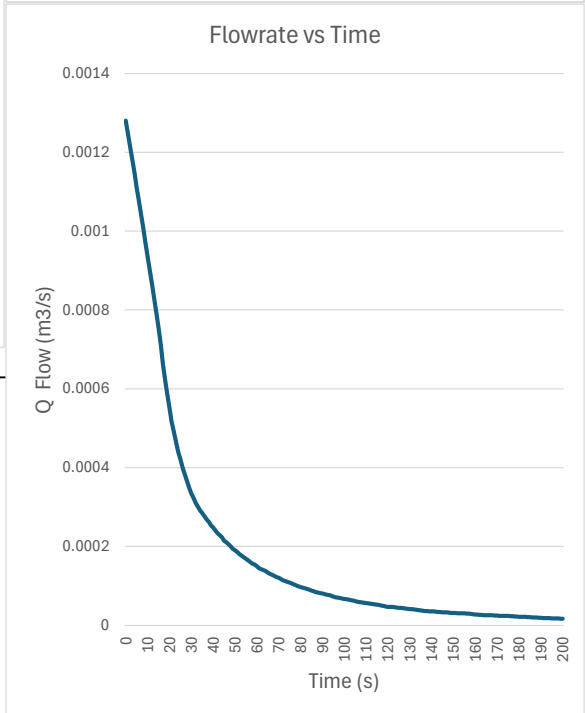

Results:

Primary Initial (Max) Flowrate Q:	0 m3/s
Secondary Initial (Max) Flowrate Q:	0.001281 m3/s
Total Initial (Max) Flowrate Q:	0.001281 m3/s
Intake Factor Estimation F:	10.91033
Initial (Max) Permeability K:	1.32E-05 m/s
Model Flow Factor Fr:	0.065
Initial Flowrate Q Difference:	1.6666 %

FULL STEADY STATE CONDITION (t=0) - SECONDARY PERMEABILITY

100 segments: (#)	Depth from Surface: (m)	Depth from Water Surface: (m)	Velocity Discharge t=0: (m/s) v	Fissure Num per Segment: (#)	Fissure Area per Segment: (m2) A	Q flow through fissures (m3/s) Q=Av
0	0	0	0	0.9	0.00028557	0
1	0.09	0.09	0.08637421	0.9	0.00028557	0
2	0.18	0.18	0.12215159	0.9	0.00028557	0
3	0.27	0.27	0.14960453	0.9	0.00028557	0
4	0.36	0.36	0.17274843	0.9	0.00028557	0
5	0.45	0.45	0.19313862	0.9	0.00028557	0
6	0.54	0.54	0.21157275	0.9	0.00028557	0
7	0.63	0.63	0.22852469	0.9	0.00028557	0
8	0.72	0.72	0.24430317	0.9	0.00028557	0
9	0.81	0.81	0.25912264	0.9	0.00028557	0
10	0.9	0.9	0.27313925	0.9	0.00028557	0
11	0.99	0.99	0.28647086	0.9	0.00028557	0
12	1.08	1.08	0.29920906	0.9	0.00028557	0
13	1.17	1.17	0.31142666	0.9	0.00028557	0
14	1.26	1.26	0.32318272	0.9	0.00028557	0
15	1.35	1.35	0.3345259	0.9	0.00028557	0
16	1.44	1.44	0.34549686	0.9	0.00028557	0
17	1.53	1.53	0.35613001	0.9	0.00028557	0
18	1.62	1.62	0.36645476	0.9	0.00028557	0
19	1.71	1.71	0.37649647	0.9	0.00028557	0
20	1.8	1.8	0.38627723	0.9	0.00028557	0
21	1.89	1.89	0.39581638	0.9	0.00028557	0
22	1.98	1.98	0.40513098	0.9	0.00028557	0
23	2.07	2.07	0.41423618	0.396	0.00012565	5.20492E-05
24	2.16	2.16	0.42314551	0.396	0.00012565	5.31687E-05
25	2.25	2.25	0.43187107	0.396	0.00012565	5.42651E-05
26	2.34	2.34	0.44042381	0.396	0.00012565	5.53398E-05
27	2.43	2.43	0.44881359	0.396	0.00012565	5.63939E-05
28	2.52	2.52	0.45704938	0.396	0.00012565	5.74288E-05
29	2.61	2.61	0.46513938	0.396	0.00012565	5.84453E-05
30	2.7	2.7	0.47309106	0.396	0.00012565	5.94444E-05
31	2.79	2.79	0.48091128	0.396	0.00012565	6.0427E-05
32	2.88	2.88	0.48860634	0.396	0.00012565	6.13939E-05
33	2.97	2.97	0.49618209	0.396	0.00012565	6.23458E-05
34	3.06	3.06	0.50364389	0.162	5.1403E-05	2.58887E-05
35	3.15	3.15	0.51099675	0.162	5.1403E-05	2.62666E-05
36	3.24	3.24	0.51824529	0.162	5.1403E-05	2.66392E-05
37	3.33	3.33	0.52539384	0.162	5.1403E-05	2.70067E-05
38	3.42	3.42	0.53244642	0.162	5.1403E-05	2.73692E-05
39	3.51	3.51	0.5394068	0.162	5.1403E-05	2.7727E-05
40	3.6	3.6	0.5462785	0.162	5.1403E-05	2.80802E-05
41	3.69	3.69	0.55306483	0.162	5.1403E-05	2.8429E-05
42	3.78	3.78	0.55976889	0.162	5.1403E-05	2.87737E-05
43	3.87	3.87	0.5663936	0.162	5.1403E-05	2.91142E-05
44	3.96	3.96	0.57294172	0.162	5.1403E-05	2.94508E-05
45	4.05	4.05	0.57941585	0.162	5.1403E-05	2.97836E-05
46	4.14	4.14	0.58581843	0.162	5.1403E-05	3.01127E-05
47	4.23	4.23	0.59215178	0.162	5.1403E-05	3.04382E-05
48	4.32	4.32	0.59841811	0.162	5.1403E-05	3.07603E-05
49	4.41	4.41	0.6046195	0.162	5.1403E-05	3.10791E-05
50	4.5	4.5	0.61075793	0.162	5.1403E-05	3.13946E-05
51	4.59	4.59	0.61683527	0.162	5.1403E-05	3.1707E-05
52	4.68	4.68	0.62285332	0.162	5.1403E-05	3.20164E-05
53	4.77	4.77	0.62881378	0.162	5.1403E-05	3.23228E-05
54	4.86	4.86	0.63471826	0.162	5.1403E-05	3.26263E-05
55	4.95	4.95	0.64056832	0.162	5.1403E-05	3.2927E-05
56	5.04	5.04	0.64636544	0	0	0
57	5.13	5.13	0.65211102	0	0	0
58	5.22	5.22	0.65780642	0	0	0
59	5.31	5.31	0.66345293	0	0	0
60	5.4	5.4	0.66905179	0	0	0
61	5.49	5.49	0.67460418	0	0	0
62	5.58	5.58	0.68011125	0	0	0
63	5.67	5.67	0.68557408	0	0	0
64	5.76	5.76	0.69099372	0	0	0
65	5.85	5.85	0.69637118	0	0	0
66	5.94	5.94	0.70170744	0	0	0
67	6.03	6.03	0.70700342	0	0	0
68	6.12	6.12	0.71226002	0	0	0
69	6.21	6.21	0.71747811	0	0	0
70	6.3	6.3	0.72265853	0	0	0
71	6.39	6.39	0.72780207	0	0	0
72	6.48	6.48	0.73290952	0	0	0
73	6.57	6.57	0.73798162	0	0	0
74	6.66	6.66	0.74301909	0	0	0
75	6.75	6.75	0.74802264	0	0	0
76	6.84	6.84	0.75299295	0	0	0
77	6.93	6.93	0.75793066	0	0	0
78	7.02	7.02	0.76283641	0	0	0
79	7.11	7.11	0.76771081	0	0	0
80	7.2	7.2	0.77255446	0	0	0
81	7.29	7.29	0.77736793	0	0	0
82	7.38	7.38	0.78215178	0	0	0
83	7.47	7.47	0.78690655	0	0	0
84	7.56	7.56	0.79163276	0	0	0
85	7.65	7.65	0.79633091	0	0	0
86	7.74	7.74	0.80100152	0	0	0
87	7.83	7.83	0.80564504	0	0	0
88	7.92	7.92	0.81026196	0	0	0
89	8.01	8.01	0.81485271	0	0	0
90	8.1	8.1	0.81941775	0	0	0
91	8.19	8.19	0.8239575	0	0	0
92	8.28	8.28	0.82847237	0	0	0
93	8.37	8.37	0.83296276	0	0	0
94	8.46	8.46	0.83742908	0	0	0
95	8.55	8.55	0.84187171	0	0	0
96	8.64	8.64	0.84629101	0	0	0
97	8.73	8.73	0.85068736	0	0	0
98	8.82	8.82	0.8550611	0	0	0
99	8.91	8.91	0.85941259	0	0	0
100	9	9	0.86374215	0	0	0

			Fissure Q
Total BH Depth :	9	m	0.001280615 m3/s
BH Diameter:	0.101	m	*[Summed]*
Water Start Depth :	0	m	
Total Casing Depth :	2	m	**Pore Q**
Flow Resistance Factor :	0.065		0 m3/s

FISSURE DISTRIBUTION TABLE [Borehole Log Runs]

Original RQD

Core Run: (#)	Core Length Input Values: (m)	RQD Input Values: (%)	Core Run Max Depth: (m)	Fissured Lengths: (m)	Fissure Number per Run: (#)	Fissure Number per Segment: (#)
-	-	-	-	-	-	-
1	1	0	1	1	10	0.9
2	1	0	2	1	10	0.9
3	1	56	3	0.44	4.4	0.396
4	2	82.5	5	0.175	1.8	0.162
5	2	100	7	0	0	0
6	2	100	9	0	0	0
7						
8						
9						
10						
11						
12						
13						
14						
15						
16						
17						
18						
19						
20						
21						
22						
23						
24						
25						
26						
27						
28						
29						
30						
31						
32						
33						
34						
35						
36						
37						
38						
39						
40						
41						
42						
43						
44						
45						
46						
47						
48						
49						
50						

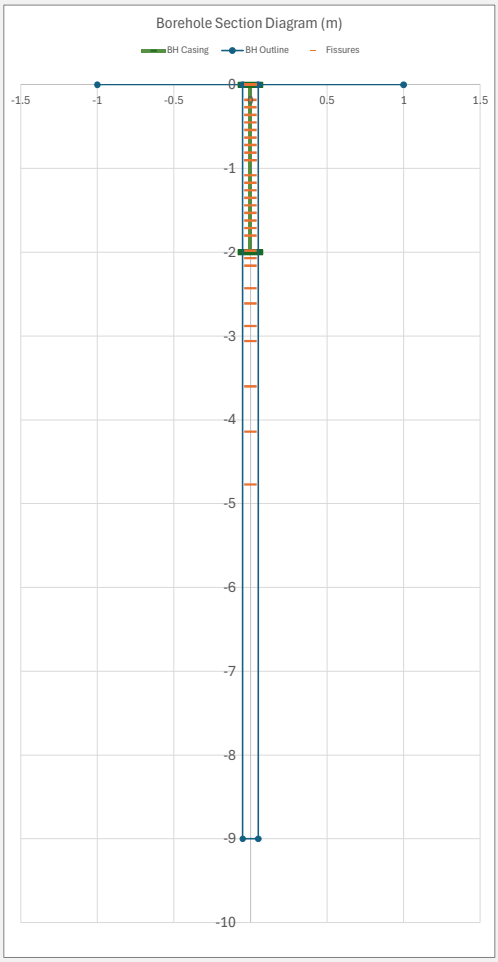

Parametric Ground Model for Infiltration Dry Well (Adjusted RQD)

Borehole Input Data

BH Depth:	9 m
BH Diameter:	0.101 m
BH Casing Depth:	2 m
BH Filter Medium:	No Filter Material

Ground Data

Limestone Type:	Globigerina Limestone
Pore Hydraulic Conductivity:	0 m/s

Fissure Input Data

Avg Fissure Width:	1 mm
Fissure Spread:	Upper Concentration
Fissure Infill:	No Infill

Other Data

On-Site Test ID:	Att.T1
Starting Water Depth:	0 m
Timestep:	1 s

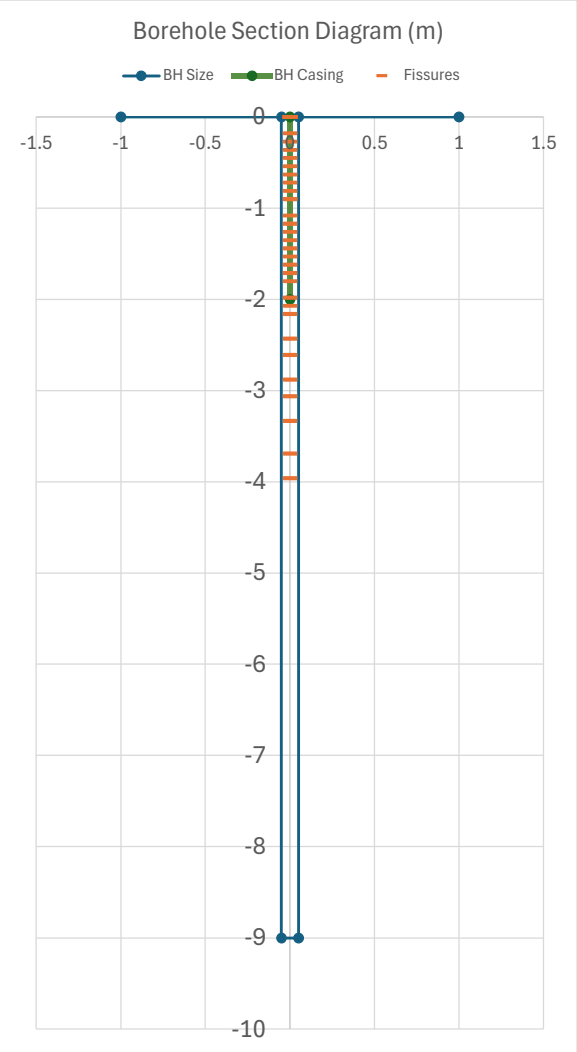

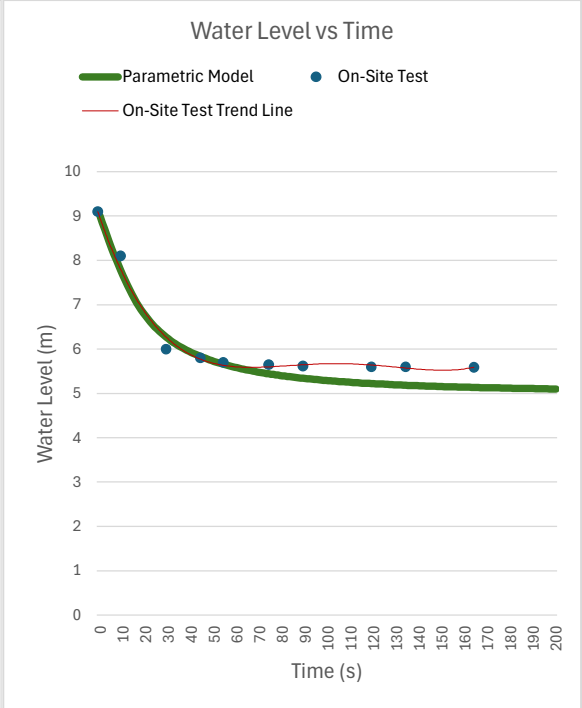

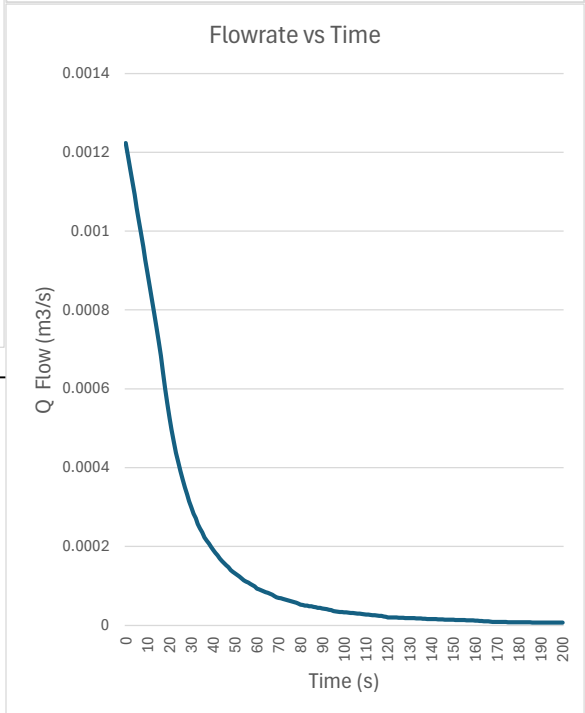

Results:

Primary Initial (Max) Flowrate Q:	0 m3/s
Secondary Initial (Max) Flowrate Q:	0.001223 m3/s
Total Initial (Max) Flowrate Q:	0.001223 m3/s
Intake Factor Estimation F:	10.91033
Initial (Max) Permeability K:	1.26E-05 m/s
Model Flow Factor Fr:	0.065
Initial Flowrate Q Difference:	2.8866 %

FULL STEADY STATE CONDITION (t=0) - SECONDARY PERMEABILITY

100 segments: (#)	Depth from Surface: (m)	Depth from Water Surface: (m)	Velocity Discharge t=0: (m/s) v	Fissure Num per Segment: (#)	Fissure Area per Segment: (m2) A	Q flow through fissures (m3/s) Q=Av
0	0	0	0	0.9	0.00028557	0
1	0.09	0.09	0.08637421	0.9	0.00028557	0
2	0.18	0.18	0.12215159	0.9	0.00028557	0
3	0.27	0.27	0.14960453	0.9	0.00028557	0
4	0.36	0.36	0.17274843	0.9	0.00028557	0
5	0.45	0.45	0.19313862	0.9	0.00028557	0
6	0.54	0.54	0.21157275	0.9	0.00028557	0
7	0.63	0.63	0.22852469	0.9	0.00028557	0
8	0.72	0.72	0.24430317	0.9	0.00028557	0
9	0.81	0.81	0.25912264	0.9	0.00028557	0
10	0.9	0.9	0.27313925	0.9	0.00028557	0
11	0.99	0.99	0.28647086	0.9	0.00028557	0
12	1.08	1.08	0.29920906	0.9	0.00028557	0
13	1.17	1.17	0.31142666	0.9	0.00028557	0
14	1.26	1.26	0.32318272	0.9	0.00028557	0
15	1.35	1.35	0.3345259	0.9	0.00028557	0
16	1.44	1.44	0.34549686	0.9	0.00028557	0
17	1.53	1.53	0.35613001	0.9	0.00028557	0
18	1.62	1.62	0.36645476	0.9	0.00028557	0
19	1.71	1.71	0.37649647	0.9	0.00028557	0
20	1.8	1.8	0.38627723	0.9	0.00028557	0
21	1.89	1.89	0.39581638	0.9	0.00028557	0
22	1.98	1.98	0.40513098	0.9	0.00028557	0
23	2.07	2.07	0.41423618	0.396	0.00012565	5.20492E-05
24	2.16	2.16	0.42314551	0.396	0.00012565	5.31687E-05
25	2.25	2.25	0.43187107	0.396	0.00012565	5.42651E-05
26	2.34	2.34	0.44042381	0.396	0.00012565	5.53398E-05
27	2.43	2.43	0.44881359	0.396	0.00012565	5.63939E-05
28	2.52	2.52	0.45704938	0.396	0.00012565	5.74288E-05
29	2.61	2.61	0.46513938	0.396	0.00012565	5.84453E-05
30	2.7	2.7	0.47309106	0.396	0.00012565	5.94444E-05
31	2.79	2.79	0.48091128	0.396	0.00012565	6.0427E-05
32	2.88	2.88	0.48860634	0.396	0.00012565	6.13939E-05
33	2.97	2.97	0.49618209	0.396	0.00012565	6.23458E-05
34	3.06	3.06	0.50364389	0.315	9.995E-05	5.03391E-05
35	3.15	3.15	0.51099675	0.315	9.995E-05	5.1074E-05
36	3.24	3.24	0.51824529	0.315	9.995E-05	5.17985E-05
37	3.33	3.33	0.52539384	0.315	9.995E-05	5.2513E-05
38	3.42	3.42	0.53244642	0.315	9.995E-05	5.32179E-05
39	3.51	3.51	0.5394068	0.315	9.995E-05	5.39136E-05
40	3.6	3.6	0.5462785	0.315	9.995E-05	5.46004E-05
41	3.69	3.69	0.55306483	0.315	9.995E-05	5.52787E-05
42	3.78	3.78	0.55976889	0.315	9.995E-05	5.59488E-05
43	3.87	3.87	0.5663936	0.315	9.995E-05	5.66109E-05
44	3.96	3.96	0.57294172	0.315	9.995E-05	5.72654E-05
45	4.05	4.05	0.57941585	0	0	0
46	4.14	4.14	0.58581843	0	0	0
47	4.23	4.23	0.59215178	0	0	0
48	4.32	4.32	0.59841811	0	0	0
49	4.41	4.41	0.6046195	0	0	0
50	4.5	4.5	0.61075793	0	0	0
51	4.59	4.59	0.61683527	0	0	0
52	4.68	4.68	0.62285332	0	0	0
53	4.77	4.77	0.62881378	0	0	0
54	4.86	4.86	0.63471826	0	0	0
55	4.95	4.95	0.64056832	0	0	0
56	5.04	5.04	0.64636544	0	0	0
57	5.13	5.13	0.65211102	0	0	0
58	5.22	5.22	0.65780642	0	0	0
59	5.31	5.31	0.66345293	0	0	0
60	5.4	5.4	0.66905179	0	0	0
61	5.49	5.49	0.67460418	0	0	0
62	5.58	5.58	0.68011125	0	0	0
63	5.67	5.67	0.68557408	0	0	0
64	5.76	5.76	0.69099372	0	0	0
65	5.85	5.85	0.69637118	0	0	0
66	5.94	5.94	0.70170744	0	0	0
67	6.03	6.03	0.70700342	0	0	0
68	6.12	6.12	0.71226002	0	0	0
69	6.21	6.21	0.71747811	0	0	0
70	6.3	6.3	0.72265853	0	0	0
71	6.39	6.39	0.72780207	0	0	0
72	6.48	6.48	0.73290952	0	0	0
73	6.57	6.57	0.73798162	0	0	0
74	6.66	6.66	0.74301909	0	0	0
75	6.75	6.75	0.74802264	0	0	0
76	6.84	6.84	0.75299295	0	0	0
77	6.93	6.93	0.75793066	0	0	0
78	7.02	7.02	0.76283641	0	0	0
79	7.11	7.11	0.76771081	0	0	0
80	7.2	7.2	0.77255446	0	0	0
81	7.29	7.29	0.77736793	0	0	0
82	7.38	7.38	0.78215178	0	0	0
83	7.47	7.47	0.78690655	0	0	0
84	7.56	7.56	0.79163276	0	0	0
85	7.65	7.65	0.79633091	0	0	0
86	7.74	7.74	0.80100152	0	0	0
87	7.83	7.83	0.80564504	0	0	0
88	7.92	7.92	0.81026196	0	0	0
89	8.01	8.01	0.81485271	0	0	0
90	8.1	8.1	0.81941775	0	0	0
91	8.19	8.19	0.8239575	0	0	0
92	8.28	8.28	0.82847237	0	0	0
93	8.37	8.37	0.83296276	0	0	0
94	8.46	8.46	0.83742908	0	0	0
95	8.55	8.55	0.84187171	0	0	0
96	8.64	8.64	0.84629101	0	0	0
97	8.73	8.73	0.85068736	0	0	0
98	8.82	8.82	0.8550611	0	0	0
99	8.91	8.91	0.85941259	0	0	0
100	9	9	0.86374215	0	0	0

			Fissure Q
Total BH Depth :	9	m	0.001223262
BH Diameter:	0.101	m	m3/s
Water Start Depth :	0	m	*[Summed]*
Total Casing Depth :	2	m	**Pore Q**
Flow Resistance Factor :	0.065		0
			m3/s

FISSURE DISTRIBUTION TABLE [Borehole Log Runs] **Adjusted RQD**

Core Run: (#)	Core Length Input Values: (m)	RQD Input Values: (%)	Core Run Max Depth: (m)	Fissured Lengths: (m)	Fissure Number per Run: (#)	Fissure Number per Segment: (#)
-	-	-	-	-	-	-
1	1	0	1	1	10	0.9
2	1	0	2	1	10	0.9
3	1	56	3	0.44	4.4	0.396
4	1	65	4	0.35	3.5	0.315
5	1	100	5	0	0	0
6	1	100	6	0	0	0
7	1	100	7	0	0	0
8	1	100	8	0	0	0
9	1	100	9	0	0	0
10						
11						
12						
13						
14						
15						
16						
17						
18						
19						
20						
21						
22						
23						
24						
25						
26						
27						
28						
29						
30						
31						
32						
33						
34						
35						
36						
37						
38						
39						
40						
41						
42						
43						
44						
45						
46						
47						
48						
49						
50						

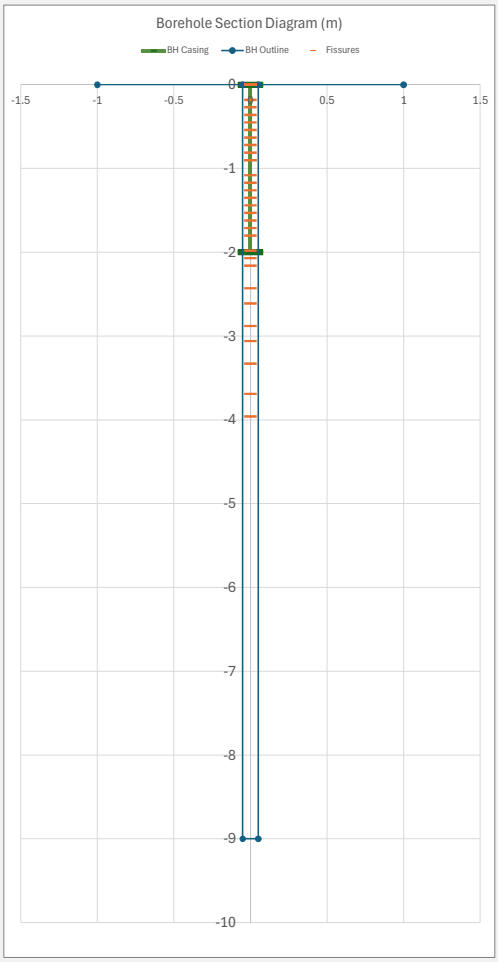

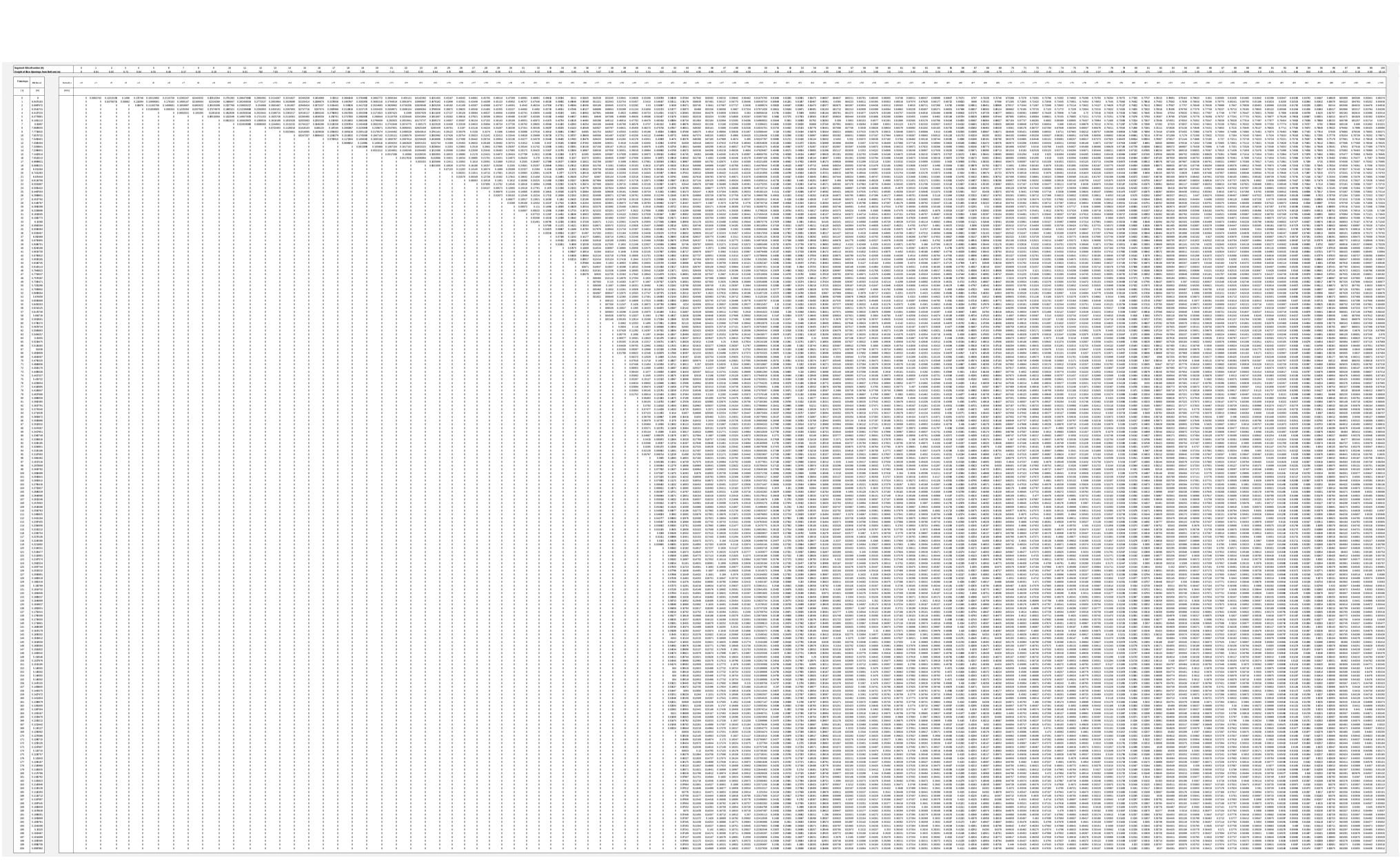

PARAMETRIC MODEL HEAD-LOSS VELOCITY TABLE [TIMESTEP vs BH SEGMENT] : Att.T1 (2)

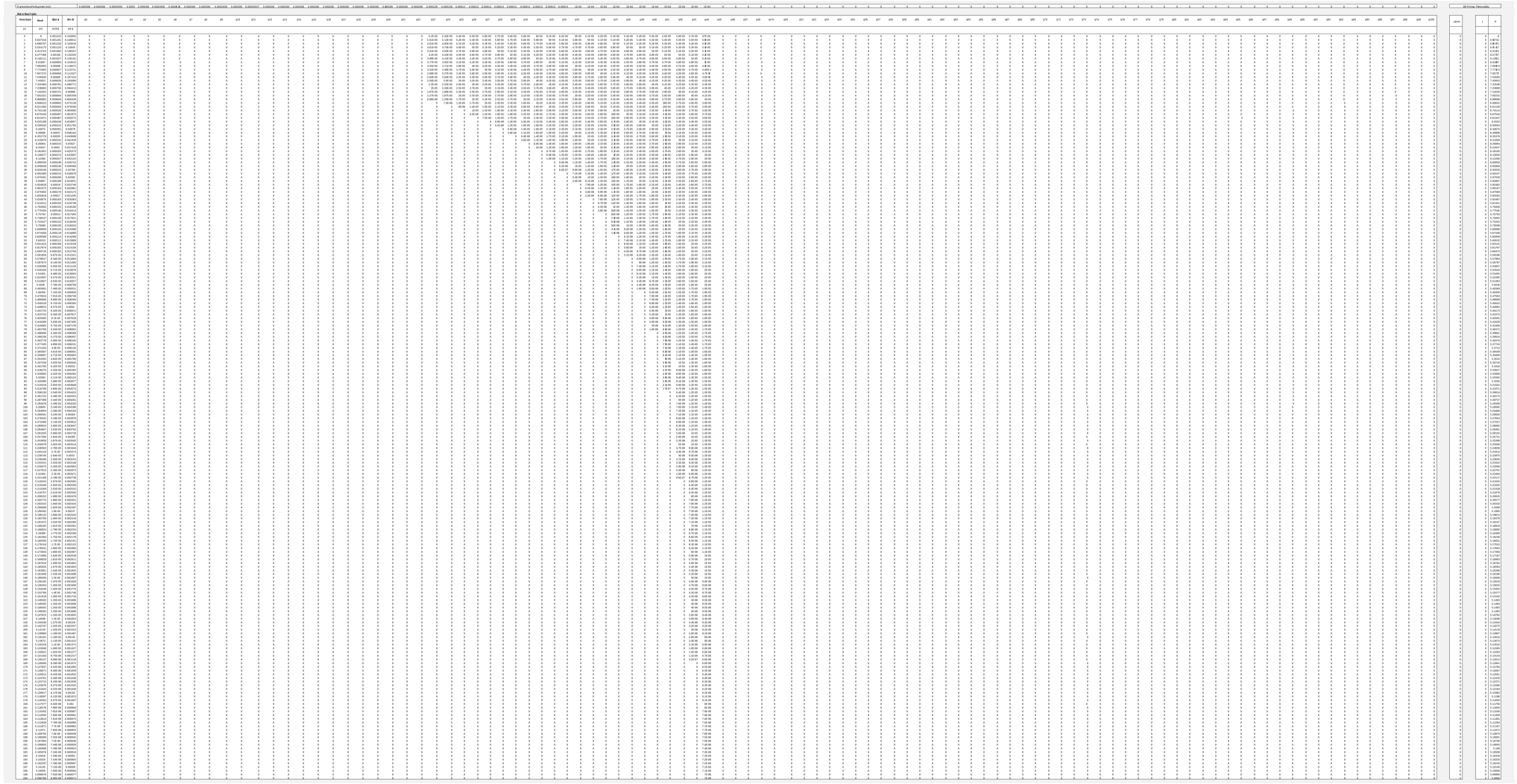

PARAMETRIC MODEL HEAD-LOSS FLOWRATE TABLE [TIMESTEP vs BH SEGMENT] : Att.T1 (2)

Borehole Drilling Record

solidbase LABORATORY LTD.

BH1

Client:	Location:	Weather:	Date started:	Date completed:
	Il-Kalkara	Fair	06/06/2024	06/06/2024
			Northings:	Eastings:

Job No:	Drill type:	Bit type/diameter:	Orientation:	Drilling fluid:	Ground level:	Water level:
J4281	CMV 600	Simple Sampler	0	Water	37.6	0

Description	Depth (Actual depth)	Run (Drill time)	TCR %	SCR %	RQD %	f/m /m	Sampling/testing	Drilling progress	Returns
Light Grey (2.5Y 7/2), moderately weak, fine, limestone gravel in cement matrix - MAN MADE, Concrete	0.00 37.60	1 0.0	96.7					Coring using simple sampler	
Pale Brown (2.5Y 7/4), firm, fine to coarse, with patches of soil, silty gravel - MAN MADE, Limestone Fill									
Olive Brown (2.5Y 4/3), firm, fine to coarse, silty, clayey gravel - MAN MADE, Soil Fill									
Pale Brown (2.5Y 7/4), firm to stiff, fine, retrieved as soil due to use of simple sampler, (wackestone) limestone - GLOBIGERINA, Lower member	1.00 36.60	2 0.0	100.0					Coring using simple sampler	
	2.00 35.60								
	3.00 34.60	3 0.0	100.0					Coring using simple sampler	
	4.00 33.60								

Legend:

GL: Ground level
AOD: Above Ordinance Datum
AMSL: Above mean sea level
RQD: Rock Quality Designation
TCR: Total core recovery
SCR: Solid core recovery
f: Fracture frequency
O/H: Open hole drilling

Clay, Silt, Sand, Gravel, Cobbles/ Boulders, Marl, Limestone, Recent

Topsoil (Recent deposits)
Man-made material (Recent deposits)
Quaternary Deposits (PLEISTOCENE, to HOLOCENE)
Upper Coralline Limst., Tal-Pitkal (MIOCENE, Tortonian to early Messinian)
Upper Coralline Limst., Mtarfa (MIOCENE, Tortonian to early Messinian)
Blue Clay - top weathered strata (MIOCENE, Langhian to Tortonian)
Blue Clay (MIOCENE, Langhian to Tortonian)
Upper Globigerina Limestone (MIOCENE, Burdigalian to early Langhian)
Middle Globigerina Limestone (MIOCENE, Aquitanian to Burdigalian)
Lower Globigerina Limestone (MIOCENE, Aquitanian)
Lower Coralline Limestone, Xlendi Member (OLIGOCENE, Chattian)
Lower Coralline Limestone, Attard Member (OLIGOCENE, Chattian)

UCS: Unconfined comp.strength
BD: Bulk density
MC: Moisture content
PP: Pocket penetrometer
PSV: Pocket shear vane
OED: Oedometer
SPT: Standard Penetration Test

Soil & rock colour references: Munsell notation (2009 charts)

Soil & rock strength descriptors: to BS 5930:1999

Borehole Drilling Record

solidbase LABORATORY LTD.

BH1

Client:	Location:	Weather:	Date started:	Date completed:
	Il-Kalkara	Fair	06/06/2024	06/06/2024
			Northings:	Eastings:

Job No:	Drill type:	Bit type/diameter:	Orientation:	Drilling fluid:	Ground level:	Water level:
J4281	CMV 600	Simple Sampler	0	Water	37.6	0

Description	Depth (Actual depth)	Run (Drill time)	TCR %	SCR %	RQD %	f/m /m	Sampling/testing	Drilling progress	Returns
Pale Brown (2.5Y 7/4), firm to stiff, fine, retrieved as soil due to use of simple sampler, (wackestone) limestone - GLOBIGERINA, Lower member									
Discontinuity at 55°, very rough sides, soil traces, with shiny surface, unclear Discontinuity at 80°, rough sides, soil traces, black mottling, rust mottling, unclear		4 0.1	96.7	34.0	16.0			Coring using double core sampler	Full, Yellow
Pale Brown (2.5Y 7/4), weak, fine, (wackestone) limestone - GLOBIGERINA, Lower member	5.00 32.60								
Discontinuity, sub-vertical, rough sides, rust staining, black mottling, slickenside with striated and shiny surface, unclear									
White (2.5Y 8.5/1), moderately weak to moderately strong, fine to coarse, (packstone) limestone - LOWER CORALLINE, Xlendi member									
Discontinuity, randomly oriented, rough sides, soil traces, rust staining, unclear									
Discontinuity at 55°, rough sides, black staining, unclear	6.00 31.60	5 0.1	100.0	55.0	55.0		6.20 MC: 15.06% BD: 1974.6Kg/m³ UCS: 5N/mm² 6.45 MC: 15.16% BD: 1981.61Kg/m³ UCS: 8.93N/mm²	Coring using double core sampler	Full,
Pale Yellow (2.5Y 8/2), weak, fine, all stratum retrieved fractured, (wackestone) limestone - LOWER CORALLINE, Xlendi member	7.00 30.60	6 0.1	90.0	4.0				Coring using double core sampler	Full,
Discontinuity at 45°, rough sides, soil traces, black mottling, unclear									
End of borehole	8.00 29.60								

Legend:

GL: Ground level
AOD: Above Ordinance Datum
AMSL: Above mean sea level
RQD: Rock Quality Designation
TCR: Total core recovery
SCR: Solid core recovery
f: Fracture frequency
O/H: Open hole drilling

Clay, Silt, Sand, Gravel, Cobbles/ Boulders, Marl, Limestone, Recent

Topsoil (Recent deposits)
Man-made material (Recent deposits)
Quaternary Deposits (PLEISTOCENE, to HOLOCENE)
Upper Coralline Limst., Tal-Pitkal (MIOCENE, Tortonian to early Messinian)
Upper Coralline Limst., Mtarfa (MIOCENE, Tortonian to early Messinian)
Blue Clay - top weathered strata (MIOCENE, Langhian to Tortonian)
Blue Clay (MIOCENE, Langhian to Tortonian)
Upper Globigerina Limestone (MIOCENE, Burdigalian to early Langhian)
Middle Globigerina Limestone (MIOCENE, Aquitanian to Burdigalian)
Lower Globigerina Limestone (MIOCENE, Aquitanian)
Lower Coralline Limestone, Xlendi Member (OLIGOCENE, Chattian)
Lower Coralline Limestone, Attard Member (OLIGOCENE, Chattian)

UCS: Unconfined comp.strength
BD: Bulk density
MC: Moisture content
PP: Pocket penetrometer
PSV: Pocket shear vane
OED: Oedometer
SPT: Standard Penetration Test

Soil & rock colour references: Munsell notation (2009 charts)

Soil & rock strength descriptors: to BS 5930:1999

Kal.T1 BH1 (2024)

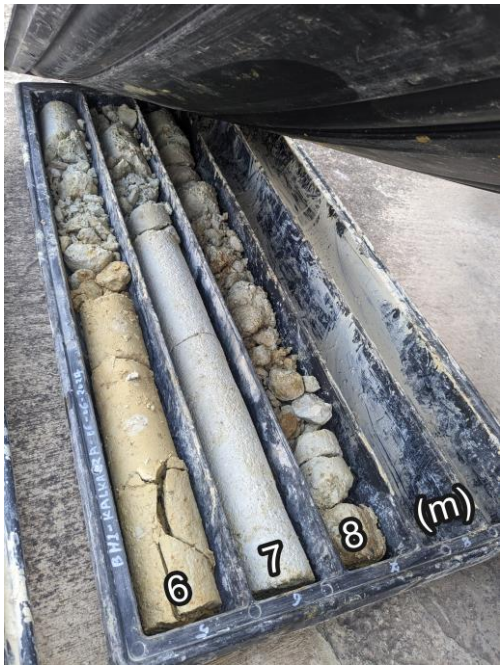

Falling Head Permeability Test (In-Situ)

Location: Kalkara
Company: Solidbase Laboratory

Test ID: Kal.T1
Date: 06.06.2024

Borehole Data

BH Depth:	8 m
BH Diameter:	0.101 m
BH Casing Depth:	0 m
Site BH Number:	BH1

Ground Data

Avg Fissure Width:	1 mm
Fissure Spread:	Surface Weathering & Deep Fissures
Fissure Infill:	Clayey Soil
Ground Material:	Weak Globigerina + Coralline

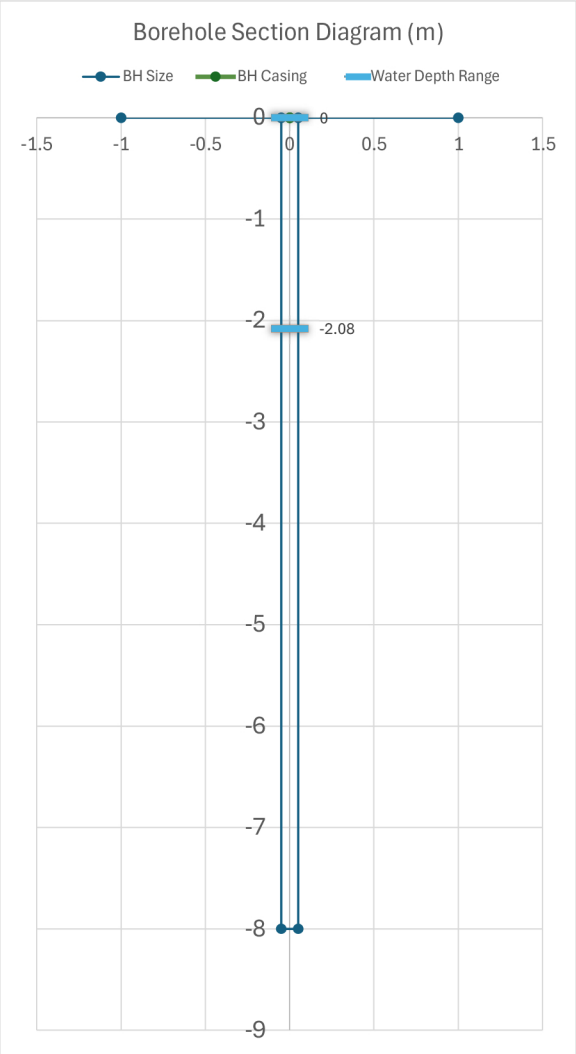

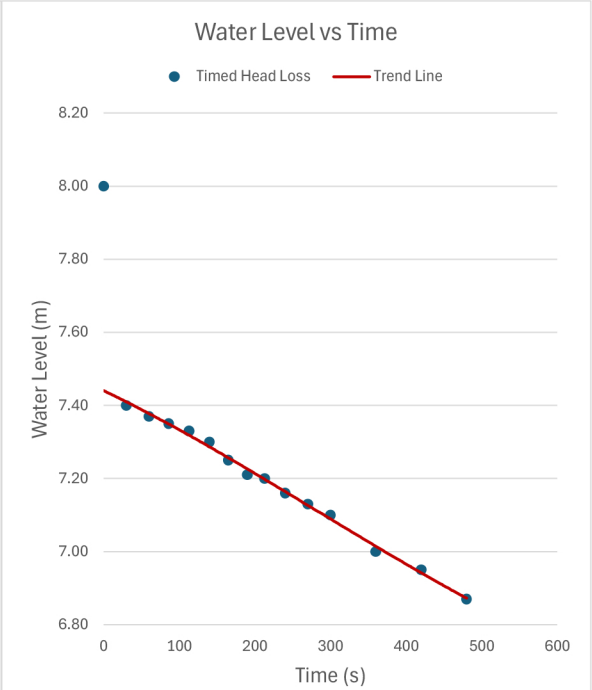

Notes:
Measurements taken in already saturated ground.
No casing used. ~0.5m fill material at surface.
Fragmented core + BH wall coated with mud due to single sampler.

Results:

Initial Water Level (Depth):	0 m
Final Water Level (Depth):	-2.08 m
Initial (Max) Flowrate Q:	8.01E-06 m3/s
Intake Factor Estimation F:	9.923567
Initial (Max) Permeability K:	2.1E-06 m/s

Time	Time Passed (s)	Water Level Depth (m) Surface (-)	Base (+)
16:30	0	0	8.00
	30	0.60	7.40
	60	0.63	7.37
	86	0.65	7.35
	113	0.67	7.33
	140	0.70	7.30
	165	0.75	7.25
	190	0.79	7.21
	213	0.80	7.20
	240	0.84	7.16
	270	0.87	7.13
	300	0.90	7.10
	360	1.00	7.00
	420	1.05	6.95
	480	1.13	6.87
	600	1.25	6.75
	900	1.28	6.72
	1200	1.7	6.3
	1500	1.9	6.1
17:00	1800	2.08	5.92

Parametric Ground Model for Infiltration Dry Well

Borehole Input Data

BH Depth:	8 m
BH Diameter:	0.101 m
BH Casing Depth:	0 m
BH Filter Medium:	No Filter Material

Ground Data

Limestone Type:	Globigerina + Coralline
Pore Hydraulic Conductivity:	5E-07 m/s

Fissure Input Data

Avg Fissure Width:	1 mm
Fissure Spread:	Lower Concentration
Fissure Infill:	Clayey Soil

Other Data

On-Site Test ID:	Kal.T1
Starting Water Depth:	0.55 m
Timestep:	3 s

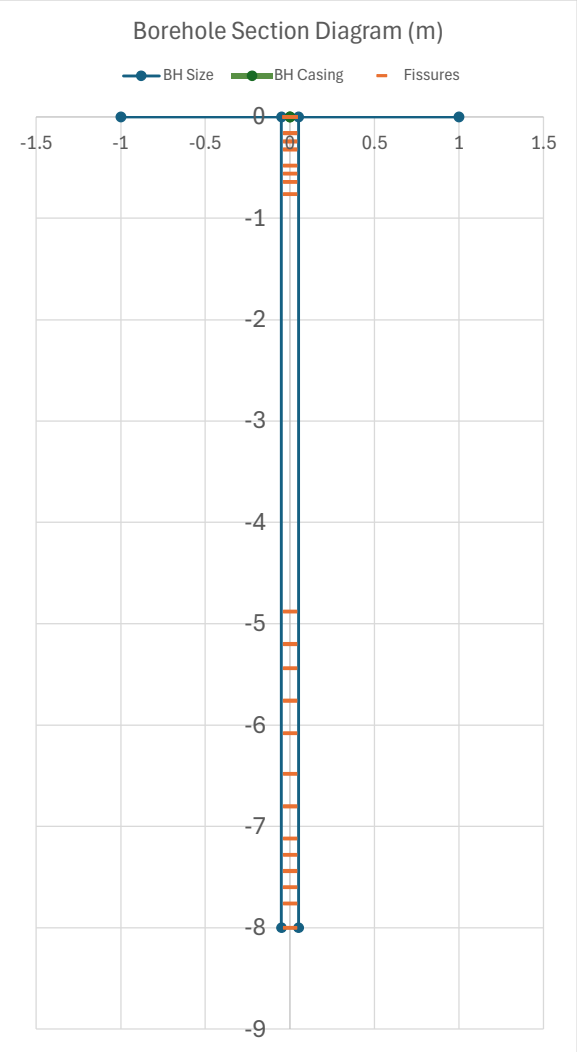

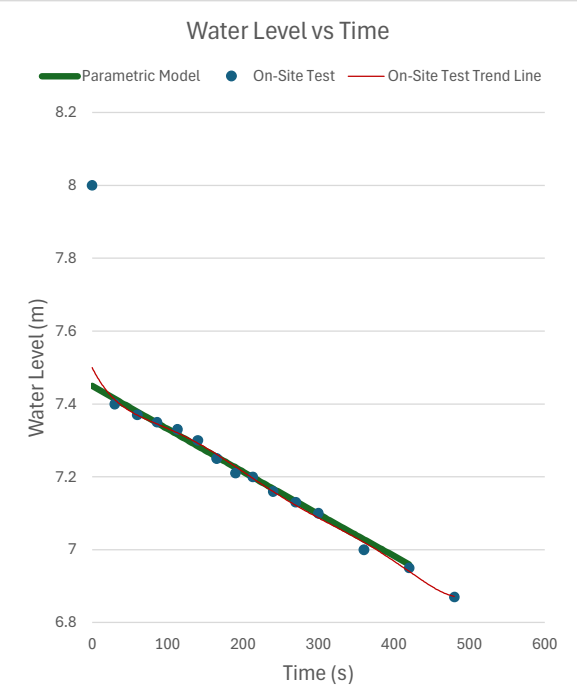

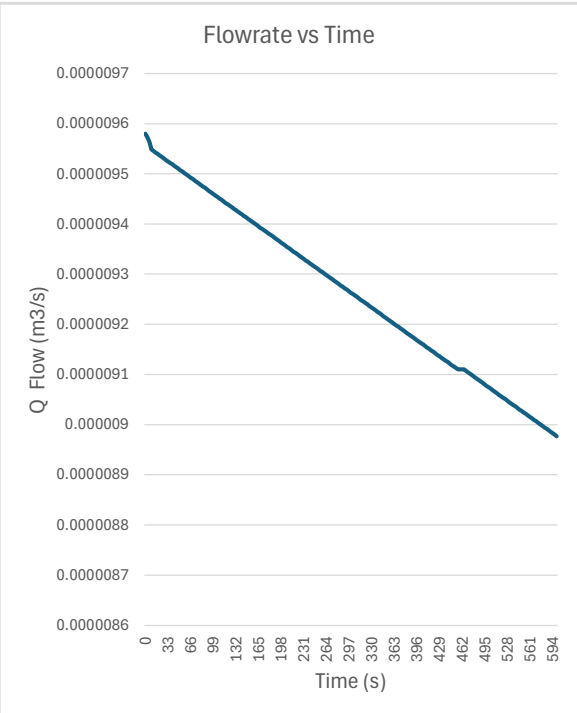

Results:

Primary Initial (Max) Flowrate Q:	2.5E-09 m3/s
Secondary Initial (Max) Flowrate Q:	9.55E-06 m3/s
Total Initial (Max) Flowrate Q:	9.55E-06 m3/s
Intake Factor Estimation F:	9.923567
Initial (Max) Permeability K:	1.3E-07 m/s
Model Flow Factor Fr:	0.00021
Initial Flowrate Q Difference:	19.2158 %

STEADY STATE CONDITION (t=0) - SECONDARY PERMEABILITY

100 segments: (#)	Segment Depth from Surface: (m)	Depth from Water Surface: (m)	Velocity Discharge t=0: (m/s) v	Fissure Num per Segment: (#)	Fissure Area per Segment: (m2) A	Q flow through fissures (m3/s) Q=Av
0	0		0	0.76	0.00024115	0
1	0.08		0	0.76	0.00024115	0
2	0.16		0	0.76	0.00024115	0
3	0.24		0	0.76	0.00024115	0
4	0.32		0	0.76	0.00024115	0
5	0.4		0	0.76	0.00024115	0
6	0.48		0	0.76	0.00024115	0
7	0.56	0	0	0.76	0.00024115	0
8	0.64	0.08	0.0002631	0	0	0
9	0.72	0.16	0.00037207	0	0	0
10	0.8	0.24	0.0004557	0	0	0
11	0.88	0.32	0.00052619	0	0	0
12	0.96	0.4	0.0005883	0	0	0
13	1.04	0.48	0.00064445	0	0	0
14	1.12	0.56	0.00069609	0	0	0
15	1.2	0.64	0.00074415	0	0	0
16	1.28	0.72	0.00078929	0	0	0
17	1.36	0.8	0.00083198	0	0	0
18	1.44	0.88	0.00087259	0	0	0
19	1.52	0.96	0.00091139	0	0	0
20	1.6	1.04	0.00094861	0	0	0
21	1.68	1.12	0.00098441	0	0	0
22	1.76	1.2	0.00101897	0	0	0
23	1.84	1.28	0.00105238	0	0	0
24	1.92	1.36	0.00108477	0	0	0
25	2	1.44	0.00111622	0	0	0
26	2.08	1.52	0.00114681	0	0	0
27	2.16	1.6	0.0011766	0	0	0
28	2.24	1.68	0.00120566	0	0	0
29	2.32	1.76	0.00123403	0	0	0
30	2.4	1.84	0.00126176	0	0	0
31	2.48	1.92	0.0012889	0	0	0
32	2.56	2	0.00131548	0	0	0
33	2.64	2.08	0.00134153	0	0	0
34	2.72	2.16	0.00136709	0	0	0
35	2.8	2.24	0.00139217	0	0	0
36	2.88	2.32	0.00141681	0	0	0
37	2.96	2.4	0.00144103	0	0	0
38	3.04	2.48	0.00146485	0	0	0
39	3.12	2.56	0.00148829	0	0	0
40	3.2	2.64	0.00151137	0	0	0
41	3.28	2.72	0.0015341	0	0	0
42	3.36	2.8	0.0015565	0	0	0
43	3.44	2.88	0.00157857	0	0	0
44	3.52	2.96	0.00160035	0	0	0
45	3.6	3.04	0.00162183	0	0	0
46	3.68	3.12	0.00164303	0	0	0
47	3.76	3.2	0.00166396	0	0	0
48	3.84	3.28	0.00168463	0	0	0
49	3.92	3.36	0.00170506	0	0	0
50	4	3.44	0.00172523	0	0	0
51	4.08	3.52	0.00174518	0	0	0
52	4.16	3.6	0.0017649	0	0	0
53	4.24	3.68	0.0017844	0	0	0
54	4.32	3.76	0.00180369	0	0	0
55	4.4	3.84	0.00182278	0	0	0
56	4.48	3.92	0.00184167	0	0	0
57	4.56	4	0.00186037	0.26666667	8.4614E-05	1.57412E-07
58	4.64	4.08	0.00187888	0.26666667	8.4614E-05	1.58979E-07
59	4.72	4.16	0.00189721	0.26666667	8.4614E-05	1.6053E-07
60	4.8	4.24	0.00191537	0.26666667	8.4614E-05	1.62066E-07
61	4.88	4.32	0.00193335	0.26666667	8.4614E-05	1.63588E-07
62	4.96	4.4	0.00195117	0.26666667	8.4614E-05	1.65095E-07
63	5.04	4.48	0.00196883	0.26666667	8.4614E-05	1.6659E-07
64	5.12	4.56	0.00198633	0.26666667	8.4614E-05	1.6807E-07
65	5.2	4.64	0.00200368	0.26666667	8.4614E-05	1.69538E-07
66	5.28	4.72	0.00202088	0.26666667	8.4614E-05	1.70994E-07
67	5.36	4.8	0.00203793	0.26666667	8.4614E-05	1.72437E-07
68	5.44	4.88	0.00205484	0.26666667	8.4614E-05	1.73868E-07
69	5.52	4.96	0.00207162	0.26666667	8.4614E-05	1.75287E-07
70	5.6	5.04	0.00208826	0.26666667	8.4614E-05	1.76695E-07
71	5.68	5.12	0.00210477	0.26666667	8.4614E-05	1.78092E-07
72	5.76	5.2	0.00212115	0.26666667	8.4614E-05	1.79478E-07
73	5.84	5.28	0.0021374	0.26666667	8.4614E-05	1.80853E-07
74	5.92	5.36	0.00215353	0.26666667	8.4614E-05	1.82218E-07
75	6	5.44	0.00216954	0.216	6.8537E-05	1.48694E-07
76	6.08	5.52	0.00218544	0.216	6.8537E-05	1.49783E-07
77	6.16	5.6	0.00220122	0.216	6.8537E-05	1.50865E-07
78	6.24	5.68	0.00221688	0.216	6.8537E-05	1.51939E-07
79	6.32	5.76	0.00223244	0.216	6.8537E-05	1.53005E-07
80	6.4	5.84	0.00224789	0.216	6.8537E-05	1.54064E-07
81	6.48	5.92	0.00226323	0.216	6.8537E-05	1.55115E-07
82	6.56	6	0.00227848	0.216	6.8537E-05	1.5616E-07
83	6.64	6.08	0.00229362	0.216	6.8537E-05	1.57197E-07
84	6.72	6.16	0.00230866	0.216	6.8537E-05	1.58228E-07
85	6.8	6.24	0.0023236	0.216	6.8537E-05	1.59252E-07
86	6.88	6.32	0.00233845	0.216	6.8537E-05	1.6027E-07
87	6.96	6.4	0.0023532	0.216	6.8537E-05	1.61281E-07
88	7.04	6.48	0.00236786	0.48	0.0001523	3.60636E-07
89	7.12	6.56	0.00238243	0.48	0.0001523	3.62855E-07
90	7.2	6.64	0.00239692	0.48	0.0001523	3.65061E-07
91	7.28	6.72	0.00241131	0.48	0.0001523	3.67253E-07
92	7.36	6.8	0.00242562	0.48	0.0001523	3.69433E-07
93	7.44	6.88	0.00243985	0.48	0.0001523	3.716E-07
94	7.52	6.96	0.00245399	0.48	0.0001523	3.73754E-07
95	7.6	7.04	0.00246806	0.48	0.0001523	3.75896E-07
96	7.68	7.12	0.00248204	0.48	0.0001523	3.78026E-07
97	7.76	7.2	0.00249595	0.48	0.0001523	3.80143E-07
98	7.84	7.28	0.00250977	0.48	0.0001523	3.8225E-07
99	7.92	7.36	0.00252353	0.48	0.0001523	3.84344E-07
100	8	7.44	0.0025372		0	0

Total BH Depth :	8	m	**Fissure Q** 9.54889E-06 m3/s *[Summed]*
BH Diameter:	0.101	m	
Water Start Depth :	0.55	m	
Total Casing Depth :	0	m	**Pore Q** 2.49503E-09 m3/s
Flow Resistance Factor :	0.00021		

FISSURE DISTRIBUTION TABLE [Borehole Log Runs]

Core Run: (#)	Core Length Input Values: (m)	RQD Input Values: (%)	Core Run Max Depth: (m)	Fissured Lengths: (m)	Fissure Number per Run: (#)	Fissure Number per Segment: (#)
-	-	-	-	-	-	-
1.1	0.6	5	0.6	0.57	5.7	0.76
1.2	0.9	100	1.5	0	0	0
2	1.5	100	3	0	0	0
3	1.5	100	4.5	0	0	0
4	1.5	16	6	0.504	5	0.26666667
5	1	55	7	0.27	2.7	0.216
6	1	0	8	0.6	6	0.48
7						
8						
9						
10						
11						
12						
13						
14						
15						
16						
17						
18						
19						
20						
21						
22						
23						
24						
25						
26						
27						
28						
29						
30						
31						
32						
33						
34						
35						
36						
37						
38						
39						
40						

Rock Type:		Rock Length:
Upper Rock:	Globigerina Limestone	5.5 m
Lower Rock:	Coralline Limestone	2.5 m

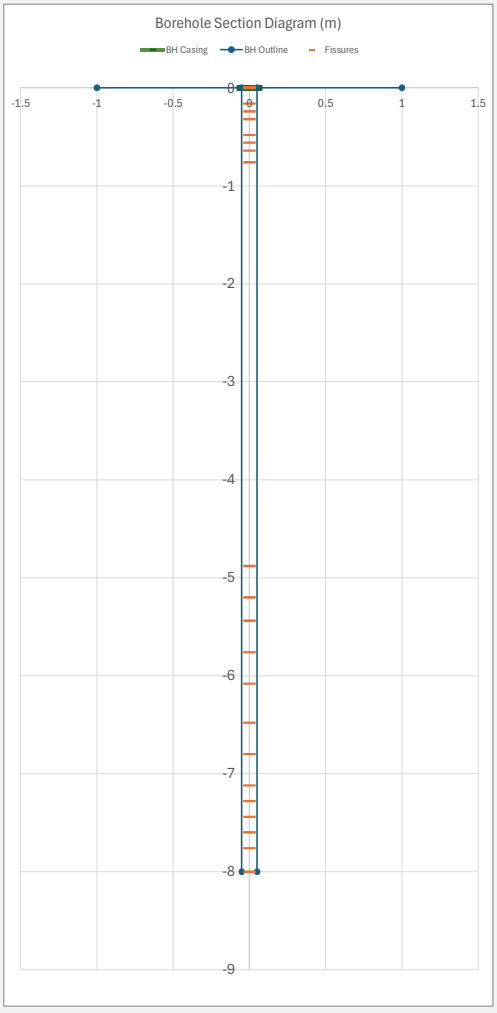

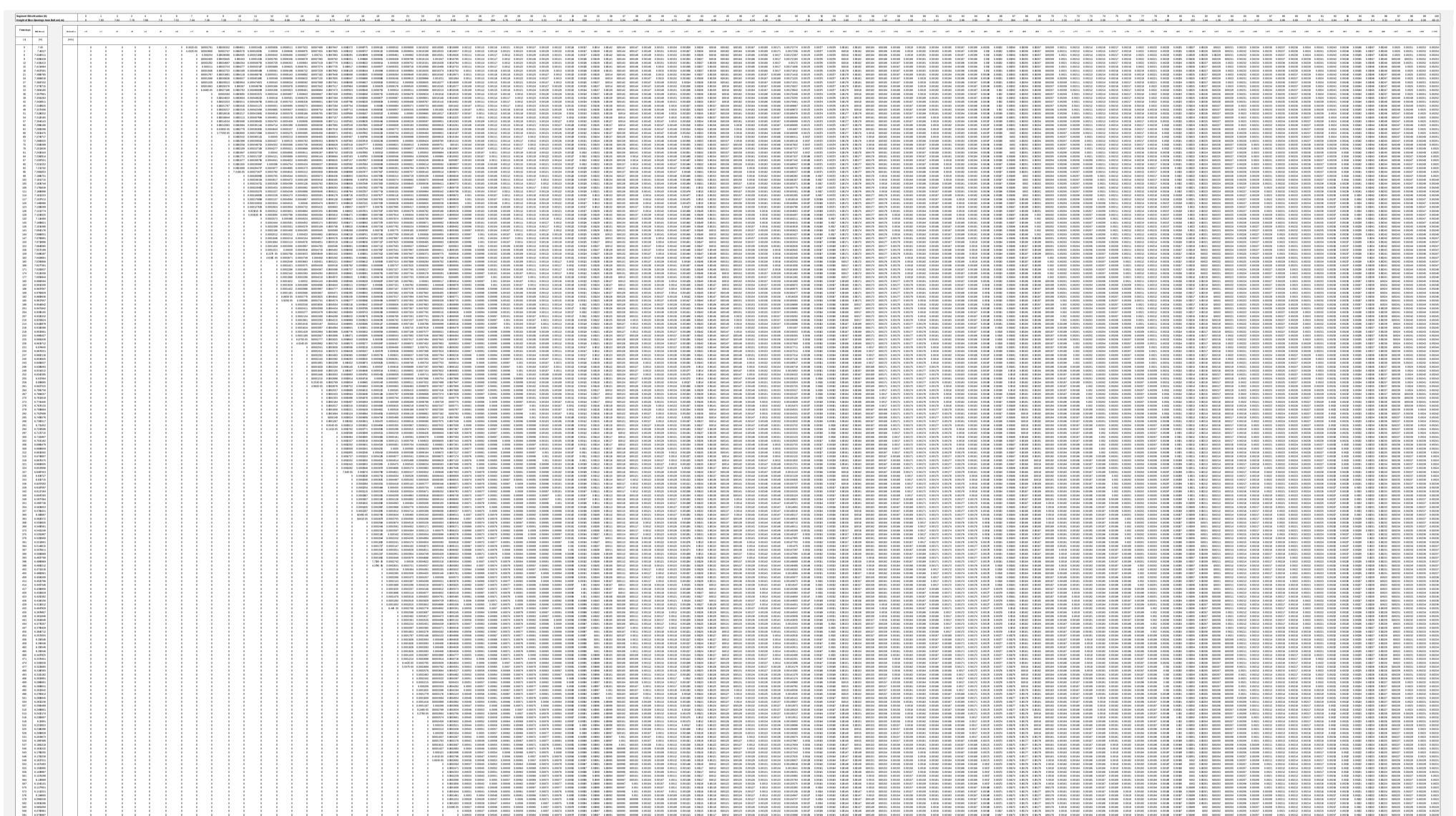

PARAMETRIC MODEL HEAD-LOSS VELOCITY TABLE [TIMESTEP vs BH SEGMENT] : Kal.T1

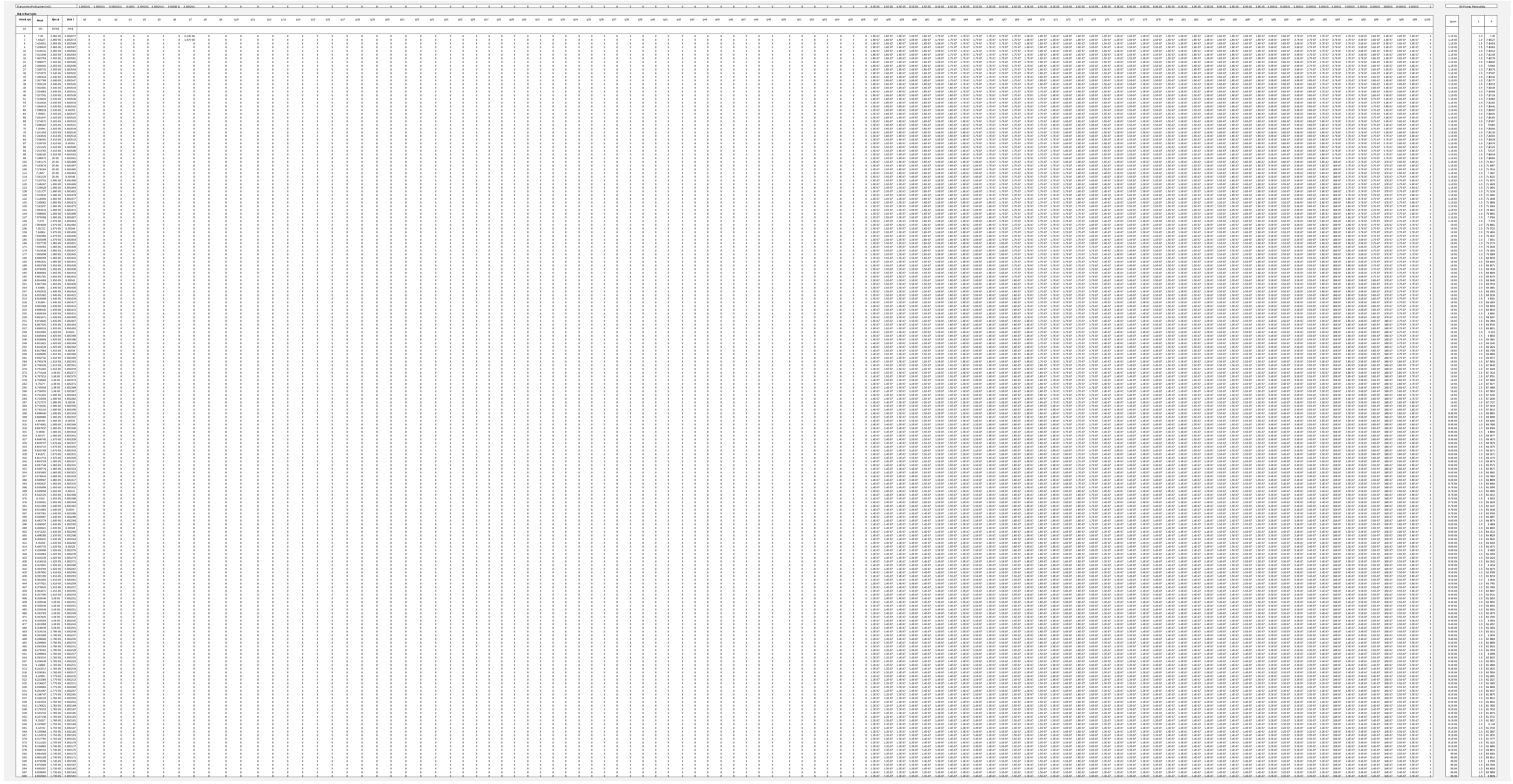

PARAMETRIC MODEL HEAD-LOSS FLOWRATE TABLE [TIMESTEP vs BH SEGMENT] : Kal.T1

solidbase LABORATORY LTD — Borehole Drilling Record

page 1 of 2 | **BH1**

NF research project	Location: Fleur de Lys Primary School		Weather: Sunny	Date started: 18/08/2011	Date completed: 18/08/2011
				Northings: 0	Eastings: 0
	Drill type: CMV -600	Bit type/diameter: Double core	Orientation: vertical	Drilling fluid: Fresh Water	Ground level: 0	Water level: 0

Description	Depth (Actual depth)	Run (Drill time)	TCR %	SCR %	RQD %	f/m /m	Sampling/testing	Drilling progress	Returns
own (2.5Y 7/3), moderately weak, fine to ı grained limestone, GLOBIGERINA, nember	0.00	1 0: 0	100	100			0.05m ▽ Falling head Slug test (A) original level at 9:50hrs	Coring using double core sampler	Full, Whitish Cream
uity, sub-horizontal, rough & calcified sides, terrarossa idurated), aperture unclear uity at 10°, rough sides, calcified terrarossa , tight uity, sub-horizontal, rough sides, calcified sand deposits aperture unclear uity at 75°, rough sides, terrarossa traces & ootlets, tight uity, sub-horiz., rough sides, calcified sand deposits, tight uity at 20°, rough sides, no infill, tight uity at 25°, rough sides, no infill, tight uity, sub-horizontal, rough sides, no infill, tight uity at 10°, rough sides, calcified mud, tight uity at 10°, rough sides, no infill, tight uity, sub-horizontal, rough sides, no infill, tight uity at 25°, rough sides, calcified terrarossa infill, 1.0mm uity at 25°, rough sides, calcified terrarossa infill, tight uity at 15°, rough sides, no infill, aperture unclear uity at 20°, rough & calcified sides, no infill, aperture unclear uity at 15°, rough & calcified sides, no infill, tight uity at 10°, rough sides, terrarossa infill, aperture unclear uity at 10°, rough sides, terrarossa infill, aperture unclear uity, sub-horizontal, rough sides, terrarossa traces, unclear	1.00	2 0: 0	100	100	80			Coring using double core sampler	Full, Whitish Cream
	2.00	3 0: 0	80	80	70			Coring using double core sampler	Full, Whitish Cream
	3.00	4 0: 0	90	90	70		3.0m ▽ Falling head Slug test (A) final level at 11:15hrs	Coring using double core sampler	Full, Whitish Cream
	4.00	5 0: 0	100	100	100			Coring using double core sampler	Full, Whitish Cream
	5.00	6 0: 0	100	100	100			Coring using double core sampler	Full, Whitish Cream
ased with 150mm dia,. pipe up to this depth. Annulus between l borehole wall filled with cement grout (bottom>up)	6.00	7 0: 0	100	100	100			Coring using double core sampler	Full, Whitish Cream
Discontinuity, horizontal, rough & calcified sides, terrarossa traces, tight							6.7m ▽ Falling head Slug test (C) original level at 8:20hrs		
	7.00	8 0: 0	100	100	100			Coring using double core sampler	Full, Whitish Cream
	8.00	9 0: 0	100	100	100		8.4m ▽ Falling head Slug test (C) final level at 9:40hrs	Coring using double core sampler	Full, Whitish Cream
	9.00	10 0: 0	100	100	100		9.0m ▽ Falling head Slug test (B) initial level at 14:35hrs 9.4m Falling head Slug test (A) when borehole drilling had reached this level	Coring using double core sampler	Full, Whitish Cream
	10.00	11 0: 0	100	100	100			Coring using double core sampler	Full, Whitish Cream

ground level
above Ordinance Datum
below ground level
above mean sea level
Rock Quality Designation
total core recovery
solid core recovery
fracture frequency
open hole

Limestone fill (Recent deposits)

Quaternary Deposits (PLEISTOCENE, to HOLOCENE)

Upper Globigerina Limestone (MIOCENE, Burdigalian to early Langhian)

Middle Globigerina Limestone (MIOCENE, Aquitanian to Burdigalian)

Lower Globigerina Limestone (MIOCENE, Aquitanian)

Legend:

UCS:	uniaxial compressive strength
BD:	Bulk density
ABS:	Absorption
MC:	Moisture content
PP:	Pocket penetrometer
PSV:	Pocket shear vane

Soil and rock colour references are according to the Munsell notation (Munsell soil colour charts 2009)

solidbase LABORATORY LTD.	Borehole Drilling Record	page 2 of 2	BH1

INF research project	Location: Fleur de Lys Primary School	Weather: Sunny	Date started: 18/08/2011	Date completed: 18/08/2011
			Northings: 0	Eastings: 0

	Drill type: CMV -600	Bit type/diameter: Double core	Orientation: vertical	Drilling fluid: Fresh Water	Ground level: 0	Water level: 0

cription	Depth (Actual depth)	Run (Drill time)	TCR %	SCR %	RQD %	f/m /m	Sampling/testing	Drilling progress	Returns
rown (2.5Y 7/3), ately weak, fine to m grained limestone, IGERINA, Lower er							10.77m ▽ Falling head Slug test (B) final level at 15:12hrs		
	11.00 -11.00	12 0: 0	100	100	100			Coring using double core sampler	Full, Whitish Cream
	12.00 -12.00	13 0: 0	100	100	100			Coring using double core sampler	Full, Whitish Cream
	13.00 -13.00	14 0: 0	100	100	100			Coring using double core sampler	Full, Whitish Cream
	14.00 -14.00	15 0: 0	100	100	100			Coring using double core sampler	Full, Whitish Cream
	15.00 -15.00	16 0: 0	100	66	66			Coring using double core sampler	Full, Whitish Cream
	16.00 -16.00	17 0: 0	100	100	100			Coring using double core sampler	Full, Whitish Cream
	17.00 -17.00	18 0: 0	100	100	100			Coring using double core sampler	Full, Whitish Cream
	18.00 -18.00	19 0: 0	100	100	85			Coring using double core sampler	Full, Whitish Cream
	19.00 -19.00	20 0: 0	100	100	90			Coring using double core sampler	Full, Whitish Cream
	20.00 -20.00	21 0: 0	100	100	100		Falling head Slug tests (B) and (C) carried out when borehole drilling had reached final level	Coring using double core sampler	Full, Whitish Cream
rehole at 20.8m		Discontinuity at 25°, rough sides, no infill, aperture unclear							

d:

ground level
above Ordinance Datum
below ground level
above mean sea level
Rock Quality Designation
total core recovery
solid core recovery
fracture frequency
open hole

Limestone fill (Recent deposits)

Quaternary Deposits (PLEISTOCENE, to HOLOCENE)

Upper Globigerina Limestone (MIOCENE, Burdigalian to early Langhian)

Middle Globigerina Limestone (MIOCENE, Aquitanian to Burdigalian)

Lower Globigerina Limestone (MIOCENE, Aquitanian)

Legend:

UCS: uniaxial compressive strength
BD: Bulk density
ABS: Absorption
MC: Moisture content
PP: Pocket penetrometer
PSV: Pocket shear vane

Soil and rock colour references are according to the Munsell notation (Munsell soil colour charts 2009)

Falling Head Permeability Test (In-Situ)

Location: Fleur de Lys School, Birkirkara
Company: Solidbase Laboratory + GEO-INF

Test ID: Bir.T2
Date: 2011

Borehole Data

BH Depth:	21 m
BH Diameter:	0.14 m
BH Casing Depth:	5.4 m
Site BH Number:	Null

Ground Data

Avg Fissure Width:	1 mm
Fissure Spread:	Surface Weathering
Fissure Infill:	Mainly Terrarossa Infill
Ground Material:	Globigerina

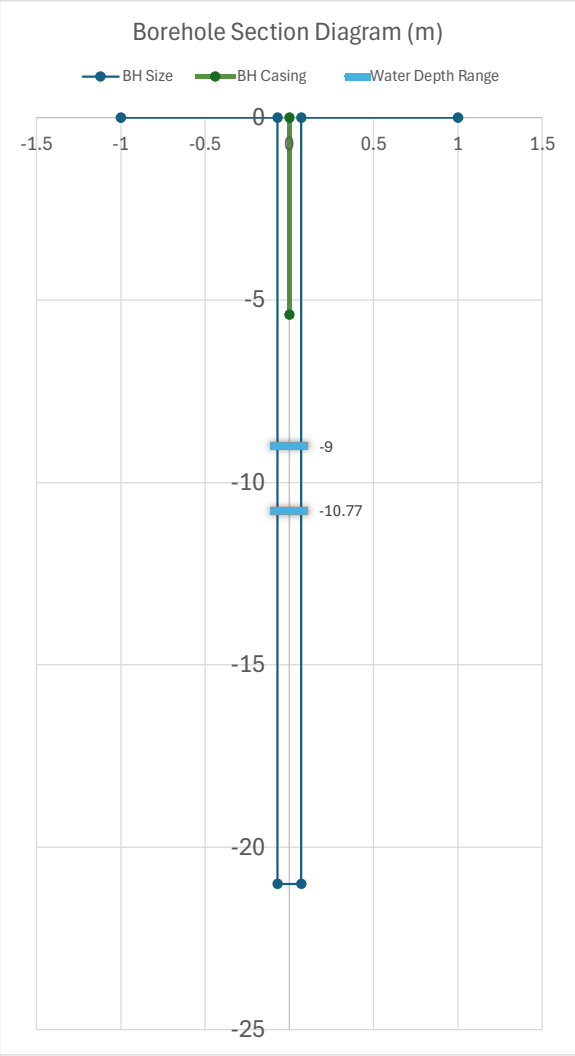

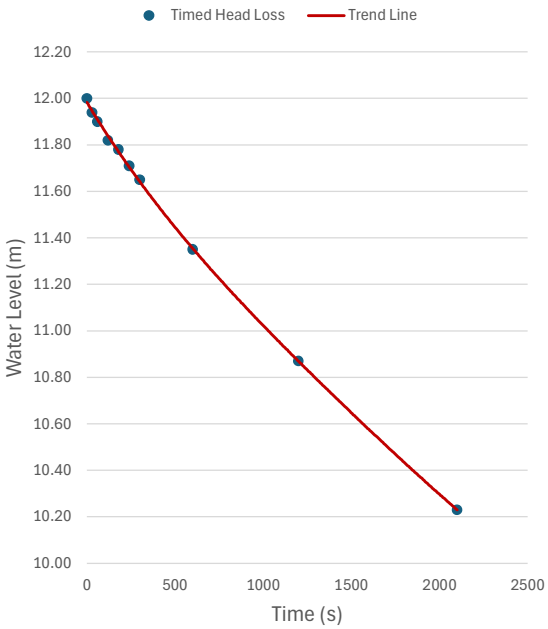

Time	Time Passed (s)	Water Level Depth (m) Surface (-)	Base (+)
02:35	0	9	12.00
	30	9.06	11.94
	60	9.10	11.90
	120	9.18	11.82
	180	9.22	11.78
	240	9.29	11.71
	300	9.35	11.65
	600	9.65	11.35
	1200	10.13	10.87
03:55	2100	10.77	10.23

[N. Borg (2012)]

Notes:
Water level recordings commenced at a depth of 9m.
Very slow flowrate.
Tight and infilled fissures.

Results:

Initial Water Level (Depth):	-9 m
Final Water Level (Depth):	-10.77 m
Initial (Max) Flowrate Q:	3.08E-05 m3/s
Intake Factor Estimation F:	23.13318
Initial (Max) Permeability K:	1.11E-07 m/s

Parametric Ground Model for Infiltration Dry Well

Borehole Input Data		**Fissure Input Data**	
BH Depth:	21 m	Avg Fissure Width:	1 mm
BH Diameter:	0.14 m	Fissure Spread:	Upper Concentration
BH Casing Depth:	5.4 m	Fissure Infill:	Clayey Soil
BH Filter Medium:	No Filter Material		
Ground Data		**Other Data**	
Limestone Type:	Globigerina Limestone	On-Site Test ID:	Bir.T2
Pore Hydraulic Conductivity:	0 m/s	Starting Water Depth:	9 m
		Timestep:	1 s

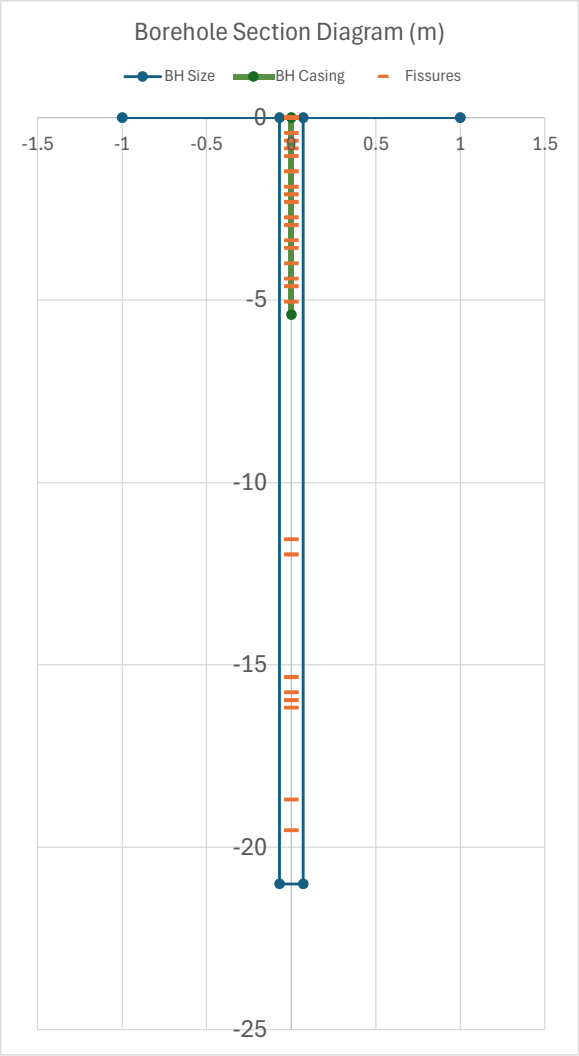

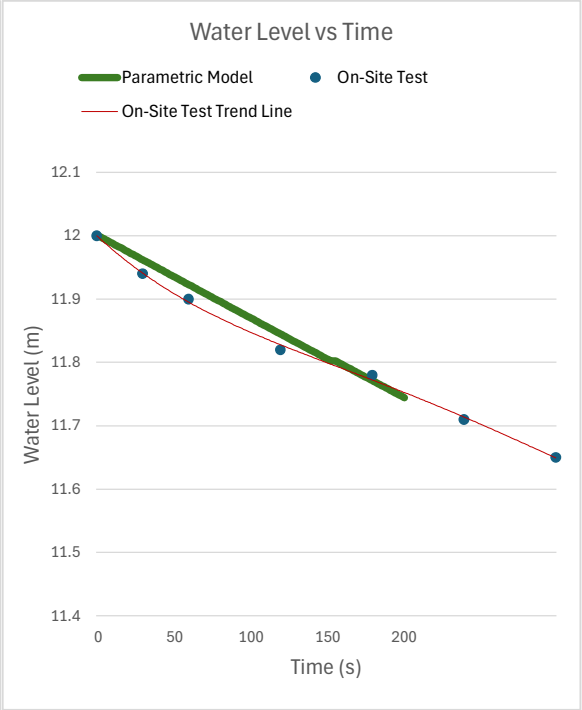

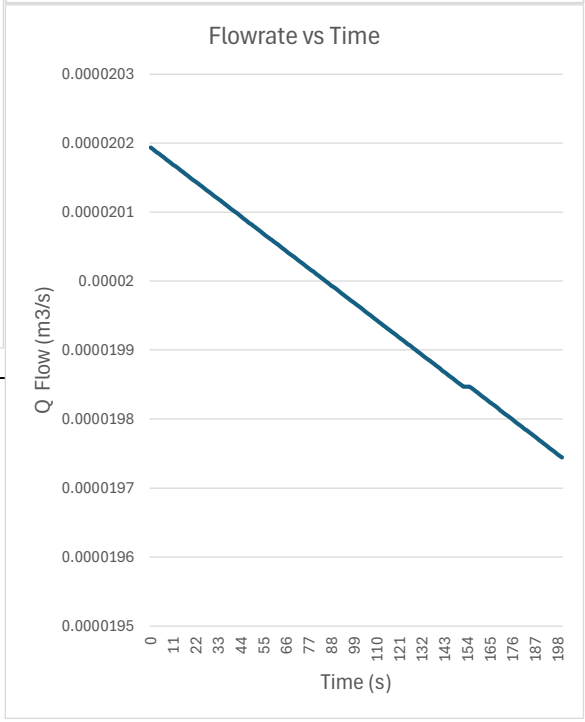

Results:

Primary Initial (Max) Flowrate Q:	0	m3/s
Secondary Initial (Max) Flowrate Q:	3.18E-05	m3/s
Total Initial (Max) Flowrate Q:	3.18E-05	m3/s
Intake Factor Estimation F:	23.13318	
Initial (Max) Permeability K:	7.27E-08	m/s
Model Flow Factor F_F:	0.0005	
Initial Flowrate Q Difference:	3.2044	%

STEADY STATE CONDITION (t=0) - SECONDARY FLOW

100 segments: (#)	Segment Depth from Surface: (m)	Depth from Water Surface: (m)	Velocity Discharge t=0: (m/s) v	Fissure Num per Segment: (#)	Fissure Area per Segment: (m2) A	Q flow through fissures (m3/s) Q=Av
0	0		0	2.1	0.00092363	0
1	0.21		0.00101491	2.1	0.00092363	0
2	0.42		0.0014353	2.1	0.00092363	0
3	0.63		0.00175788	2.1	0.00092363	0
4	0.84		0.00202983	2.1	0.00092363	0
5	1.05		0.00226942	0.42	0.00018473	0
6	1.26		0.00248602	0.42	0.00018473	0
7	1.47		0.00268521	0.42	0.00018473	0
8	1.68		0.00287061	0.42	0.00018473	0
9	1.89		0.00304474	0.42	0.00018473	0
10	2.1		0.00320944	0.63	0.00027709	0
11	2.31		0.00336609	0.63	0.00027709	0
12	2.52		0.00351576	0.63	0.00027709	0
13	2.73		0.00365932	0.63	0.00027709	0
14	2.94		0.00379746	0.63	0.00027709	0
15	3.15		0.00393074	0.63	0.00027709	0
16	3.36		0.00405966	0.63	0.00027709	0
17	3.57		0.0041846	0.63	0.00027709	0
18	3.78		0.00430591	0.63	0.00027709	0
19	3.99		0.00442391	0.63	0.00027709	0
20	4.2		0.00453883	0.63	0.00027709	0
21	4.41		0.00465092	0.63	0.00027709	0
22	4.62		0.00476037	0.63	0.00027709	0
23	4.83		0.00486736	0.63	0.00027709	0
24	5.04		0.00497204	0	0	0
25	5.25		0.00507457	0	0	0
26	5.46		0.00517507	0	0	0
27	5.67		0.00527365	0	0	0
28	5.88		0.00537042	0	0	0
29	6.09		0.00546548	0	0	0
30	6.3		0.00555891	0	0	0
31	6.51		0.0056508	0	0	0
32	6.72		0.00574122	0	0	0
33	6.93		0.00583024	0	0	0
34	7.14		0.00591791	0	0	0
35	7.35		0.00600431	0	0	0
36	7.56		0.00608948	0	0	0
37	7.77		0.00617348	0	0	0
38	7.98		0.00625635	0	0	0
39	8.19		0.00633813	0	0	0
40	8.4		0.00641888	0	0	0
41	8.61		0.00649862	0	0	0
42	8.82		0.00657739	0	0	0
43	9.03	0	0.00665523	0	0	0
44	9.24	0.21	0.00673218	0	0	0
45	9.45	0.42	0.00680825	0	0	0
46	9.66	0.63	0.00688348	0	0	0
47	9.87	0.84	0.0069579	0	0	0
48	10.08	1.05	0.00703153	0	0	0
49	10.29	1.26	0.0071044	0	0	0
50	10.5	1.47	0.00717652	0	0	0
51	10.71	1.68	0.00724793	0	0	0
52	10.92	1.89	0.00731865	0	0	0
53	11.13	2.1	0.00738868	0.42	0.00018473	1.36488E-06
54	11.34	2.31	0.00745806	0.42	0.00018473	1.3777E-06
55	11.55	2.52	0.0075268	0.42	0.00018473	1.39039E-06
56	11.76	2.73	0.00759492	0.42	0.00018473	1.40298E-06
57	11.97	2.94	0.00766243	0.42	0.00018473	1.41545E-06
58	12.18	3.15	0.00772935	0	0	0
59	12.39	3.36	0.0077957	0	0	0
60	12.6	3.57	0.00786149	0	0	0
61	12.81	3.78	0.00792673	0	0	0
62	13.02	3.99	0.00799144	0	0	0
63	13.23	4.2	0.00805563	0	0	0
64	13.44	4.41	0.00811931	0	0	0
65	13.65	4.62	0.0081825	0	0	0
66	13.86	4.83	0.0082452	0	0	0
67	14.07	5.04	0.00830743	0	0	0
68	14.28	5.25	0.00836919	0	0	0
69	14.49	5.46	0.00843051	0	0	0
70	14.7	5.67	0.00849138	0	0	0
71	14.91	5.88	0.00855182	0	0	0
72	15.12	6.09	0.00861183	0.714	0.00031403	2.7044E-06
73	15.33	6.3	0.00867143	0.714	0.00031403	2.72312E-06
74	15.54	6.51	0.00873062	0.714	0.00031403	2.74171E-06
75	15.75	6.72	0.00878941	0.714	0.00031403	2.76017E-06
76	15.96	6.93	0.00884781	0.714	0.00031403	2.77851E-06
77	16.17	7.14	0.00890583	0	0	0
78	16.38	7.35	0.00896348	0	0	0
79	16.59	7.56	0.00902075	0	0	0
80	16.8	7.77	0.00907766	0	0	0
81	17.01	7.98	0.00913422	0	0	0
82	17.22	8.19	0.00919044	0	0	0
83	17.43	8.4	0.0092463	0	0	0
84	17.64	8.61	0.00930184	0	0	0
85	17.85	8.82	0.00935704	0	0	0
86	18.06	9.03	0.00941192	0.315	0.00013854	1.30397E-06
87	18.27	9.24	0.00946649	0.315	0.00013854	1.31153E-06
88	18.48	9.45	0.00952074	0.315	0.00013854	1.31904E-06
89	18.69	9.66	0.00957468	0.315	0.00013854	1.32652E-06
90	18.9	9.87	0.00962832	0.315	0.00013854	1.33395E-06
91	19.11	10.08	0.00968166	0.21	9.2363E-05	8.94226E-07
92	19.32	10.29	0.00973471	0.21	9.2363E-05	8.99125E-07
93	19.53	10.5	0.00978747	0.21	9.2363E-05	9.03999E-07
94	19.74	10.71	0.00983995	0.21	9.2363E-05	9.08846E-07
95	19.95	10.92	0.00989216	0.21	9.2363E-05	9.13667E-07
96	20.16	11.13	0.00994408	0	0	0
97	20.37	11.34	0.00999574	0	0	0
98	20.58	11.55	0.01004713	0	0	0
99	20.79	11.76	0.01009826	0	0	0
100	21	11.97	0.01014914	0	0	0

Total BH Depth :	21	m	**Fissure Q** 3.17742E-05 m3/s *[Summed]*
BH Diameter:	0.14	m	
Water Start Depth :	9	m	
Total Casing Depth :	5.4	m	**Pore Q** 0 m3/s
Flow Resistance Factor :	0.0005		

FISSURE DISTRIBUTION TABLE [Borehole Log Runs]

Core Run: (#)	Core Length Input Values: (m)	RQD Input Values: (%)	Core Run Max Depth: (m)	Fissured Lengths: (m)	Fissure Number per Run: (#)	Fissure Number per Segment: (#)
-	-	-	-	-	-	-
1	1	0	1	1	10	2.1
2	1	80	2	0.2	2	0.42
3	1	70	3	0.3	3	0.63
4	1	70	4	0.3	3	0.63
5	1	70	5	0.3	3	0.63
6	6	100	11	0	0	0
7	1	80	12	0.2	2	0.42
8	3	100	15	0	0	0
9	1	66	16	0.34	3.4	0.714
10	1	100	17	0	0	0
11	1	100	18	0	0	0
12	1	85	19	0.15	1.5	0.315
13	1	90	20	0.1	1	0.21
14	1	100	21	0	0	0
15						
16						
17						
18						
19						
20						
21						
22						
23						
24						
25						
26						
27						
28						
29						
30						
31						
32						
33						
34						
35						
36						
37						
38						
39						
40						
41						
42						
43						
44						
45						
46						
47						
48						
49						
50						

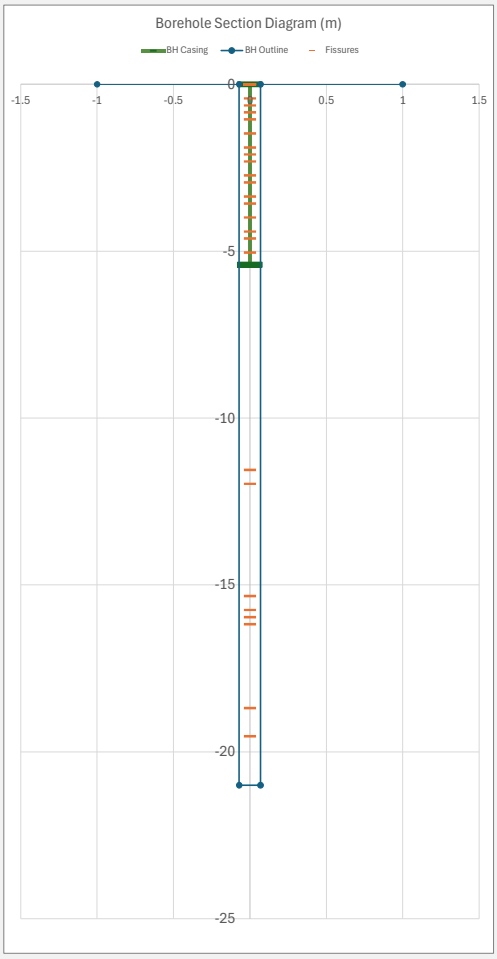

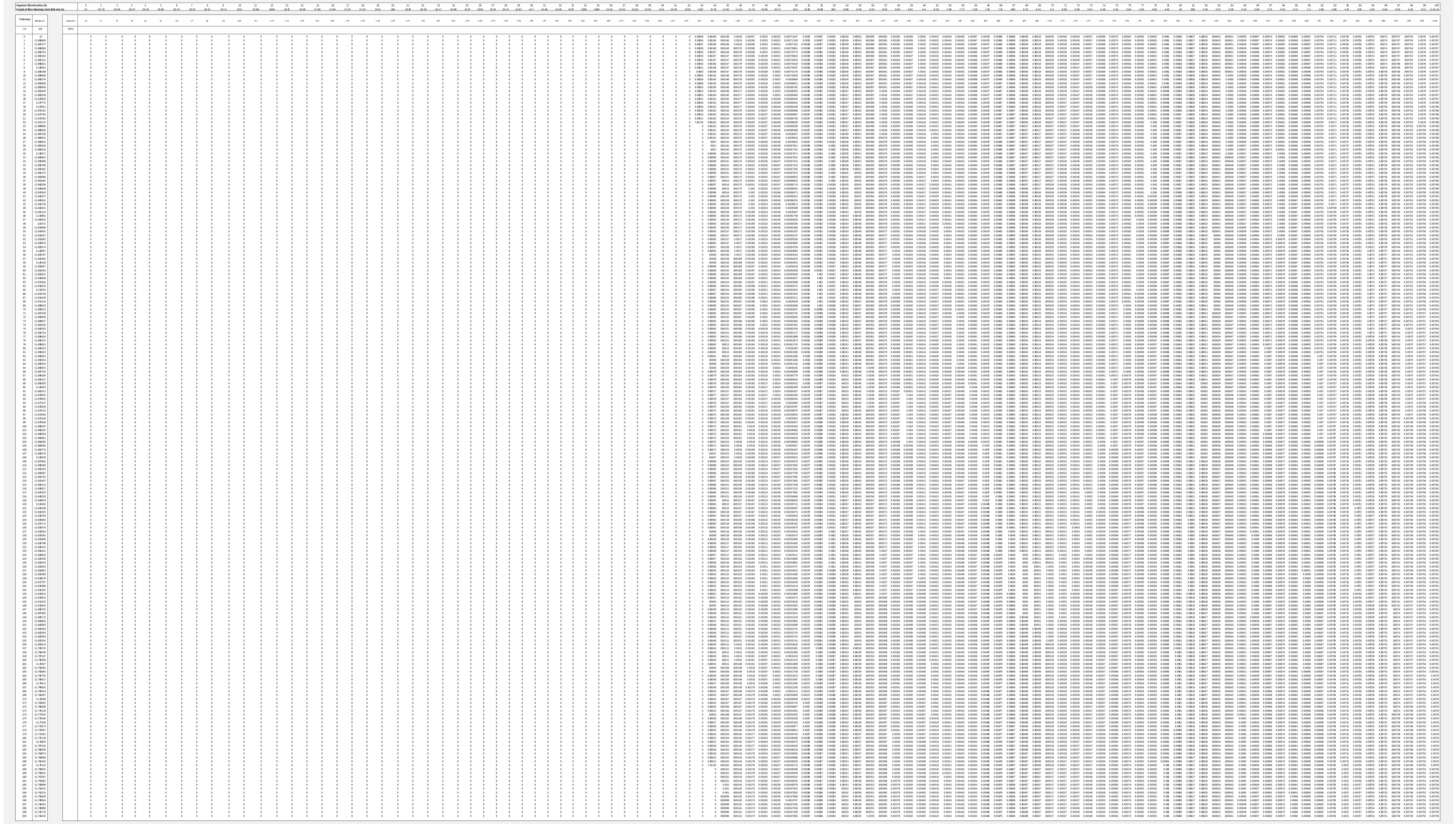

PARAMETRIC MODEL HEAD-LOSS VELOCITY TABLE [TIMESTEP vs BH SEGMENT] : Bir.T2

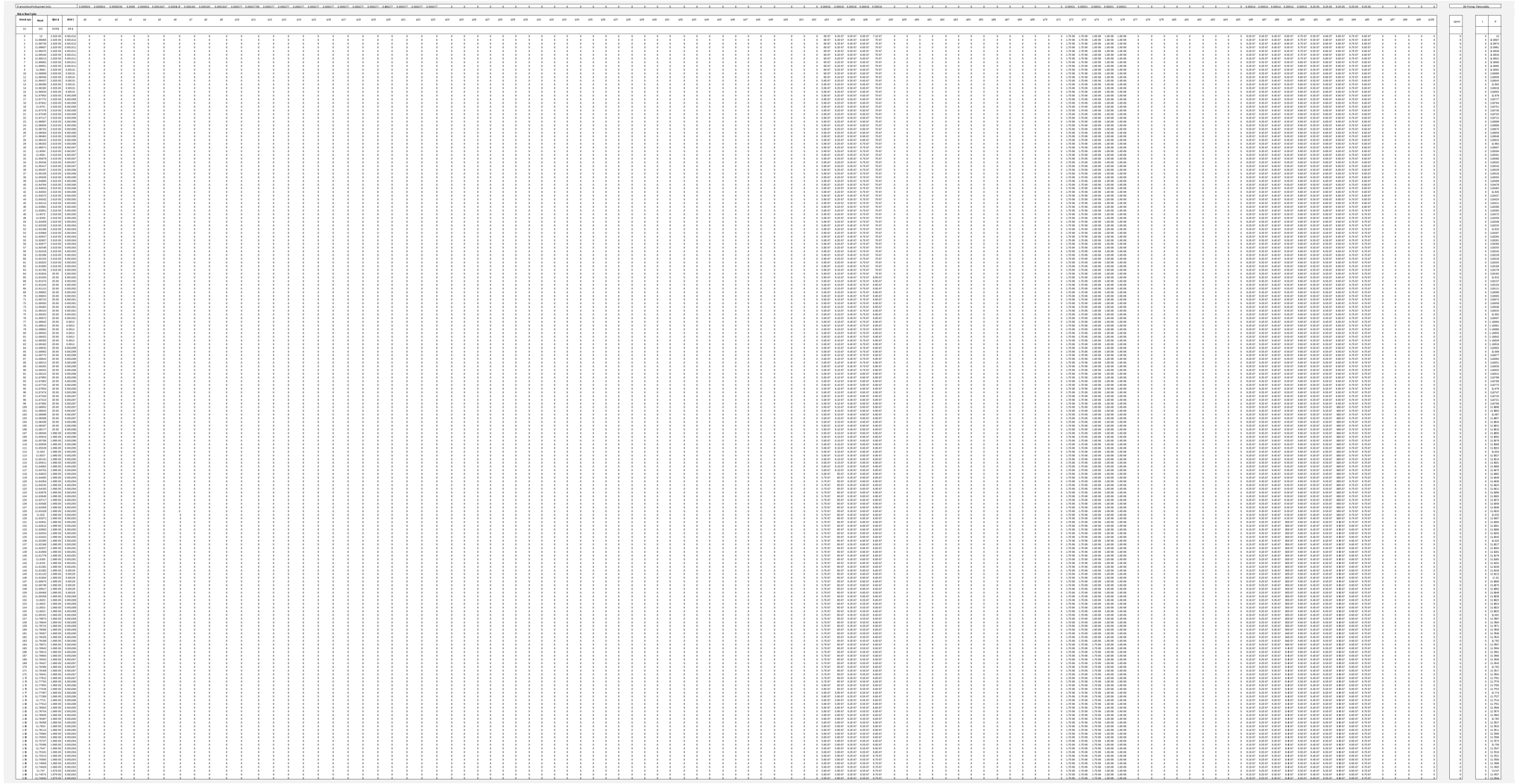

PARAMETRIC MODEL HEAD-LOSS FLOWRATE TABLE [TIMESTEP vs BH SEGMENT] : Bir.T2

solidbase LABORATORY LTD

Borehole Drilling Record

BH1

INF research project	Location: Fgura A Primary school		Weather: Sunny	Date started: 04/05/2012	Date completed: 04/05/2012
				Northings: 0	Eastings: 0
	Drill type: CMV -600	Bit type/diameter: Double core	Orientation: vertical	Drilling fluid: Fresh Water	Ground level: 0	Water level: 0

cription	Depth (Actual depth)	Run (Drill time)	TCR %	SCR %	RQD %	f/m /m	Sampling/testing	Drilling progress	Returns
strong, coarse grained concrete, CONCRETE made	0.00	1 0: 0	100	33.3	33.3			Advance casing Coring using double core sampler	Lost,
ellowish Brown (10YR 3/4), hard (soil), fine to grained clayey silt - several rootlets, ERNARY DEPOSITS, Terrarossa soil	1.00								
rown (2.5Y 7/4), moderately strong, m grained limestone, GLOBIGERINA, member		2 0: 0	100	100	90			Coring using double core sampler	Lost
Discontinuity at 45°, rough sides, no infill, aperture < 5mm	2.00								
Discontinuity at 15°, rough & calcified sides, terrarossa infill, aperture unclear									
Discontinuity at 25°, rough & calcified/ calcified terrarossa sides, aperture < 5mm									
Discontinuity at 25°, rough sides, terrarossa infill, aperture > 15mm	3.00	3 0: 0	100	100	77.8			Coring using double core sampler	Lost,
Discontinuity at 55°, rough & calcified/ calcified terrarossa sides, aperture < 5mm							3.7m ▽ Falling head Slug test (A) original level at 9.50hrs		
Discontinuity at 40°, rough sides, terrarossa infill, aperture < 5mm							4.22m ▽ Falling head Slug test (A) final level at 10:35hrs		
rown (2.5Y 8/3), moderately , medium grained limestone - rystalline, GLOBIGERINA, member	4.00								
Discontinuity at 45°, rough & calcified/calcified terrarossa sides, aperture 1-2mm		4 0: 0	100	100	80			Coring using double core sampler	Lost,
rown (2.5Y 7/4) IGERINA, Lower er	5.00								
Discontinuity, sub-horizontal, very rough sides, terrarossa infill, aperture unclear		5 0: 0						Core retrieval with double core sampler	Lost,
Hole hole drilling through ited plastic casing	6.00								
rown (2.5Y 8/3), moderately strong, medium d limestone - semi crystalline, GLOBIGERINA, member	7.00	5 0: 0	100	34.6	34.6			Coring using double core sampler	Full, Cream
rown (2.5Y 7/4), ately strong ing moderately weak , medium grained ne, GLOBIGERINA, member									
Discontinuity at 15°, rough sides, terrarossa traces, aperture unclear									
Discontinuity, sub-horizontal, rough sides, terrarossa infill, aperture unclear	8.00								
Discontinuity at 60°, smooth & slickensided sides, terrarossa infill, tight									
Discontinuity at 60°, smooth & slickensided sides, terrarossa infill, aperture unclear	9.00								
		6 0: 0	100	91.3	73.9			Coring using double core sampler	Full, Cream
	10.00								
Discontinuity, sub-horizontal, rough sides, terrarossa infill, aperture unclear									
	11.00								

d:

- ground level
- above Ordinance Datum
- below ground level
- above mean sea level
- Rock Quality Designation
- total core recovery
- solid core recovery
- fracture frequency
- open hole

- Limestone fill (Recent deposits)
- Quaternary Deposits (PLEISTOCENE, to HOLOCENE)
- Upper Globigerina Limestone (MIOCENE, Burdigalian to early Langhian)
- Middle Globigerina Limestone (MIOCENE, Aquitanian to Burdigalian)
- Lower Globigerina Limestone (MIOCENE, Aquitanian)

Legend:

UCS:	uniaxial compressive strength
BD:	Bulk density
ABS:	Absorption
MC:	Moisture content
PP:	Pocket penetrometer
PSV:	Pocket shear vane

Soil and rock colour references are according to the Munsell notation (Munsell soil colour charts 2009)

solidbase LABORATORY LTD

Borehole Drilling Record

page 2 of 2

BH1

-INF research project	Location: Fgura A Primary school		Weather: Sunny	Date started: 04/05/2012	Date completed: 04/05/2012
				Northings: 0	Eastings: 0
:	Drill type: CMV -600	Bit type/diameter: Double core	Orientation: vertical	Drilling fluid: Fresh Water	Ground level: 0
					Water level: 0

cription	Depth (Actual depth)	Run (Drill time)	TCR %	SCR %	RQD %	f/m /m	Sampling/testing	Drilling progress	Returns
	11.00								
Discontinuity, horizontal, rough sides, terrarossa infill, tight Discontinuity at 60°, rough sides, terrarossa infill, aperture unclear	12.00	7 0: 0	100	100	96.7			Coring using double core sampler	Full, Cream
	13.00								
	14.00								
3rown (2.5Y 7/4), ately weak to weak, m to fine grained marl - ely bioturbated, IGERINA, Lower er	15.00	8 0: 0	100	100	100		15.0m Falling head Slug test (A) when borehole drilling had reached this level	Coring using double core sampler	Full, Cream
	16.00								
	17.00								
3rown (2.5Y 7/4), ately weak, medium d limestone - onally bioturbated, IGERINA, Lower er	18.00	9 0: 0	100	100	55			Coring using double core sampler	Full, Cream
	19.00								
Discontinuity at 55°, rough sides, terrarossa infill, aperture unclear	20.00	10 0: 0	100	90	90			Coring using double core sampler	Full, Cream
	21.00								
orehole at 22.0m	22.00								

d:

- ground level
- above Ordinance Datum
- below ground level
- above mean sea level
- Rock Quality Designation
- total core recovery
- solid core recovery
- fracture frequency
- open hole

- Limestone fill (Recent deposits)
- Quaternary Deposits (PLEISTOCENE, to HOLOCENE)
- Upper Globigerina Limestone (MIOCENE, Burdigalian to early Langhian)
- Middle Globigerina Limestone (MIOCENE, Aquitanian to Burdigalian)
- Lower Globigerina Limestone (MIOCENE, Aquitanian)

Legend:

UCS:	uniaxial compressive strength
BD:	Bulk density
ABS:	Absorption
MC:	Moisture content
PP:	Pocket penetrometer
PSV:	Pocket shear vane

Soil and rock colour references are according to the Munsell notation (Munsell soil colour charts 2009)

Falling Head Permeability Test (In-Situ)

Location: St. Thomas More, Fgura
Company: Solidbase Laboratory + GEO-INF

Test ID: Fgu.T2
Date: 2012

Borehole Data

BH Depth:	22 m
BH Diameter:	0.1 m
BH Casing Depth:	5.77 m
Site BH Number:	Null

Ground Data

Avg Fissure Width:	1 mm
Fissure Spread:	Surface Weathering
Fissure Infill:	Mainly Terrarossa Infill
Ground Material:	Globigerina

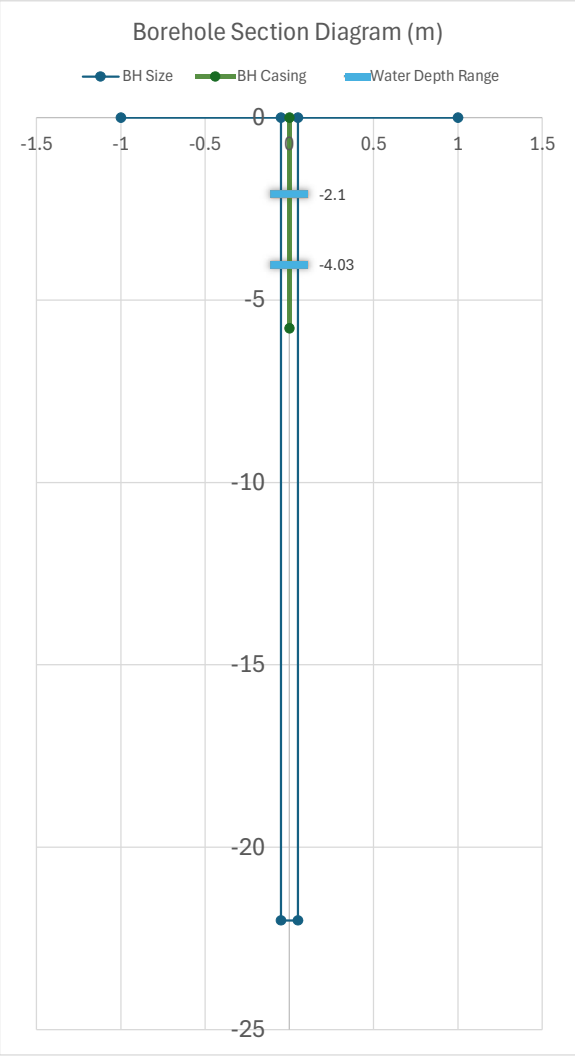

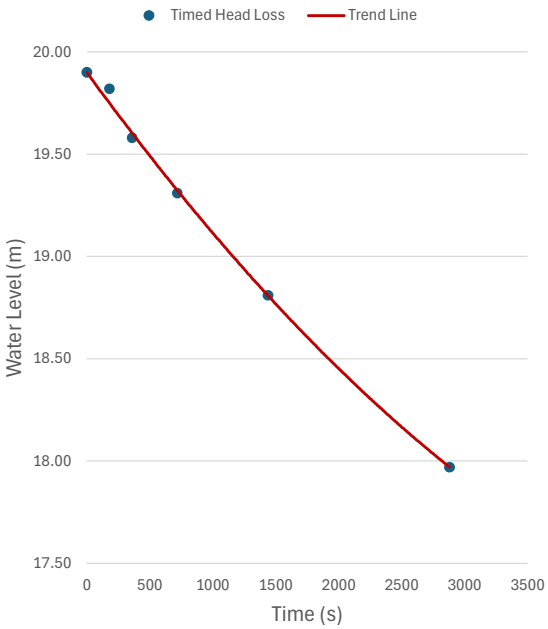

Time	Time Passed (s)	Water Level Depth (m) Surface (-)	Base (+)
09:50	0	2.1	19.90
	180	2.18	19.82
	360	2.42	19.58
	720	2.69	19.31
	1440	3.19	18.81
11:23	2880	4.03	17.97

[N. Borg (2012)]

Notes:
Water level recordings commenced at a depth of 2.1m.
Very slow flowrate.
Infilled fissures.

Results:

Initial Water Level (Depth):	-2.1 m
Final Water Level (Depth):	-4.03 m
Initial (Max) Flowrate Q:	6.44E-06 m3/s
Intake Factor Estimation F:	22.70989
Initial (Max) Permeability K:	1.56E-08 m/s

Parametric Ground Model for Infiltration Dry Well

Borehole Input Data

BH Depth:	22	m
BH Diameter:	0.1	m
BH Casing Depth:	5.77	m
BH Filter Medium:	No Filter Material	

Ground Data

Limestone Type:	Globigerina Limestone	
Pore Hydraulic Conductivity:	0	m/s

Fissure Input Data

Avg Fissure Width:	1	mm
Fissure Spread:	Average Concentration	
Fissure Infill:	Clayey Soil	

Other Data

On-Site Test ID:	Fgu.T2	
Starting Water Depth:	2.1	m
Timestep:	10	s

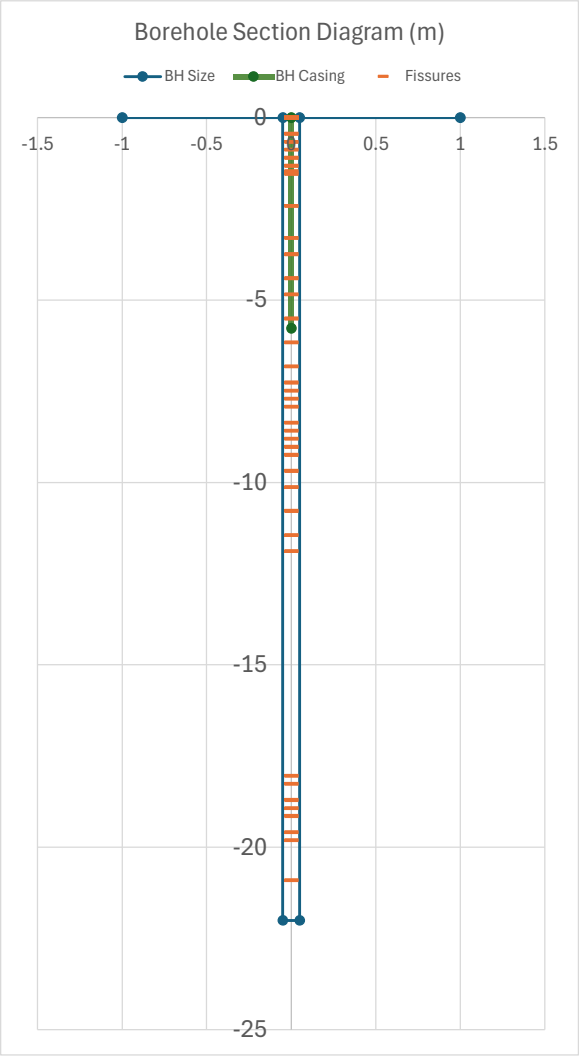

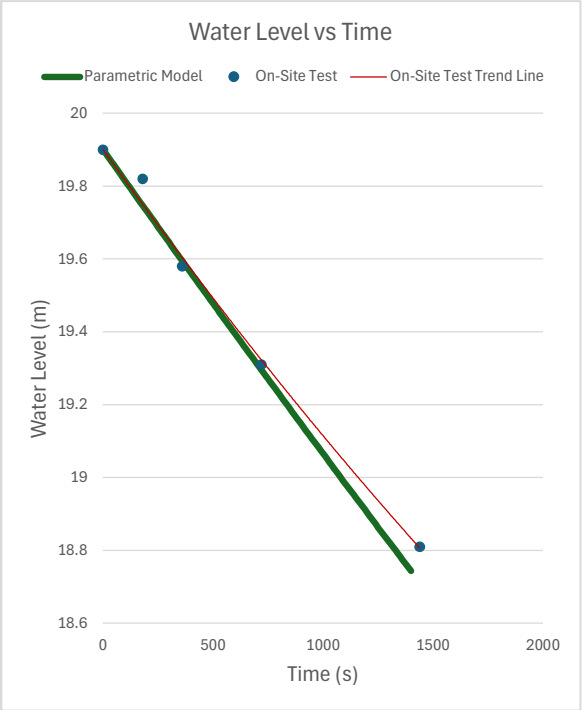

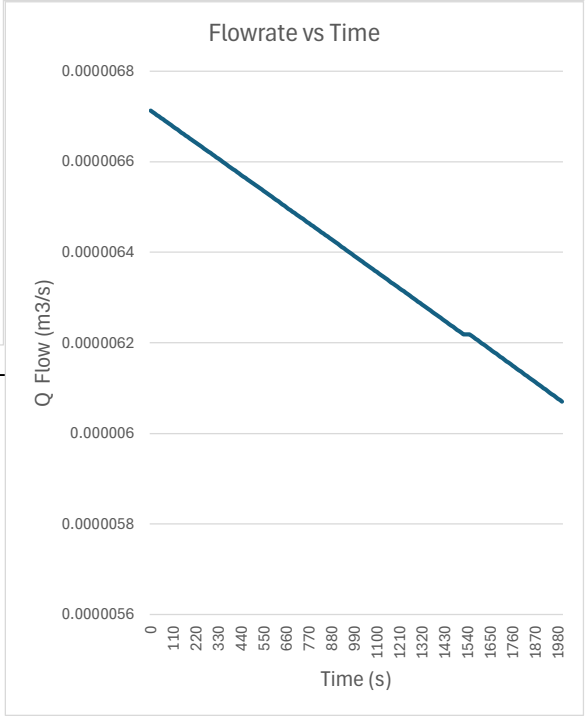

Results:

Primary Initial (Max) Flowrate Q:	0	m3/s
Secondary Initial (Max) Flowrate Q:	6.67E-06	m3/s
Total Initial (Max) Flowrate Q:	6.67E-06	m3/s
Intake Factor Estimation F:	22.70989	
Initial (Max) Permeability K:	1.49E-08	m/s
Model Flow Factor F_F:	0.000065	
Initial Flowrate Q Difference:	3.7130	%

STEADY STATE CONDITION (t=0) - SECONDARY PERMEABILITY

100 segments: (#)	Segment Depth from Surface: (m)	Depth from Water Surface: (m)	Velocity Discharge t=0: (m/s) v	Fissure Num per Segment: (#)	Fissure Area per Segment: (m2) A	Q flow through fissures (m3/s) Q=Av
0	0		0	1.46666667	0.00046077	0
1	0.22		0	1.46666667	0.00046077	0
2	0.44		0	1.46666667	0.00046077	0
3	0.66		0	1.46666667	0.00046077	0
4	0.88		0	1.46666667	0.00046077	0
5	1.1		0	1.46666667	0.00046077	0
6	1.32		0	1.46666667	0.00046077	0
7	1.54		0	0.22	6.9115E-05	0
8	1.76		0	0.22	6.9115E-05	0
9	1.98		0	0.22	6.9115E-05	0
10	2.2	0	0	0.22	6.9115E-05	0
11	2.42	0.22	0.00013504	0.22	6.9115E-05	0
12	2.64	0.44	0.00019098	0.22	6.9115E-05	0
13	2.86	0.66	0.0002339	0.22	6.9115E-05	0
14	3.08	0.88	0.00027009	0.40333333	0.00012671	0
15	3.3	1.1	0.00030197	0.40333333	0.00012671	0
16	3.52	1.32	0.00033079	0.40333333	0.00012671	0
17	3.74	1.54	0.00035729	0.40333333	0.00012671	0
18	3.96	1.76	0.00038196	0.40333333	0.00012671	0
19	4.18	1.98	0.00040513	0.40333333	0.00012671	0
20	4.4	2.2	0.00042705	0.40333333	0.00012671	0
21	4.62	2.42	0.00044789	0.40333333	0.00012671	0
22	4.84	2.64	0.0004678	0.33	0.00010367	0
23	5.06	2.86	0.00048691	0.33	0.00010367	0
24	5.28	3.08	0.00050529	0.33	0.00010367	0
25	5.5	3.3	0.00052302	0.33	0.00010367	0
26	5.72	3.52	0.00054017	0.33	0.00010367	0
27	5.94	3.74	0.0005568	0.33	0.00010367	5.77248E-08
28	6.16	3.96	0.00057294	0.33	0.00010367	5.93983E-08
29	6.38	4.18	0.00058864	0.33	0.00010367	6.1026E-08
30	6.6	4.4	0.00060393	0.33	0.00010367	6.26113E-08
31	6.82	4.62	0.00061885	0.82923077	0.00026051	1.61216E-07
32	7.04	4.84	0.00063341	0.82923077	0.00026051	1.6501E-07
33	7.26	5.06	0.00064765	0.82923077	0.00026051	1.68719E-07
34	7.48	5.28	0.00066158	0.82923077	0.00026051	1.72348E-07
35	7.7	5.5	0.00067522	0.82923077	0.00026051	1.75901E-07
36	7.92	5.72	0.00068859	0.82923077	0.00026051	1.79385E-07
37	8.14	5.94	0.00070171	0.82923077	0.00026051	1.82802E-07
38	8.36	6.16	0.00071458	0.82923077	0.00026051	1.86157E-07
39	8.58	6.38	0.00072723	0.82923077	0.00026051	1.89452E-07
40	8.8	6.6	0.00073966	0.82923077	0.00026051	1.9269E-07
41	9.02	6.82	0.00075189	0.82923077	0.00026051	1.95876E-07
42	9.24	7.04	0.00076392	0.82923077	0.00026051	1.9901E-07
43	9.46	7.26	0.00077577	0.37304348	0.0001172	9.0916E-08
44	9.68	7.48	0.00078743	0.37304348	0.0001172	9.22833E-08
45	9.9	7.7	0.00079893	0.37304348	0.0001172	9.36305E-08
46	10.12	7.92	0.00081026	0.37304348	0.0001172	9.49587E-08
47	10.34	8.14	0.00082144	0.37304348	0.0001172	9.62685E-08
48	10.56	8.36	0.00083247	0.37304348	0.0001172	9.75608E-08
49	10.78	8.58	0.00084335	0.37304348	0.0001172	9.88362E-08
50	11	8.8	0.00085409	0.37304348	0.0001172	1.00095E-07
51	11.22	9.02	0.0008647	0.37304348	0.0001172	1.01339E-07
52	11.44	9.24	0.00087518	0.37304348	0.0001172	1.02567E-07
53	11.66	9.46	0.00088554	0.37304348	0.0001172	1.03781E-07
54	11.88	9.68	0.00089578	0.03666667	1.1519E-05	1.03186E-08
55	12.1	9.9	0.0009059	0.03666667	1.1519E-05	1.04352E-08
56	12.32	10.12	0.00091591	0.03666667	1.1519E-05	1.05505E-08
57	12.54	10.34	0.00092581	0.03666667	1.1519E-05	1.06646E-08
58	12.76	10.56	0.00093561	0.03666667	1.1519E-05	1.07775E-08
59	12.98	10.78	0.00094531	0.03666667	1.1519E-05	1.08891E-08
60	13.2	11	0.0009549	0.03666667	1.1519E-05	1.09997E-08
61	13.42	11.22	0.0009644	0.03666667	1.1519E-05	1.11091E-08
62	13.64	11.44	0.00097381	0.03666667	1.1519E-05	1.12175E-08
63	13.86	11.66	0.00098313	0.03666667	1.1519E-05	1.13249E-08
64	14.08	11.88	0.00099236	0.03666667	1.1519E-05	1.14312E-08
65	14.3	12.1	0.00100151	0.03666667	1.1519E-05	1.15366E-08
66	14.52	12.32	0.00101057	0.03666667	1.1519E-05	1.1641E-08
67	14.74	12.54	0.00101956	0	0	0
68	14.96	12.76	0.00102846	0	0	0
69	15.18	12.98	0.00103729	0	0	0
70	15.4	13.2	0.00104604	0	0	0
71	15.62	13.42	0.00105472	0	0	0
72	15.84	13.64	0.00106333	0	0	0
73	16.06	13.86	0.00107188	0	0	0
74	16.28	14.08	0.00108035	0	0	0
75	16.5	14.3	0.00108876	0	0	0
76	16.72	14.52	0.0010971	0	0	0
77	16.94	14.74	0.00110538	0	0	0
78	17.16	14.96	0.0011136	0	0	0
79	17.38	15.18	0.00112176	0	0	0
80	17.6	15.4	0.00112986	0	0	0
81	17.82	15.62	0.0011379	0.748	0.00023499	2.67396E-07
82	18.04	15.84	0.00114588	0.748	0.00023499	2.69272E-07
83	18.26	16.06	0.00115381	0.748	0.00023499	2.71136E-07
84	18.48	16.28	0.00116169	0.748	0.00023499	2.72987E-07
85	18.7	16.5	0.00116951	0.748	0.00023499	2.74825E-07
86	18.92	16.72	0.00117728	0.748	0.00023499	2.76651E-07
87	19.14	16.94	0.001185	0.748	0.00023499	2.78465E-07
88	19.36	17.16	0.00119267	0.748	0.00023499	2.80268E-07
89	19.58	17.38	0.00120029	0.748	0.00023499	2.82059E-07
90	19.8	17.6	0.00120787	0.165	5.1836E-05	6.26113E-08
91	20.02	17.82	0.00121539	0.165	5.1836E-05	6.30014E-08
92	20.24	18.04	0.00122287	0.165	5.1836E-05	6.33892E-08
93	20.46	18.26	0.00123031	0.165	5.1836E-05	6.37745E-08
94	20.68	18.48	0.0012377	0.165	5.1836E-05	6.41575E-08
95	20.9	18.7	0.00124504	0.165	5.1836E-05	6.45383E-08
96	21.12	18.92	0.00125234	0.165	5.1836E-05	6.49168E-08
97	21.34	19.14	0.0012596	0.165	5.1836E-05	6.52932E-08
98	21.56	19.36	0.00126682	0.165	5.1836E-05	6.56673E-08
99	21.78	19.58	0.001274	0	0	0
100	22	19.8	0.00128114		0	0

Total BH Depth :	22	m	**Fissure Q** 6.67487E-06 m3/s *[Summed]*
BH Diameter:	0.1	m	
Water Start Depth :	2.1	m	
Total Casing Depth :	5.77	m	**Pore Q** 0 m3/s
Flow Resistance Factor :	0.000065		

FISSURE DISTRIBUTION TABLE [Borehole Log Runs]

Core Run: (#)	Core Length Input Values: (m)	RQD Input Values: (%)	Core Run Max Depth: (m)	Fissured Lengths: (m)	Fissure Number per Run: (#)	Fissure Number per Segment: (#)
-	-	-	-	-	-	-
1	1.5	33.3	1.5	1.0005	10	1.46666667
2	1.5	90	3	0.15	1.5	0.22
3	1.8	77.8	4.8	0.333	3.3	0.40333333
4	2	80	6.8	0.3	3	0.33
5	2.6	34.6	9.4	0.981	9.8	0.82923077
6	2.3	73.9	11.7	0.3915	3.9	0.37304348
7	3	96.7	14.7	0.0495	0.5	0.03666667
8	3	100	17.7	0	0	0
9	2	55	19.7	0.675	6.8	0.748
10	2	90	21.7	0.15	1.5	0.165
11	0.3	100	22	0	0	0
12						
13						
14						
15						
16						
17						
18						
19						
20						
21						
22						
23						
24						
25						
26						
27						
28						
29						
30						
31						
32						
33						
34						
35						
36						
37						
38						
39						
40						
41						
42						
43						
44						
45						
46						
47						
48						
49						
50						

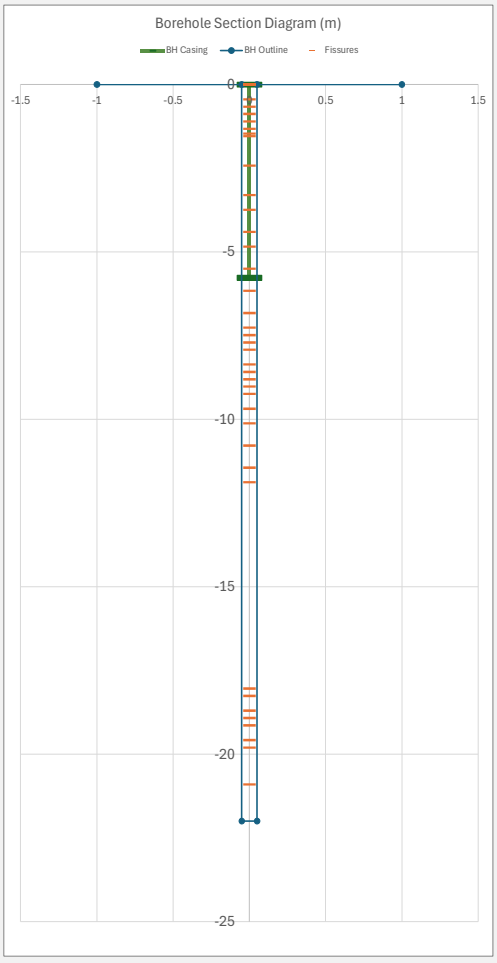

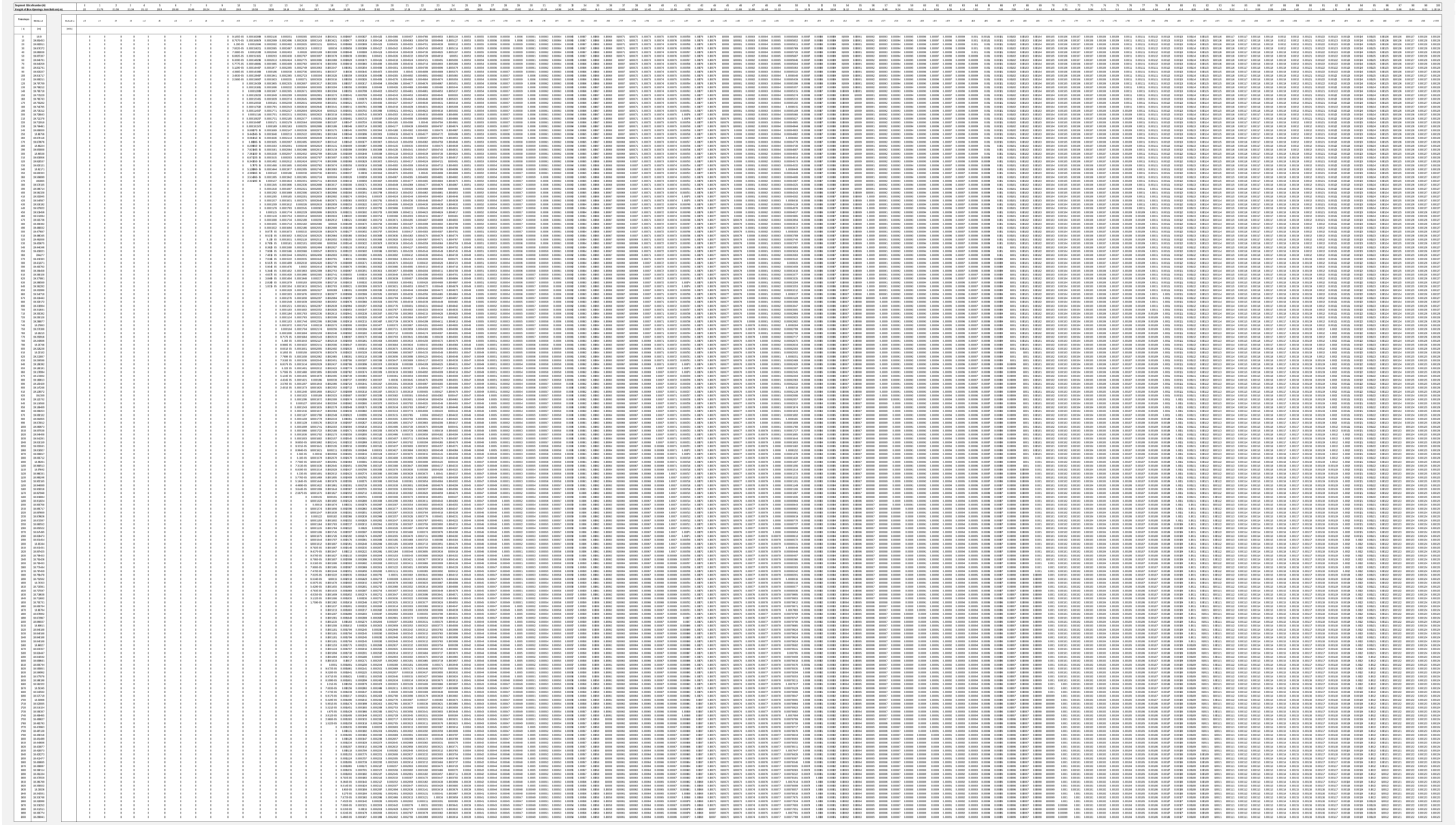

PARAMETRIC MODEL HEAD-LOSS VELOCITY TABLE [TIMESTEP vs BH SEGMENT] : Fgu.T2

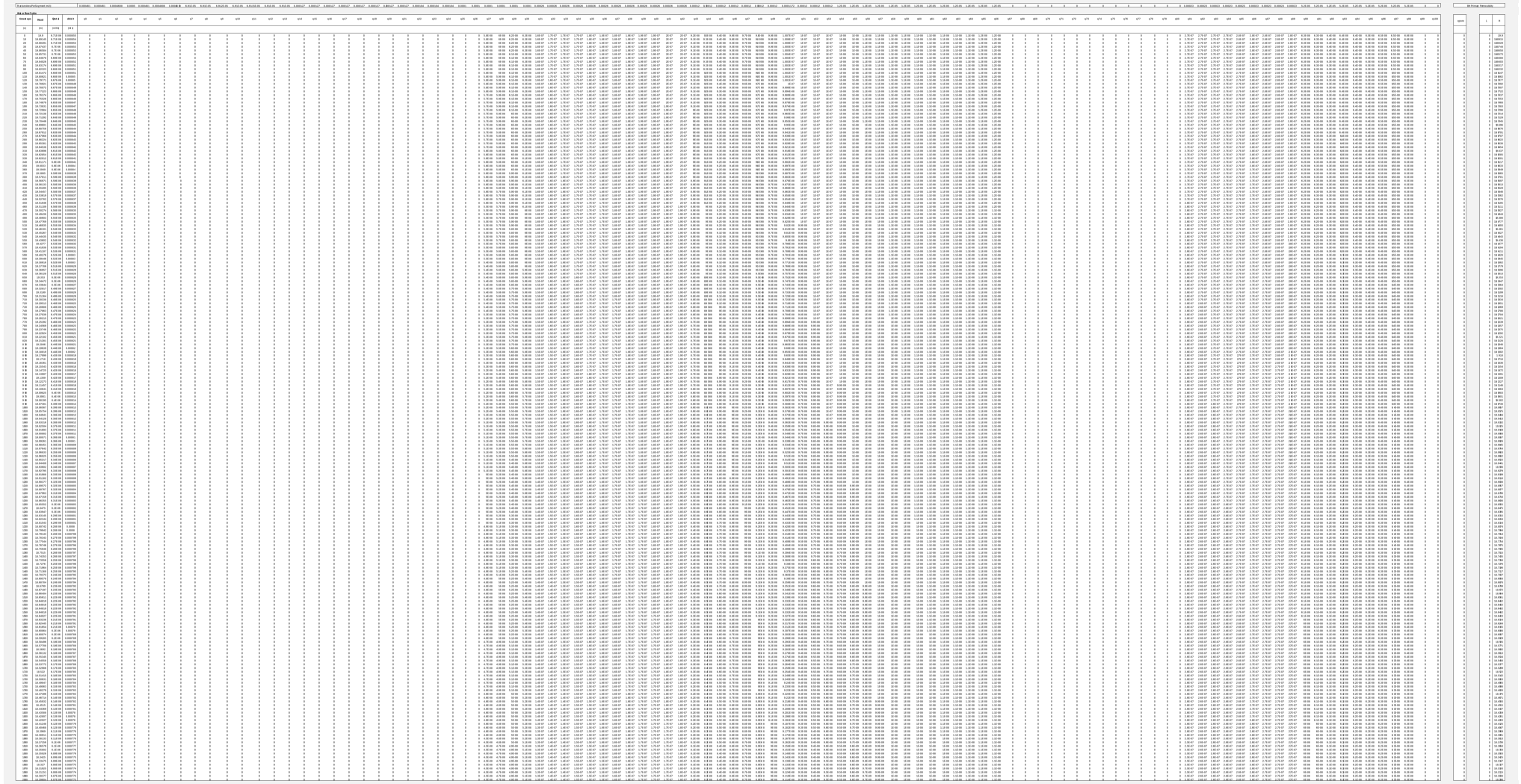

PARAMETRIC MODEL HEAD-LOSS FLOWRATE TABLE [TIMESTEP vs BH SEGMENT] : Fgu.T2